

File Copy
DOE/BC/10082-8
(DE82009072)

ADSORPTION FROM FLOODING SOLUTIONS IN POROUS MEDIA

A Study of Interactions of Surfactants and Polymers with Reservoir
Minerals Second Annual Report

By
P. Somasundaran
C. C. Gryte
Philip B. Lorenz

April 1982
Date Published

Work Performed Under Contract No. AC19-79BC10082

Columbia University
New York, New York



U. S. DEPARTMENT OF ENERGY

DISCLAIMER

"This report was prepared as an account of work sponsored by an agency of the United States Government. Neither the United States Government nor any agency thereof, nor any of their employees, makes any warranty, express or implied, or assumes any legal liability or responsibility for the accuracy, completeness, or usefulness of any information, apparatus, product, or process disclosed, or represents that its use would not infringe privately owned rights. Reference herein to any specific commercial product, process, or service by trade name, trademark, manufacturer, or otherwise, does not necessarily constitute or imply its endorsement, recommendation, or favoring by the United States Government or any agency thereof. The views and opinions of authors expressed herein do not necessarily state or reflect those of the United States Government or any agency thereof."

This report has been reproduced directly from the best available copy.

Available from the National Technical Information Service, U. S. Department of Commerce, Springfield, Virginia 22161.

Price: Printed Copy A11
Microfiche A01

Codes are used for pricing all publications. The code is determined by the number of pages in the publication. Information pertaining to the pricing codes can be found in the current issues of the following publications, which are generally available in most libraries: *Energy Research Abstracts, (ERA)*; *Government Reports Announcements and Index (GRA and I)*; *Scientific and Technical Abstracts, (STAR)*; and publication, NTIS-PR-360 available from (NTIS) at the above address.

ADSORPTION FROM FLOODING SOLUTIONS IN POROUS MEDIA
A Study of Interactions of Surfactants and Polymers with Reservoir Minerals
Second Annual Report

P. Somasundaran, *Principal Investigator*
C. C. Gryte, *Co-Principal Investigator*
Columbia University
School of Engineering and Applied Science
P.O. Box 20
New York, New York 10027

Philip B. Lorenz, *Technical Project Officer*
Bartlesville Energy Technology Center
P.O. Box 1398
Bartlesville, Oklahoma 74005

Work Performed for the Department of Energy
Under Contract No. DE-AC19-79BC10082

Date Published—April 1982

CONTENTS

LIST OF FIGURES.	vi
LIST OF TABLES	xv
SYMBOLS AND ABBREVIATIONS.	xvi
SUMMARY.	xix
I. PRECIPITATION/REDISSOLUTION/REPRECIPITATION PHENOMENA	1
A. Introduction.	1
B. Materials and Methods	3
B1. SURFACTANTS AND OTHER CHEMICALS.	3
B2. METHODS.	4
B2a. Turbidity Measurements	4
B2b. Precipitation Tests.	4
B2c. Conductivity Measurements.	5
B2d. Dye Solubilization	5
B2e. Surface Tension Measurements	5
B2f. Free Na Ion Measurements	6
B2g. Free Ca Ion Measurements	7
C. Effect of Chain Length.	7
D. Effect of Temperature	19
E. Effect of Alcohols and Oils	28
E1. EFFECT OF n-PROPANOL	28
E2. EFFECT OF n-DODECANE	32
F. A Thermodynamic Model for Precipitation/ Redissolution	35
F1. OUTLINE OF THE MODEL	36
F2. COMPARISON OF THE MODEL PREDICTIONS WITH THE EXPERIMENTAL DATA.	52
F3. SPECIES ACTIVITIES Vs. NaDDBS CONCENTRATION.	54

G.	Molecular Mechanism of Precipitation/ Redissolution.	56
G1.	INTRODUCTION	56
G2.	MOLECULAR MECHANISMS	58
G3.	ANALYSIS OF THE DIFFERENCES IN THE SOLU- BILIZATION POWERS OF NaDDS AND NaDDBS.	64
G3a.	Conductivity Results	64
G3b.	Extent of Na Ion Binding	66
G4.	HEAT OF ADSORPTION OF CALCIUM ON MICELLES	69
G5.	A CALCIUM ADSORPTION MODEL FOR TEMPERA- TURE DEPENDENCE OF REDISSOLUTION	72
II.	ADSORPTION OF SURFACTANTS ON RESERVOIR MINERALS	77
A.	Introduction.	77
B.	Materials and Methods	79
B1.	MINERALS	80
B1a.	Kaolinite.	80
B1b.	Alumina.	80
B2.	SURFACTANTS AND OTHER CHEMICALS.	80
B2a.	n-Na Alkylbenzenesulfonates.	80
B2b.	Recrystallized Na Dodecylbenzene- sulfonate.	83
B2c.	Alipal Co-436.	83
B2d.	Hydrocarbon Oils	83
B2e.	Alcohols	83
B2f.	Inorganic Reagents	83
B2g.	Water.	84
B3.	SYNTHESIS AND CHARACTERIZATION OF ISOMER- ICALLY PURE n-ALKYLBENZENESULFONATES	84
B3a.	n-Na Dodecylbenzenesulfonate	84
B3b.	n-Na Decylbenzenesulfonate	89
B4.	ADSORPTION EXPERIMENTS	94
B5.	ADSORPTION TESTS IN THE PRESENCE OF OIL.	97

C.	Results and Discussion.	99
C1.	KINETICS OF ADSORPTION OF n-NaDDBS ON ALUMINA.	99
C2.	KINETICS OF n-DODECANE UPTAKE BY ALUMINA IN n-NaDDBS SOLUTIONS.	99
C3.	ADSORPTION OF ISOMERICALLY PURE n-ALKYLBENZENESULFONATES ON ALUMINA. . .	102
	C3a. n-Na Dodecylbenzenesulfonate . . .	102
	C3b. n-Na Decylbenzenesulfonate	108
	C3c. Chain Length Effect and Free Energy of Hemimicellization. . . .	109
	C3d. Plateau Adsorption-Comparison Between n-NaDDBS and n-NaDBS . . .	113
C4.	EFFECT OF OIL ON SURFACTANT ADSORPTION AND THE UPTAKE OF OIL.	114
	C4a. Effect of Oil on Sulfonate Adsorption	120
	C4b. Abstraction of Oil	120
C5.	EFFECT OF TEMPERATURE.	129
C6.	EFFECT OF ALCOHOL.	131
C7.	ADSORPTION OF ALIPAL Co-436 ON ALUMINA AND Na-KAOLINITE	136
III.	POLYMER SURFACTANT INTERACTIONS	145
	A. Introduction.	145
	B. Wettability of Reservoir Rock Minerals in Polymer-Surfactant Solutions.	147
	B1. INTRODUCTION	147
	B2. METHODS AND MATERIALS.	148
	B2a. Materials.	148
	B2b. Methods.	149
	B3. RESULTS AND DISCUSSION	151
	B3a. Wettability of Quartz in Amine Solutions.	151
	B3b. Non-Ionic Polymer.	154
	B3c. Cationic Polymer	158
	B3d. Anionic Polymer.	158
	B3e. NaDDS/PAMD/Quartz.	166

C.	PAMD/NaDDBS-Interactions in Bulk Solutions- Precipitation/Redissolution Phenomenon. . . .	168
C1.	INTRODUCTION	168
C2.	MATERIALS AND METHODS.	170
C2a.	Materials.	170
C2b.	Methods.	170
C3.	RESULTS AND DISCUSSION	171
C3a.	NaDDBS/PAMD Precipitation Behavior	171
C3b.	Effect of NaCl on PAMD/NaDDBS Precipitation.	179
C3c.	Effect of CaCl ₂ on PAMD/NaDDBS Precipitation.	180
IV.	FLOW DISTRIBUTIONS IN CONSOLIDATED SANDSTONE UTILIZING A TOMOGRAPHIC TECHNIQUE	185
A.	Introduction.	185
B.	Fluids That Can Be Observed in Berea Sand- stone	185
C.	Initial Results for 1M KI Displacing Oil from Berea Core.	188
	REFERENCES	197

LIST OF FIGURES

Chapter I

- I:1. Ratio of residual (C_{Ca-r}) to initial (C_{Ca-i}) concentration of labelled calcium as a function of the initial sulfonate concentration for different chain length sulfonates 9
- I:2. Variation of solubility product as a function of the chain length of alkyl sulfonates 11
- I:3. CMC and solubilization constant of alkylsulfonates as a function of chain length 15
- I:4. Solubilization pattern of $Ca(C_{16}SO_3)_2$ in the aqueous solutions of $NaC_{10}SO_3$ and $NaC_{18}SO_3$ 18
- I:5. Effect of temperature on the precipitation/redissolution behavior of the $NaDDBS/CaCl_2$ system; light transmission of the solutions as a function of sulfonate concentration 21
- I:6. Effect of temperature on the precipitation/redissolution behavior of the $NaDDS/CaCl_2$ system; light transmission of the solutions as a function of sulfonate concentration. 22

I:7.	Solubility product of $\text{Ca}(\text{DDS})_2$ and $\text{Ca}(\text{DDBS})_2$ as a function of the reciprocal of the absolute temperature	25
I:8.	Effect of n-propanol on the precipitation/redissolution behavior of the $\text{NaDDBS}/\text{CaCl}_2$ system	29
I:9.	Effect of n-dodecane on the precipitation/redissolution behavior of the $\text{NaDDBS}/\text{CaCl}_2$ system	34
I:10.	A schematic diagram of the mechanism of the precipitation/redissolution/precipitation process	37
I:11.	Surface tension of NaDDBS as a function of sulfonate concentration at various NaCl levels . .	47
I:12.	Surface tension of NaDDBS as a function of sulfonate concentrations at various levels of CaCl_2	48
I:13.	Dependence of CMC as a function of total counterion concentration.	51
I:14.	Comparison of the experimentally obtained precipitation/redissolution patterns of $\text{NaDDS}/\text{CaCl}_2$ system with that predicted using the micellar solubilization model	53

I:15.	Comparison of the experimentally obtained precipitation/redissolution patterns of NaDDS / CaCl ₂ system at three different temperatures with that predicted using the micellar solubilization model.	55
I:16	Experimentally obtained variations in the activities of different species in NaDDBS/CaCl ₂ system as a function of sulfonate concentration	57
I:17.	Conductivity of NaDDS and NaDDBS solutions as a function of sulfonate concentration	65
I:18.	Free Na ⁺ ion concentration determined in NaDDBS and NaDDS solutions under various conditions. .	67
I:19.	Specific conductivity of NaDDS/CaCl ₂ system as a function of sulfonate concentration at different temperatures	71

Chapter II

II:1.	Electron micrograph of Linde Alumina.	81
II:2.	Solubility of alumina at 75°C, as a function of pH.	82
II:3.	Proton NMR spectrum of n-dodecane, n-NaDBS, and n-NaDDBS.	86

II:4.	Proton decoupled Fourier transform $^{13}\text{C}\{\text{H}\}$ NMR spectrum of n-dodecylbenzene sulfonic acid (70% by weight) in deuterio chloroform. Upper: full spectrum; Middle: expansion of alkyl region; Lower: expansion of aryl region.	87
II:5.	TIC and fragmentation pattern of n-dodecylbenzenesulfonic acid (obtained by chemical ionization method).	88
II:6.	Conductivity of n-NaDDBS and n-NaDBS as a function of concentration at 65°C	91
II:7.	Proton decoupled Fourier-transform $^{13}\text{C}\{\text{H}\}$ NMR spectrum of n-decylbenzenesulfonic acid (70% by weight) in deuterio chloroform. Upper: full spectrum; Middle: expansion of alkyl region; Lower: expansion of aryl region.	92
II:8.	Fragmentation pattern of n-decylbenzenesulfonic acid (obtained by chemical ionization method) .	93
II:9.	Calibration curve for the titration of Alipal Co-436 with hexadecyl trimethyl ammonium bromide [HTAB]	96
II:10.	Calibration curve for the estimation of n-dodecane by C-14 counting (using liquid scintillation technique)	98

II:11.	Kinetics of Adsorption of n-DDBS on alumina at two levels of sulfonate, at 10^{-2} kmol/m ³ NaCl .	100
II:12.	Abstraction of n-dodecane as a function of time at two levels of NaCl	101
II:13.	Kinetics of abstraction of oil and adsorption of n-DDBS on alumina.	103
II:14.	Adsorption of n-DDBS on alumina at three levels of NaCl at 75°C	104
II:15.	Adsorption of n-DBS on alumina at three levels of NaCl at 75°C	110
II:16.	Effect of chain length of alkyl-benzenesulfonates on their adsorption on alumina at 10^{-1} kmol/m ³ NaCl at 75°C.	111
II:17.	Effect of oil, n-dodecane, on the adsorption of n-DDBS on alumina at 75°C	116
II:18.	Effect of oil, n-dodecane, on the adsorption of n-DBS on alumina at 75°C.	117
II:19.	Abstraction of n-dodecane by alumina in the presence of n-DDBS at 75°C.	118
II:20.	Abstraction of n-dodecane from n-DBS solutions by alumina at three NaCl levels at 75°C	119
II:21.	Abstraction of n-dodecane by alumina in the presence of n-DBS at 75°C	122

II:22.	Alumina particles showing spherical agglomeration with increase in oil abstraction. Initial oil concentrations (Vol. %): Left = 0.5, Center = 4.9, Right = 11.6	123
II:23.	Abstraction of oil by alumina in the presence of n-DDBS at 2.5% by volume of n-dodecane at 75°C.	126
II:24.	The effect of solid to liquid ratio on the adsorption of n-DDBS and abstraction of n-dodecane on alumina at 75°C	127
II:25.	Adsorption of n-DDBS on alumina at two levels of NaCl at 65°C	130
II:26.	Effect of oil, n-dodecane, on the adsorption of n-DDBS on alumina at 65°C	132
II:27.	Abstraction of n-dodecane by alumina at 65°C in the presence of n-DDBS.	133
II:28.	Effect of alcohol, n-propanol, on the adsorption of n-DDBS on alumina	134
II:29.	Kinetics of abstraction of Alipal Co-436 on alumina at 75° and 27°C and on Na-kaolinite at 27°C.	138
II:30.	Adsorption of Alipal Co-436 on alumina at three levels of NaCl at 75°C.	139
II:31.	Adsorption of Alipal Co-436 on Na-kaolinite at three levels of NaCl at 27°C.	140

II:32.	Effect of salinity on the adsorption of Alipal Co-436 on Alumina at 75°C	141
II:33.	Effect of salinity on the adsorption of Alipal Co-436 on Na-kaolinite.	142

Chapter III

III:1.	Hydrophobicity of quartz, as measured by flotation, as a function of concentration of DDA-HCl	152
III:2.	Effect of the non-ionic polymer, PAM, on the wettability of quartz, as measured by its flotation in DDA-HCl solutions	155
III:3.	Adsorption of PAM on silica as a function of time at three pH values	156
III:4.	Effect of the cationic polymer, PAMD, on the wettability of quartz, as measured by its flotation, in DDA-HCl solutions.	159
III:5.	Adsorption of PAMD on silica as a function of the polymer concentrations at three pH values .	160
III:6.	A schematic diagram showing the polymer, PAMD, masking the effect of the adsorbed DDA ⁺ on quartz.	161
III:7.	Effect of the anionic polymer, PAMS, on the wettability of quartz, as measured by its flotation, in DDA-HCl solutions.	162

III:8.	A schematic diagram showing the aggregation between the surfactant coated bubble and quartz in the presence of a polymer charged oppositely to the surfactant--the aggregation process is referred to as "Sandwiching Effect."	165
III:9.	Effect of the cationic polymer, PAMD, on the wettability of quartz, as measured by flotation, in NaDDS solutions.	167
III:10.	A schematic diagram showing the activation of the adsorption of DDS^- on quartz in PAMD solutions	169
III:11.	Precipitation behavior of DDBS and PAMD as a function of sulfonate concentration	172
III:12.	Relative viscosity of PAMD/NaDDBS solutions as a function of sulfonate concentration	173
III:13.	The effect of NaCl on the precipitation behavior of PAMD, both in the presence and absence of NaDDBS	175
III:14.	Surface tension of NaDDBS/PAMD and NaDDBS/PAMD/ CaCl_2 systems as a function of sulfonate concentration.	178
III:15.	Precipitation behavior of NaDDBS/ CaCl_2 system as a function of sulfonate concentration	182
III:16.	Precipitation behavior of NaDDBS/ CaCl_2 /PAMD system as a function of sulfonate concentration	183

Chapter IV

IV:1.	CAT scan image of oil-rich (white) and water-rich (black) regions in Berea core cross-section.	187
IV:2.	Traverse of Berea Sandstone core.	189
IV:3.	Local oil fraction for traverse of core shown in Figure 4	189
IV:4.	Profiles of traverse local oil fraction at different axial positions, 1M KI displacing oil, 3 percent of pore volumes injected.	190
IV:5.	Initial attempt at graphic representation of cross-section and fraction matrix	194
IV:6.	Pixel composition as a function of injected 1M KI volume (time); Position: 5 cm from injection point	196
IV:7.	Area average oil fraction as a function of axial positions for 1M KI displacing oil from Berea core.	196

LIST OF TABLES

Chapter I

- I:1. Dependence of $\log K_{sp}$, onset of precipitation, CMC, K_s and K_d on alkylbenzenesulfonate chain length. 10a
- I:2. Temperature dependence of solubility product, CMC, and solubilization constant of $\text{Ca}(\text{DDBS})_2$ and $\text{Ca}(\text{DDS})_2$ 23
- I:3. Comparison of CMC values determined by surface tension and dye solubilization techniques. 50

Chapter II

- II:1. Elemental analysis of n-NaDDBS. 90
- II:2. Experimental conditions for adsorption tests. 95
- II:3a. Plateau adsorption of alkylbenzenesulfonate on alumina 115
- II:3b. Break points in sulfonate adsorption and dodecane abstraction isotherms 115
- II:4. A comparison of plateau adsorption of surfactants on alumina. 143

Chapter III

- III:1. Properties of polymers used in the present investigation. 150
- III:2. Adsorption of PAM under natural pH conditions. 157

Chapter IV

- IV:1. Displacing fluid/displaced fluid combinations that can be observed in Berea Sandstone. 186

SYMBOLS AND ABBREVIATIONS

c_s	=	concentration in the interfacial region
c_b	=	concentration in the bulk solution
c	=	concentration
c_{Ca-i}	=	initial concentration of calcium
c_{Ca-r}	=	residual concentration of calcium
c_{CaR_2-rd}	=	amount in moles of CaR_2 redissolved
c_{CMC}	=	initial sulfonate concentration corresponding to CMC
c_{CR}	=	sulfonate concentration corresponding to complete redissolution
c_{R-CaR_2}	=	amount in moles of sulfonate precipitated
c_{R-i}	=	initial sulfonate concentration
c_{R-M}	=	concentration of sulfonate in micelle form
c_{R-r}	=	residual sulfonate concentration
CMC	=	residual concentration corresponding to onset of micellization

DDA-HCl	=	dodecylaminehydrochloride
DBS	=	decylbenzenesulfonate
DDBS	=	dodecylbenzenesulfonate
DDS	=	dodecylsulfonate
e	=	fundamental unit of charge
k	=	Boltzmann constant
K_d	=	dimerization constant
K_s	=	solubilization constant
K_{sp}	=	solubility product
n	=	number of $-CH_2-$ groups in the hydrocarbon chain
NaDBS	=	sodium decylbenzenesulfonate
NaDDBS	=	sodium dodecylbenzenesulfonate
NaDDS	=	sodium dodecylsulfonate
P	=	polymer
PAM	=	polyacrylamide
PAMD	=	aminated polyacrylamide

PAMS	=	sulfonated polyacrylamide
R	=	gas constant
R^-	=	surfactant monomer
R_2^{2-}	=	surfactant dimer
T	=	absolute temperature
Z	=	valency of ion
ΔG_{ad}°	=	free energy of adsorption
ΔG_M°	=	free energy of micellization
$\Delta G_{pptn.}^\circ$	=	free energy of precipitation
ΔH	=	heat of reaction
ΔH_{ad}	=	heat of adsorption
ΔH_M	=	heat of micellization
ΔH_s	=	heat of solubilization
ΔH_{sp}	=	heat of dissolution

SUMMARY

Precipitation/Redissolution/ Reprecipitation Phenomena

Our past studies on the interactions of sulfonates with dissolved inorganics showed that sulfonates precipitated by multivalent ions can undergo redissolution upon increasing either the sulfonate or NaCl concentration. At higher sulfonate and NaCl levels the surfactant reprecipitated. These studies also showed redissolution to occur only in the presence of micelles. The role of mechanisms involving such factors as complexation seems to be minimal under the conditions studied.

Since the phenomenon of redissolution can be beneficially used for minimizing the surfactant loss due to precipitation, investigation of this phenomenon was continued during the current year. The objectives of this study were to develop a quantitative understanding of the molecular mechanisms involved and to formulate a model with predictive capabilities for the precipitation behavior of surfactant/inorganic ions systems. Towards this purpose, precipitation/redissolution/reprecipitation behavior of sulfonates was studied as a function of relevant variables including surfactant and salt

concentration, surfactant chain length, alcohol and oil concentration and temperature.

Study of the precipitation/redissolution behavior of $\text{CaCl}_2/\text{Na-alkylsulfonate}$ as a function of chain length showed that the C_{18} sulfonate which did not form micelles could not solubilize its calcium sulfonate precipitate. This observation supports our earlier contention that the redissolution is caused by micelles. Most interestingly, the solubilization patterns of $\text{Ca}(\text{C}_{16}\text{SO}_3)_2$ and $\text{Ca}(\text{C}_{10}\text{SO}_3)_2$ in C_{10} sulfonate micelle were identical indicating that the solubilization power of the micelle is independent of the chain length of the precipitate. This led to the conclusion that the surface of the micelle rather than the interior plays a major role in this solubilization process. Results obtained for the effect of chain length were used to determine the free energy contribution per $-\text{CH}_2-$ group towards micellization (0.4 kcal/mol) and precipitation (2.1 kcal/mol).

The effect of alcohols and oils, both of which are relevant to micellar flooding, on precipitation/redissolution was tested under selected conditions. Alcohol was found to decrease the precipitation and even eliminate it at higher levels. The solubilization power of the micelle itself was, however, found to decrease in the presence of alcohol or oil. Possible reasons for these effects are discussed.

Examination of the results obtained for $\text{CaCl}_2/\text{NaDDS}$ and $\text{CaCl}_2/\text{NaDDBS}$ systems showed that the precipitation regions can be characterized by the solubility product and the redissolution region by a term that we have called solubilization constant. A model has been developed to predict the precipitation behavior and the composition of the system. The model was tested using experimental data and was found to predict the system behavior accurately.

The molecular mechanism for the redissolution phenomenon, proposed on the basis of all the results that we have obtained for the $\text{CaCl}_2/\text{sulfonate}$ systems, involves the uptake of Ca^{2+} by the micelle followed by the redissolution of the precipitate to replenish the system with Ca^{2+} ions and the formation of additional micelles by the released sulfonate.

Marked differences in the solubilization powers of sodium dodecylbenzenesulfonate and sodium dodecylsulfonate for their calcium salts were correlated with the charge characteristics and counter ion bindings of their micelles and the resultant capability to adsorb calcium ions.

A thermodynamic model involving the adsorption of Ca^{2+} on micelles was formulated to test the proposed series of molecular processes leading to the redissolution.

The results obtained for the dependence of precipitation/redissolution on temperature were used to test the above model and the temperature dependence predicted by the model was found to be in agreement with the experimental results.

A complete understanding of the precipitation/redissolution/reprecipitation will result from an investigation of sulfonate precipitation with other multivalent and mixed salt systems.

Adsorption of Surfactants on Reservoir Minerals

Adsorption of surfactant on reservoir rock minerals has been shown from our past studies to be a complex process, dependent upon a number of system parameters such as the nature and concentration of surfactants and inorganic electrolytes, pH, temperature and solid to liquid ratio. Also, in certain cases, the isotherms exhibited a maximum followed by a minimum in the region of critical micelle concentration (CMC). These studies clearly showed the need for conducting tests with well characterized minerals and surfactants in order to elucidate the mechanisms involved. During the current year, most of our adsorption studies were therefore conducted using isomerically pure n-alkylbenzenesulfonates synthesized in our laboratory and characterized using p-NMR, C-13 NMR and mass spectrometric techniques.

Investigations of the effect of oils (e.g., n-dodecane) on the adsorption of sulfonates on a well characterized mineral, alumina, were given major emphasis during the current year. Most importantly, in all such tests, the uptake of oils by the mineral also was measured simultaneously.

Adsorption of n-dodecylbenzenesulfonate and n-decylbenzenesulfonate on alumina at 75°C increased with increase in sulfonate concentration and reached a plateau above a certain concentration. The onset of plateau as determined by the dye solubilization techniques corresponded to CMC. Addition of NaCl to sulfonate/alumina system increased the surfactant adsorption and shifted the onset of plateau to lower sulfonate concentrations. Addition of oil, n-dodecane, did not affect the surfactant adsorption significantly under any of the above conditions.

The uptake of oil by alumina in the presence of sulfonate was markedly affected by the changes in the surfactant concentration. At low sulfonate concentrations the abstraction of oil (initial oil - 0.5% vol) was equivalent to about 3 to 4 monolayers. The oil uptake decreased with increase in sulfonate and in some cases exhibited a minimum. The high abstraction of n-dodecane at low sulfonate levels is attributed to coating of oil on alumina surface that is partially hydrophobic

because of surfactant adsorption. The decrease in oil uptake above a certain sulfonate level is due to the solubilization of oil by the micelles as well as decreased coating owing to the partially restored hydrophilicity of the solid with surfactant adsorbed with a reverse orientation under these conditions.

At a given sulfonate level, abstraction of n-dodecane was found to increase with increase in oil concentration. The oil coated particles were found to agglomerate in the system. Such agglomeration can affect the permeability of the reservoir and its implications in micellar flooding are discussed.

The results for the adsorption of n-DDBS and n-DBS on alumina were analyzed using a modified Stern-Grahame model. By comparing the bulk concentrations required for a given adsorption density, the free energy contribution per $-\text{CH}_2-$ group towards adsorption has been calculated to be 1:1 kT.

A study on the effect of temperature on sulfonate adsorption, in the presence and absence of oil was initiated during the current year. Both in the presence and absence of oil, increase in temperature caused a decrease in adsorption.

A study of the effect of alcohol was also initiated during the current year. For a few conditions studied, alcohol was found to decrease the surfactant adsorption markedly.

In addition to the above studies using isomerically pure n-alkylbenzenesulfonates, adsorption of a commercial surfactant, Alipal CO-436 on alumina and homoionic sodium kaolinite was also begun recently. This ethoxylated sulfate is considered to be a potential surfactant for micellar flooding, since it has a higher salt tolerance than alkylbenzenesulfonates. Preliminary results obtained with this surfactant are included.

Polymer/Surfactant Interactions

Surfactants come in contact with the polymers during flooding and hence interactions between them can have an influence on the efficiency of the micellar flooding process. Polymers and surfactants can react to form complexes and precipitates. In addition, adsorption properties of surfactants and polymers at various interfaces can be affected markedly by the presence of one another and this can in turn affect the wettability of the reservoir rocks and therefore the oil displacement efficiency. For these reasons, during the current year, an investigation of the wettability of reservoir rock

minerals such as quartz in the presence of acrylamide based cationic, anionic and nonionic polymers and surfactants was initiated. Adsorption and precipitation of surfactants and polymers have also been determined simultaneously under selected conditions. In order to develop a full understanding of the manner in which the polymeric and surfactant species interact, C-13 NMR, p-NMR, viscosity, surface tension and conductivity properties of solutions containing these reagents have been successfully initiated.

Wettability of quartz as measured by the Hallimond tube flotation technique was altered markedly by the nature of charge on the surfactant as well as polymer. A non-ionic polymer, polyacrylamide (PAM) which did not adsorb on quartz was found not to influence the wettability of quartz. A cationic polymer, aminated polyacrylamide (PAMD), on the other hand, was found to increase the water wettability of quartz in dodecylaminehydrochloride (DDA·HCl) solutions. This is attributed to the peculiar configuration of the adsorbed polymer which helps to mask the adsorbed surfactant. The polymer is believed to adsorb at the solid/liquid interface with its segments and loops extended into the solution.

Addition of an anionic polymer, sulfonated polyacrylamide (PAMS) was found to decrease the water wettability

of quartz at all levels of DDA·HCl. The effect of PAMS at low concentrations of amine is attributed to its influence on the solvent power of water and the consequent increase in the effective concentration of amine in the system (salting out). At high amine concentrations where the surfactant can adsorb with a reverse orientation at the solid/liquid interface, PAMS is suggested to bridge the particle with bubble and thus enhance flotation.

Quartz which remained water wettable in sodium dodecylsulfonate (NaDDS) solutions became hydrophobic upon the addition of the cationic polymer, PAMD. The polymer can be considered in this case to adsorb at the solid/liquid interface and provide adsorption sites for the anionic surfactant and thus make the particles hydrophobic.

In addition to changing the wettability of the solid, PAMD and sulfonate interacted in the bulk to form a precipitate under certain conditions. It was found that at a fixed PAMD level, an increase in NaDDBS concentration resulted in precipitation with further addition of the sulfonate causing redissolution of the precipitate. This behavior is similar to that of the sulfonates in the presence of multivalent ions such as Ca^{2+} . Unlike in the case of calcium sulfonate, however, redissolution in polymer-surfactant system appears to occur before

micellization. This is attributed to the interaction of the precipitate with the excess sulfonate to form charged complexes.

I. PRECIPITATION/REDISSOLUTION/ REPRECIPITATION PHENOMENA

A. Introduction

Interaction of sulfonates with various mono and multivalent ions is of major importance in tertiary oil recovery by micellar flooding. We have reported earlier that interaction of such species can affect the loss of surfactant due to precipitation (1-4). It was also reported that the precipitate can be redissolved by excess surfactant or NaCl. During the current year, major emphasis was placed on developing a quantitative understanding of the precipitation/redissolution process, the knowledge of which can possibly be used to reduce the surfactant loss.

The precipitation/redissolution/reprecipitation behavior of sulfonates with mono and multivalent ions was continued this year with the aim of quantifying the interactions involved. Detailed investigation of this phenomenon as a function of type and chain length of sulfonate, ionic strength, and temperature showed micelles to be responsible for the redissolution of multivalent ion/surfactant precipitates.

A model with capabilities to predict the nature and concentrations of various species under different solution conditions, given the thermodynamic constants and the initial levels of surfactants and inorganic ions, has been developed. The model was tested using different sets of experimental data and was found to predict the system behavior satisfactorily.

We have now extended the precipitation/redissolution study to systems containing alcohols and oils.

Based upon the information that we have obtained from the precipitation/redissolution studies and the data for the conductivity and counterion binding to micelles, a molecular mechanism to explain the redissolution of the precipitate has also been proposed.

The data for the dependence of precipitation/redissolution on temperature was used to obtain various thermodynamic parameters such as heats of dissolution, micellization, solubilization and calcium adsorption on micelles. Also, the validity of the proposed molecular mechanism for the redissolution process was tested by developing a suitable model and testing with the results obtained for the temperature dependence of redissolution.

The investigation of the precipitation/redissolution process is now being extended to multi component systems containing sulfonates and inorganic ions such as Al^{3+} .

B. Materials and Methods

B1. SURFACTANTS AND OTHER REAGENTS

Sodium dodecylbenzenesulfonate (NaDDBS) specified to be 90% pure by Lachat Chemicals was purified by deoiling, recrystallization and desalting techniques (3).

Sodium dodecylsulfonate (NaDDS), (>99% purity according to the manufacturer's chromatographic analysis) was purchased from Aldrich chemicals and used without further purification. Conductivity versus concentration data obtained for NaDDS showed the CMC to be 9.8×10^{-3} kmol/m³. This is in agreement with the reported CMC values (5).

C₁₀, C₁₂, C₁₆, and C₁₈ alkyl sulfonates used in the current study were purchased from Aldrich Chemicals and C₁₄ sulfonate was purchased from Pfaltz and Bauer. All these sulfonates were specified to be >98% pure.

Radioactive Ca⁴⁵ used in the preparation of labelled calcium sulfonates was purchased from ICN Inc.

NaCl, NaOH and HCl used were also of A.R. grade. When higher purity reagents were required, ultrapure NaCl purchased from J.T. Baker Chemical Co. and CaCl₂ purchased from Aldrich Chemicals Co. were used. Triply distilled water was used in all experiments.

B2. METHODS

B2a. Turbidity Measurements

A Brinkman PC-600 probe colorimeter was used to measure the turbidity of the solutions. Equal amounts of surfactant and inorganic electrolyte solutions were mixed in a test tube, shaken for 10 seconds and then kept at the desired temperature in a thermostat. The electrolyte solutions were always introduced before the surfactant solutions. The dependence of the turbidity on the surfactant and electrolyte concentrations was determined from the values for light transmission ($\lambda=670$ nm) 24 hours after the mixing.

B2b. Precipitation Tests

Solutions containing the surfactant and the inorganic electrolytes in glass vials were mixed by shaking them vigorously for about 10 seconds and were left undisturbed at the desired temperature for 24 hours. The vials were then centrifuged at 17,000 RPM for sixty minutes or until all the precipitate settled. The supernatant was analyzed for sulfonate. The amount precipitated was determined by calculating the difference between the initial and final sulfonate concentrations.

The analysis of the sulfonate was done by a two-phase titration technique using a mixture of dimidium bromide and disulphine blue as indicators.

The residual calcium concentration was determined by standard EDTA titration using Mg-EDTA and Erichrome Black-T the latter being the indicator.

B2c. Conductivity Measurements

Specific conductivity measurements for the determination of CMC of sulfonate solutions were performed with a linear conductance/resistance meter (A.H. Thomas Co., Model 275 at 1000 Hz).

B2d. Dye Solubilization

Dye solubilization technique (7,8) used here is based on the spectral changes on either side of the CMC. Below the CMC, the dye (pinacyanol chloride) exhibits a pink color due to the formation of a highly insoluble salt of the surfactant anion with the dye cation (6). Above the CMC the solution turns blue apparently due to the solubilization of the dye by the micelles. The tests were conducted by mixing the surfactant solution with a 10^{-5} kmol/m³ dye solution. The solutions were then equilibrated in the dark for two hours and measurements were made using a Hitachi model spectrophotometer.

B2e. Surface Tension Measurements

Wilhelmy plate technique was used to measure the surface tension of solutions. A sandblasted platinum sensor plate of known width was immersed in the solution

and the pull exerted by the solution on the sensor was directly measured using a Cahn-2000 microbalance.

Reproducibility of the results checked using duplicate samples was found to be ± 0.2 mN/m.

B2f. Free Na Ion Measurements

Orion model 96-11 sodium ion combination electrode was used along with an Orion Model 701A digital pH/mV meter to measure the concentration of free Na^+ ions in solution. The sodium electrode consisted of a sodium containing glass membrane. When the membrane is in contact with a sodium containing solution, a difference in electrode potential is developed. The pH of the solutions was always kept above six as recommended by the manufacturer. Since the introduction of electrolytes can disturb the micellar equilibrium no ionic strength adjustment was made in this case. The required activity corrections were made only below CMC but no such attempt was made above it because the activity of Na^+ ions on the micelle was not available. Depending on the temperature, the slope of the electrode response varied in the range of 55 to 59 mV which is close to the Nernstian Slope. Measurements at high temperatures (25 to 70°C) required longer equilibrium time as compared to about 5 minutes for room temperature measurements. Reproducibility of measurements was better than

±3%. After prolonged use, a hydrated layer formed on the surface of the sodium-sensitive glass which made the response slower. This was rectified by removing the layer by a short exposure of the electrode to a dilute ammonium bifluoride solution (9).

B2g. Free Ca Ion Measurement

The calcium electrode purchased from Orion (Model 93-20) was tried initially for the activity measurements with no success. Since the membrane is a liquid organic ion exchanger, the presence of micelles in surfactant solutions renders the electrode ineffective. A solid substrate membrane made of PVC produced by Ionetics Inc. was finally found to permit measurements of calcium activity in micellar solutions. Reproducibility of the data varied, however, in the range of ±10% to ±20% the latter being for lower calcium activities.

C. Effect of Chain Length

Our previous studies of precipitation/redissolution of NaDDBS/CaCl₂ and NaDDS/CaCl₂ systems in the presence and absence of NaCl, discussed in detail in the 1980 Annual Report indicated the important role of micelles in the solubilization of multivalent ion/sulfonate precipitates.

Pronounced differences in the solubilization capacity of two different sulfonates having varying structure were also noted. To further test the generality of our findings, we have used commercially available laboratory grade C_{10} , C_{12} , C_{14} , C_{16} and C_{18} alkylsulfonates. Precipitation/redissolution pattern of these sulfonates was determined by analyzing the residual sulfonate using the two-phase titration technique and the residual calcium by using Ca^{45} labelled $CaCl_2$ solutions. Experiments were conducted at $65^\circ C$ which is above the Krafft temperature of all the sulfonates in the absence of salt.

The effect of chain length on precipitation/redissolution of sulfonates in $3 \times 10^{-3} \text{ kmol/m}^3$ $CaCl_2$ solutions is illustrated in Figure I:1. It is seen that the $Ca-C_{10}$ sulfonate has the highest solubility and the $Ca-C_{18}$ sulfonate, the lowest. This is in accord with the increase in hydrophobicity of the sulfonate with the increase in the chain length.

The precipitation behavior of calcium salts of C_{14} , C_{16} and C_{18} sulfonates, was, however, almost identical. In the redissolution region, on the other hand, the behavior of these three sulfonates differed markedly. While the C_{14} sulfonate exhibited complete redissolution, and the C_{16} partial redissolution, the C_{18}

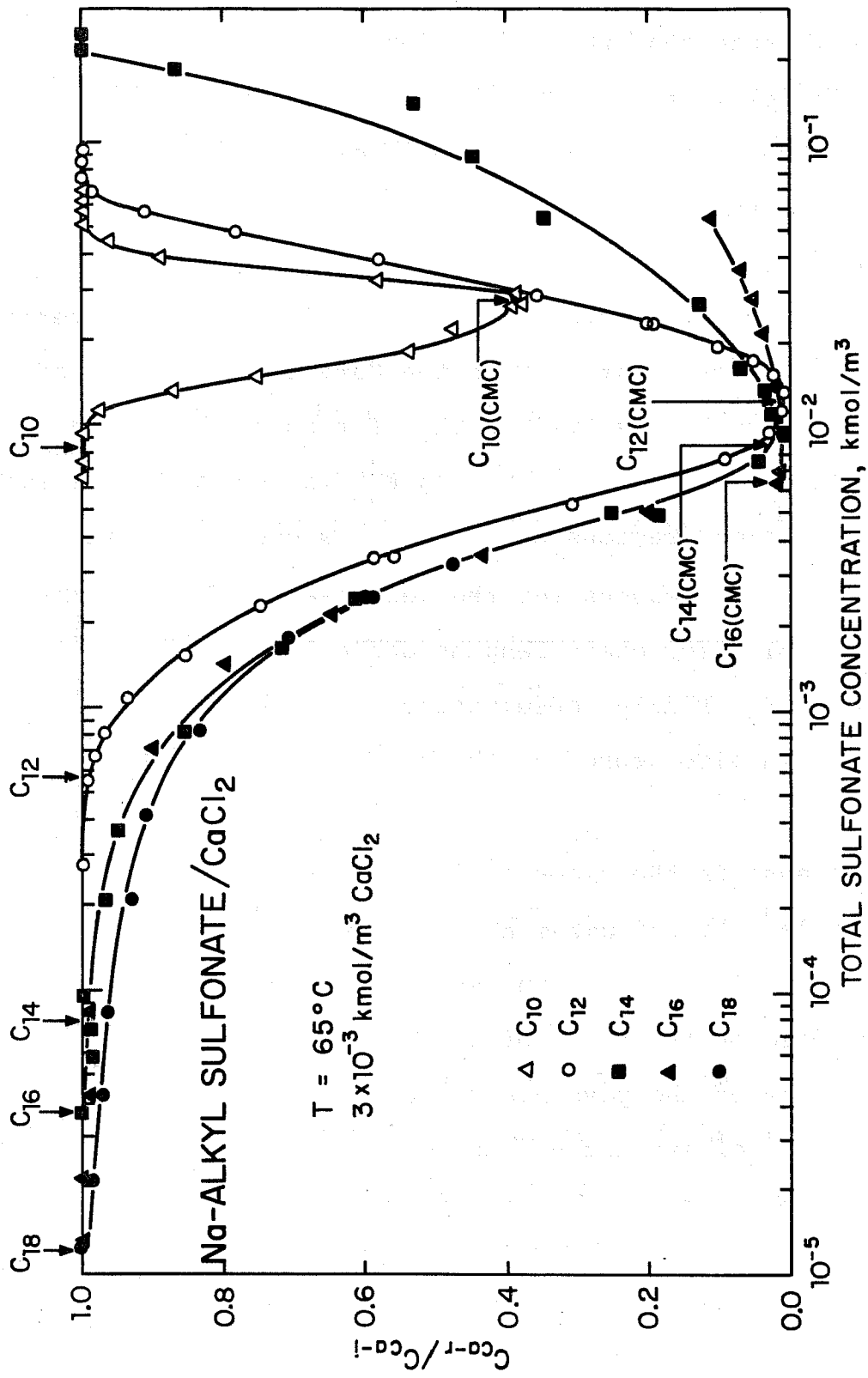


Figure I:1. Ratio of residual (C_{Ca-r}) to initial (C_{Ca-i}) concentration of labelled calcium as a function of the initial sulfonate concentration for different chain length sulfonates.

sulfonate did not undergo any redissolution. It is interesting to note that the C_{18} sulfonate also did not undergo any micellization. This finding confirms our earlier observations that the redissolution of multivalent ion/sulfonate precipitate occurs only in the presence of micelles.

The solubility products of calcium sulfonates of different chain length were calculated using the data for the onset of precipitation from Figure I:1 and that for onset of turbidity (See also Table I:1). The plot of $\log K_{sp}$ vs. chain length in Figure I:2 shows two linear regions differing in slope by almost a factor of 2. The reasons for the decrease in slope of the $\log K_{sp}$ vs. n plot for chain lengths above 16 are not clear at present. Similar observations have been reported also in literature for the solubility of fatty acids (10).

The decrease in the slope of $\log K_{sp}$ vs. n for higher chain lengths indicates that the system has a higher tolerance for calcium and sulfonate, compared to what is expected on the basis of the behavior of shorter sulfonates. One of the possible reasons for this is the self association of surfactants to form complexes such as dimers and other multimers and the resultant decrease in the activity of the monomer in the solution.

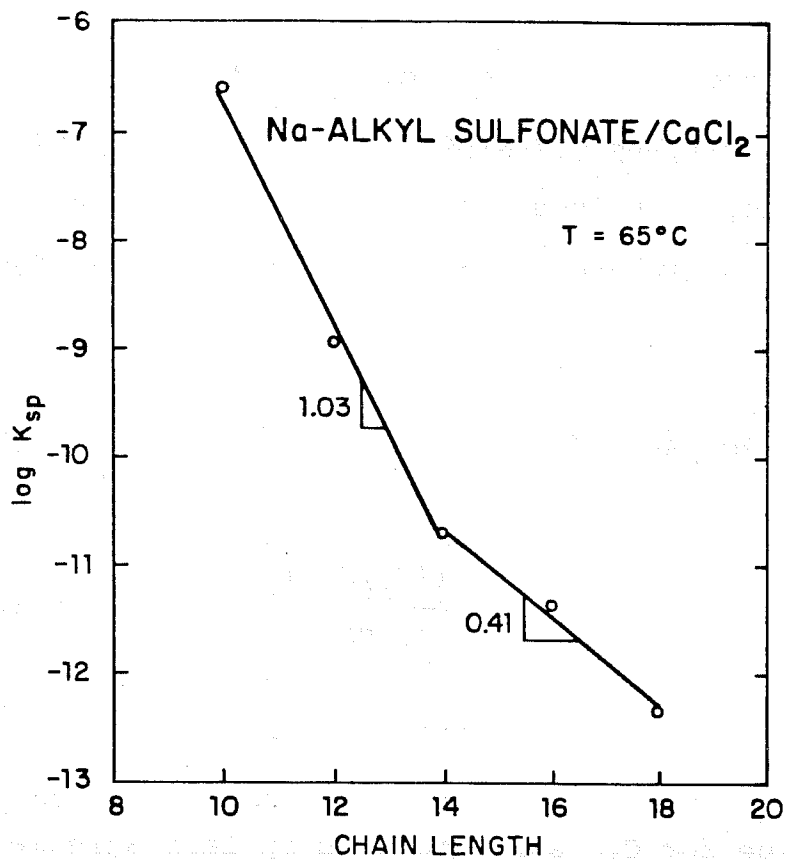


Figure I:2. Variation of solubility product as a function of the chain length of alkyl sulfonates.

Table 1:1

Dependence of $\log K_{sp}$, onset of precipitation, CMC, K_s and K_d on alkylsulfonate chain length

Chain Length (n)	$\log K_{sp}^{**}$	Sulfonate at onset of precipitation*** ($K_{sp}/3 \times 10^{-3}$) ^{1/2}	CMC, 3 kmol/m ³	CaR ₂ Redissolved kmol/m ³	$K_s = CaR_2 / C_{cr}^{-C_{cmc}}$	K_d
10	-6.62	8.94×10^{-3}	2.3×10^{-2}	1.86×10^{-3}	0.085	
12	-8.96	6.03×10^{-4}	6.6×10^{-3}	2.97×10^{-3}	0.044	
14	-10.72	8.00×10^{-5}	2.0×10^{-3}	3.00×10^{-3}	0.016	
16	-11.36(m) -12.87(e)	3.81×10^{-5} 6.71×10^{-6}	6.9×10^{-4}	3.00×10^{-3}	0.006(e)	3.5×10^5
18	-12.36(m) -14.92(e)	1.20×10^{-5} 6.33×10^{-7}				1.4×10^7

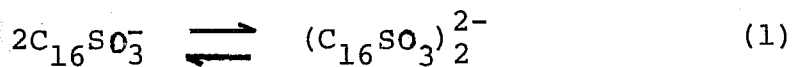
* (m) - measured

* (e) - extrapolated

** Calculated using the onset of turbidity

*** Indicated by arrow in Figure

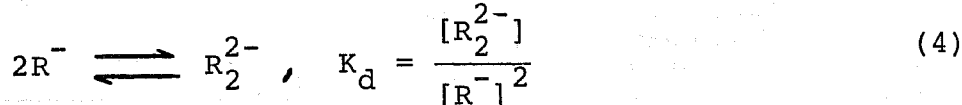
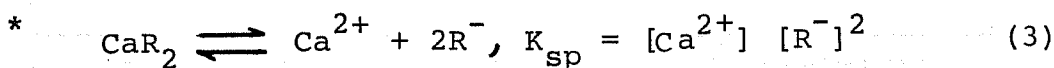
Assuming that the variation of $\log K_{sp}$ with n is linear and that the observed deviations in K_{sp} at higher chain length values are due to dimerization alone, we have evaluated the dimerization constant for the reaction.*



$$K_d = \frac{[(C_{16}SO_3)_2^{2-}]}{[C_{16}SO_3^-]^2} \quad (2)$$

$$= 3.5 \times 10^5$$

This value for C_{16} surfactant is in fair agreement with the K_d values reported for fatty acids and amines (12, 13) and higher by two orders of magnitude than the constant obtained for oleic acid (18).



$$\text{Total Sulfonate} = [R^-] + 2K_d[R^-]^2 \quad (5)$$

For C_{16} sulfonate, K_{sp} (extrapolated) = $10^{-12.87}$, $Ca^{2+} = 3 \times 10^{-3}$ kmol/m³, $(R^-) = 6.7 \times 10^{-6}$, total sulfonate = 3.8×10^{-5}
 Therefore, $K_d = 3.5 \times 10^5$

The deviations in K_{sp} at higher chain lengths can result also from the partial coiling of surfactant chains. On the other hand, the inaccuracies in the determination of the exact onset of precipitation at such low levels of sulfonate can also contribute to deviations in K_{sp} .

The observed linear dependence of $\log K_{sp}$ on chain length can be utilized to obtain the free energy contribution from the $-CH_2-$ groups towards precipitation in the following manner:

$$\log K_{sp} = - \frac{\Delta G_{ppt}^{\circ}}{2.3 RT} = \frac{-n\phi}{2.3 RT} + \frac{\Delta G_c^{\circ}}{2.3 RT} \quad (6)$$

where ΔG_{ppt}° is the free energy change accompanying the precipitation, ϕ is the free energy contribution per $-CH_2-$ group towards precipitation and ΔG_c° is the free energy of precipitation from all other factors such as chemical and electrostatic interactions. Using the slope of $\log K_{sp}$ vs. chain length the free energy contribution for chain lengths up to 14 is found to be 1.6 kcal/mol of $-CH_2-$ group.

In the redissolution region, as mentioned earlier, sulfonates of varying chain length exhibited marked differences. A comparison of the abilities of the micelles of these sulfonates to solubilize a given calcium disulfonate precipitate was made by examining the

solubilization constant defined as:

$$K_s = \frac{[\text{CaR}_2 \text{ Precipitate Redissolved}]}{C_{cr} - \text{CMC}} \quad (7)$$

where C_{cr} is the sulfonate concentration corresponding to complete redissolution. A plot of $\log K_s$ vs. chain length given in Figure I:3 shows that the solubilization constant decreases linearly with increase in chain length. It can be represented by the equation:

$$\log K_s = -0.195n + 0.919 \quad (8)$$

This equation which is valid for alkylsulfonates was used to determine the effective number of $-\text{CH}_2-$ groups in alkylbenzenesulfonate. Since the K_s for dodecylbenzenesulfonate/ CaCl_2 is known from our earlier work, the effective 'n' was calculated from the above equation to be 7.4. The superior solubilization power of NaDDBS compared to NaDDS, thus suggests effective number of $-\text{CH}_2-$ groups in the benzene ring to be -4.6. It is interesting to note that this value is close to the one suggested for benzene ring from the data for adsorption of alkylbenzenesulfonates at the solid/liquid interface (14); the implications of the apparent lowering in chain length by 4.6, as opposed to an increase normally suggested needs further analysis.

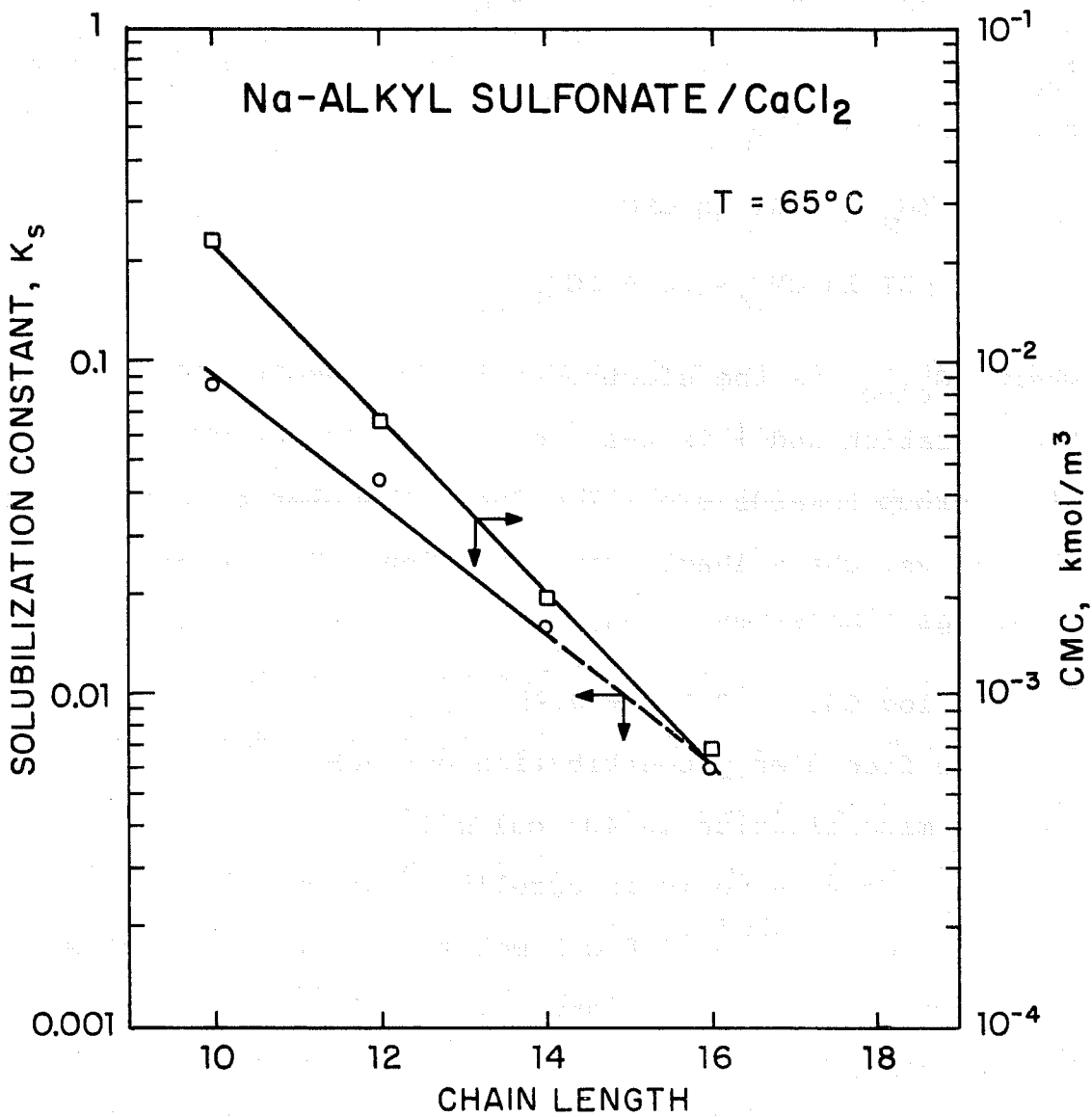


Figure I:3. CMC and solubilization constant of alkylsulfonates as a function of chain length.

The residual concentration of the surfactant at the onset of redissolution, as discussed earlier, corresponded to the CMC of the system. The data for CMC as a function of chain length can conveniently be used to determine the contribution of $-\text{CH}_2-$ groups to micellization. Since the free energy of micellization can be written as:

$$\Delta G_M^\circ = -RT \ln \text{CMC}, \quad (9)$$

$$-RT \ln \text{CMC} = n\phi + \Delta G_{\text{elec}}^\circ. \quad (10)$$

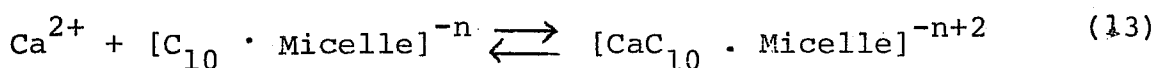
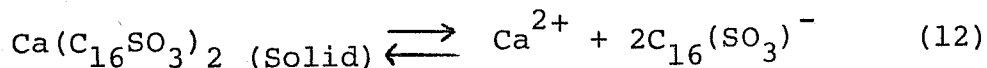
where $\Delta G_{\text{elec}}^\circ$ is the electrostatic free energy of micellization and ϕ is the free energy contribution per $-\text{CH}_2-$ group towards micellization. The plot of $\log \text{CMC}$ vs. chain length given in Figure I:3 can be represented by the equation

$$\log \text{CMC} = -0.26n + 0.95 \quad (11)$$

The free energy contribution per $-\text{CH}_2-$ group towards micellization is 403 cal/mol at 65°C. This value is in excellent agreement with the reported value of 418 cal/mol for the alkylsulfates (15). Other ionic surfactants also yield similar values (16).

It was pointed out earlier that the redissolution of the calcium sulfonate precipitates occurred only in

the presence of micelles. The role of micelles in solubilizing the precipitates was further tested by dissolving labelled solid $\text{Ca}(\text{C}_{16}\text{SO}_3)_2$ in $\text{NaC}_{10}\text{SO}_3$ and $\text{NaC}_{18}\text{SO}_3$ sulfonates. The data shown in Figure I:4 clearly demonstrate the superior solubilization power of C_{10} sulfonate. This again confirms our earlier contention that the lower chain length sulfonate is a more powerful solubilizer for calcium sulfonate precipitates. Most importantly, the identical redissolution behavior of calcium precipitates of C_{10} and C_{16} sulfonates in C_{10} micelles (see Figures I:1 and I:4) indicates that the solubilization power of C_{10} micelle (for Ca-sulfonate precipitates) is independent of the chain length of the calcium sulfonate precipitate. This finding clearly suggests that it is the exterior of the micelle rather than the interior that is responsible for the redissolution in this case. This process can be written as



The uptake of calcium by the micelle would enhance reaction (12) to proceed to the right, resulting in the redissolution of the precipitate. It should be noted that the activity of the monomeric C_{16}

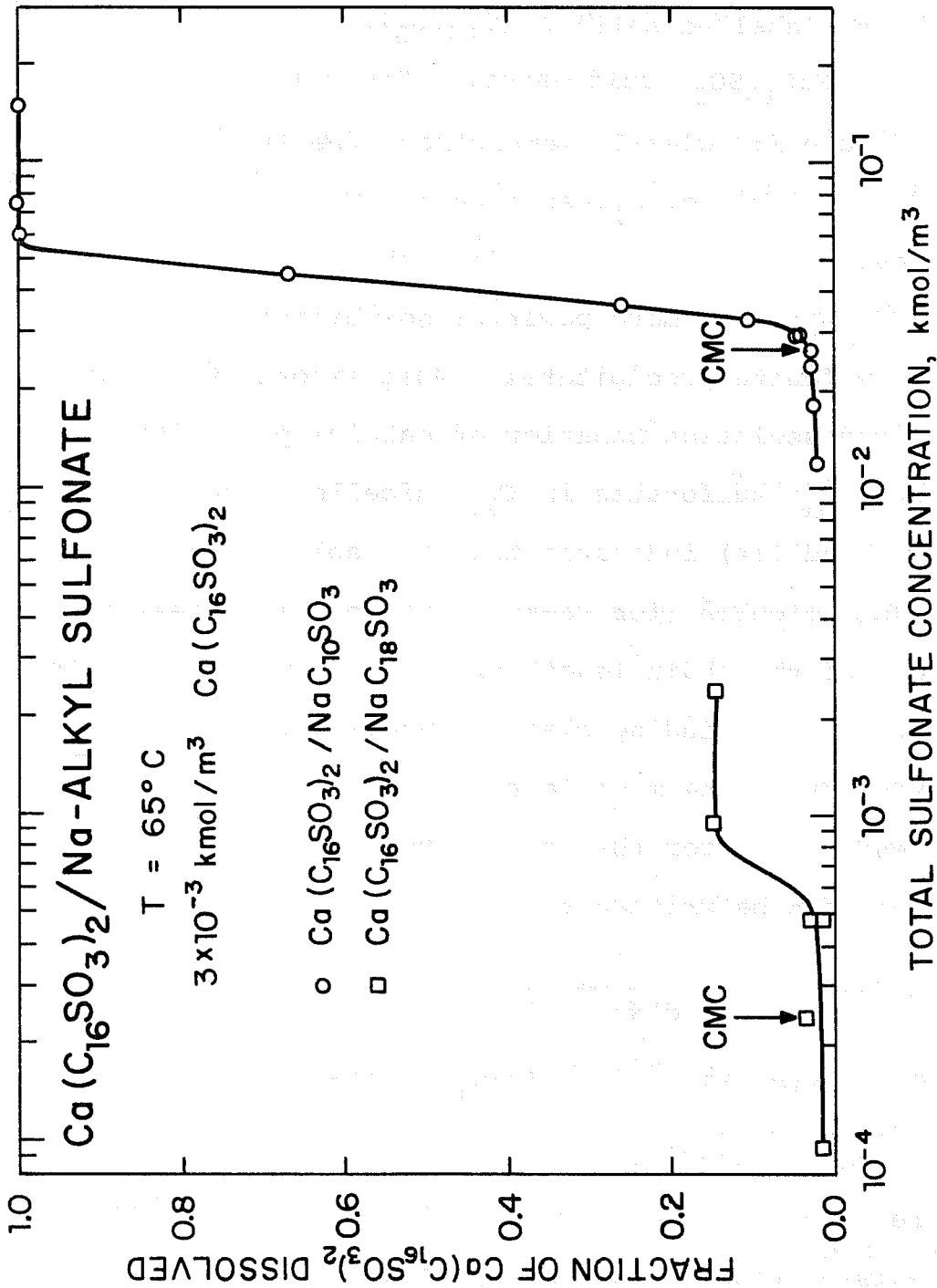


Figure I:4. Solubilization pattern of Ca(C₁₆SO₃)₂ in the aqueous solutions of NaC₁₀SO₃ and NaC₁₈SO₃.

sulfonate is controlled only by the solubility product of C_{16} sulfonate as opposed to the case where the precipitate is redissolved by the micelles of the same surfactant. In the latter case, since the monomer concentration is fixed by the CMC of the surfactant and the calcium in the bulk by $K_{sp}/(CMC)^2$, redissolved sulfonate has to form micelles. Therefore, when C_{16} precipitate is redissolved in C_{10} micelles, an increase in the activity of monomeric C_{16} sulfonate can be expected. Such changes should reflect in properties like surface tension which are being investigated at present.

The above discussion indicates that the precipitate solubilization by micelles is initiated by an uptake of calcium by the micelle. The redissolved surfactant monomers may form either micelles or remain as monomers depending upon the system. A detailed discussion of the molecular aspects of redissolution is given in Section G.

D. Effect of Temperature

An understanding of the effect of temperature on precipitation/redissolution phenomenon is important both from a practical and fundamental point of view. Such information can be useful in predicting the

precipitation behavior of surfactants in reservoirs of different temperature and even different locations in the same reservoir. Also, the dependence of precipitation/redissolution on temperature can yield important thermodynamic information regarding the process. During the current year, we have investigated the temperature dependence of precipitation/redissolution of NaDDBS/CaCl₂ and NaDDS/CaCl₂ systems. The results have been analyzed to obtain the heats of reaction of various sub-processes involved in precipitation/redissolution.

The temperature dependence of precipitation of NaDDBS and NaDDS in the presence of CaCl₂ (3×10^{-3} kmol/m³) is shown in Figures I:5 and I:6 in terms of % light transmitted through the solution. The solubilities of calcium dodecylsulfonate and calcium dodecylbenzenesulfonate are found to increase with increase in temperature. The solubility products of these sulfonates calculated from the data for the onset of precipitation are given in Table 2. The solubility product of Ca(DDS)₂ increased by an order of magnitude for an increase in temperature from 40° to 70°C. On the other hand, the solubility product of Ca(DDBS)₂ increased only by a factor of 4 over a wider temperature range (25° to 70°). In the redissolution region, similarly the Ca(DDS)₂ exhibited a marked dependence on temperature compared to Ca(DDBS)₂. In all these cases, the

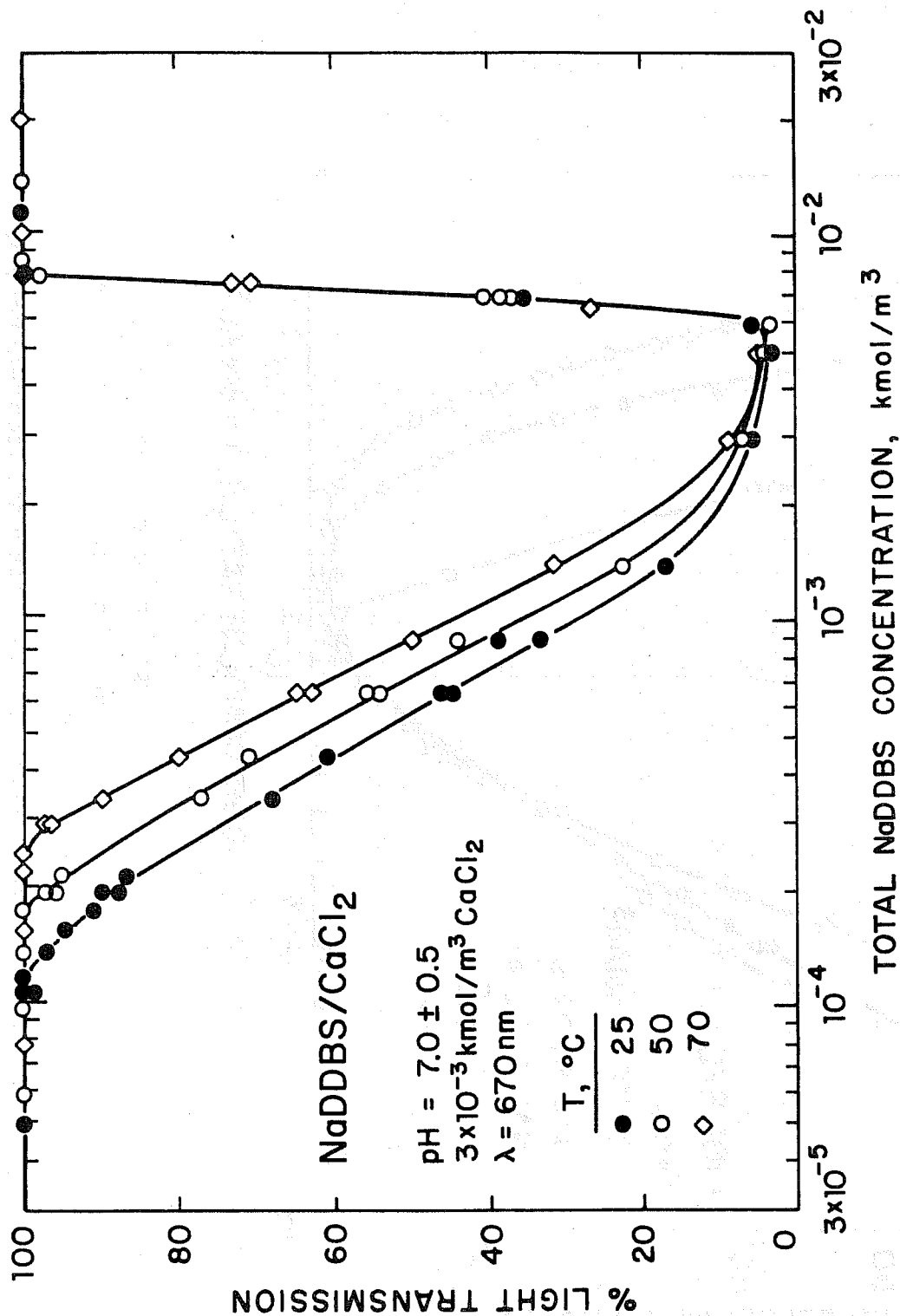


Figure I:5. Effect of temperature on the precipitation/ redissolution behavior of the NaDDBS/CaCl₂ system; light transmission of the solutions as a function of sulfonate concentration.

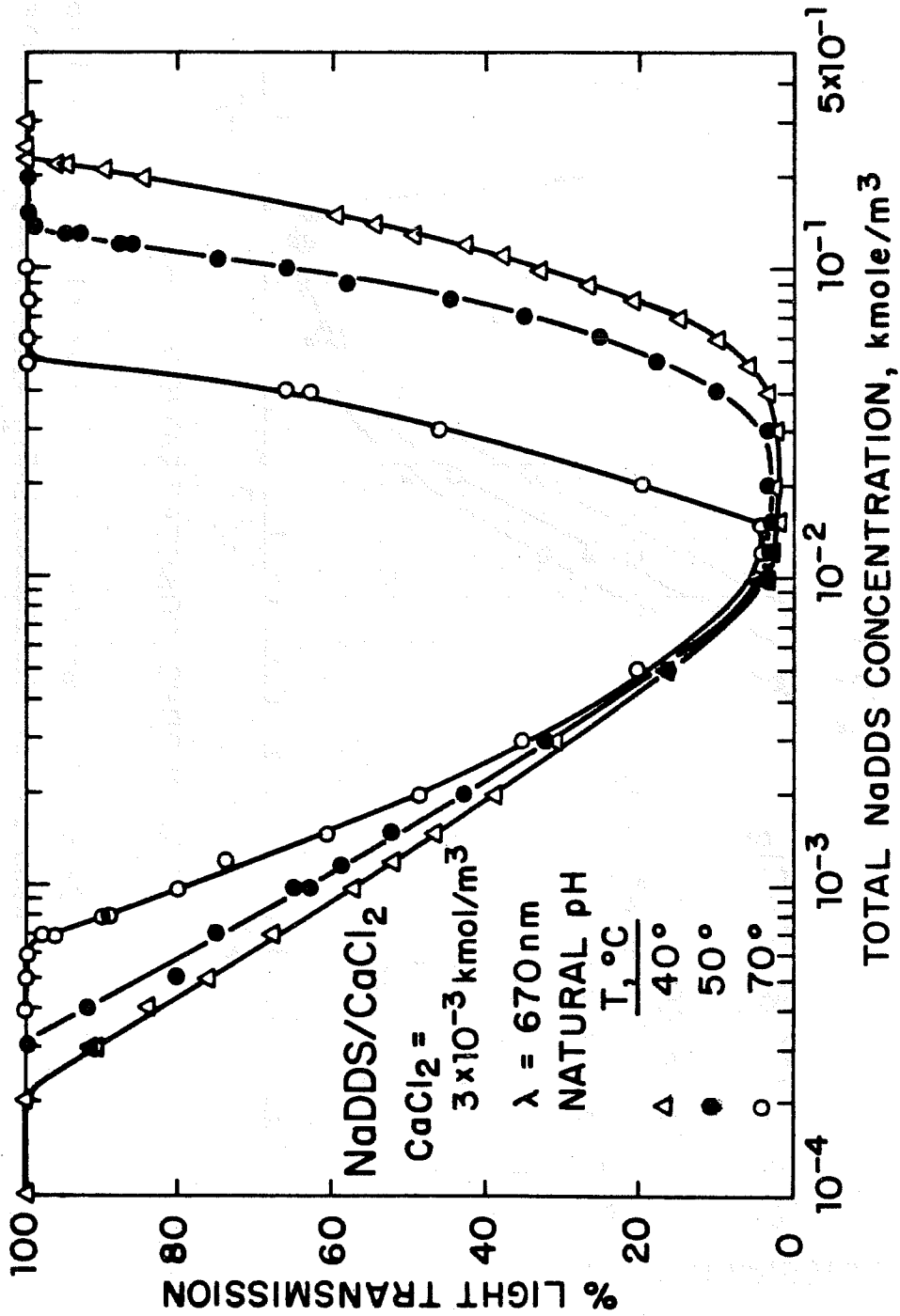


Figure I:6. Effect of temperature on the precipitation/redissolution behavior of the NaDDS/CaCl₂ system; light transmission of the solutions as a function of sulfonate concentration.

TABLE I:2

Temperature Dependence of Solubility Product, CMC and Solubilization Constant of $\text{Ca}(\text{DDBS})_2$ and $\text{Ca}(\text{DDS})_2$

Systems	T, °C	K_{sp}	CMC kmol/m ³	K_s
$\text{Ca}(\text{DDS})_2$	40	1.2×10^{-10}	8.5×10^{-3}	0.014
	50	2.7×10^{-10}	9.5×10^{-3}	0.023
	70	1.4×10^{-9}	1.1×10^{-2}	0.077
$\text{Ca}(\text{DDBS})_2$	25	4.3×10^{-11}	4.5×10^{-4}	0.37
	50	1.03×10^{-10}	5.3×10^{-4}	0.35
	70	1.88×10^{-10}	5.9×10^{-4}	0.33

onset of redissolution coincided with the CMC of the system, thus, once again, confirming the contention that the redissolution of calcium sulfonate precipitate occurs only in the presence of micelles.

The data for the temperature dependence of dissolution can be made use of as shown below, to determine the heat of dissolution.



$$K_{\text{sp}} = [\text{Ca}^{2+}] [\text{R}^-]^2 \quad (15)$$

$$\frac{\partial \ln K_{\text{sp}}}{\partial (1/T)} = \frac{-\Delta H}{R} \quad (16)$$

$$\ln K_{\text{sp}} = \frac{-\Delta H}{RT} + \text{constant} \quad (17)$$

A plot of $\log K_{\text{sp}}$ vs. $1/T$ should yield $-\Delta H/R$ as the slope. The $\log K_{\text{sp}}$ vs. $1/T$ plots are given in Figure I:7 and the values of ΔH_{sp} are

$$\Delta H_{\text{sp-Ca(DDS)}_2} = 18,500 \text{ cal/mol}$$

$$\Delta H_{\text{sp-Ca(DDBS)}_2} = 6,000 \text{ cal/mol}$$

These values for ΔH_{sp} reflect the earlier conclusion that the temperature dependence of dissolution of Ca(DDS)_2 is stronger than that of Ca(DDBS)_2 .

The ΔH_{sp} obtained above corresponds to a process

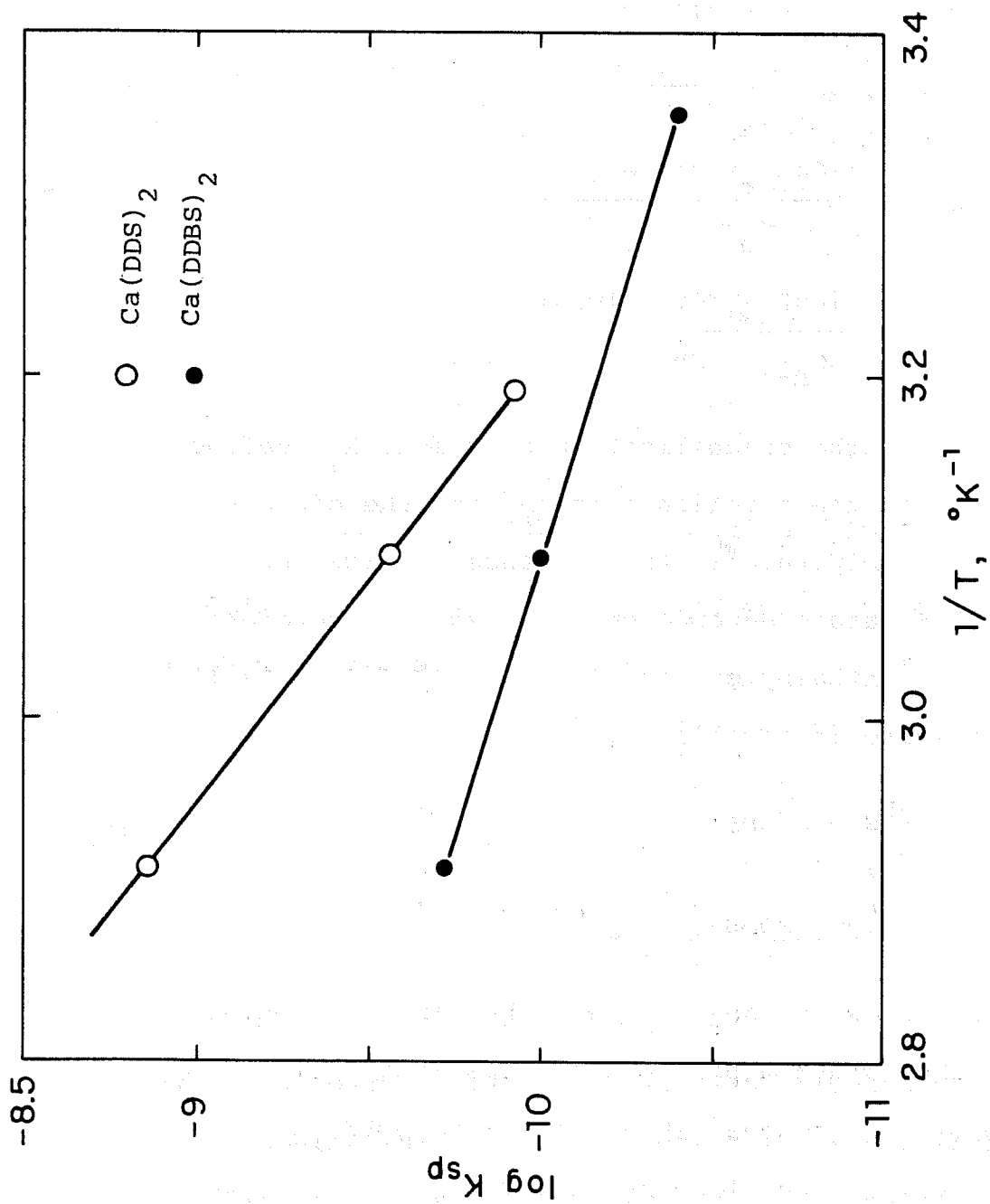
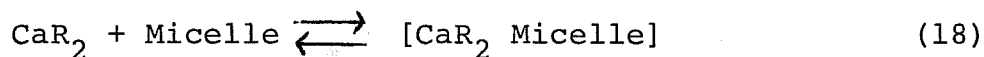


Figure I:7. solubility product of Ca(DDS)₂ and Ca(DBBS)₂ as a function of the reciprocal of the absolute temperature.

in which the calcium sulfonate dissolves in water to give rise to Ca^{2+} and 2R^- ions. Redissolution of the precipitate at higher surfactant concentrations, however, results from the reaction :



$$K_s = \frac{[\text{CaR}_2 \text{ Micelle}]}{[\text{Micelle}]} \quad (19)$$

$$= \frac{[\text{CaR}_2 \text{ Redissolved}]}{C_{\text{R-r}} - \text{CMC}} \quad (20)$$

Thus, the solubilization constant, K_s , defined earlier is the reaction constant for the dissolution of the precipitate in the presence of micelles.

The temperature dependence of K_s should therefore give the enthalpy of dissolution of calcium sulfonate precipitate in micelles.

$$\frac{\partial \ln K_s}{\partial (1/T)} = \frac{-\Delta H}{R} \quad (21)$$

$$\ln K_s = -\frac{\Delta H}{RT} + \text{Constant} \quad (22)$$

The $\ln K_s$ for both NaDDS and NaDDBS was obtained from the precipitation/redissolution curves given in Figures I:5 and I:6 (see Table I:2). The values of ΔH_s obtained from $\ln K_s$ vs. $1/T$ plots are as follows:

$$\Delta H_{s-\text{Ca}(\text{DDS})_2} = 12,375 \text{ cal/mol}$$

$$\Delta H_{s-\text{Ca}(\text{DDBS})_2} = -4 \text{ cal/mol}$$

It is interesting to note that the heat of redissolution of $\text{Ca}(\text{DDBS})_2$ is almost zero in contrast to the large positive value (12,375 cal/mol) for $\text{Ca}(\text{DDS})_2$.

The heat of dissolution obtained from the K_{sp} values, as mentioned earlier, corresponds to the reaction



The heat of dissolution in the presence of micelles, on the other hand, represents the heat involved in the solubilization of CaR_2 by the micelle. This process can be considered to be equivalent to a dissolution reaction given by equation 23 and subsequent adsorption of calcium on the micelle surface followed by the formation of more micelles by the released surfactant. A detailed analysis along these lines to obtain the heat of adsorption of Ca^{2+} on the micelle and a model based upon the temperature dependence data to test the validity of the above proposed molecular mechanism of redissolution are given in Section G.

E. Effect of Alcohols and Oils

Most of the past work on precipitation of surfactants conducted at Columbia was limited to mono and multivalent ions/surfactant systems. Multivalent ion/sulfonate systems upon increasing the surfactant concentration exhibited a precipitation, redissolution and a reprecipitation stage. The influence of alcohols and oils on such precipitation/redissolution phenomenon is important in micellar flooding systems, since the former is a co-surfactant in micellar flooding and the latter is always present under the flooding conditions. The results for the precipitation behavior of $\text{CaCl}_2/\text{NaDDBS}$ system in the presence of n-Propanol and n-dodecane are included in this report and this study will be extended to other solution conditions and to other alcohols and oils in the future.

E1. EFFECT OF n-PROPANOL

Precipitation behavior of $\text{NaDDBS}/\text{CaCl}_2$ (3×10^{-3} kmol/m³) at three levels of n-propanol is given in Figure I:8. Our past work has identified the precipitate under these concentrations of sulfonate in CaCl_2 solutions (in the absence of n-Propanol) to be calcium dodecylbenzenesulfonate (See Annual Report, 1980).

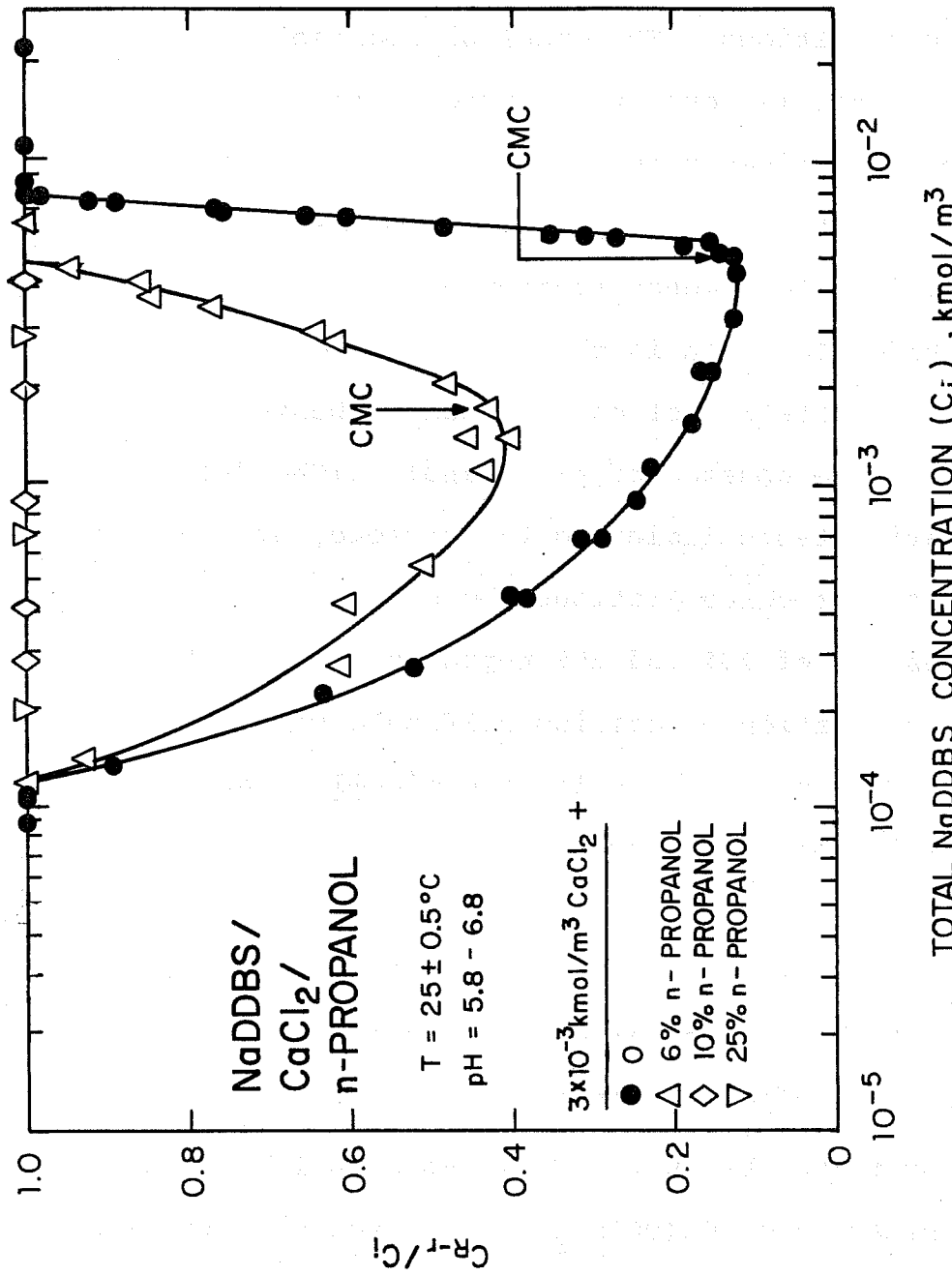


Figure I:8. Effect of n-propanol on the precipitation/ redissolution behavior of the NaDDBS/CaCl₂ system.

It is evident from the data in Figure I:8 that 6% n-propanol reduced the precipitation and 10% and 25% n-propanol completely eliminated the precipitation under all tested conditions. The onset of redissolution at 6% n-propanol is found to coincide with the CMC of the system determined using the dye solubilization technique. Most interestingly, 10% n-propanol reduced the CMC of DDBS to a concentration below 1.35×10^{-4} kmol/m³ sulfonate which is the concentration for the onset of precipitation of calcium dodecylbenzene-sulfonate in the absence of n-propanol. (The dye solubilization tests indicated the presence of micelles at all sulfonate concentrations above 1.35×10^{-4} kmol/m³ in the presence of 10% and 25% n-propanol.) In these cases, precipitation of calcium sulfonate was not observed. Evidently, the sulfonate micelles can cause the redissolution of the precipitates (or prevent the precipitation).

It is clear from Figure I:8 that the effect of alcohol is to reduce the amount of precipitate under all the tested sulfonate concentrations. It is to be noted that even below the CMC, n-propanol reduced the precipitation of Ca(DDBS)₂. The effect of n-propanol on Ca(DDBS)₂ precipitation is therefore, not only by shifting the CMC, but also by affecting the precipitation below CMC. Even though the mechanism by

which short chain alcohols such as n-propanol affect the CMC has not been well established, the speculations involve the effect of alcohol on the structure and hence the solvent power of water as well as the incorporation of alcohols between the charged heads of sulfonate in the micelle (17). The role of the former effect can be estimated by examining the influence of n-propanol on the precipitation below CMC. The role of the latter effect, i.e., the incorporation of alcohol molecules between the charged heads of the micelle can be evaluated by estimating the solubilization constant of the micelles defined earlier, as the amount in moles of the precipitate redissolved per mole of sulfonate above CMC,

$$\text{i.e., } K_s = \frac{[\text{CaR}_2 \text{ (Redissolved)}]}{C_{R-r} - \text{CMC}} \quad (24)$$

where CMC is the residual sulfonate at the onset of redissolution and C_{R-r} is the residual concentration at which $[\text{CaR}_2]$ moles of precipitate has redissolved.

$$K_s \text{ (6\% n-propanol)} = 0.12$$

$$K_s \text{ (0\% n-propanol)} = 0.3$$

Assuming a constant micelle size, the lower solubilization power of micelles for the precipitates in the presence of alcohol can be interpreted to be due to the competition of the alcohol with precipitate for the

micelle. On the other hand, a short chain alcohol such as n-propanol cannot be expected to get solubilized within the micelle. Incorporation of alcohols between the charged heads of the micelle is conceivable. Since the redissolution of calcium sulfonate precipitate involves either the incorporation of the precipitate with the calcium on the exterior of the micelle and sulfonate in the interior, or the uptake of calcium by the micelle and the formation of new micelles by the released sulfonate (see Section G), both of which involve the incorporation of Ca on the charged head of the micelle, the redissolution process can be expected to be influenced by the presence of n-propanol.

E2. EFFECT OF n-DODECANE

The effect of n-dodecane on the precipitation-redissolution of NaDDBS/CaCl₂ was tested in the following manner. n-Dodecane and an aqueous solution containing Na-dodecylbenzenesulfonate and CaCl₂ (6×10^{-3} kmol/m³) were taken in 1:1 ratio in a vial and were hand shaken vigorously for ten seconds. The vial was left undisturbed for 24 hours. Subsequently, the vial was centrifuged for 1 hour at 17,000 RPM. Samples from the aqueous phase were taken and analyzed for calcium and sulfonate. Analysis of the oil phase showed the

amounts of calcium and sulfonate in the oil phase to be below their detection limits.

At sulfonate concentrations above CMC, a turbid phase appeared separating the oil and aqueous phase. The volume of this phase was found to increase with increase in sulfonate concentration. Centrifugation of the system for 1 hour at 17,000 RPM, however, eliminated this middle phase.

The ratio C_{R-r}/C_{R-i} is plotted in Figure I:9 as a function of C_{R-i} . The continuous curve in this figure represents the expected sulfonate precipitation behavior in $6 \times 10^{-3} \text{ kmol/m}^3$ CaCl_2 solution in the absence of any oil. This curve has been obtained from the data for the precipitation of sulfonate in $5 \times 10^{-3} \text{ kmol/m}^3$ and $1 \times 10^{-2} \text{ kmol/m}^3$ CaCl_2 by interpolation. It is evident from this figure that the precipitation behavior of CaCl_2 is not affected by the presence of oil. The onset of redissolution, however, has shifted to a lower initial sulfonate concentration in the presence of n-dodecane.

Thus, the effect of n-dodecane on calcium dodecylbenzenesulfonate precipitation/redissolution is apparently only to shift the point of onset of precipitate redissolution to lower sulfonate concentrations.

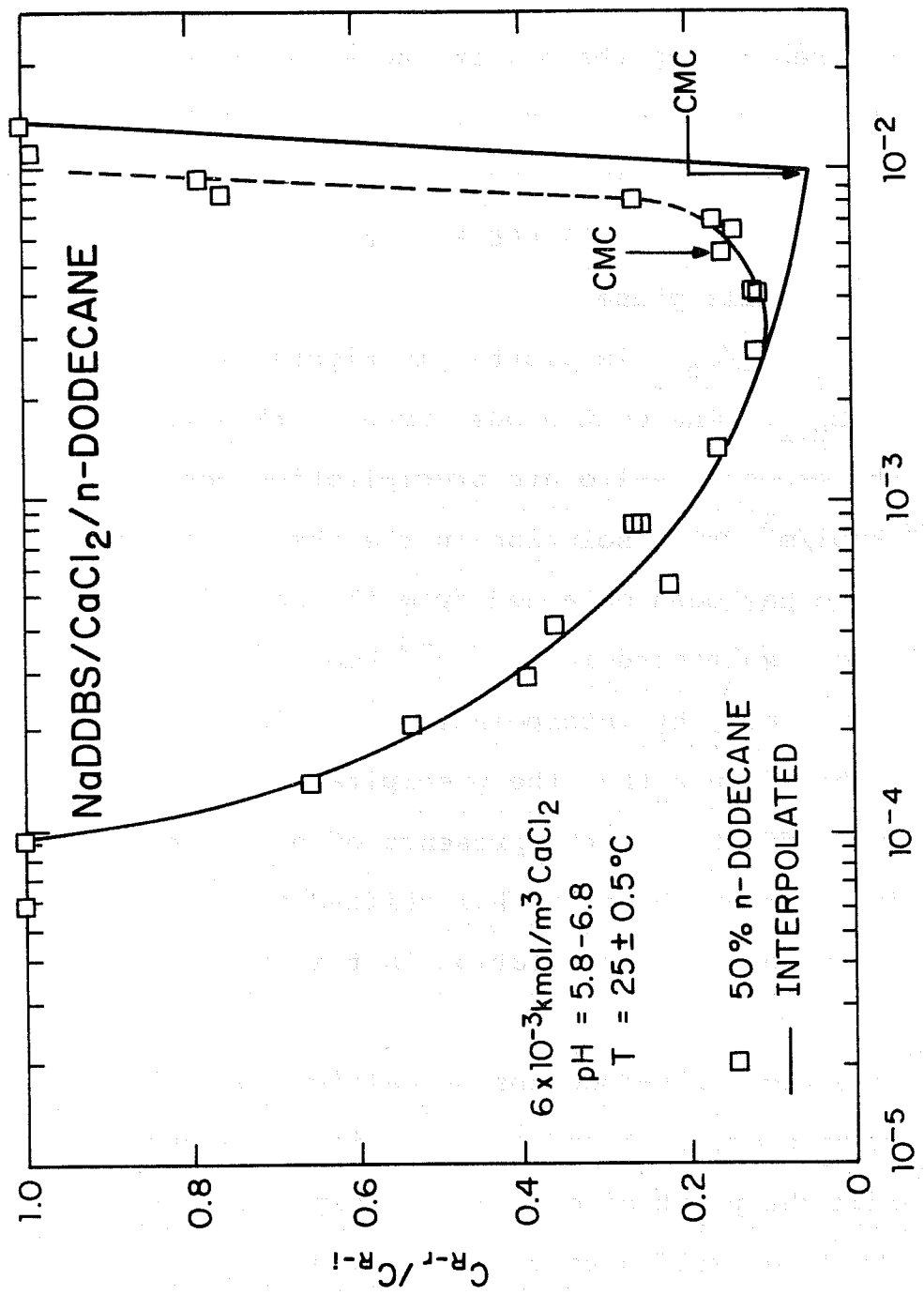


Figure I:9. Effect of n-dodecane on the precipitation/redissolution behavior of the NaDDBS/CaCl₂ system.

Since n-dodecane does affect the CMC of the sulfonate, a comparison of the precipitate dissolution in the presence and in the absence of oil in terms of the solubilization constant (as defined in the earlier section) of the micelle in these systems can be useful.

$$K_s \text{ (in the presence of oil)} = 0.21$$

$$K_s \text{ (no oil)} = 0.35$$

These figures indicate a lower solubilization power in the presence of oil suggesting as in the case of alcohol, competition of oil molecules with the precipitate for the micelle (see Section G).

F. A THERMODYNAMIC MODEL FOR PRECIPITATION/REDISSOLUTION

Our work on precipitation/redissolution of multivalent ion/sulfonate systems conducted so far has conclusively proved that the redissolution of multivalent ion-sulfonate precipitate occurs only in the presence of micelles. Our studies have identified also the chemical composition of the surfactant/multivalent ion precipitates and the conditions for the formation of mixed surfactant/mono and multivalent ions precipitates. With this background, we have now developed a thermodynamic model to predict the precipitation/redissolution

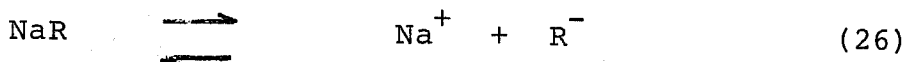
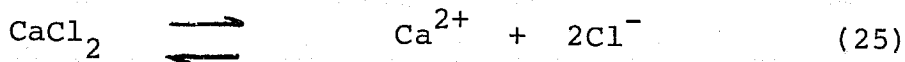
behavior of multivalent ion/surfactant systems. Given the initial concentrations of the multivalent ion and the thermodynamic constants involved in various sub-processes, this model can predict the nature and amounts of various species in the system. This model which has been developed for a simple multivalent ion/surfactant system can be easily, suitably modified to predict the behavior of other multi-component systems.

F1. OUTLINE OF THE MODEL

The model is based upon the micellar solubilization mechanism for the redissolution of multivalent ion/sulfonate precipitates. A schematic diagram of the precipitation/redissolution process indicating the regions of various interactions is given in Figure I:10.

The equations representing the various regions are written for the model system CaCl_2/NaR .

Region I. In this region, all the added CaCl_2 and NaR dissociate to form the corresponding ions in aqueous solution:



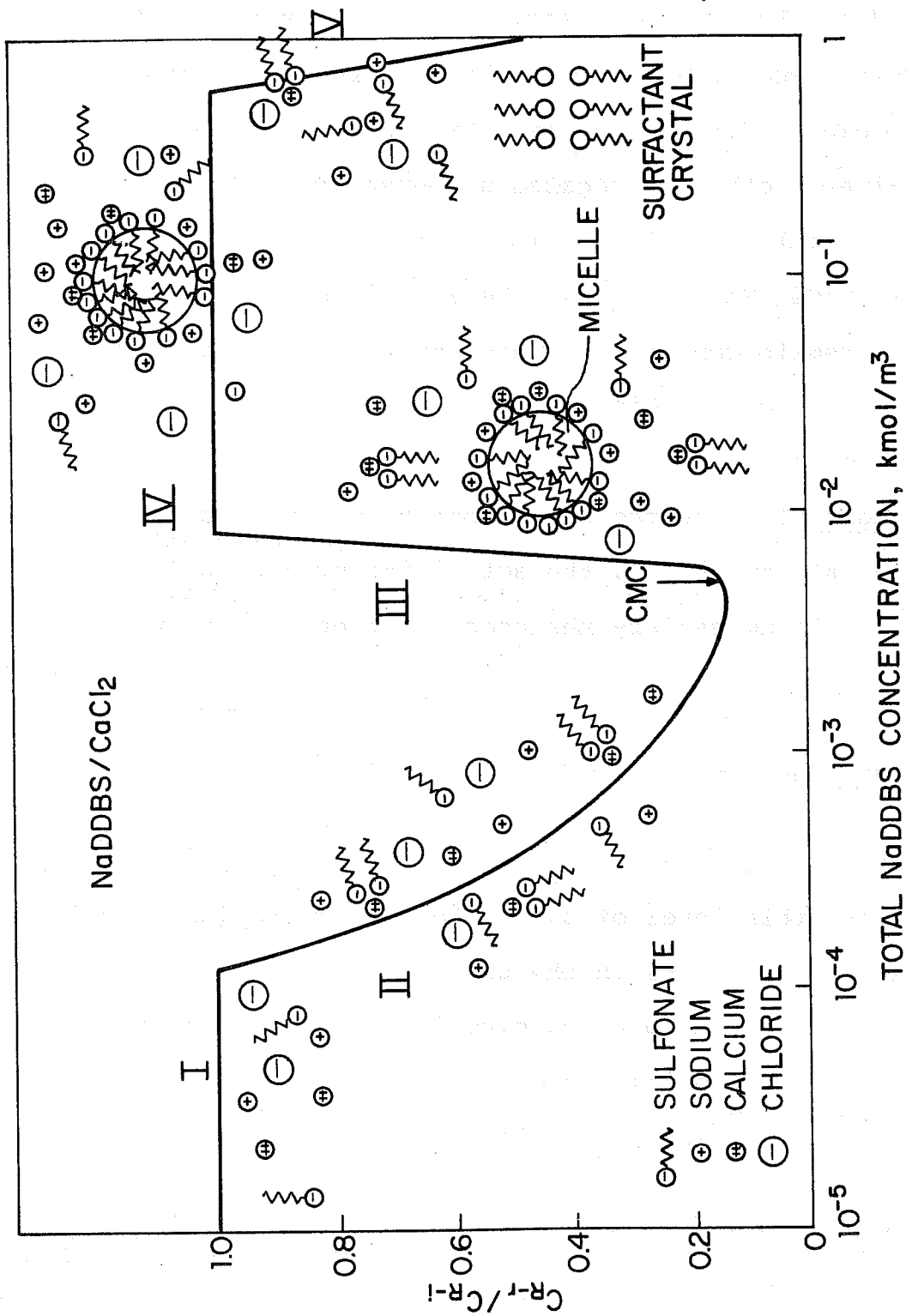


Figure I:10. A schematic diagram of the mechanism of the precipitation/redissolution/reprecipitation process.

In the case of multivalent ions such as Al^{3+} which can undergo hydrolysis reactions to form various aqueous complexes, such reactions should also be considered in this region. Similarly, long chain surfactants can form dimers, other aggregates and even hydrolyzed products (18).

In $\text{CaCl}_2/\text{NaDDS}$ system, the activities of Ca^{2+} and Cl^- remain constant in this region. Na^+ and R^- activities increase linearly with increase in the concentration of sulfonate.

Region II. As the concentration of sulfonate is increased, at some point, the activities of the sulfonate and the calcium satisfy the precipitation condition that

$$K_{\text{sp}} = [\text{Ca}^{2+}] \cdot [\text{R}^-]^2 \quad (27)$$

Above this level of sulfonate, precipitation of calcium sulfonate occurs in the system. Part of the added sulfonate is taken up by calcium in such a manner that the residual concentration of sulfonate and calcium satisfy equation (27) which can be rewritten as

$$K_{\text{sp}} = (C_{\text{Ca-i}} - x) (C_{\text{R-i}} - 2x)^2 \quad (28)$$

where 'i' refers to the initial concentration and 'x' to the amount of CaR_2 precipitated. Substituting for x as

$$C_{\text{Ca-i}} - C_{\text{Ca-r}} = x \quad (29)$$

equation (28) can be modified to yield

$$C_{\text{Ca-r}}^3 + C_{\text{Ca-r}}^2 (C_{\text{R-i}} - 2C_{\text{Ca-i}}) + \frac{1}{4} C_{\text{Ca-r}} (C_{\text{R-i}} - 2C_{\text{Ca-i}}) - \frac{1}{4} K_{\text{sp}} = 0 \quad (30)$$

The above third order equation involves the initial concentrations of surfactant, and calcium, and the solubility product K_{sp} . Using a suitable computer program (or by numerical methods) one can determine the residual activity of calcium and in turn, that of the surfactant.

In region II, the activity of the sulfonate will not increase in the same manner as it did in Region I, mainly because part of the sulfonate precipitated. The bulk activity will, however, continue to increase and at a certain concentration the system will reach the CMC of the surfactant. The activity of the surfactant monomer remains constant equal to CMC above this level

of sulfonate.

The changes in the activities of calcium and sulfonate in Region II can therefore be determined using equations (27) and (30).

Maximum precipitation of calcium sulfonate for any given initial level of calcium can be calculated as:

$$CaR_{2-MAX} = C_{Ca-i} - \frac{K_{sp}}{(CMC)^2} \quad (31)$$

Thus, knowing C_{Ca-i} , K_{sp} , and CMC, maximum precipitation can be determined.

Region III. In this region the redissolution of the precipitated calcium sulfonate occurs. It should be noted that the activity of the surfactant monomer in this region is equal to CMC and the bivalent calcium activity is governed by

$$C_{Ca-r} = \frac{K_{sp}}{(CMC)^2} \quad (32)$$

Therefore, the activities of both calcium and sulfonate remain constant in this region. The redissolution of the precipitate, however, takes place in such a way that the excess sulfonate and calcium

introduced into the solution are taken up by the micelles. The actual molecular mechanism involved in the redissolution process itself is discussed in Section G. Most importantly, our past work has shown that the redissolution region can be characterized by a solubilization constant, K_s , defined as

$$K_s = \frac{CaR_{2-rd}}{(C_{R-r} - CMC)} \quad (33)$$

where C_{R-r} is the residual concentration of sulfonate in solution, and CaR_{2-rd} is the amount in moles of calcium sulfonate precipitate redissolved. (The subscript 'rd' refers to "redissolved".) The residual concentration C_{R-r} can be obtained by knowing the initial concentration C_{R-i} in the following manner.

$$\begin{aligned} C_{R-r} &= \text{Excess sulfonate added above the onset of} \\ &\quad \text{redissolution} + CMC + 2(\text{amount of calcium} \\ &\quad \text{sulfonate redissolved}). \\ &= [C_{R-i} - C_{CMC}] + CMC + 2CaR_{2-rd} \quad (34) \end{aligned}$$

combining equations (33) and (34) and rearranging,

$$CaR_{2-rd} = \frac{K_s}{(1-2K_s)} [C_{R-i} - C_{CMC}] \quad (35)$$

Thus, knowing the solubilization constant, initial sulfonate concentration and C_{CMC} (the initial sulfonate concentration corresponding to the onset of micellization) one can determine the amount of CaR_2 redissolved. The latter term C_{CMC} can also be determined by simply knowing the initial calcium concentration and CMC of the system.

At the onset of micellization,

$$C_{Ca-r} = \frac{K_{sp}}{(CMC)^2} \quad (36)$$

If the initial calcium is C_{Ca-i} , the amount of calcium precipitated would be

$$[CaR_2] = C_{Ca-i} - \frac{K_{sp}}{(CMC)^2} \quad (37)$$

Therefore,

$$C_{CMC} = CMC + 2 \left[C_{Ca-i} - \frac{K_{sp}}{(CMC)^2} \right] \quad (38)$$

Using equations (36) and (38) and the CMC of the system, the amount of calcium redissolved can be determined.

The amount of sulfonate in the micelle form can be obtained from equations (34) and (35) as

$$C_{R-M} = C_{R-i} - CMC = [C_{R-i} - C_{CMC}] + \frac{2K_s}{1-2K_s} [C_{R-i} - C_{CMC}] \quad (39)$$

$$C_{R-M} = [C_{R-i} - C_{CMC}] \frac{1}{1-2K_s} \quad (40)$$

The amount of sulfonate precipitated can be obtained from the material balance equation as

$$C_{R-CaR_2} = C_{R-i} - C_{R-M} - CMC \quad (41)$$

Thus, the amounts of calcium and sulfonate in various forms can be determined from their initial concentrations, the solubility product, the solubilization constant and the CMC of the system.

Region IV. In this region, the sulfonate exists as monomers (activity = CMC) and micelles. The amount of sulfonate in the micelle form can be readily calculated as:

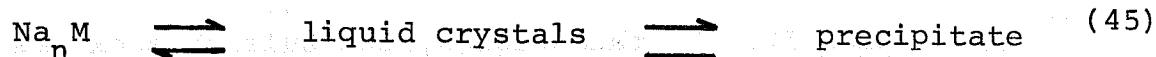
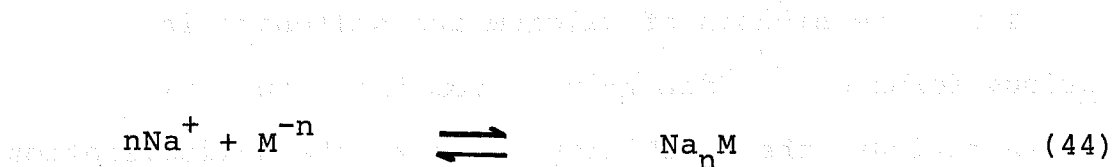
$$C_{R-M} = C_{R-i} - CMC \quad (42)$$

The activity of bivalent calcium cannot exceed $K_{sp}/(CMC)^2$ in this region. On the other hand, continued uptake of calcium by the micelle, even above the point of complete redissolution of CaR_2 can lead to

$$C_{Ca-r} < K_{sp}/(CMC)^2 \quad (43)$$

It should be noted that, while increasing the concentration of surfactant in the system, the Na^+ concentration also increases simultaneously. Therefore, at relatively high surfactant concentrations the sodium ions can compete with calcium for the micelle surface.

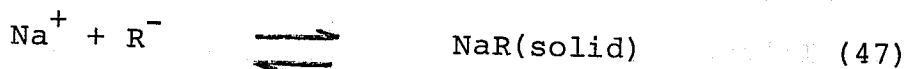
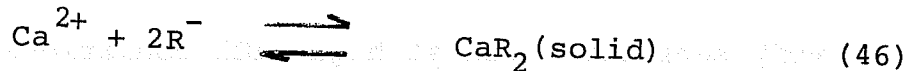
Region V. Increase in sulfonate concentration above a certain limit leads to the precipitation of NaR itself. This limit of precipitation can be obtained experimentally and can be represented as



Mixed Precipitation. If the concentration of calcium in the system is significantly high, such that the C_{CMC} is raised (see equations (37) and (38)) then the amount of $C_{\text{R-i}}$ required for complete redissolution of the precipitate also will correspondingly increase. It is, therefore, possible to envisage a system in which the calcium concentration is high enough that NaR itself starts precipitating prior to reaching the values of

C_{R-i} which can bring about the complete redissolution of the calcium sulfonate precipitate. Under these conditions, co-precipitation of calcium and sodium sulfonates can be expected.

On similar arguments, it is possible that at certain levels of calcium, sulfonate activity may never become even equal to CMC prior to the precipitation of NaR, in which case, no redissolution can be expected.



It is possible that the morphology of NaR precipitates obtained in this manner is different from that formed through a micellization process.

Importance of CMC. The above discussion of the model clearly showed that a prior knowledge of the 'CMC' of the system under various conditions is extremely important to be able to predict its precipitation/redissolution behavior. CMC, on the other hand, is very sensitive to the nature and concentration of counter ions present. In the present study, therefore, the CMC's of NaDDS and NaDDBS were determined under various

solution conditions.

The techniques used for the determination of the CMC of sulfonates under various conditions include surface tension, conductivity, Krafft point solubility and dye solubilization. Use of more than one technique was necessary to determine the CMC, because no single technique from the above was applicable to all the desired solution conditions. For example, the conductivity technique was not quite sensitive under high salinity conditions. Surface tension technique, on the other hand, was very sensitive even at high NaCl conditions (see Figure I:11). However, this technique failed to identify the CMC in precipitation systems (for example, see Figure I:12).

The technique that was found to be quite successful in precipitating systems was the dye solubilization technique. In this technique, the change in color of the solution upon the solubilization of the dye-surfactant complex in the micelle is taken as an indication of the onset of micellization.

Even though Mukerjee and Mysels (6) have criticized that this technique yields CMC values lower than other techniques, it was possible, from available literature, to identify certain dyes which were more suitable for certain surfactants. Thus, a cationic dye (pinacyanol

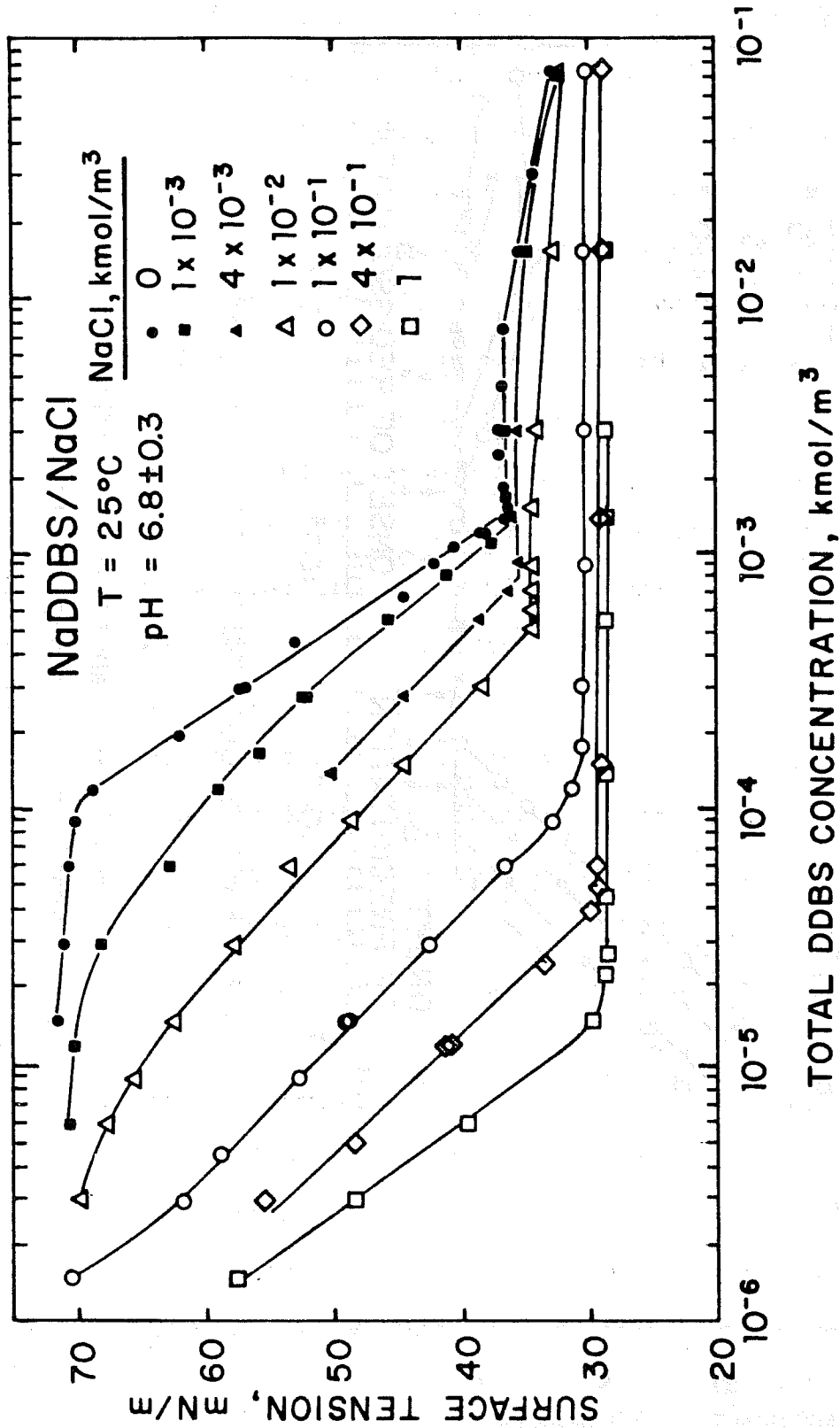


Figure I:11. Surface tension of NaDDBS as a function of sulfonate concentration at various NaCl levels.

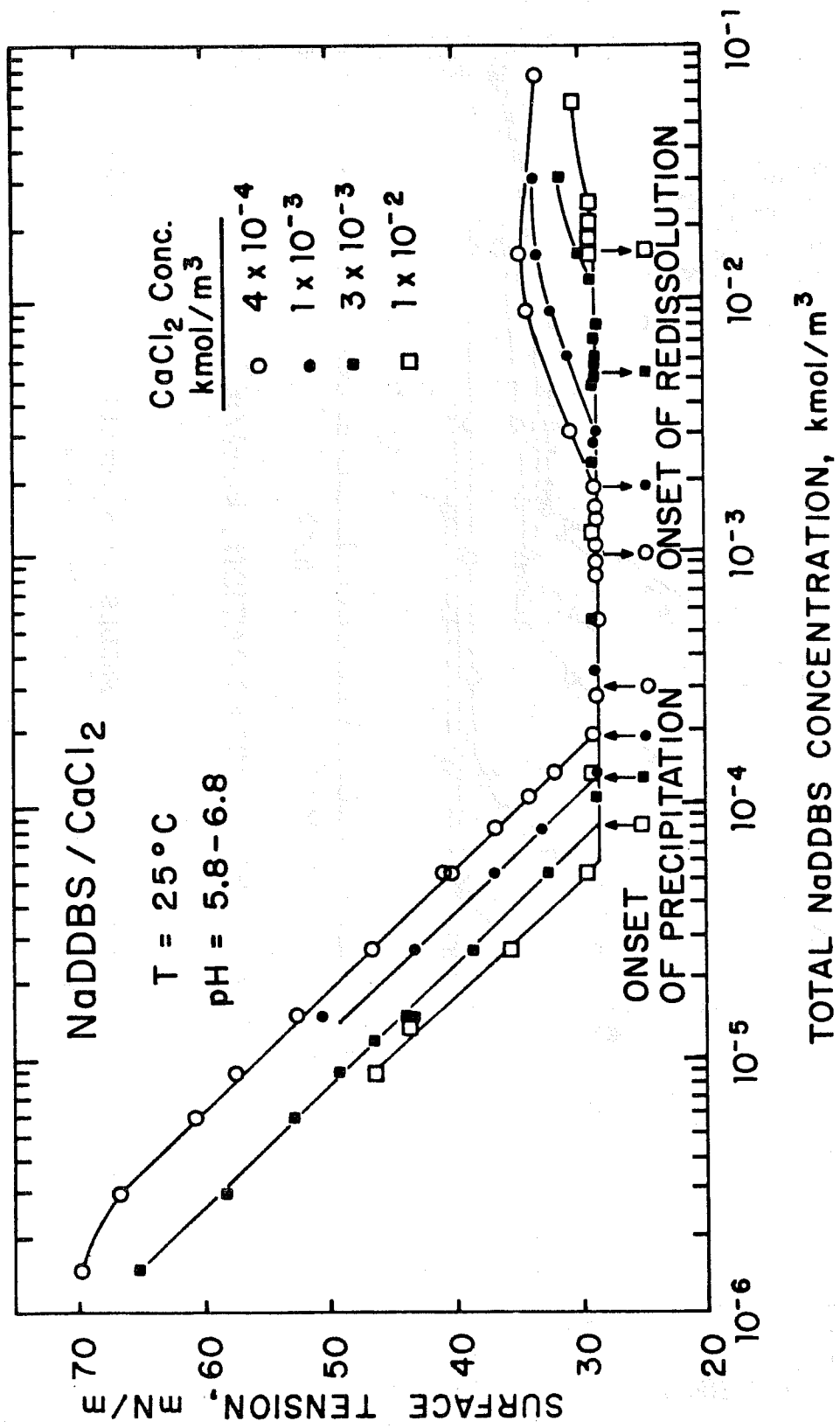


Figure I:12. Surface tension of NaDDBS as a function of sulfonate concentrations at various levels of CaCl₂.

chloride) was selected for the present studies. The performance of this technique was tested by determining the CMC of NaDDBS at different NaCl concentrations and by comparing them with the results obtained from the surface tension technique. It is evident from the data given in Table 3 that the dye technique yields CMC values which are in reasonable agreement with those obtained from the surface tension measurements.

The CMC of NaDDBS in NaCl and CaCl₂ solutions is given in Figure I:13 as a function of total counter ion concentration. The results of CMC for NaDDS/NaCl system is also included.

The data given in Figure I:13 is fitted to a general equation of the type

$$\log \text{CMC} = -a \log C_i + b \quad (48)$$

where C_i is the counterion concentration. The dependence of CMC of NaDDS and NaDDBS can be represented by the equations

For NaDDS

$$\log \text{CMC} = -0.68 \log C_i - 3.4 \quad (49)$$

For NaDDBS

$$\log \text{CMC} = -0.60 \log C_i - 4.5 \quad (50)$$

TABLE I: 3

Comparison of CMC values of NaDDBS determined by surface tension and dye solubilization techniques.

Added NaCl Conc., kmol/m ³	CMC, kmol/m ³	
	Surface tension	Dye solubilization
0	1.5 x 10 ⁻³	1.55 x 10 ⁻³
10 ⁻³	1.25 x 10 ⁻³	1.2 x 10 ⁻³
4 x 10 ⁻³	7.5 x 10 ⁻⁴	7.3 x 10 ⁻⁴
10 ⁻²	5.0 x 10 ⁻⁴	5.6 x 10 ⁻⁴
10 ⁻¹	1.4 x 10 ⁻⁴	2.8 x 10 ⁻⁴

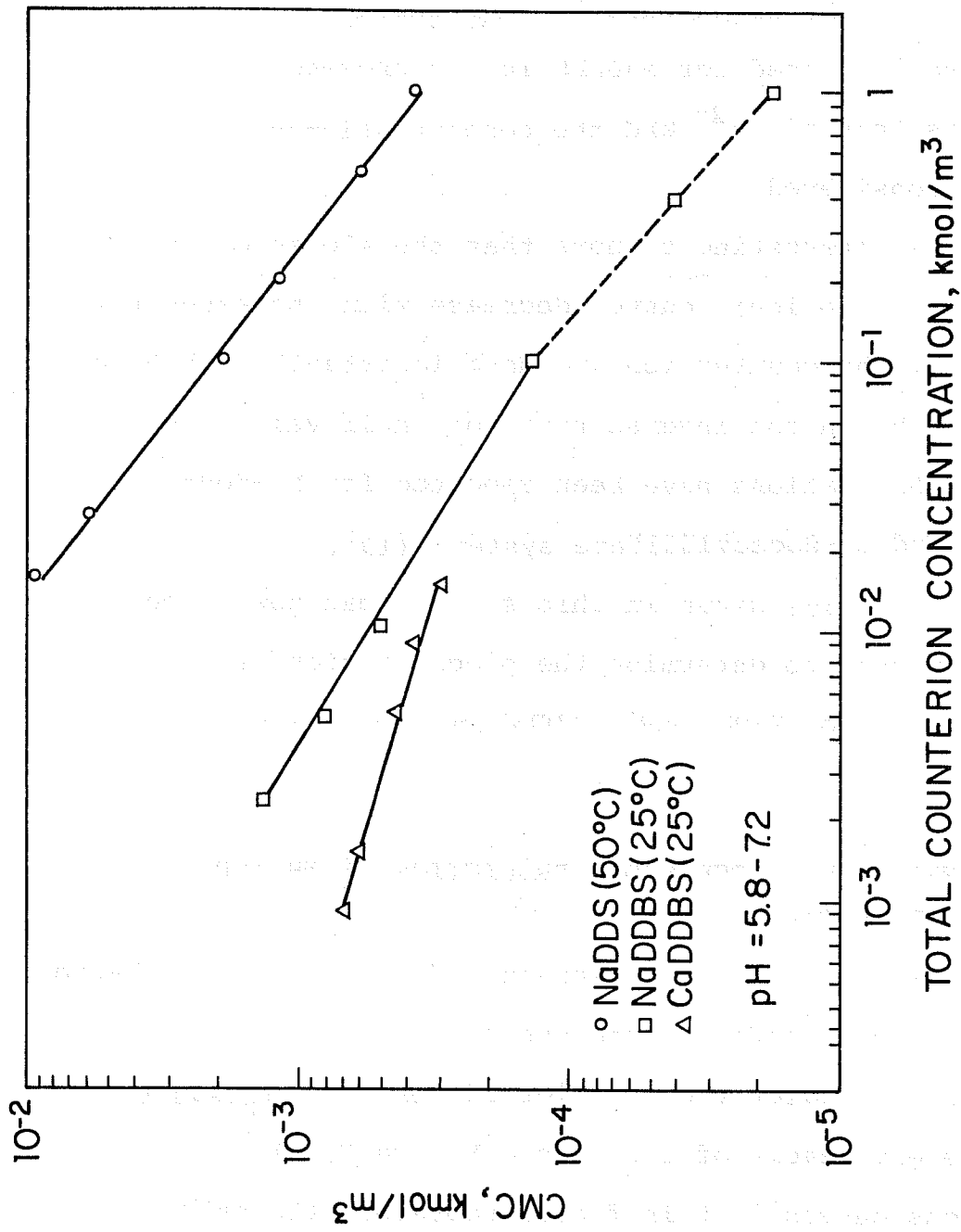


Figure I:13. Dependence of CMC as a function of total counterion concentration.

For NaDDBS/CaCl₂

$$\log \text{CMC} = -0.28 \log C_i - 4.01 \quad (51)$$

It is to be noted that the C_i , the counterion concentration, used for NaDDBS in the presence of CaCl₂ was that of Ca²⁺ and the concentration of Na⁺ was not considered.

It is interesting to note that the slopes of log CMC vs. log (counterion) curves decrease with increase in the valency of the counter ion and most importantly, the slopes appear to be in the inverse ratio of their valencies. Similar observations have been reported for Na-dodecylsulfate and Ca-dodecylsulfate systems (19).

The CMC data given in this section can now be conveniently used to determine the precipitation/redissolution behavior of NaDDS and NaDDBS under various conditions.

F2. COMPARISON OF THE MODEL PREDICTIONS WITH THE EXPERIMENTAL DATA

The model for the precipitation/redissolution behavior of multivalent ion/sulfonate systems outlined earlier was used to predict the behavior of NaDDS/CaCl₂ system at different levels of CaCl₂ (see Figure I:14). The continuous curves in this figure represent the calculated model predictions. The excellent agreement between

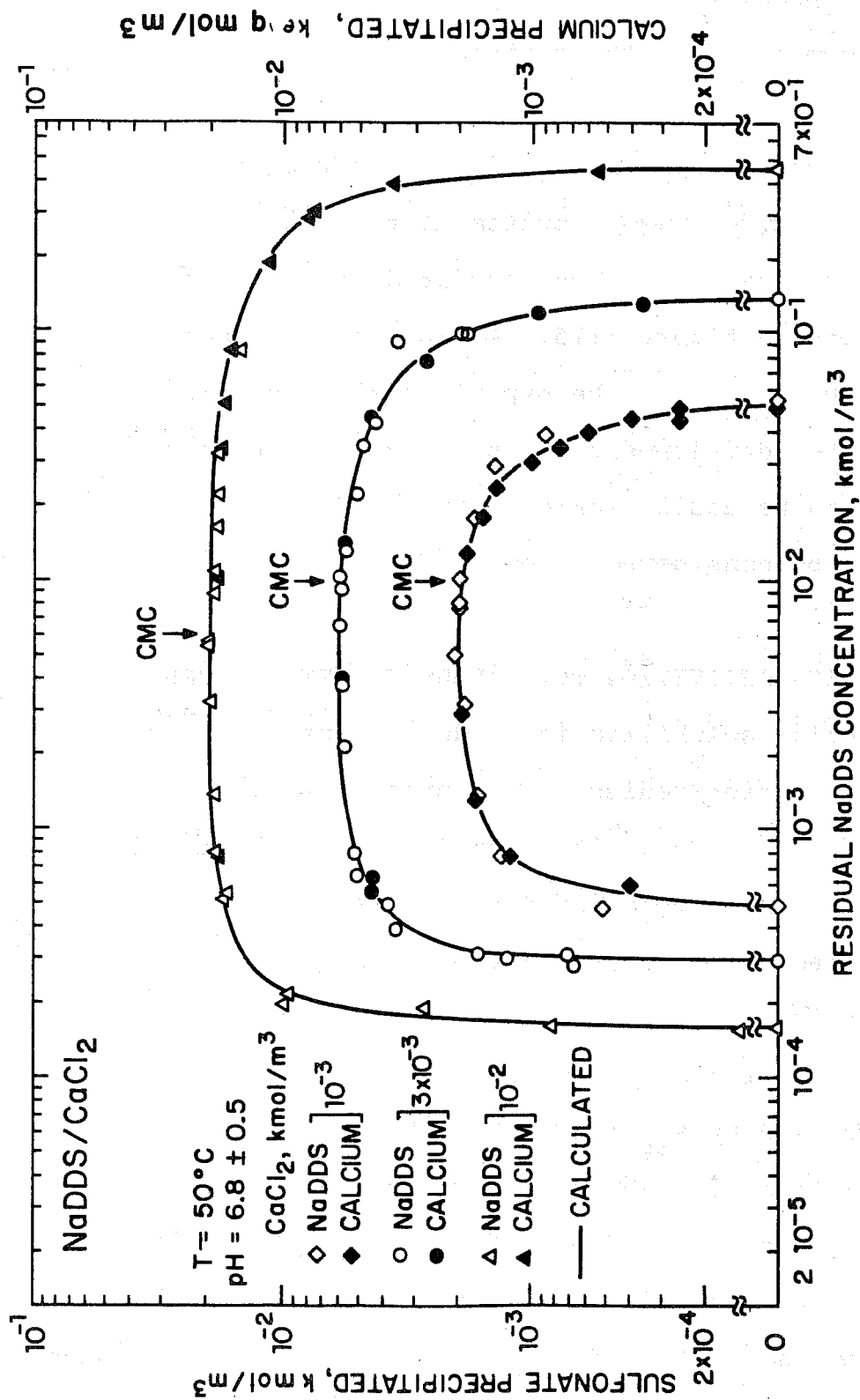


Figure I:14. Comparison of the experimentally obtained precipitation/redissolution patterns of NaDDS /CaCl₂ system with that predicted using the micellar solubilization model.

the model predictions and the experimental data, clearly demonstrates the predictive capabilities of the model.

The results for the precipitation/redissolution behavior of NaDDS/CaCl₂ system at three different temperatures have also been compared with the model predictions in Figure I:15. Again, the agreement between the model and the experimental values is good.

Further development of this model to multi-component systems can be easily achieved by suitable modifications. This will be considered in our future work.

F3. SPECIES ACTIVITIES vs. NaDDS CONCENTRATIONS

Micellar solubilization model proposed earlier for the precipitation/redissolution process suggests specific variations in the activities of different species in solution. For example, in Region I (see Figure I:10), while the activity of Ca²⁺ remained constant, those of Na⁺ and R⁻ increased linearly with the concentration of NaR. In Region II, the activity variations of Ca²⁺ and R⁻ are controlled by K_{sp} and in III, by both K_{sp} and K_s. In Region III, activities of both Ca²⁺ and R⁻ remain constant. With the experimental data available for the concentration of sulfonate and calcium and the activity of Na⁺ and Ca²⁺ (obtained using ion selective electrodes)

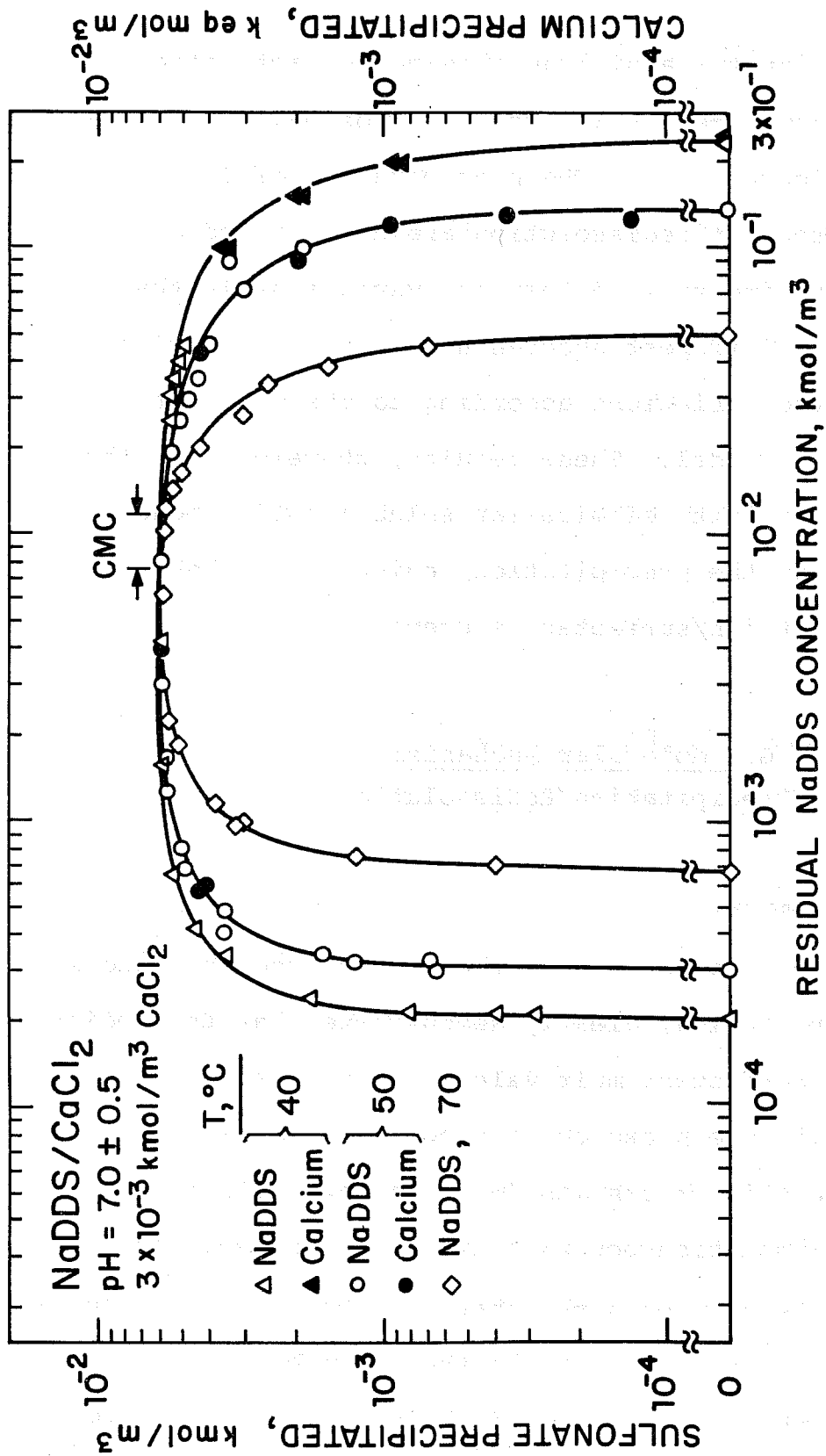


Figure I:15. Comparison of the experimentally obtained precipitation/redissolution patterns of NaDDS/CaCl₂ system at three different temperatures with that predicted using the micellar solubilization model.

we have constructed a diagram showing the activities of all the various species as a function of NaR concentration (see Figure I:16). The precipitation of CaR_2 and its subsequent redissolution are also included.

The experimentally determined variations in the activities of different species are in agreement with their expected variations according to the micellar solubilization model. These results, therefore, further confirm the validity of micellar solubilization model to account for the precipitation/redissolution behavior of multivalent ion/surfactant systems.

G. Molecular Mechanism of Precipitation/Redissolution

G1. INTRODUCTION

The results presented in the earlier sections and in our past report (1-4) clearly demonstrate that the redissolution of surfactant multivalent ion of precipitate occurs only in the presence of micelles. We have been referring to this process as "micellar solubilization", since the dissolution occurs only in the presence of micelles. It should be noted that the above term to describe this process is strictly within the definition of "solubilization", as per the classical definition of McBain and

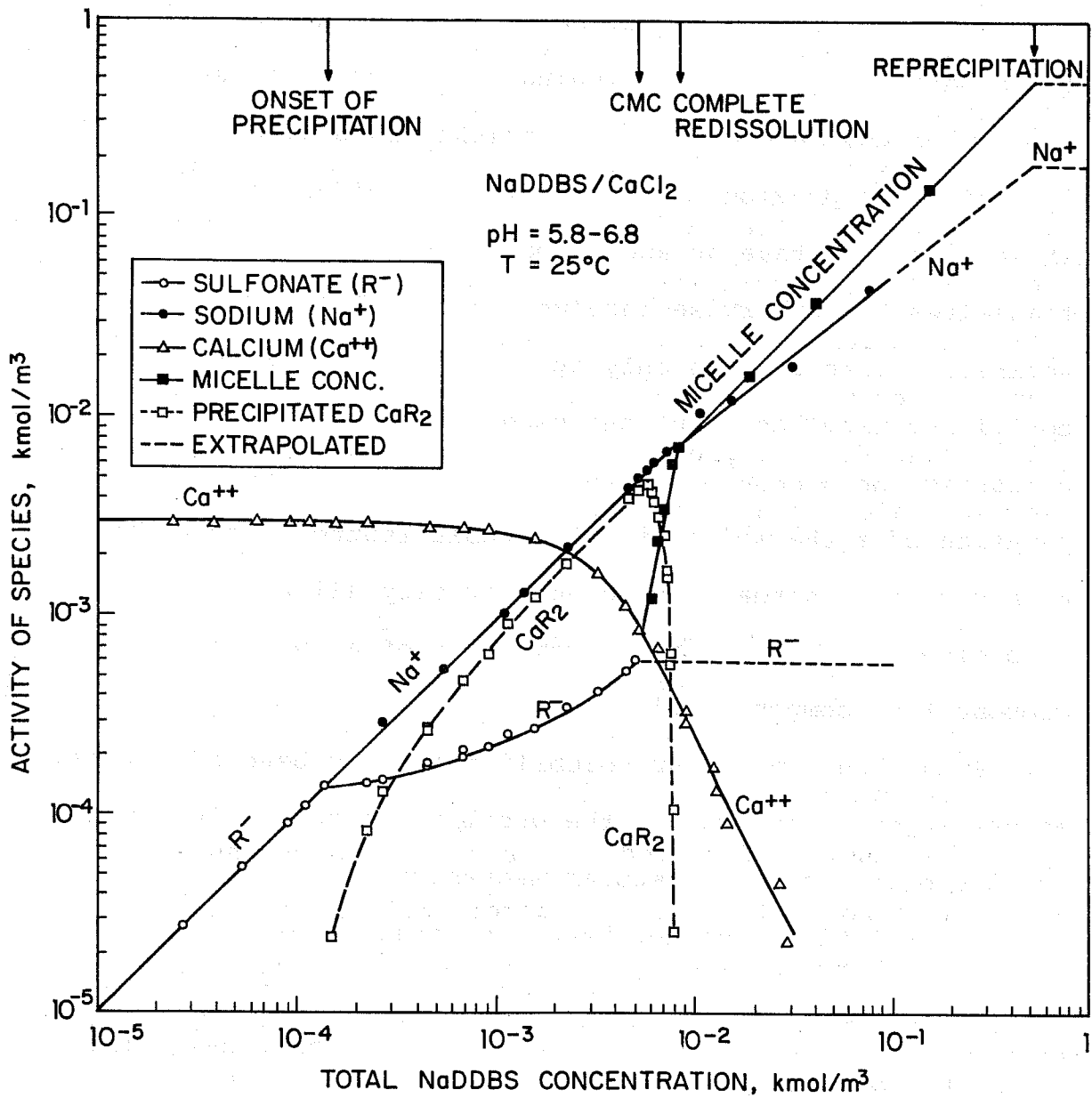


Figure I:16 Experimentally obtained variations in the activities of different species in NaDDBS/CaCl₂ system as a function of sulfonate concentration.

Hutchinson (20) and as per the current IUPAC definition. Solubilization as defined by McBain and Hutchinson (20), is 'a particular mode of bringing into a solution such substances that are otherwise insoluble in a given medium, involving the previous presence of a colloidal solution whose particles take up and incorporate within or upon themselves the otherwise insoluble material.' This definition literally is only applicable to solutions containing micelles. Current usage of the word solubilization as suggested by the definition, is 'the preparation of a thermodynamically stable isotropic solution of a substance normally insoluble or very slightly soluble in a given solvent by the introduction of an additional component or components.'

Even though micellar solubilization has been identified as the major mechanism for the precipitate redissolution, the micro-processes (molecular mechanisms) involved in the redissolution have not been discussed so far. For a complete understanding of the precipitation/redissolution process, it is important to know as to what happens to the calcium sulfonate upon dissolution.

G2. MOLECULAR MECHANISM

Solubilization by micelles can be brought about in three possible ways: (1) the uptake of the material by the micelle within its interior (2) incorporation of

the material, in a manner similar to mixed micelle formation and (3) the uptake of the material on the micelle surface (21). Non-polar substances such as hydrocarbon oils are dissolved in the interior of the micelle. Amphipathic solubilizates such as long chain alcohols are incorporated into the micelles with the hydrocarbon chain in the palisade layer and the polar heads projected on the micellar periphery. Polar solubilizates adsorb on the surface of micelles with probably some penetration into the palisade layer (22). A number of factors - polarity, polarizability, chain length and branching, molecular size, shape, and structure - have been shown to affect the solubilization capacity of substances in surfactant micelles (23). Klevens and McBain suggest that the addition of an electrolyte will increase solubilizing power toward non polar materials but will decrease solubilizing power toward polar materials (24, 25). With this background, and with the available experimental data, the solubilization of calcium sulfonate is examined from a molecular point of view in the subsequent sections.

Calcium sulfonate is amphipathic in nature. Moreover, during the redissolution of CaR_2 in micellar solutions, the activities of both bivalent calcium and sulfonate cannot increase appreciably (since surfactant monomer activity is almost a constant equal to CMC and

calcium is controlled by $K_{sp}/(\text{CMC})^2$. With these restrictions, the dissolved calcium and sulfonate of CaR_2 should become part of the micelle. This can happen in two possible ways: (1) incorporation of CaR_2 into the sulfonate micelle such that the hydrophobic part of it is in the interior of the micelle and the calcium is on the micelle surface (similar to mixed micelle formation) and (2) the uptake of Ca^{2+} by the micelle (adsorption of positively charged species on negatively charged surface), followed by the replenishment of the Ca^{2+} in solution by the dissolution of CaR_2 and finally the formation of micelles by the released sulfonate ions. It should be noted that both of the above micro processes are thermodynamically indistinguishable and equivalent. Possible methods to distinguish between these two micro processes were examined by critically analyzing the experimental data given earlier. The solubilization constant (see section C for definition) which is an indicator of the capacity of the micelles to solubilize the precipitate is used for the comparison of test results. The major conclusions from the earlier sections are reproduced below.

1. The solubilization constant of $\text{NaDDBS}/\text{CaCl}_2$ system decreased from 0.3 to 0.08 upon addition of $3 \times 10^{-2} \text{ kmol/m}^3$ NaCl .

2. Solubilization constant decreased with increase in the concentration of CaCl_2 .

3. Presence of 6% n-propanol in $\text{NaDDBS}/\text{CaCl}_2$ system decreased the solubilization constant from 0.3 to 0.12.

4. Increase in the chain length of sulfonate decreased the solubilization constant. Most importantly, the redissolution behavior of $\text{Ca}-(\text{C}_{16}\text{SO}_3)_2$ and $\text{Ca}-(\text{C}_{10}\text{SO}_3)_2$ in C-10 sulfonate micelle was identical indicating that the chain length of the sulfonate did not affect the solubilization constant of C_{10} sulfonate micelle.

5. Solubilization constant was found to decrease also in the presence of n-dodecane.

6. Solubilization increased with increase in temperature for $\text{NaDDS}/\text{CaCl}_2$ system. On the other hand, a marginal decrease in K_s was observed in the case of $\text{NaDDBS}/\text{CaCl}_2$ system.

7. The solubilization constants for $\text{NaDDS}/\text{CaCl}_2$ and $\text{NaDDBS}/\text{CaCl}_2$ differed markedly. The latter exhibited superior solubilization power for the calcium sulfonate precipitates compared to the former.

A decrease in the solubilization, in spite of the enhanced micellization with increase in NaCl indeed suggests that electrostatic interactions are important in

the redissolution process. Similarly, increase in CaCl_2 will result in an increase in the amount of NaR required to reach the onset of micellization and consequently will lead to a higher Na^+ concentration in the system. Also, the ionic strength will be increased because of the increase in NaCl. Effect of Na^+ and ionic strength again reflects the significance of electrostatic interactions in the redissolution process.

n-Propanol, as discussed in section E1, cannot be expected to get solubilized in the interior of the micelle. However, it can be expected to interact with the surface of the micelle and hence compete with other reactions that occur on the micelle surface. The decrease in the solubilization constant in the presence of n-propanol, suggests that the surface of micelles does play a significant role in the redissolution. It is assumed in this analysis that the size and shape of micelles are not affected by n-propanol.

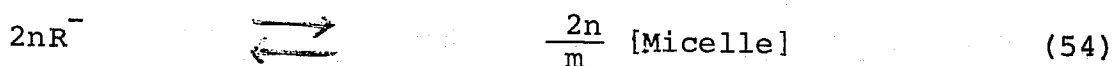
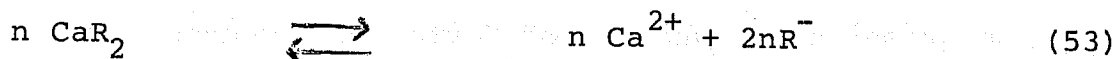
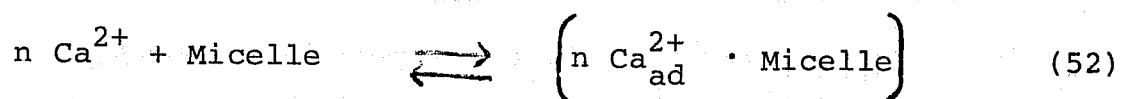
The fact that the redissolution of C_{16} and C_{10} calcium sulfonates occurs in an identical manner in C_{10} micelles shows that the interior of the micelle does not take part in the redissolution process. On the contrary, the effect of oil on K_s suggests that the interior of the micelle also has a role in the redissolution. It is, however, possible that the solubilization of oil

within the micelle leads to changes in the shape and the size of the micelle which can indirectly affect the interactions at the micelle surface.

The effect of temperature on solubilization cannot be directly interpreted, since it can affect the electrostatic interactions, solubility, and hence, the concentration of ions and the CMC of the system. A detailed analysis of temperature effects is given in a subsequent section.

The above series of arguments appear to suggest that the redissolution of calcium sulfonate involves adsorption of Ca^{2+} on the micelle surface and the subsequent dissolution of CaR_2 followed by the micellization of the released sulfonate. The changes in ionic strength and counterion concentrations can indeed influence the adsorption of Ca^{2+} on the micelle surface.

The molecular mechanisms discussed above can be represented as:



where 'm' is the number of monomers in a micelle. Since the activity of Ca^{2+} under redissolution conditions is governed by

$$C_{\text{Ca-r}} = \frac{K_{\text{sp}}}{(\text{CMC})^2} \quad (55)$$

adsorption of calcium according to equation (52) will cause redissolution of CaR_2 and micellization of (12) according to equations (53) and (54).

G3. ANALYSIS OF THE DIFFERENCES IN THE SOLUBILIZATION POWERS OF NaDDS AND NaDDBS

In the light of the above discussion on the molecular mechanisms of redissolution, it would now be interesting to examine the significant differences in the solubilization powers of NaDDS and NaDDBS for their corresponding calcium salts. Since the adsorption of calcium on the micelle surface can be markedly influenced by the charge on the micelle, the charge characteristics of the micelle of NaDDS and NaDDBS were determined by measuring conductivity of respective solutions.

G3a. Conductivity Results

The results for the conductivity of NaDDS and NaDDBS solutions as a function of surfactant concentration are given in Figure I:17. It is interesting to note that, while the slope of the conductivity vs. concentration curve decreases above CMC in the case of NaDDS, an increase

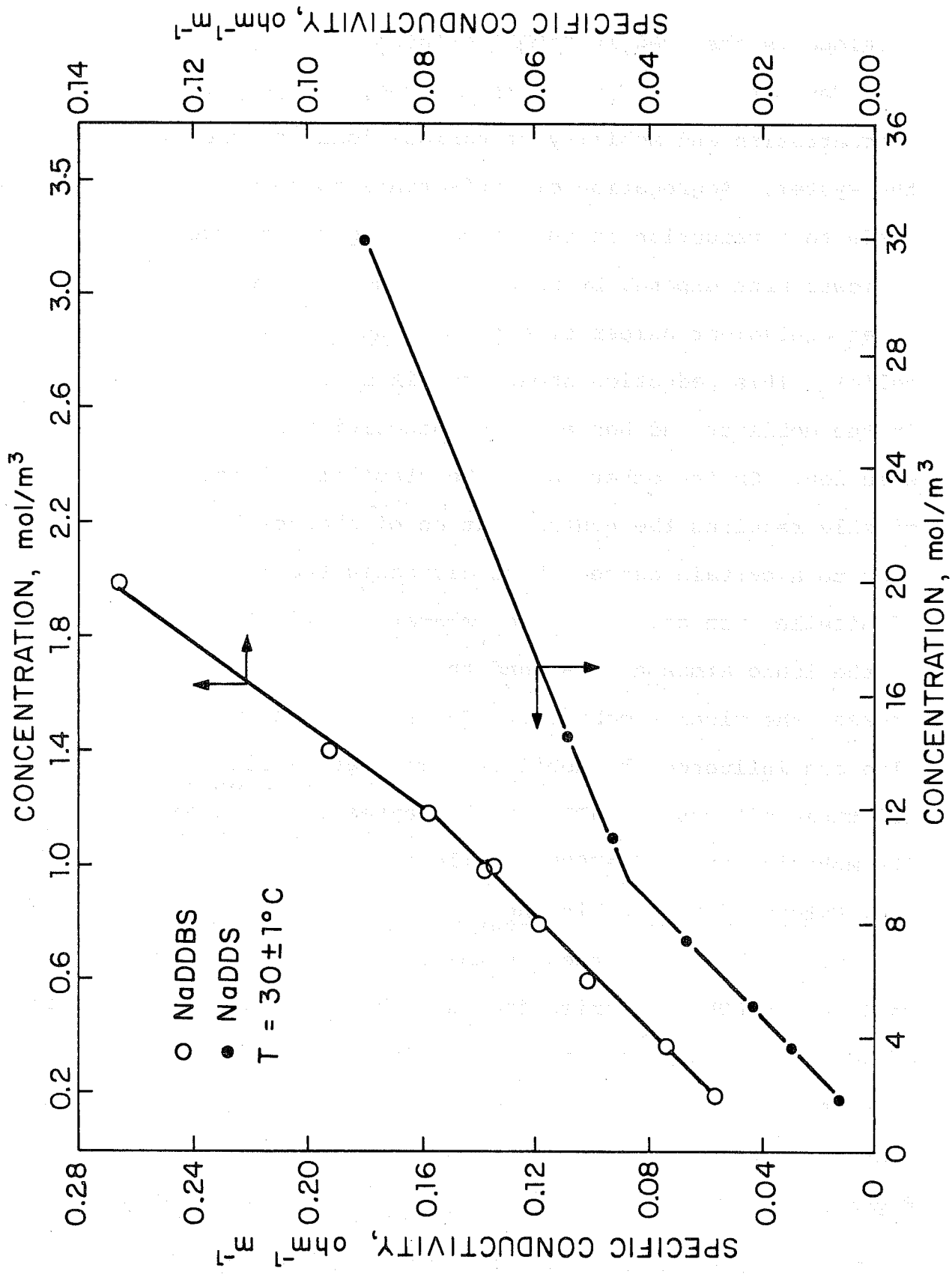


Figure I:17 Conductivity of NaDDS and NaDDBS solutions as a function of sulfonate concentration

in slope is observed in NaDDBS solutions.

Conductivity of solutions is dependent upon the concentration and mobility of various ionic species in the system. Aggregation of surfactants to form micelles leads to a reduction in the viscous drag force (due to lower area exposed by micelle to the solution compared to an equivalent number of monomers constituting the micelle). This reduction should result in an increase in the mobility and hence, the conductivity of the solution. On the other hand, the stability of the micelle requires the neutralization of charges by counterions to a certain degree which decreases the mobility of micelle. In addition, the relaxation effects caused by the ionic atmosphere around the micelle, further decrease the micelle mobility. The size of the micelle also can influence the mobility. The net result of all these effects on NaDDS micelle appears to decrease its mobility and on NaDDBS micelle to increase it.

G3b. Extent of Na ion binding

Since the differences in the conductivities of NaDDS and NaDDBS can arise from a number of reasons, the extent of counterion binding on the micelle was determined independently by measuring the activity of free Na^+ using a sodium ion electrode. The results given in Figure I:18 show that the degree of Na^+ binding is lower

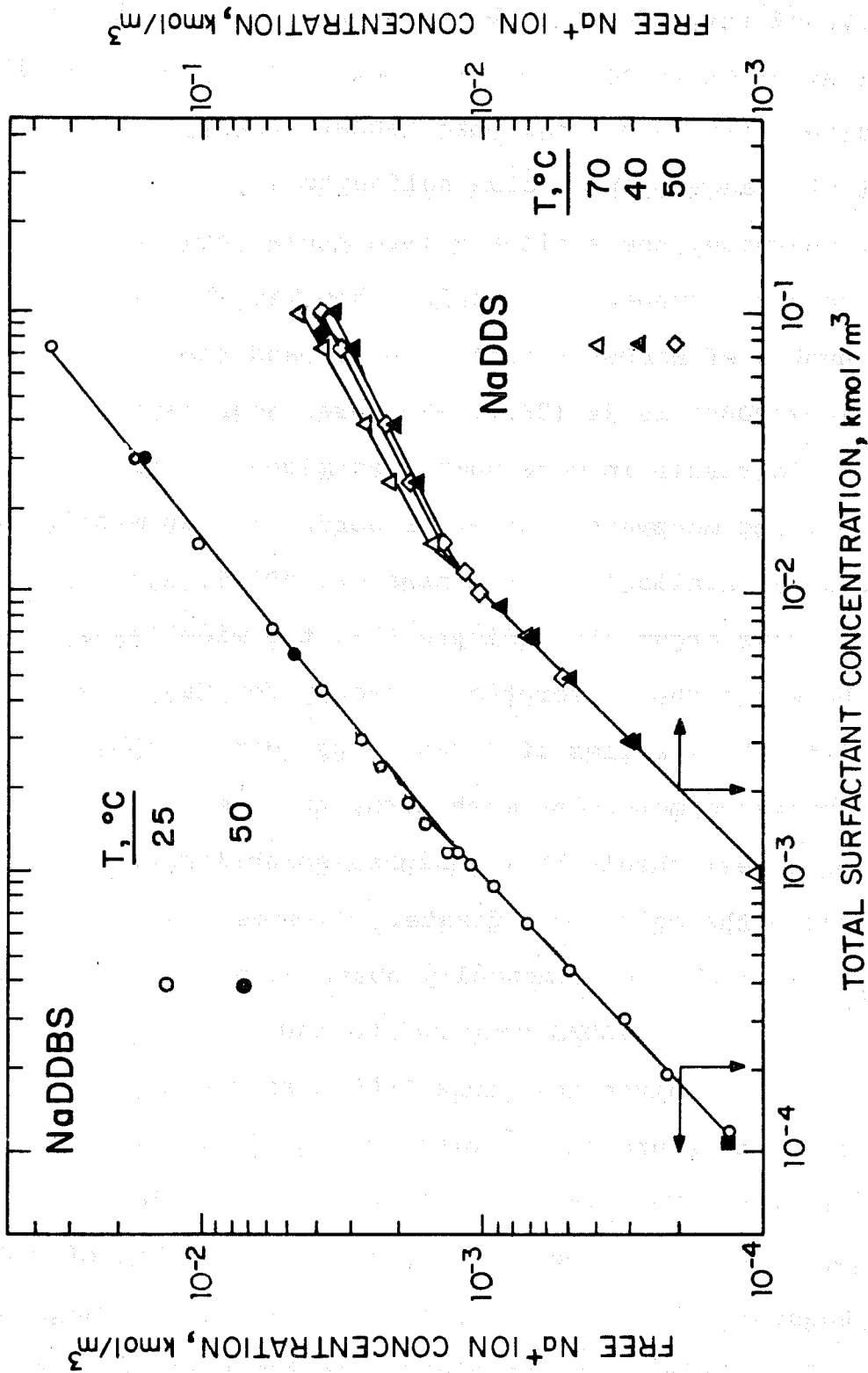


Figure I:18. Free Na⁺ ion concentration determined in NaDDBS and NaDDS solutions under various conditions.

in the case of NaDDBS compared to NaDDS. The lower degree of Na^+ binding on NaDDBS micelle would permit the accommodation of larger amounts of Ca^{2+} ions on the micelle surface and this indeed can make NaDDBS micelle a better solubilizing agent for calcium sulfonate.

Furthermore, the available literature results for the aggregation number of micelles show that the aggregation number of NaDDS is about 54 (26) and that of NaDDBS (p-NaDDBS) is 24 (28). The lower aggregation number would result in more number of micelles for the same number of monomers - in other words, larger micelle area would be available in the case of NaDDBS.

The above arguments indicate that the micelles of NaDDBS have a higher adsorption capacity for Ca^{2+} compared to the micelles of NaDDS. According to the earlier proposed molecular mechanism, therefore, the NaDDBS micelles should have a higher solubilization capacity for the calcium sulfonate. This is in agreement with the experimentally observed superior solubilization capacity of NaDDBS compared to NaDDS.

The results given in Figure I:18 also show the effect of temperature on Na^+ binding. It is interesting to note that the Na^+ binding in the case of NaDDBS is not affected at all by temperature compared to that of NaDDS. Again, these results are in agreement with the experimentally observed dependence of redissolution on temperature (see Section D). The conductivity and Na^+ ion binding data support

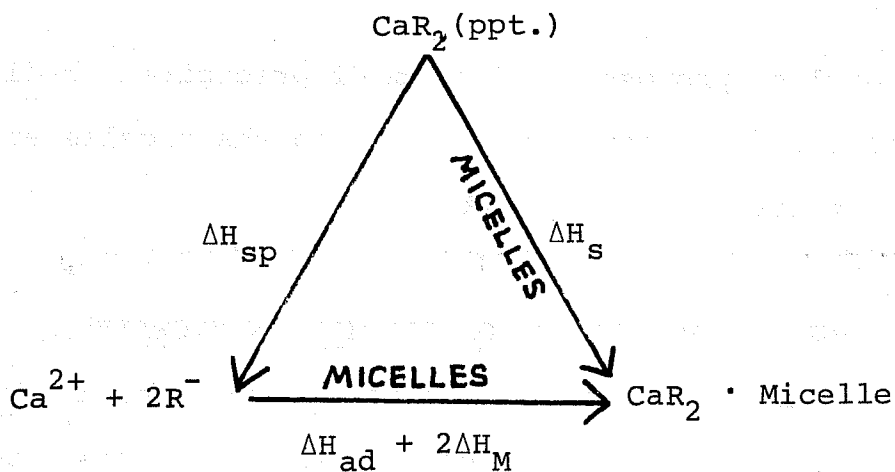
the earlier proposed mechanism of precipitate redissolution involving the adsorption of Ca^{2+} on the micelle and the subsequent dissolution of CaR_2 .

G4. HEAT OF ADSORPTION OF CALCIUM ON MICELLES

An understanding of the micro-processes involved in the redissolution process now makes it possible to further analyze and evaluate more thermodynamic information from the data for the dependence of precipitation/redissolution on temperature, given in Section D.

Based upon the temperature dependence of K_{sp} and K_{s} , the heat of reactions ΔH_{sp} and ΔH_{s} were calculated for both NaDDS and NaDDBS in CaCl_2 solutions. While the former, ΔH_{sp} , refers to the dissolution of CaR_2 to yield Ca^{2+} and 2R^- ions, the latter corresponds to the micellar solubilization of the precipitates. Since the available results strongly suggest that the redissolution occurs by a process involving the adsorption of Ca^{2+} on the micelle and the consequent redissolution of CaR_2 , one can obtain the heat of adsorption of calcium on the micelle in the following manner.

As the heat of any reaction is independent of the path taken to achieve the final state, but depends only on the initial and final states (Hess's Law), one can write (see the schematic diagram given below)



Since the values of ΔH_{sp} and ΔH_M have already been calculated and since ΔH_M can be calculated from the dependence of CMC on temperature, one can determine the heat of adsorption of calcium on the micelle.

$$\Delta H_{ad} = \Delta H_s - \Delta H_{sp} - 2\Delta H_M \quad (56)$$

The CMC of NaDDS/ CaCl_2 was determined from the conductivity data given in Figure I:19. In the case of NaDDBS/ CaCl_2 system, the CMC was determined in the following manner. The CMC of NaDDBS was determined at different temperatures using the dye technique. Assuming a similar dependence of CMC on temperature for NaDDBS/ CaCl_2 system, and by knowing the CMC of the latter at 25°C , the rest of the values were determined. The heat of micellization itself was obtained using relations

$$\frac{\partial \ln \text{CMC}}{\partial (1/T)} = \frac{\Delta H_M}{R} \quad (57)$$

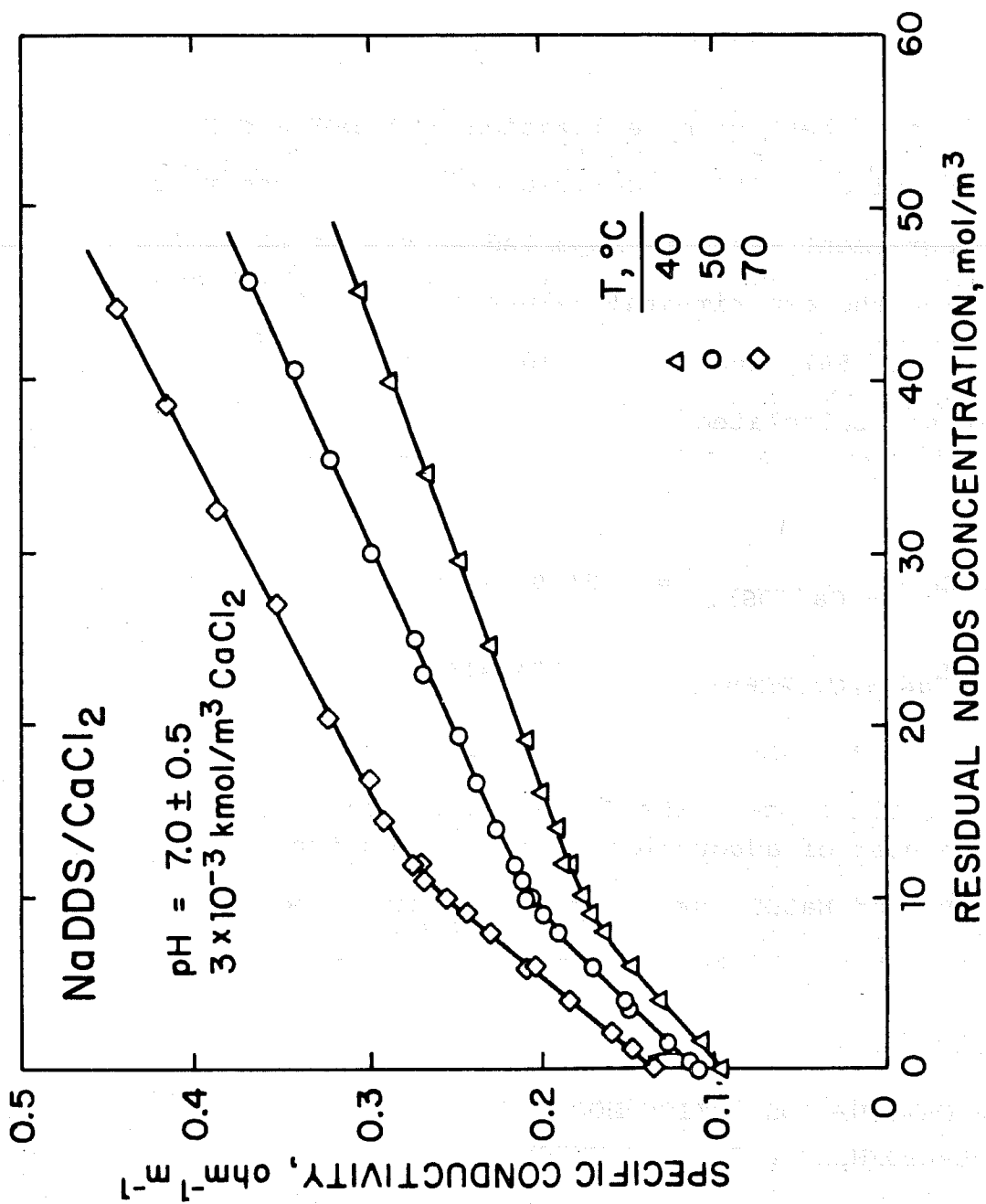


Figure I:19. Specific conductivity of NaDDS/CaCl₂ system as a function of sulfonate concentration at different temperatures.

and

$$\ln \text{CMC} = \frac{\Delta H_M}{RT} + \text{constant} \quad (58)$$

The values of heat of micellization of NaDDS and NaDDBS are respectively -1848 and -1210 cal/mol. These values are in agreement with the reported values of ΔH_m (16).

Using the experimental values of ΔH_s , ΔH_{sp} and ΔH_m in Equation (56), the heat of adsorption of Ca^{2+} on the micelle was calculated as

$$\Delta H_{\text{ad}} - \text{Ca}(\text{DDS})_2 = -2429 \text{ cal/mol}$$

$$\Delta H_{\text{ad}} - \text{Ca}(\text{DDBS})_2 = -3584 \text{ cal/mol}$$

The heat of adsorption of calcium on the micelles of NaDDBS and NaDDS comes out to be large negative values, the latter being higher by about 1000 cal/mole than the former.

G5. A CALCIUM ADSORPTION MODEL FOR TEMPERATURE DEPENDENCE OF REDISSOLUTION

For the above series of calculations, it was hypothesized that the redissolution of the precipitate occurs due to (a) adsorption of calcium by the micelle

and (b) the dissolution of calcium sulfonate to replenish the solution with calcium according to the solubility product expression and (c) the formation of micelles by the released sulfonate upon the dissolution of calcium sulfonate. If the above series of reactions in fact lead to the redissolution of the precipitate, then the amount of precipitate redissolved should be proportional to the adsorption of calcium on the micelle.

$$K_s(T_1) \propto \Gamma(T_1) \quad (59)$$

where $K_s(T_i)$ is the solubilization constant at temperature (T_i) and $\Gamma(T_i)$ is the adsorption of calcium on the micelle. For two different temperatures, this can be modified as:

$$\frac{K_s(T_1)}{K_s(T_2)} = \frac{\Gamma(T_1)}{\Gamma(T_2)} \quad (60)$$

Adsorption of calcium can in turn be expressed as:

$$\Gamma(T_1) = K_{ad} \cdot C_{Ca} \quad (61)$$

where K_{ad} is the adsorption constant and $C_{Ca^{2+}}$ is the concentration of calcium in the solution. Combining Equations (60) and (61), we obtain

$$\frac{K_s(T_1)}{K_s(T_2)} = \frac{K_{ad}(T_1)}{K_{ad}(T_2)} \cdot \frac{C_{Ca}(T_1)}{C_{Ca}(T_2)} \quad (62)$$

The concentration of calcium in the redissolution region is governed by the solubility product of calcium sulfonate and the CMC of the surfactant, i.e.,

$$C_{Ca} = K_{sp}/(CMC)^2 \quad (63)$$

Also, using the Clausius/Claypeyron Equation for the dependence of K_{ad} and K_{sp} on temperature in the following form and rearranging them one can obtain,

$$\frac{\partial \ln K_{ad}}{\partial (1/T)} = \frac{-\Delta H_{ad}}{R} \quad (64)$$

$$\ln \left[\frac{K_{ad}(T_1)}{K_{ad}(T_2)} \right] = \frac{-\Delta H_{ad}}{R} \left[\frac{1}{T_1} - \frac{1}{T_2} \right] \quad (65)$$

$$\ln \left[\frac{K_{sp}(T_1)}{K_{sp}(T_2)} \right] = \frac{-\Delta H_{sp}}{R} \left[\frac{1}{T_1} - \frac{1}{T_2} \right] \quad (66)$$

$$\ln \left(\frac{K_{ad}(T_1)}{K_{ad}(T_2)} \right) = \frac{\Delta H_{ad}}{\Delta H_{sp}} \ln \left(\frac{K_{sp}(T_1)}{K_{sp}(T_2)} \right) \quad (67)$$

$$\frac{K_{ad}(T_1)}{K_{ad}(T_2)} = \left(\frac{K_{sp}(T_1)}{K_{sp}(T_2)} \right)^{\frac{\Delta H_{ad}}{\Delta H_{sp}}} \quad (68)$$

Substituting for $K_{ad}(T_1)/K_{ad}(T_2)$ and $(C_{Ca}(T_1)/C_{Ca}(T_2))$ in Equation (62) from Equation (68) and (63), the final expression can be obtained as:

$$\frac{K_s(T_1)}{K_s(T_2)} = \left(\frac{K_{sp}(T_1)}{K_{sp}(T_2)} \right)^{\left(1 + \frac{\Delta H_{ad}}{\Delta H_{sp}} \right)} \cdot \left(\frac{CMC(T_2)}{CMC(T_1)} \right)^2 \quad (69)$$

Since we know all the parameters on the right hand side of the above expression, the ratio of $K_s(T_1)/K_s(T_2)$ can be estimated.

$$\frac{K_s(40^\circ \text{C})}{K_s(50^\circ \text{C})} = 0.62$$

The experimentally obtained value of $K_s(40)/K_s(50)$ for this system is 0.61, and is in agreement with the predictions.

$$\frac{K_s(25^\circ\text{C})}{K_s(50^\circ\text{C})} = 0.99$$

The experimentally obtained value (=1.04) is again in agreement with the predicted value based upon the adsorption of calcium on micelle.

The results for the dependence of precipitation/redissolution on temperature, thus, have been used to determine the heat of dissolution of the calcium sulfonate precipitate in water, and in the presence of micelles. Also, the heats of micellization and adsorption of calcium on micelles have been estimated. A model is proposed to check the validity of the calcium adsorption for the redissolution process. The experimental results and the model predictions are in agreement with each other, thus indicating the redissolution process to be caused by the uptake of calcium by the micelle.

II. ADSORPTION OF SURFACTANTS ON RESERVOIR MINERALS

A. Introduction

A complete understanding of the phenomenon of surfactant adsorption on reservoir rock minerals is of critical importance in enhanced oil recovery by micellar flooding. Our past work has demonstrated the complex nature of the surfactant adsorption on reservoir minerals. Specifically, adsorption tests using industrial, laboratory, and purified sulfonates on minerals such as Berea sandstone, limestone, and as-received and purified kaolinites showed adsorption to depend upon several system variables such as the nature and concentrations of surfactants and electrolytes, pH, temperature, and solid to liquid ratio. Such studies clearly revealed also the need for conducting tests with characterized surfactants and minerals in order to elucidate the mechanisms involved. During the current year most of the adsorption tests were therefore conducted using isomerically pure n-alkylbenzenesulfonates which were synthesized and characterized in our laboratory. Results for the adsorption of isomerically pure n-dodecylbenzenesulfonate on alumina as a function of surfactant

concentration, salinity, and temperature are included in this report. The studies on the effect of surfactant chain length on adsorption have also been initiated.

Adsorption of surfactants on reservoir minerals can be expected to be affected by oil which is present in the reservoir. Major emphasis was therefore placed during the current year on studying the effect of oil on the adsorption of surfactants on minerals. Effect of n-dodecane, a hydrocarbon oil, on the adsorption of n-dodecylbenzenesulfonate (n-DDBS) and n-decylbenzenesulfonate (n-DBS) on alumina has been tested as a function of surfactant concentration, salinity, solid to liquid ratio, and temperature. Most importantly, in all such tests, the uptake of oil by the solid has also been simultaneously determined. The study of the uptake of oil along with that of the surfactant is necessary because of the influence of the former on surfactant adsorption and the wettability of reservoir rocks. Moreover a complete understanding of the influence of oil on sulfonate adsorption is possible only if data for partitioning of the oil into various regions is available.

Investigation of the adsorption behavior of commercial sulfates on reservoir rock minerals was also

continued during the current year. Adsorption of Alipal Co-436 (an ethoxylated sulfate which is reported to have a high tolerance to multivalent ions and consequently a potential surfactant for micellar flooding) on Na-kaolinite and alumina was tested as a function of surfactant concentration and salinity. Additional tests to determine the adsorption behavior of this surfactant are in progress at present.

Since alcohol is used as a co-surfactant in micellar flooding, it is important to study the adsorption behavior of surfactants in the presence of alcohols also. We have currently initiated a study of the effect of alcohol on surfactant adsorption. Preliminary results obtained for the adsorption of n-dodecylbenzenesulfonate on alumina in the presence of n-propanol are discussed in this report.

B. Materials and Methods

Materials and Methods used in our investigation have been described in detail in earlier reports (1,2). Only the salient points are repeated here.

B1. MINERALS

B1a. Kaolinite

Homoionic Na-kaolinite prepared from well crystallized kaolinite samples purchased from the clay repository at the University of Missouri was used for adsorption tests. A detailed procedure for the preparation and characterization of homoionic Na-kaolinite is described elsewhere (1,2). Surface area of the kaolinite sample determined by the nitrogen adsorption technique was $9.0 \text{ m}^2/\text{g}$.

B1b. Alumina

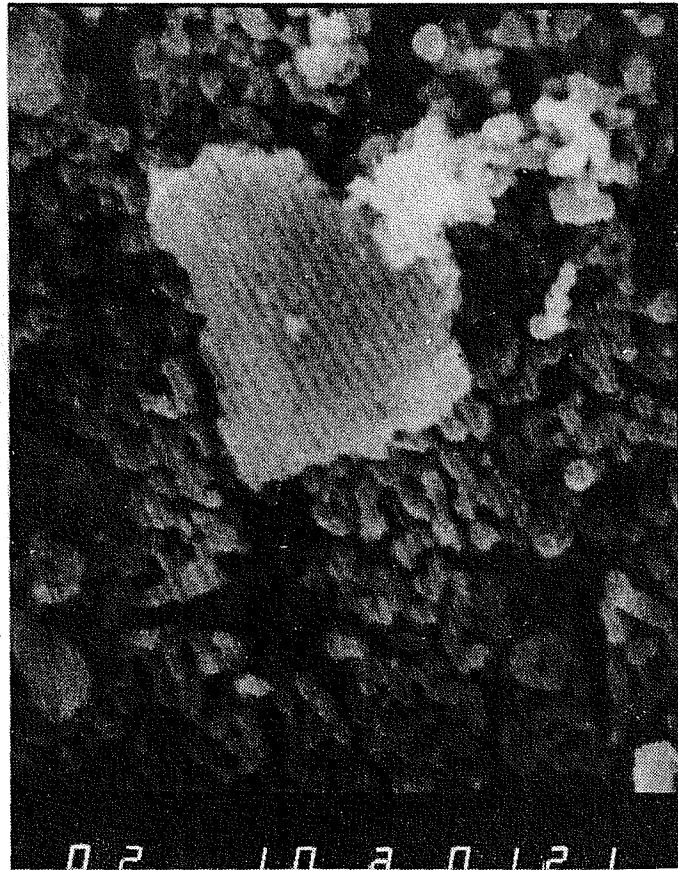
Alumina used in the present study was a Linde high purity sample obtained from Union Carbide Corp. The electron micrograph of the alumina sample given in Figure II:1 shows the irregular shape of the particles. The surface area determined by nitrogen adsorption was $15 \text{ m}^2/\text{g}$. Solubility of this sample was also measured under different solution conditions and is given in Figure II:2.

B2. SURFACTANTS AND OTHER CHEMICALS

B2a. n-Na alkylbenzenesulfonates *

n-Na dodecylbenzenesulfonate and n-Na decylbenzenesulfonate were synthesized, purified and characterized using procedures described elsewhere (see Section IIB3).

* Alkylbenzenesulfonates are given in the subsequent section, with a code VS-1. This indicates the batch number of synthesis and the person who synthesized it.



II:1. Electron Micrograph of Linde Alumina
Magnification (x10,000)

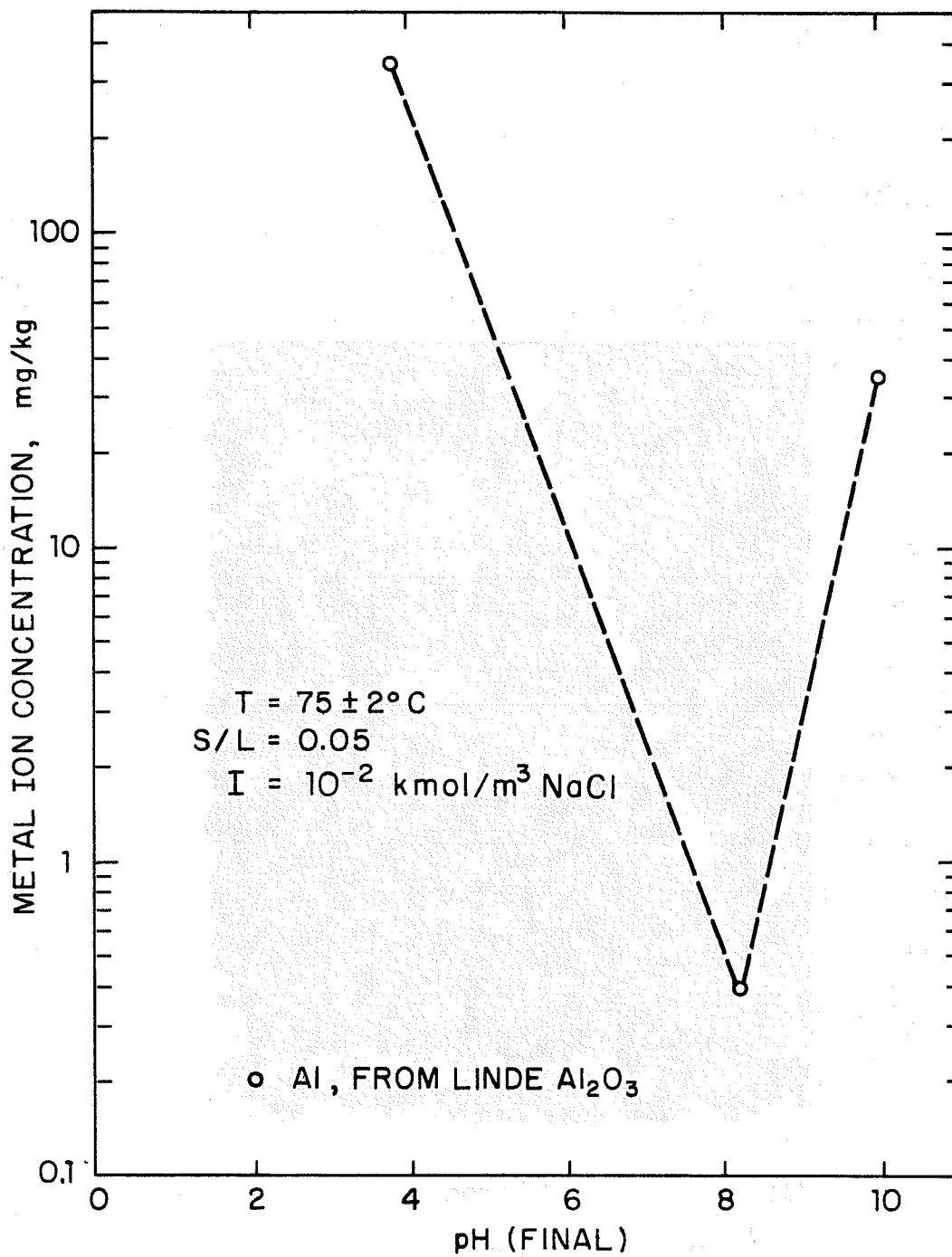


Figure II:2. Solubility of alumina at 75°C, as a function of pH.

B2b. Recrystallized Na dodecylbenzenesulfonate

Samples of Na dodecylbenzenesulfonate (>90% purity) purchased from Lachat Chemicals were purified by deoiling, recrystallization, and desalting techniques to obtain the recrystallized NaDDBS (see references 2,3 for a description of the procedure used).

B2c. ALIPAL[®] Co-436

This surfactant is an ammonium salt of sulfate ester of an alkyl (C_x) phenoxy poly (ethylene oxy)_y ethanol. The reported values (4) of x and y for this surfactant are 9 and 3 respectively. Equivalent weight of this surfactant is ~493 g.

B2d. Hydrocarbon Oils

n-dodecane (>99% pure) and n-phenyldecane (>97% pure) were purchased from Aldrich Chemicals Company, Inc. 1-phenyldodecane (>97% pure) was obtained from Pfaltz and Bauer. C-14 labelled n-dodecane (>99% pure) was purchased from ICN Chemicals.

B2e. Alcohols

n-propanol (ACS certified) was purchased from Fisher Scientific Co.

B2f. Inorganic Reagents

Inorganic reagents such as NaCl, NaOH and KOH were of ultrapure grade and were purchased from Aldrich Chemicals Company, Inc.

B2g. Water

Triple distilled water (conductivity $<10^6$ mhos) was used for preparation of all solutions.

B3. SYNTHESIS AND CHARACTERIZATION OF ISOMERICALLY PURE n-ALKYLBENZENESULFONATES

B3a. n-Na Dodecylbenzenesulfonate

The recrystallized NaDDBS, as discussed in our 1980 Annual Report, was a mixture of 1 ϕ , 2 ϕ , and 3 ϕ dodecylbenzenesulfonates. The separation of individual isomers from laboratory grade sulfonate was found to be difficult even with techniques such as liquid chromatography. Therefore, during the current year, an attempt was made to synthesize pure n-dodecylbenzenesulfonate. The procedure obtained from the Department of Energy* for the synthesis of n-decylbenzenesulfonate and 2-dodecylbenzenesulfonate was modified suitably for the synthesis of n-dodecylbenzenesulfonate.

Sulfonation of n-dodecylbenzene was carried out in a three-necked flask containing 60 g of n-dodecylbenzene and maintained at an initial temperature of 4°C by adding an equivalent amount of fuming sulfuric acid drop by drop into the system. The liquid in the reaction vessel was stirred continuously. The reaction

*Thomas E. Burchfield, private communication.

product solidified during the addition of H_2SO_4 and at that stage the temperature was raised to 30°C and the rest of the H_2SO_4 was added. After adding all the H_2SO_4 , temperature was raised to 55°C and it was maintained at that level for 90 minutes. Finally, the reaction product was cooled to 4°C and was neutralized using 20% NaOH and was left undisturbed over night. The precipitate thus obtained was washed, scrubbed with cold water (4°C), and then recrystallized from 40% ethanol solution and twice from triple distilled water.

The sulfonate prepared in the above manner was characterized using p-NMR, C-13 NMR, and mass spectrometry techniques. Principles of these techniques and the methods of interpretation of the results from such techniques were described in detail in the 1980 Annual Report (3). Only the spectra of the sulfonate prepared and the conclusions are included in this report.

For the purpose of characterization, sulfonate was converted to sulfonic acid and was analyzed using the above techniques. p-NMR, C-13 NMR, and mass spectra of this compound are given in Figures II:3-5. p-NMR and C-13 NMR results exhibited only those peaks expected for n-dodecylbenzenesulfonate and thus confirmed the absence of short chain, long chain, and isomeric impurities.

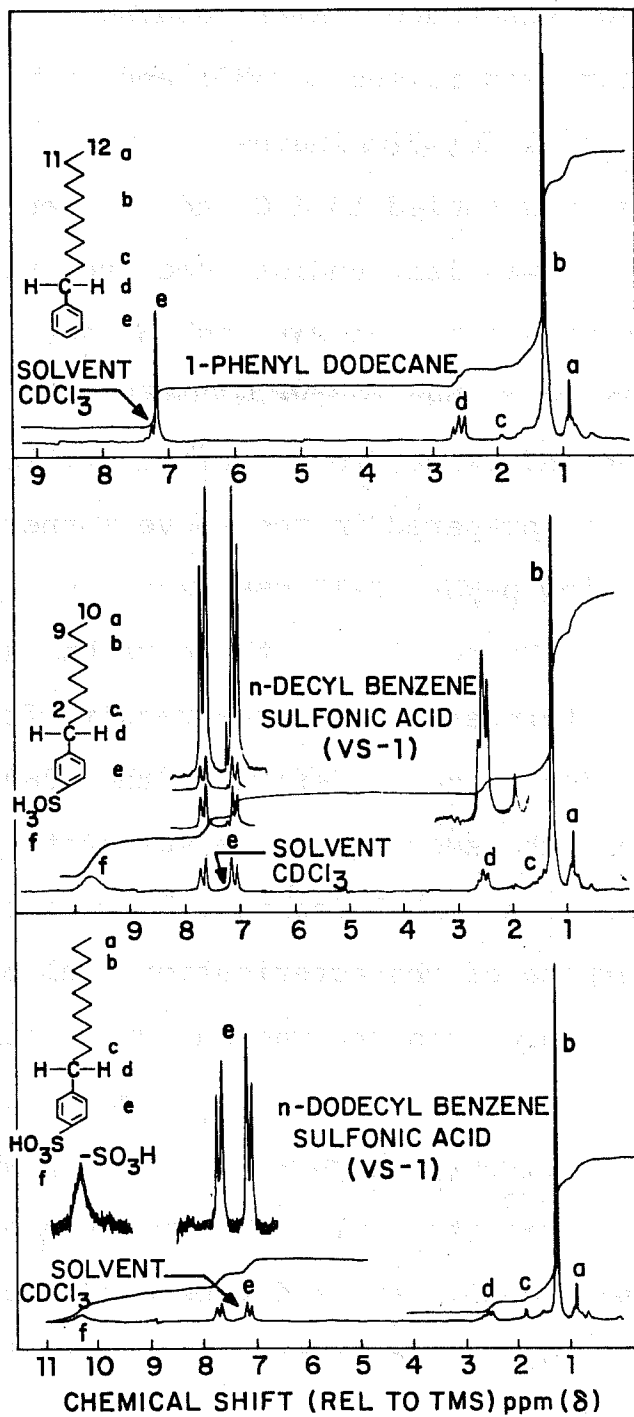


Figure II:3. Proton NMR spectrum of n-dodecane, n-NaDBS, and n-NaDDBS.

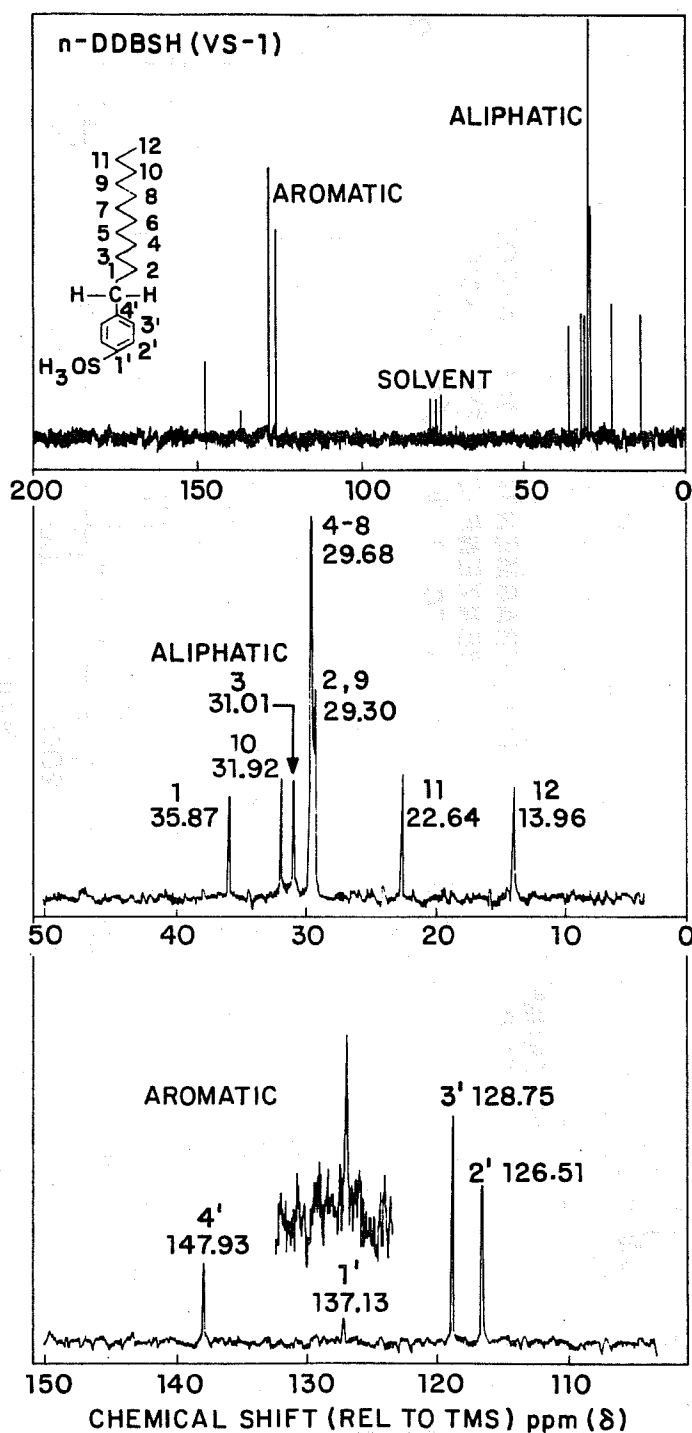


Figure II:4. Proton decoupled fourier transform ^{13}C H NMR spectrum of n-dodecylbenzene-sulfonic acid (70% by weight) in deuterio chloroform. Upper: full spectrum; Middle: expansion of alkyl region; Lower: expansion of aryl region.

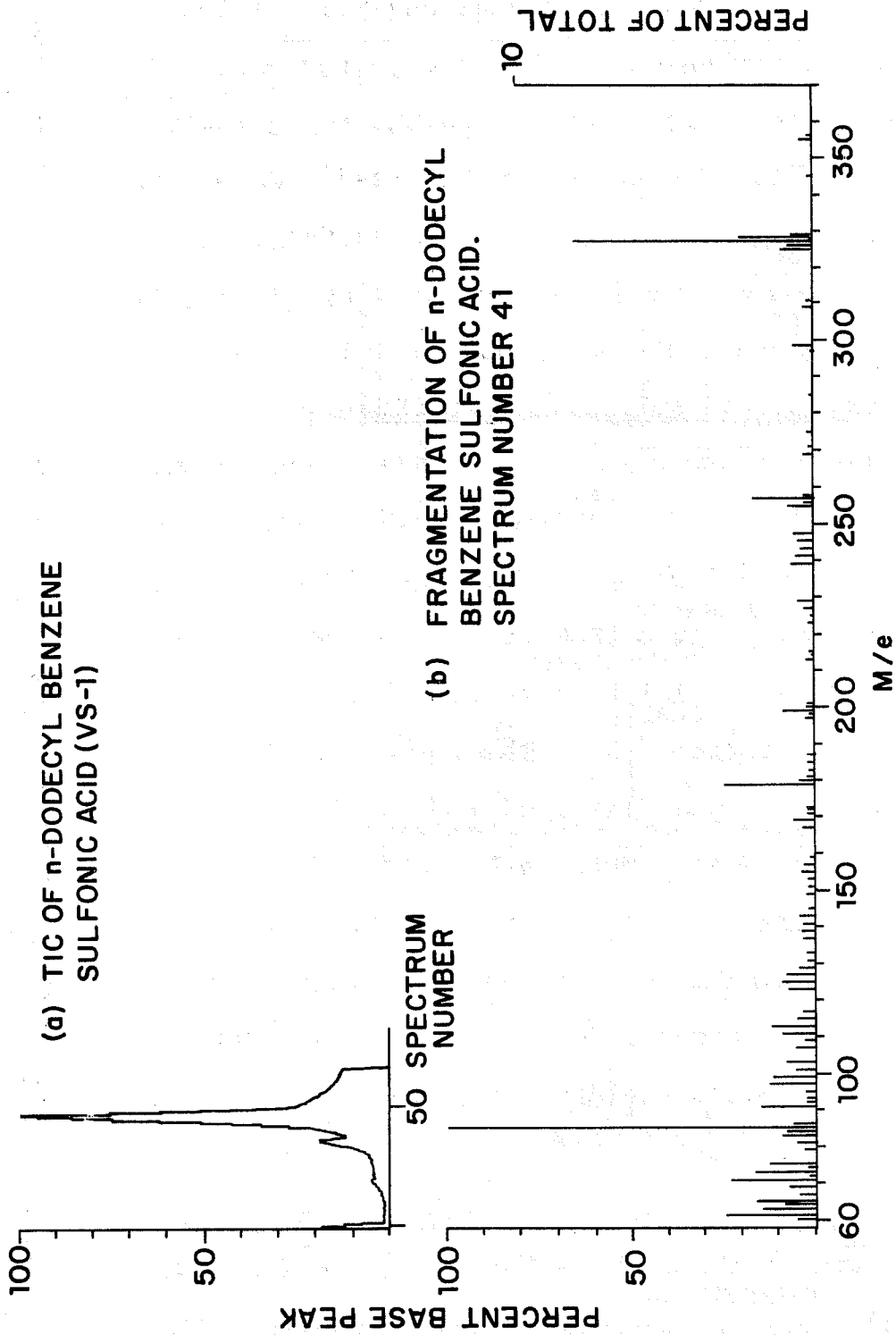


Figure II.5. TIC and fragmentation pattern of n-dodecylbenzenesulfonic acid (obtained by chemical ionization method).

Mass spectrometry showed the molecular weight of the sulfonate to be 349. Elemental analysis of the sulfonate was in agreement with the expected values for NaDDBS (see Table II:1). Based upon the above analysis, it was concluded that the synthesized n-NaDDBS is 98-99% isomerically pure. CMC of this sulfonate at 65°C was determined, using the conductivity technique, to be 1.2×10^{-3} kmol/m³ (see Figure II:6).

B3b. n-Na Decylbenzenesulfonate (n-NaDBS)

n-NaDBS was synthesized in a similar manner with minor modifications. The initial reaction temperature in this case was 75°C as opposed to the 5°C used in the case of n-DDBS preparation. Also, the solvent for recrystallization was a 1:1 mixture of ethanol and water. Final recrystallization, as in the case of n-DDBS was carried out from triple distilled water.

As in the case of n-DDBS, n-DBS was used in the sulfonic acid form for characterization purposes. p-NMR, C-13 NMR, and mass spectrometry results for n-DBS are given in Figures II:3,6,7-8. It was concluded from these results that the prepared sulfonate is isomerically pure (purity >98%).

CMC of this sulfonate at 65°C, as determined by the conductivity technique, is 3.4×10^{-3} kmol/m³ (see Figure II:6).

TABLE II:1

Results of Elemental Analysis of n-NaDDBS

Element	n-NaDDBS	Theoretical
C	61.85 ± 0.04	62.04
H	8.52 ± 0.02	8.39
S	9.11 ± 0.06	9.20
Na	6.38 ± 0.01	6.60
Subtotal	85.86 ± 0.13	86.23
O	14.24	13.77
Total	100.10	100.00

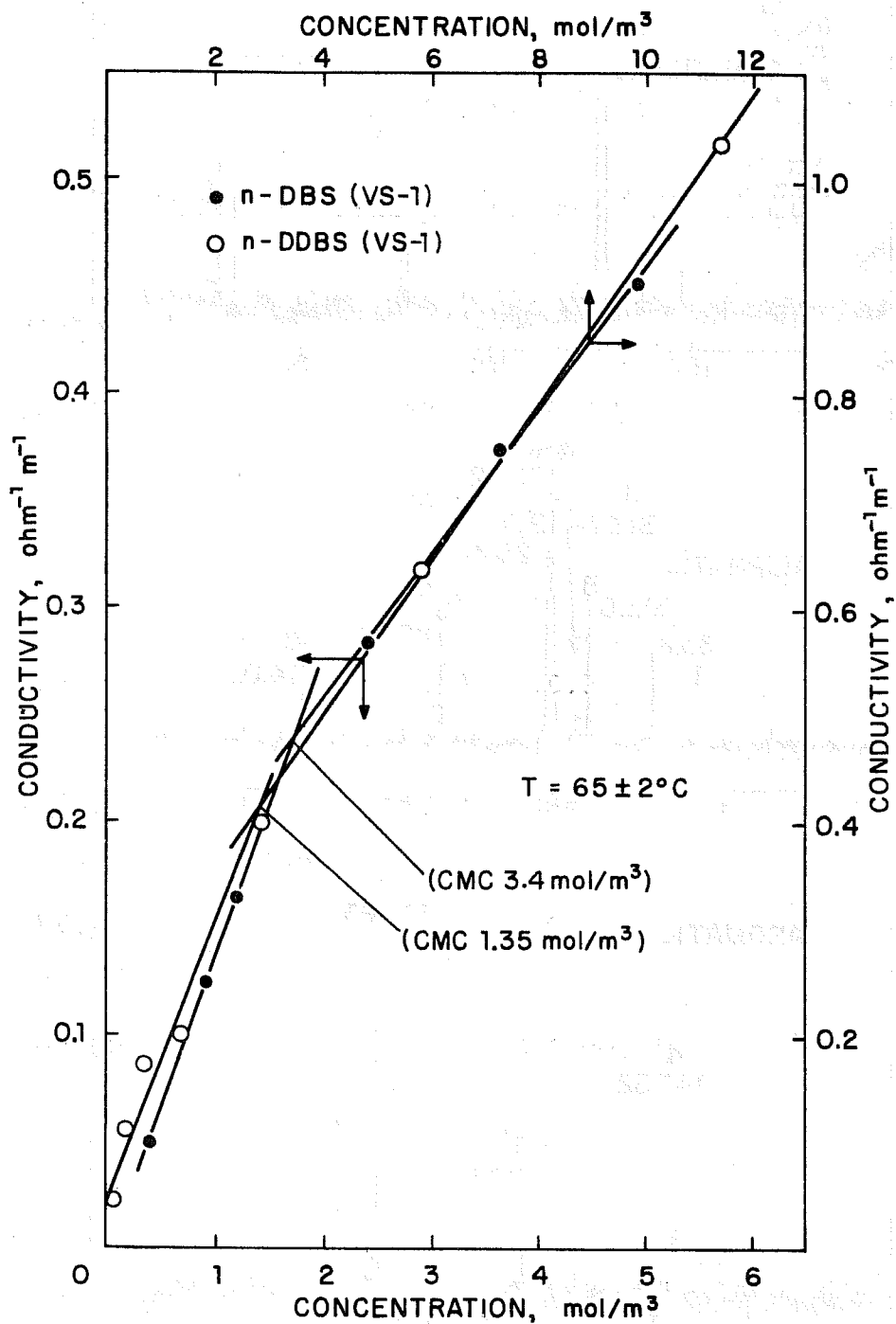


Figure II:6. Conductivity of n-NaDDBS and n-NaDBS as a function of concentration at 65°C

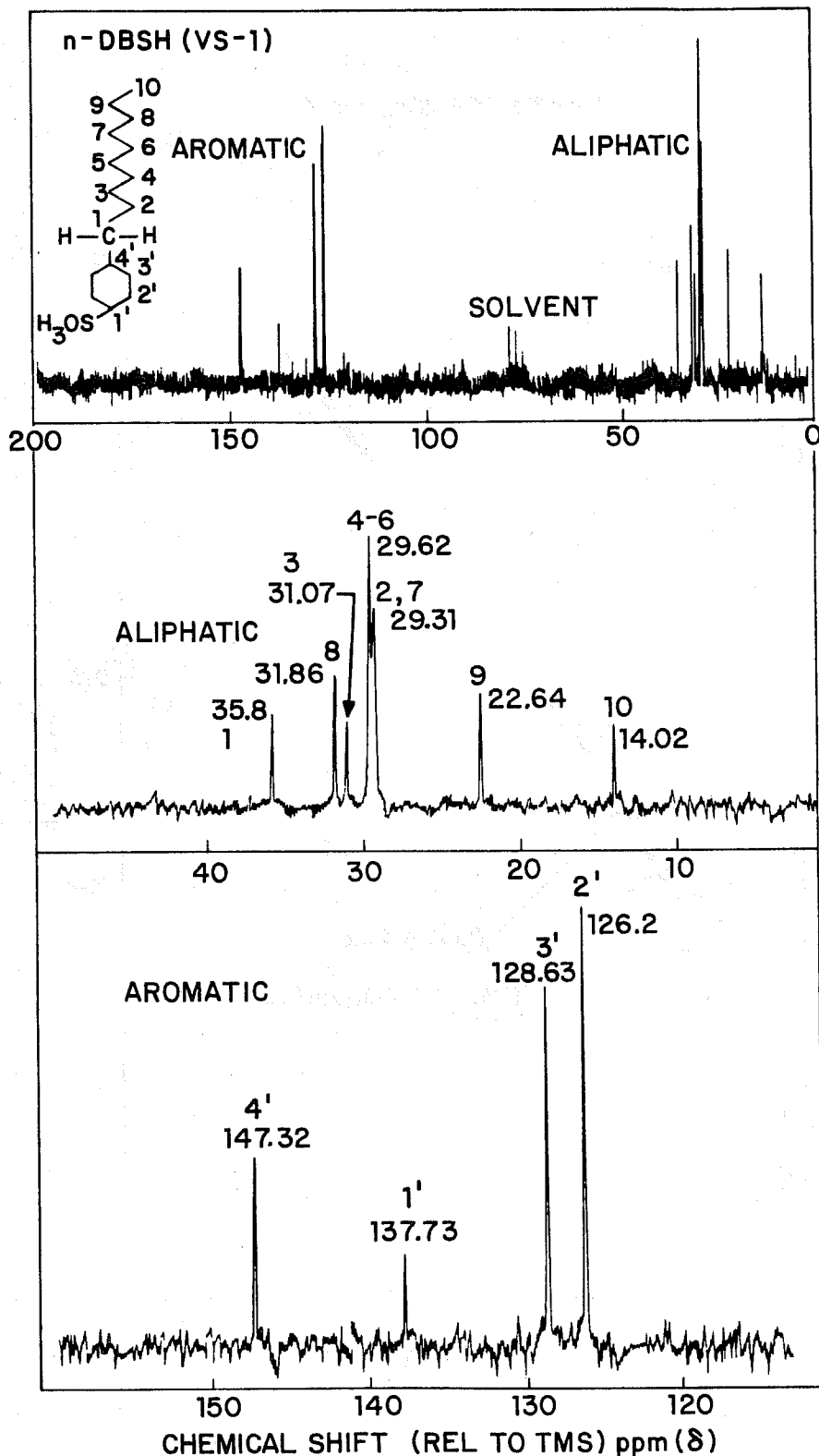


Figure II:7. Proton decoupled Fourier-transform ^{13}C H NMR spectrum of n-decylbenzene-sulfonic acid (70% by weight) in deuterio chloroform. Upper: full spectrum; Middle: expansion of alkyl region; Lower: expansion of aryl region.

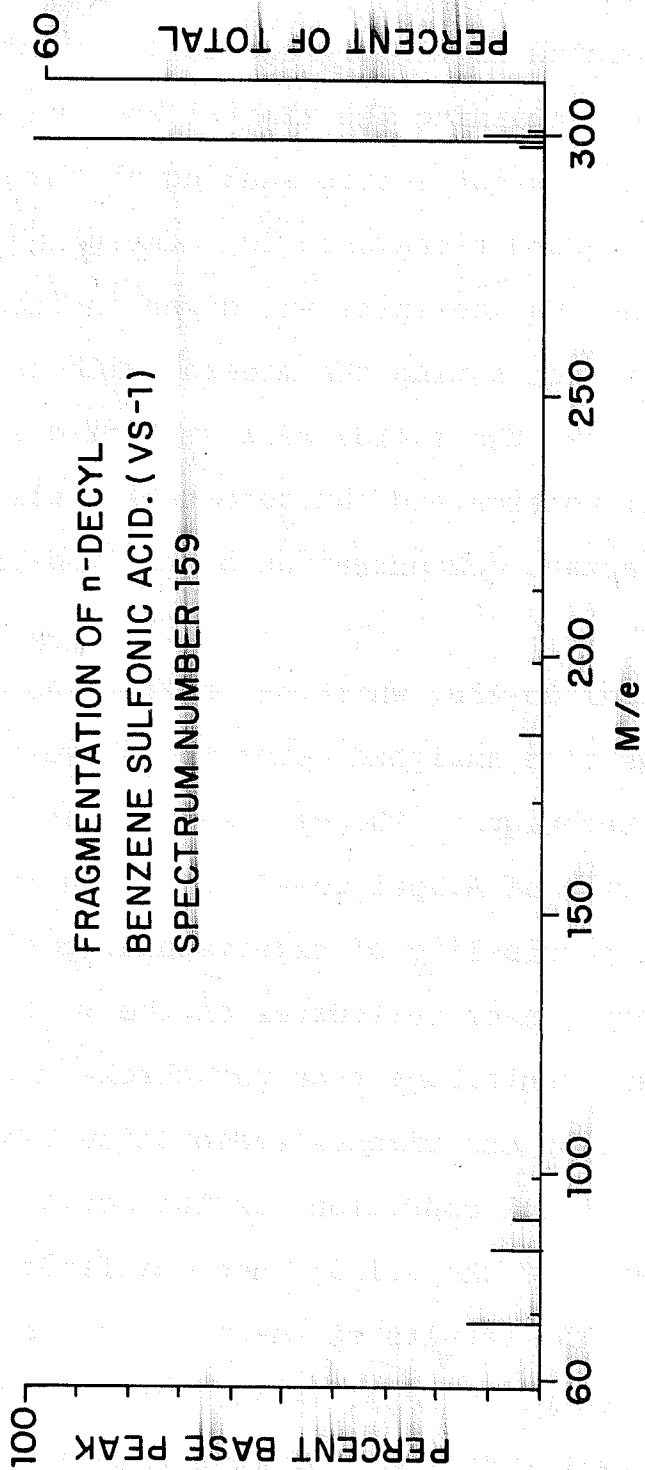


Figure II:8. Fragmentation pattern of n-decylbenzenesulfonic acid (obtained by chemical ionization method).

B4. ADSORPTION EXPERIMENTS

As during the preceding years, adsorption tests were conducted in tightly capped 5 dram vials (1-3). The vials containing the mineral and the reagents were subjected to wrist action shaking at the desired temperature. Conditions used for adsorption tests with alumina and Na kaolinite are given in Table II:2.

After contacting the mineral with reagents for the desired time, the solids were separated from the liquid by centrifugation and the supernatant was analyzed for its surfactant concentration by the two-phase titration technique (5).

Alipal Co-436, which has sulfate as the functional group was also analyzed using the above two phase titration technique. The calibration curve obtained for the analysis of Alipal Co-436 is given in Figure II:9.

The possibility of experimental artifacts due to the adsorption of sulfonates on the walls of the container and centrifuge tube was checked by conducting several blank experiments (adsorption tests conducted under identical conditions as the actual tests, but in the absence of the solid) under different solution conditions. The results of these tests did not indicate any such complications. Also there was no interference of hydrocarbon oils or polymers with the two-phase titration analysis of the sulfonate.

TABLE II:2

Experimental Conditions for Adsorption*

	Alumina	Na Kaolinite
Preconditioning time	1½ h	2 h
Conditioning time with surfactant	4 h	72 h
S/L ratio	0.05	0.2
Centrifugation time	1 h	$\frac{3}{4}$ h
Centrifugation speed	4,500 RPM	17,000 RPM
Natural pH	8.2 ± 0.2	5.1

*Centrifugation was done at the same temperature at which the adsorption tests were conducted.

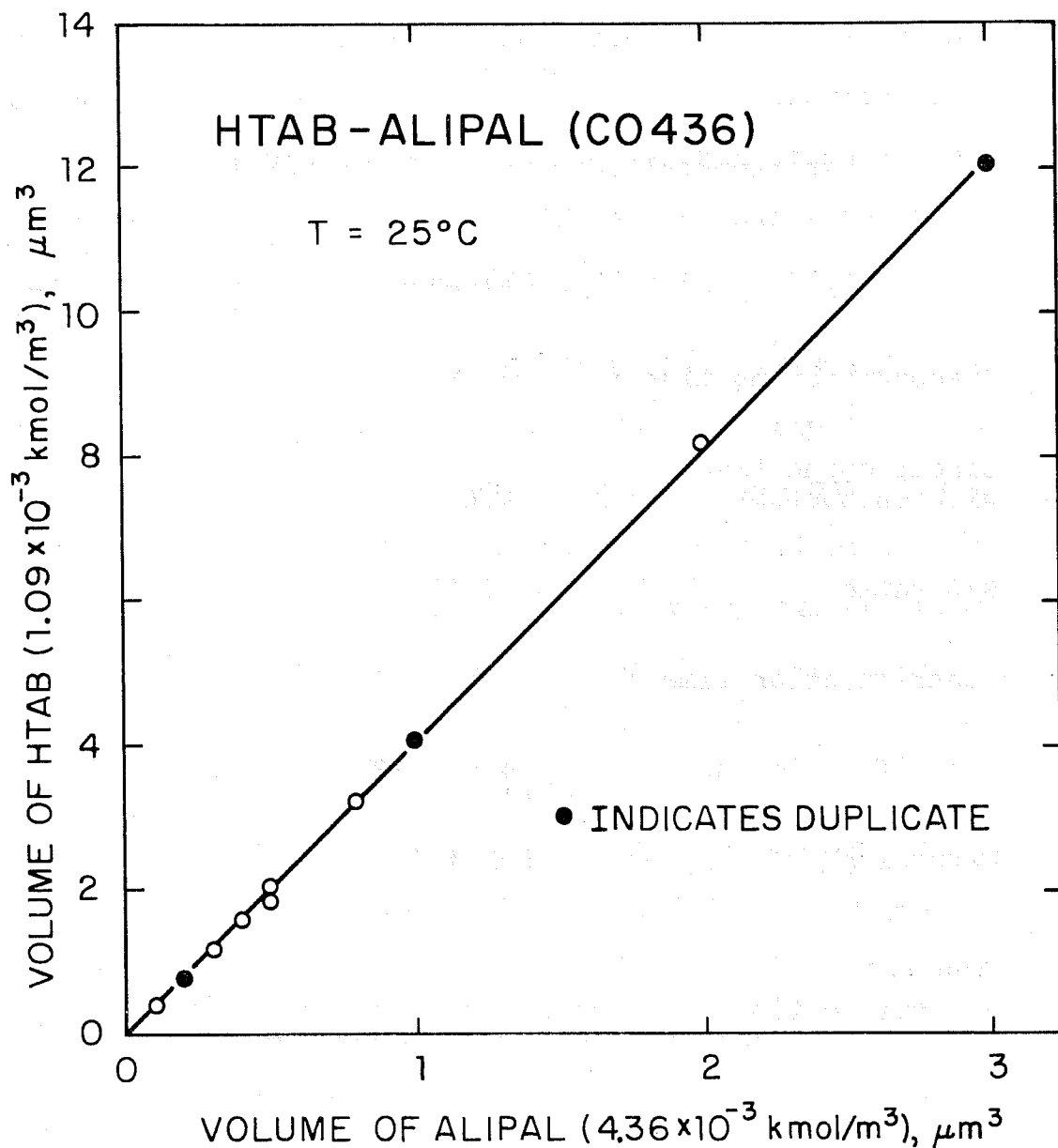


Figure II:9. Calibration curve for the titration of Alipal Co-436 with hexadecyl trimethyl ammonium bromide [HTAB].

Adsorption of n-NaDDBS and n-NaDBS were conducted at 65° and 75°C. The relatively low solubility of these isomerically pure sulfonates compared to that of the recrystallized sulfonate was one of the reasons for selecting higher temperatures for adsorption tests. Such tests are relevant also to practical systems because of the higher temperature of reservoirs.

B5. ADSORPTION TESTS IN THE PRESENCE OF OIL

Oil was introduced into the adsorption system following the procedure described below. Desired amount of oil (C-14 labelled) was pipetted into the surfactant solution and the mixture was subjected to ultrasonication for fifteen minutes. The resultant emulsion was used for adsorption tests. A sample of the emulsion was analyzed using the liquid scintillation counter to determine the initial concentration of oil. For determining the concentration of oil after adsorption tests, the supernatant was removed from the centrifuge tube, ultrasonicated, and analyzed using the liquid scintillation counter. The calibration curve for the oil is given in Figure II:10.

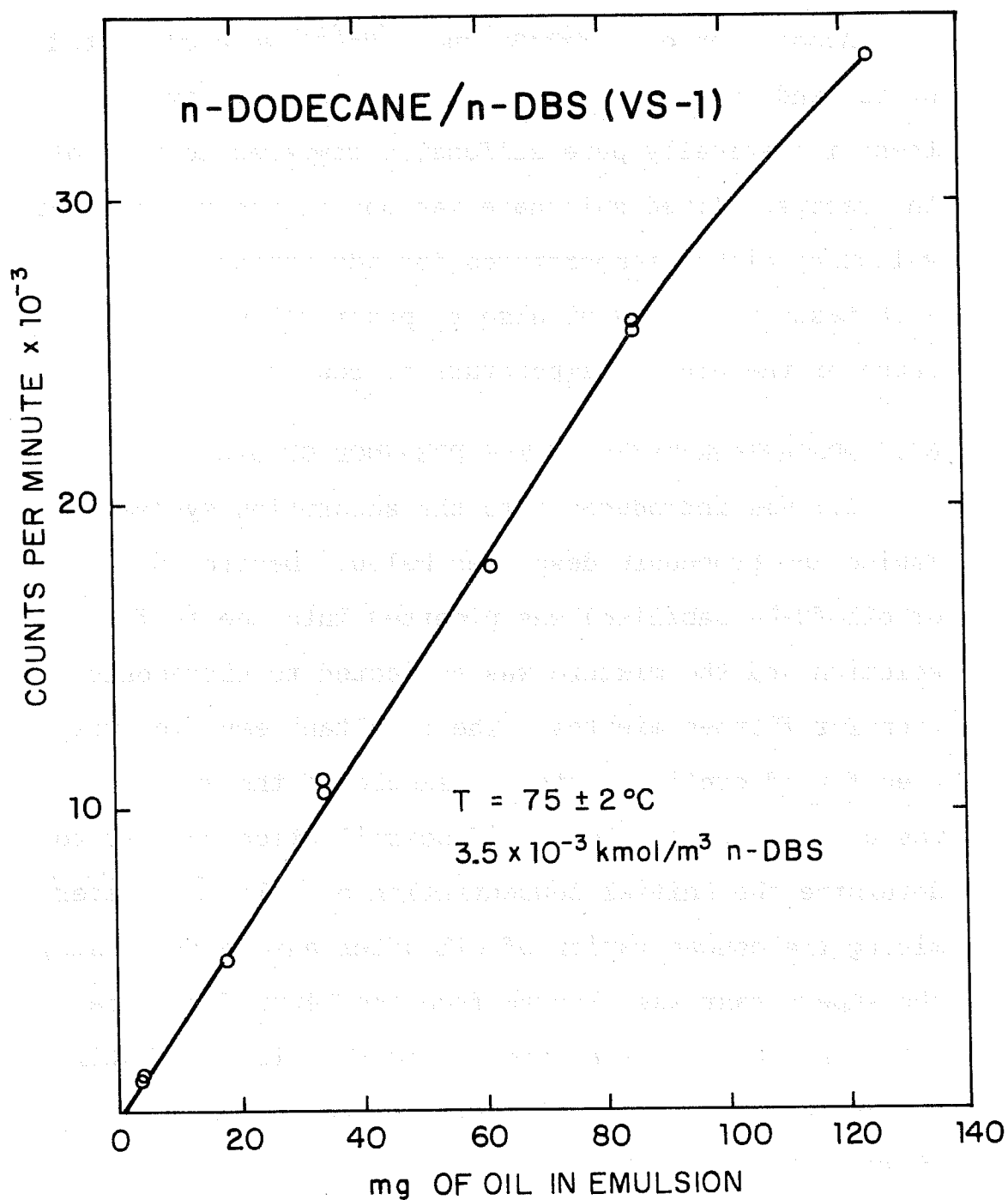


Figure II:10. Calibration curve for the estimation of n-dodecane by C-14 counting (using liquid scintillation technique).

C. Results and Discussion

C1. KINETICS OF ADSORPTION OF n-NaDDBS ON ALUMINA

Kinetics of adsorption of the isomerically pure n-NaDDBS on alumina was determined mainly for the purpose of establishing the contact time required for equilibration. Results obtained for sulfonate adsorption as a function of time at two levels of sulfonate (7×10^{-4} kmol/m³ and 5.5×10^{-3} kmol/m³) at 10^{-2} kmol/m³ NaCl are given in Figure II:11. It is evident from this figure that the equilibration time for adsorption is about 2 to 3 hours. In order to ensure the attainment of equilibrium a contact time of 4 hours was selected for all the experiments.

C2. KINETICS OF n-DODECANE UPTAKE BY ALUMINA IN n-NaDDBS SOLUTIONS

Results of the uptake of n-dodecane as a function of time at 2×10^{-3} kmol/m³ n-NaDDBS and at two levels of NaCl (0 and 10^{-1} kmol/m³) are given in Figure II:12. At 0 kmol/m³ NaCl oil uptake appears to increase even after 48 hours. In 10^{-1} kmol/m³ NaCl, however, oil uptake attained equilibrium in less than five hours. Since over 90% of oil uptake took place in less than 5 hours even in 0 kmol/m³ NaCl, a contact time of five hours was selected for all tests with oil.

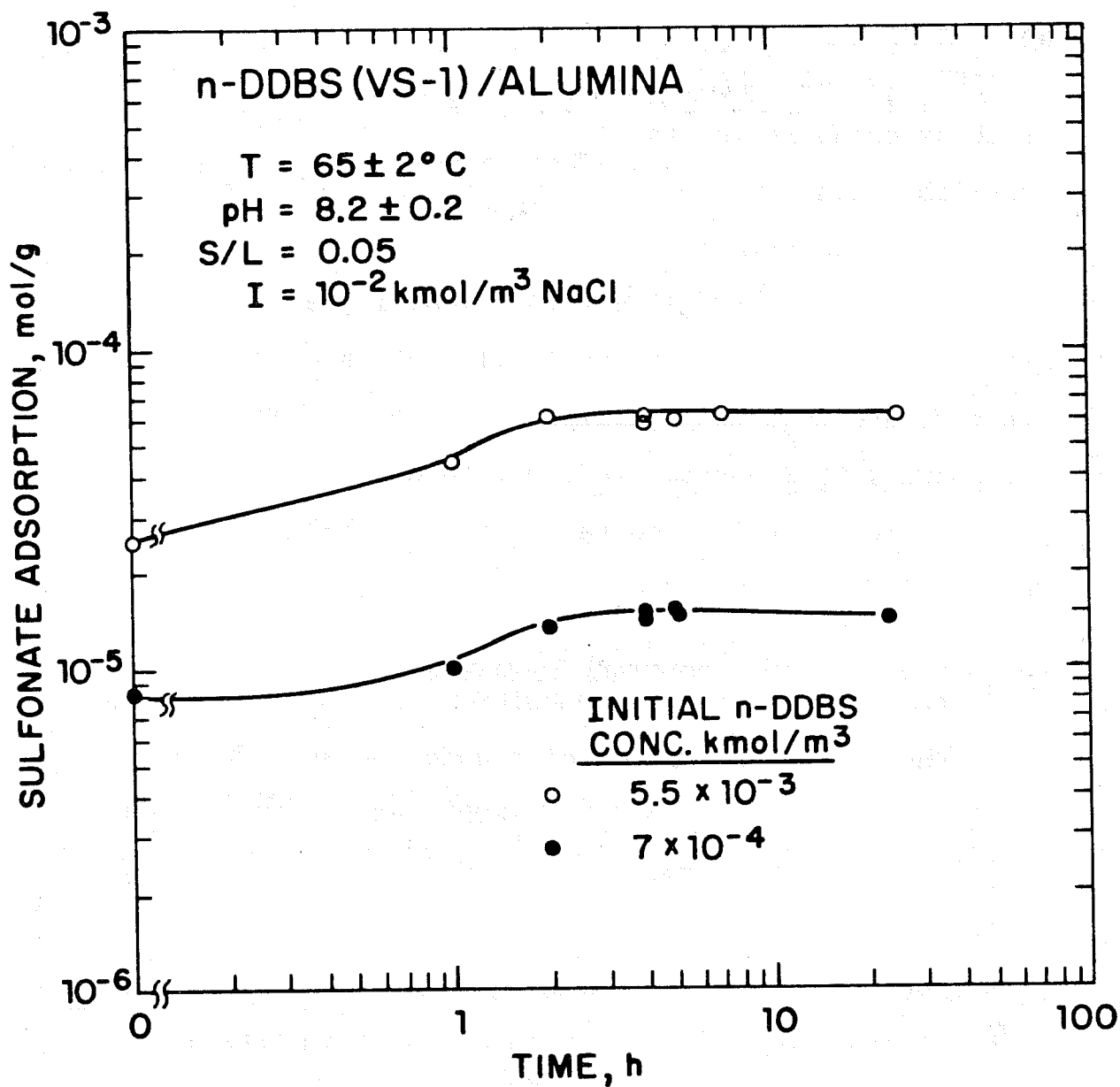


Figure II:11. Kinetics of Adsorption of n-DDBS on alumina at two levels of sulfonate, at $10^{-2} \text{ kmol/m}^3 \text{ NaCl}$.

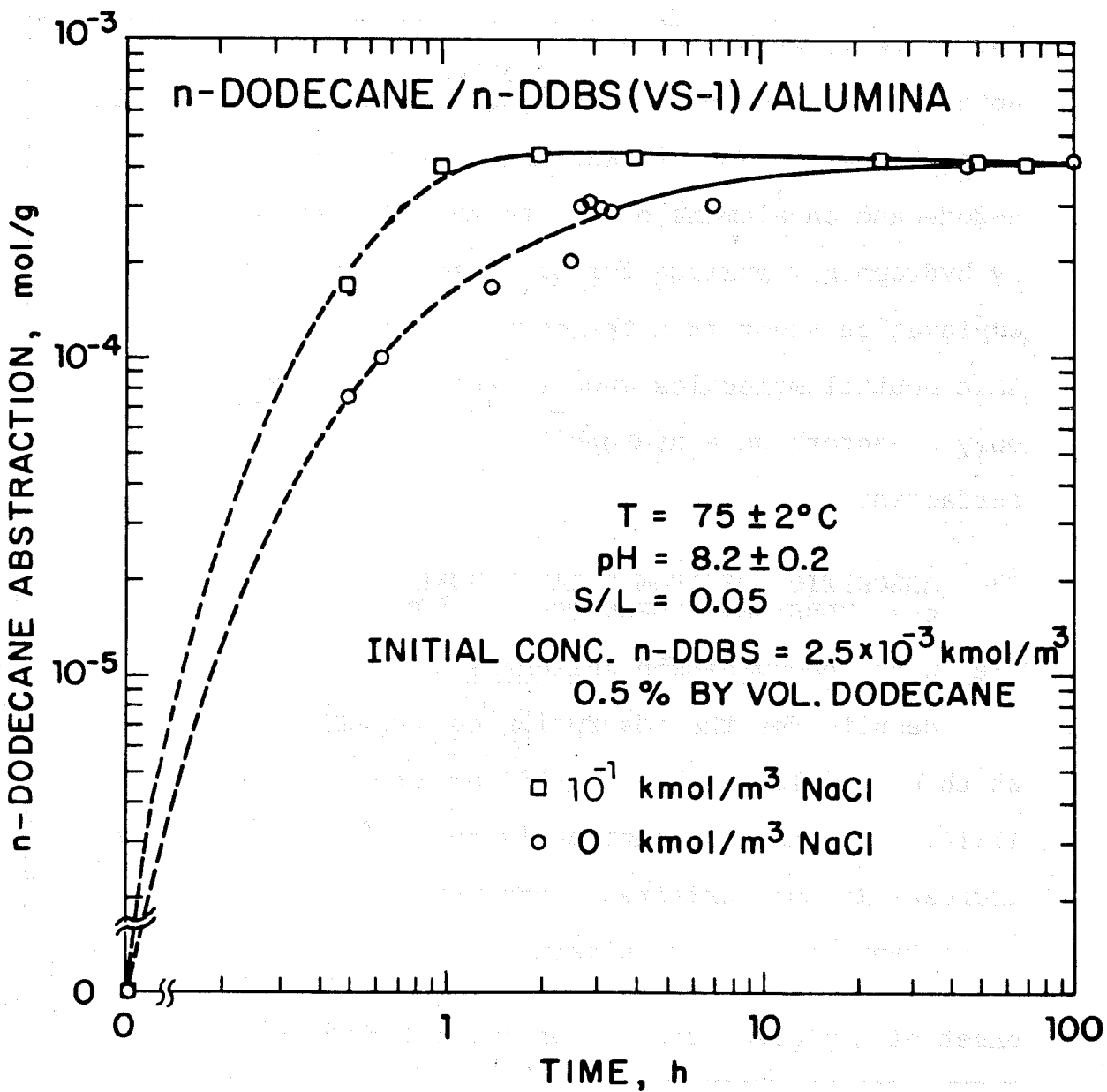


Figure II:12. Abstraction of n-dodecane as a function of time at two levels of NaCl.

A comparison of the kinetics of uptake of oil and adsorption of n-NaDDBS on alumina (see Figure II:13) shows that, while 75% of the equilibrium adsorption of sulfonate is attained in zero time*, no measurable uptake of oil is achieved during this time. This could be either due to the slower kinetics of adsorption of n-dodecane on alumina or due to the need for a partially hydrophobic surface for oil abstraction. The latter explanation stems from the currently accepted postulate that neutral molecules such as that of n-dodecane can only co-adsorb on a hydrophilic surface along with a surfactant.

C3. ADSORPTION OF ISOMERICALLY PURE n-ALKYLBENZENESULFONATES ON ALUMINA

C3a. n-Na Dodecylbenzenesulfonate

Results for the adsorption of n-NaDDBS on alumina at three levels of NaCl at 75°C are given in Figure II:14. Sulfonate adsorption is found to increase with increase in the surfactant concentration and to attain a constant value above a particular concentration. The onset of a plateau region, as evident from this figure,

* "Zero time implies zero mixing time followed by 1 hour of centrifugation. It is to be noted that there can be some adsorption during the addition of the solid to the surfactant solution as well as during centrifugation.

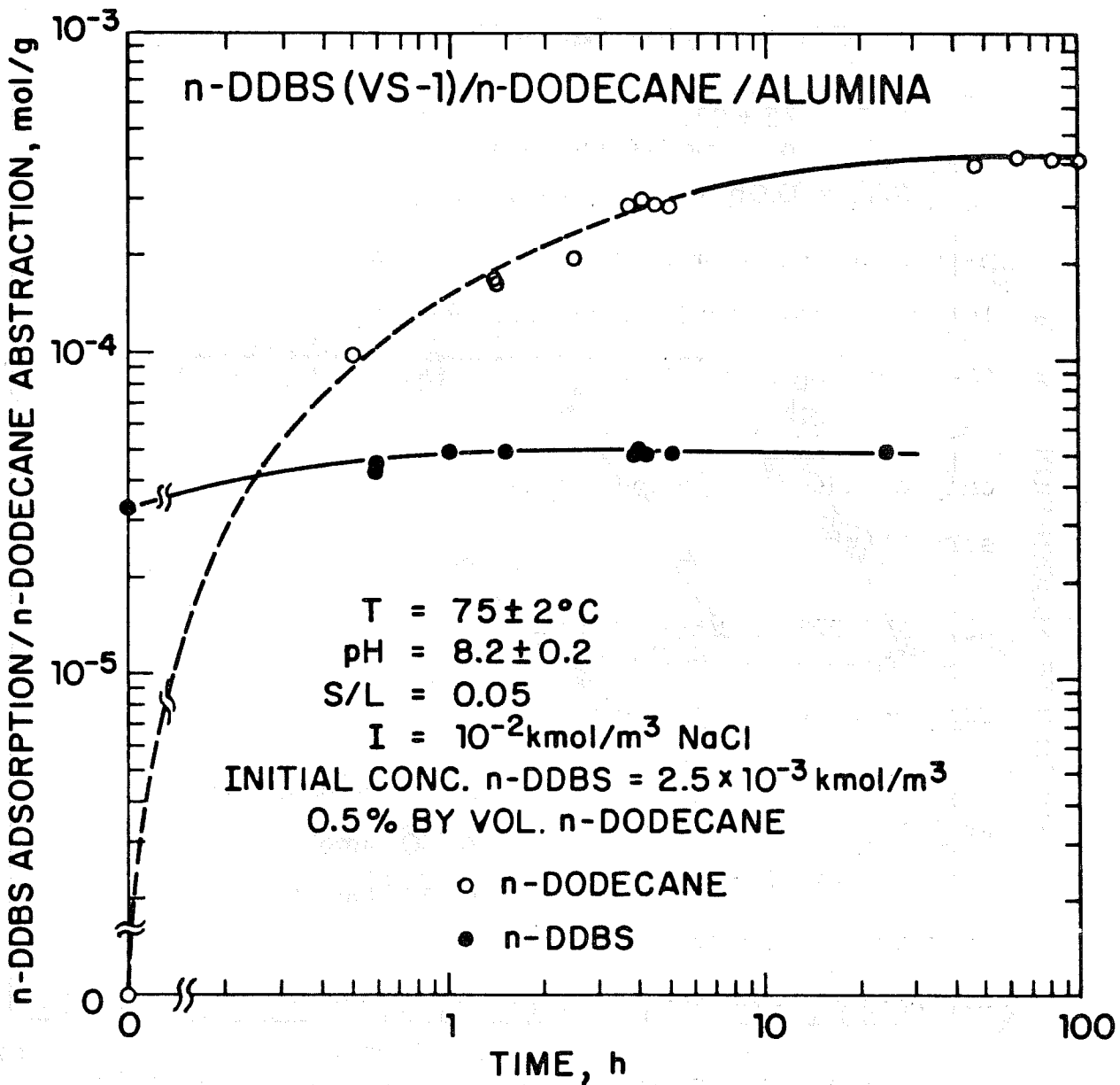


Figure II:13. Kinetics of abstraction of oil and adsorption of n-DDBS on alumina.

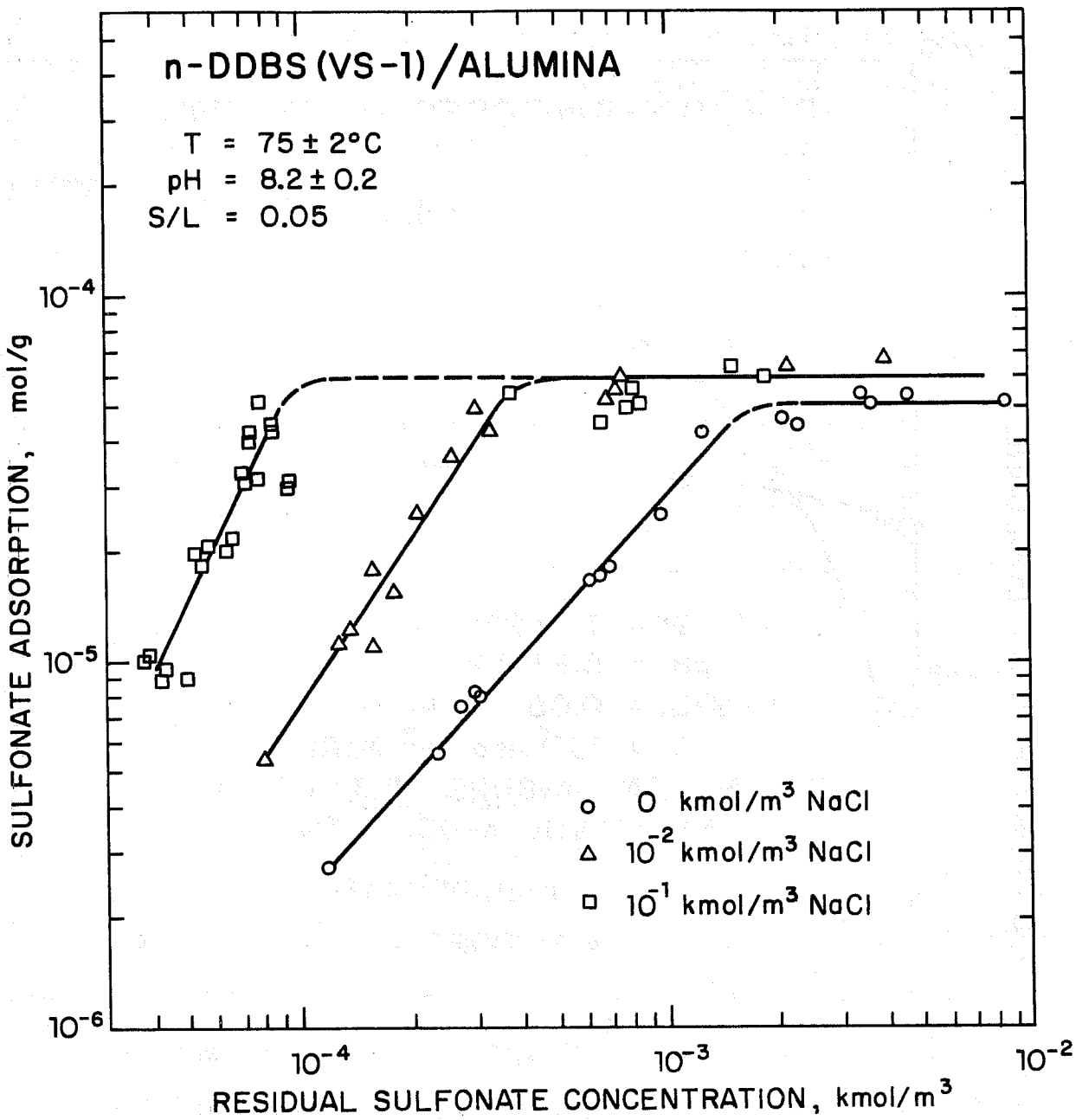


Figure II:14. Adsorption of n-DDBS on alumina at three levels of NaCl at 75°C .

shifts to lower sulfonate concentrations with increase in NaCl. Furthermore, increase in NaCl produced an increase in sulfonate adsorption, only in the rising part of the isotherm.

An increase in adsorption of sulfonate with increase in bulk concentration is in agreement with the Boltzmann distribution law,

$$c_s = c_b \exp\left(\frac{-\Delta G_{ads}^{\circ}}{RT}\right) \quad (1)$$

where c_s = concentration of surfactant in the interfacial region

c_b = concentration of surfactant in the bulk

R = Gas Constant

T = Absolute Temperature

ΔG_{ads}° , the free energy of adsorption, is given by

$$\Delta G_{ads}^{\circ} = \Delta G_{elec}^{\circ} + \Delta G_{chain-chain}^{\circ} + \Delta G_{solv}^{\circ} + \Delta G_H^{\circ} + \dots \quad (2)$$

The total free energy of adsorption is a sum total of contributions arising from factors such as electrostatic interaction, chain-chain interaction, solvation and desolvation of the surface and the adsorbate species, hydrogen bonding, etc. In the present system, under the tested pH conditions, the alumina surface is positively charged, hence electrostatic forces would play a major role in determining the sulfonate adsorption. This

mechanism has been discussed earlier for the adsorption of dodecylsulfonate on alumina (6). In addition to electrostatic forces, lateral interaction among the adsorbed surfactants (hydrophobic chain-chain interaction) was also considered to contribute towards enhanced sulfonate adsorption above a certain concentration (6). The two-dimensional surfactant aggregates resulting from such chain-chain interaction were referred to as hemi-micelles, since this process is analogous to the formation of surfactant micelles in solution. The hemimicellization which occurs at surfactant concentrations that are about two orders of magnitude lower than the CMC is accompanied by a marked increase in the slope of the adsorption isotherm. Presence of such regions in the adsorption isotherm for the n-DDBS/alumina system can be ascertained only after the data that would adequately cover the dilute sulfonate concentration region is determined. Additional adsorption tests are now being conducted for this purpose at lower sulfonate concentrations. Since the hemimicellization phenomenon has been studied and analyzed thermodynamically in detail in the past (6) it is not further discussed here.

Plateau Region. Constant adsorption density regions, such as those given in Figure II:14, can result from either the saturation of the solid/liquid inter-

face, or the attainment of a constant activity for the adsorbate species. Since the onset of plateau at all three levels of the NaCl region was found to coincide with the CMC of the surfactant as determined by the dye solubilization technique, the plateau region in this system is attributed to the constant activity of the sulfonate monomers.

Effect of NaCl. The increase in ionic strength is found to increase sulfonate adsorption at all sulfonate concentrations studied (see Figure II:14). Changes in ionic strength can be expected to affect surfactant adsorption due to (a) the compression of the electrical double layer and resultant decrease in the electrostatic potential for sulfonate adsorption and (b) the increase in the effective concentration of sulfonate in the system, this increase being due to the solvation of Na^+ and Cl^- ions and the resultant decrease in the solvent power of water. While the former effect is to decrease the adsorption, the latter is to increase it at any given level of sulfonate. The net effect in the present case is evidently to increase the adsorption. These opposing effects are being treated quantitatively using suitable models.

It is to be noted that the decrease in surface tension and CMC of surfactant solutions upon adding

NaCl is also due to a similar decrease in the solvent power of the medium and the consequent "salting out" of the surfactant. In this case ionic strength further enhances the adsorption by reducing the electrostatic repulsion in the monolayer.

C3b. n-Na Decylbenzenesulfonate

Adsorption tests using n-NaDBS are the first in a series of experiments designed to investigate the effect of chain length and branching of surfactants on adsorption. This investigation is of major practical and fundamental importance for the following reasons:

(a) Most of the commercial sulfonates being considered for micellar flooding are mixtures of sulfonates of different chain lengths and branching. In order to understand the behavior of such mixtures, pure sulfonates of different chain length, branching, etc., should be investigated individually as well as in synthetic mixture forms. The study of the effect of the chain length is a first step in that direction.

(b) From a fundamental point of view, the effect of chain length on adsorption can yield information on the hydrophobic interactions involved. Similar data for alkylsulfonates, alkylammoniumchlorides and perfluoro hydrocarbons have been obtained in the past (7-9). Results for the adsorption of n-DBS on alumina

at 75°C are given in Figure II:15. Adsorption, similar to that of n-DDBS, is found to increase up to a certain concentration above which it remained constant. Sulfonate concentration at the onset of plateau, as detected by the dye test, again corresponded to the CMC of the system. The effect of the increase in NaCl at any given sulfonate concentration is to increase the sulfonate adsorption and to shift the onset of the plateau region to lower sulfonate concentrations. These are again in agreement with the results (Quarterly Report, December, 1980) for n-DDBS discussed earlier (see Figure II:14).

C3c. Chain Length Effect and Free Energy of Hemimicellization

Comparison of the results for adsorption of n-DDBS and n-DBS on alumina given in Figure II:16 shows that the adsorption of n-DDBS is significantly higher than that for n-DBS. These observations are in agreement with the expected surface activities C_{12} and C_{10} sulfonates. It is possible to use this data to evaluate the contribution of $-\text{CH}_2-$ groups to the free energy of adsorption in the following manner. For sulfonate/alumina system (6,7),

$$c_s = c_b \exp \left(- \frac{Ze\psi_\delta + n\phi}{kT} \right) \quad (3)$$

where Z = valency of the adsorbate species

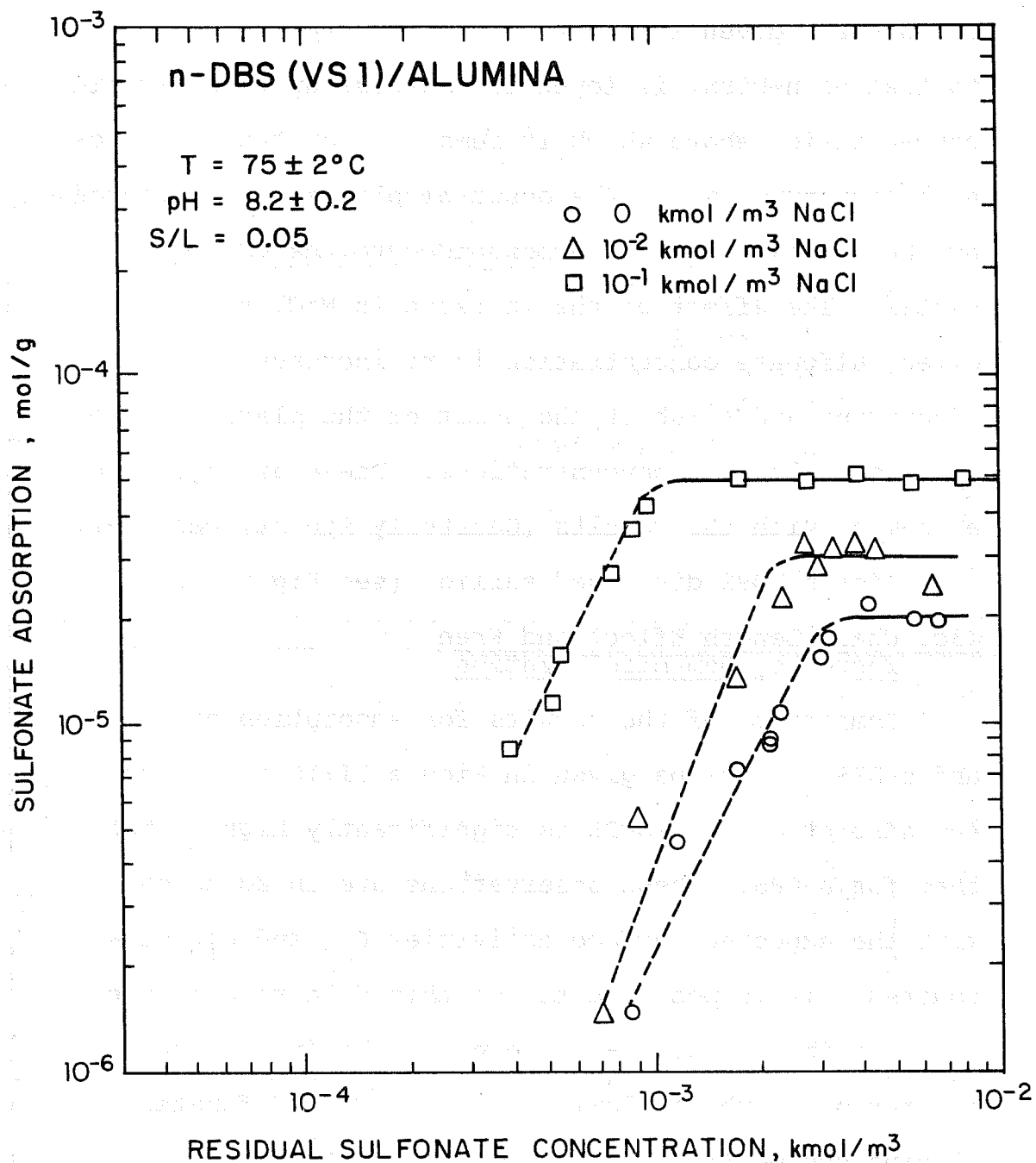


Figure II:15. Adsorption of n-DBS on alumina at three levels of NaCl at 75°C.

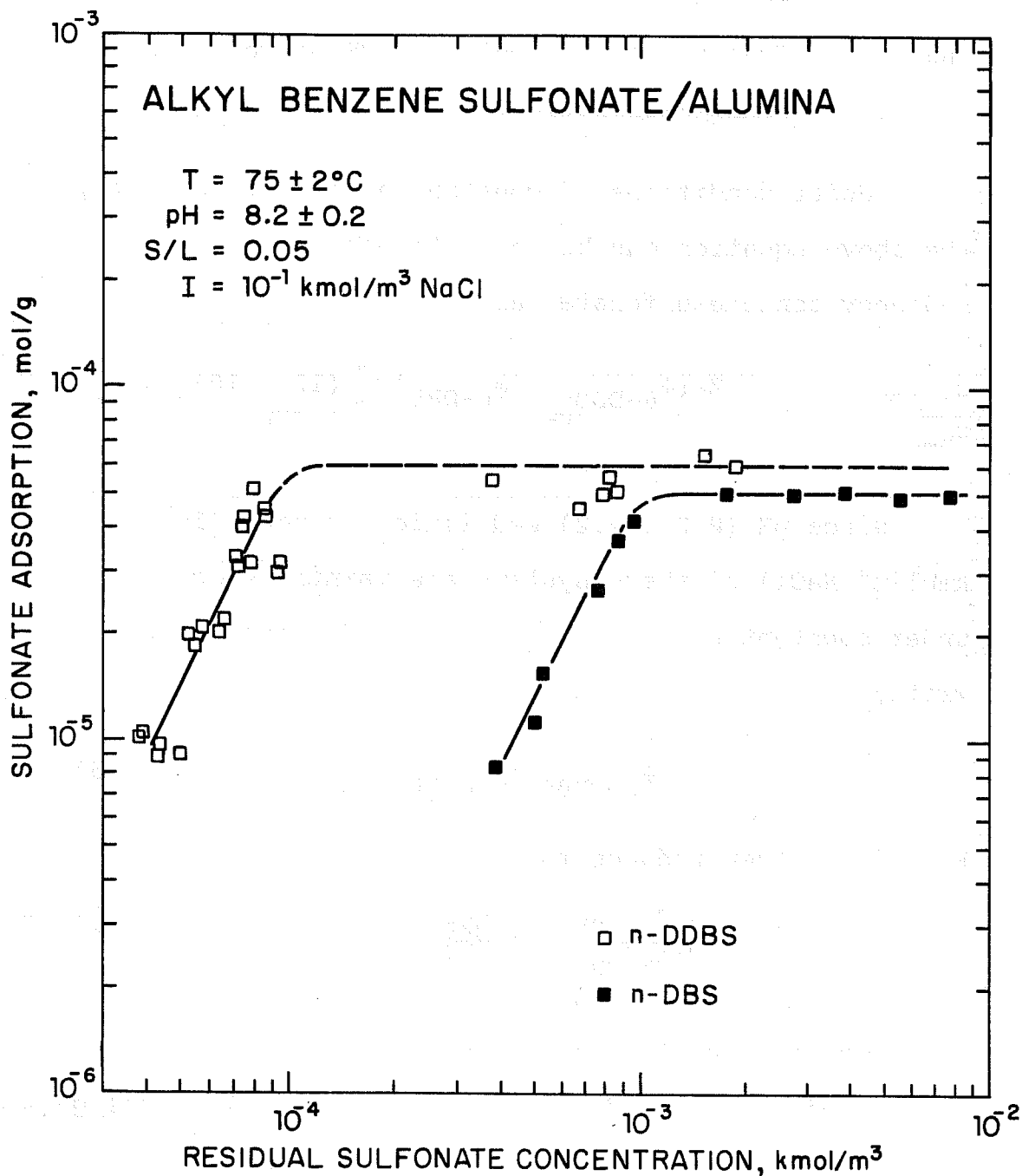


Figure II:16. Effect of chain length of alkylbenzenesulfonates on their adsorption on alumina at $10^{-1} \text{ kmol/m}^3 \text{ NaCl}$ at 75°C .

e = fundamental unit of charge

ψ_{δ} = Stern layer potential

n = number of straight chain alkyl groups in the surfactant

and ϕ = free energy per mole of $-\text{CH}_2-$ groups for hemimicellization.

Under conditions of constant adsorption density, the above equation can be rewritten for n -decyl and n -dodecylbenzenesulfonates as

$$\frac{C_{\text{b-DDBS}}}{C_{\text{b-DBS}}} = \exp \left[\frac{Ze(\psi_{\delta\text{-DDBS}} - \psi_{\delta\text{-DBS}})}{kT} + \frac{(12 - 10)\phi}{kT} \right] \quad (4)$$

Since pH (8.2 ± 0.2) and ionic strength (10^{-1} kmol/m³ NaCl) of these systems are maintained constant, under constant adsorption density conditions one can write,

$$\psi_{\delta\text{-DDBS}} = \psi_{\delta\text{-DBS}} \quad (5)$$

Equation 4 then reduces to

$$\ln \left[\frac{C_{\text{b-DDBS}}}{C_{\text{b-DBS}}} \right] = \frac{+2\phi}{kT} \quad (6)$$

Substituting the values for bulk concentrations corresponding to an adsorption density, $\Gamma = 10^{-5}$ mol/g (see Figure II:16),

$$\phi = -1.1 \text{ kT per } -\text{CH}_2- \text{ group}$$

$$\equiv -758 \text{ cal/mol } -\text{CH}_2- \text{ group}$$

This value for free energy contribution per $-\text{CH}_2-$ group (1.1kT) is in excellent agreement with the value reported by Somasundaran et al (6,7) for alkyl sulfonate adsorption on alumina.

C3d. Plateau Adsorption-Comparison Between n-NaDDBS and n-NaDBS

A comparison of the plateau adsorption of n-NaDDBS and n-NaDBS on alumina shows that the effect of NaCl on the saturation adsorption is more pronounced in the case of n-DBS than in that of n-DDBS (see Figures II:14,15). This might possibly be due to the relatively high surface coverage by surfactant at 0 NaCl itself in the case of n-DDBS as a result of which any increase in coverage with increase in NaCl is not significant. This is supported by the consideration that the sulfonate adsorption for a monolayer coverage on alumina assuming a parking area of 30\AA^2 for sulfonate is about 8.5×10^{-5} mol/g. The plateau adsorption at 0 kmol/m³ NaCl in the case of n-DDBS is about 5×10^{-5} mol/g. The plateau adsorption density in the case of n-DBS at 0 NaCl is, however, only 2×10^{-5} mol/g, which is much lower than that required for saturation adsorption. Since more sulfonate can be accommodated on alumina surface in the case of n-DBS,

the increase in plateau adsorption with increase in NaCl is sufficiently pronounced in this case.

C4. EFFECT OF OIL ON SURFACTANT ADSORPTION AND THE UPTAKE OF OIL

Results obtained for the adsorption of n-NaDDBS and n-NaDBS on alumina in the presence of n-dodecane and for the uptake of n-dodecane under the same conditions are given in Figures II:17-20. Major conclusions from these data are: (see also Table II:3)

(a) The shape of the sulfonate adsorption isotherms in the presence of oil is similar to that in the absence of oil.

(b) Increase in ionic strength increased the sulfonate adsorption and shifted the onset of the plateau region to lower concentrations.

(c) Adsorption of n-dodecane at a bulk concentration of 0.5% (vol), exhibited a minimum as a function of n-NaDDBS concentration. No such minimum was observed when the bulk oil concentration was 2.5% (vol). Also, in the presence of n-NaDBS, even at 0.5% (vol) n-dodecane no minimum was observed as a function of surfactant concentration.

(d) In most cases, surfactant concentration corresponding to onset of decrease in oil uptake is slightly lower than the onset of plateau region in the sulfonate adsorption isotherm (see Table II:3b).

TABLE II: 3a

PLATEAU ADSORPTION OF SULFONATE ON ALUMINA

SURFACTANT		PLATEAU ADSORPTION mol/g x 10 ⁵		
		0 kmol/m ³ NaCl	10 ⁻² kmol/m ³ NaCl	10 ⁻¹ kmol/m ³ NaCl
n-DDBS 75°C	No Oil	5.0	6.0	5.6
	n-Dodecane (0.5% by vol)	5.0	7.0	7.5
n-DBS 75°C	No Oil	2.0	3.2	5.2
	n-Dodecane (0.5% by vol)	2.0	3.3	5.2
n-DDBS 65°C	No Oil	5.2	5.4	-
	n-Dodecane (0.5% by vol)	5.4	8.0	16.0

TABLE II:3b

BREAK POINTS IN SULFONATE ADSORPTION AND n-DODECANE ABSTRACTION
ISOTHERMS* (solid-alumina)

SURFACTANT			SULFONATE CONCENTRATION AT BREAK POINTS, kmol/m ³ x 10 ⁴		
			0 kmol/m ³ NaCl	10 ⁻² kmol/m ³ NaCl	10 ⁻¹ kmol/m ³ NaCl
n-DDBS 75°C	No Oil	onset of plateau	17	4 (3.8)	1 (0.95)
	n-Dodecane (0.5% vol)	onset of plateau	12 (10)	8 (7.25)	1.5 (0.85)
	" "	onset of decrease in oil uptake	7.5	2-3	0.75-0.8
	" "	minimum in oil uptake	15	6-15	1.2
n-DBS 75°C	No Oil	onset of plateau	32 (29)	24 (22)	11 (10)
	n-dodecane (0.5% vol.)	onset of plateau	38 (37)	32 (28)	7 (7.3)
	" "	onset of decrease in oil uptake	35-38	24	8-15
	" "	minimum in oil uptake	-	-	-
n-DDBS 65°C	No Oil	onset of plateau	12-13	3.2-5	
	n-dodecane 0.5% vol.	onset of plateau	12	8-10.5	2.3
	" "	onset of decrease in oil uptake	2.5-5	1.5-3	1.3-2
	" "	minimum in oil uptake	12-15	6	1.8-3

*Numbers in the bracket indicate points of intersection of plateau and rising part of isotherm. Whenever the break point is not clear, a range is indicated.

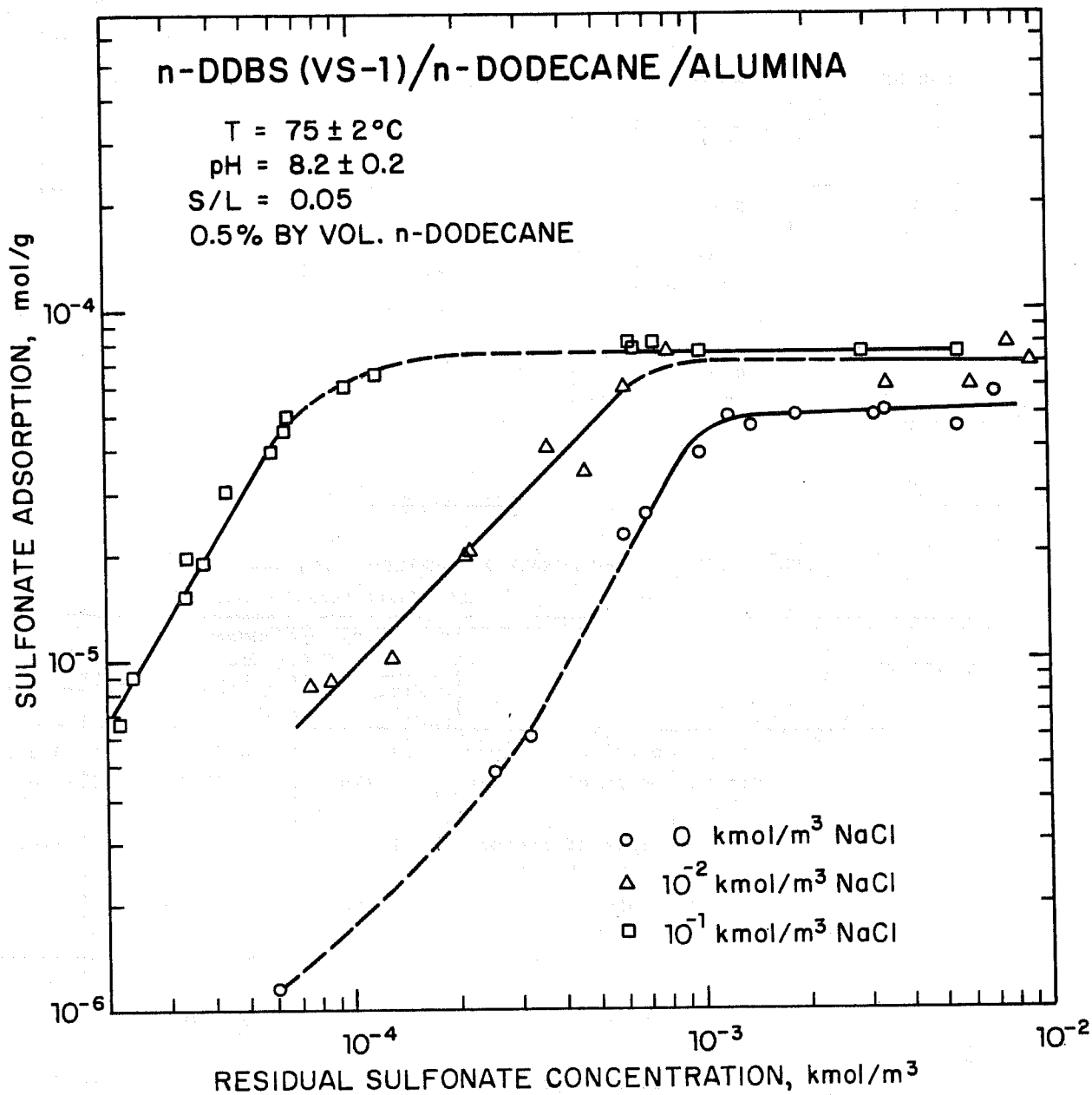


Figure II:17. Effect of oil, n-dodecane, on the adsorption of n-DDBS on alumina at 75°C.

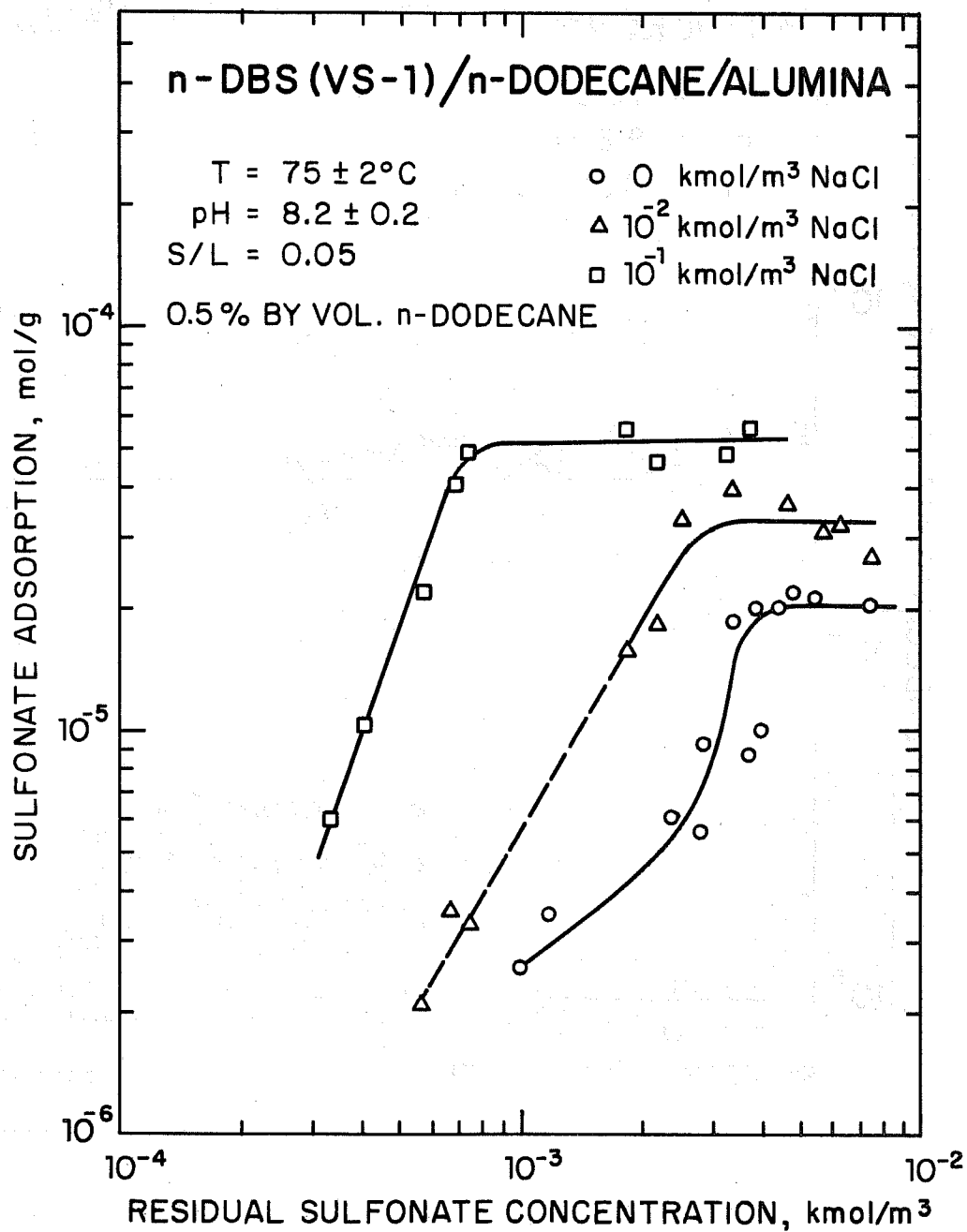


Figure II:18. Effect of oil, n-dodecane, on the adsorption of n-DBS on alumina at 75°C.

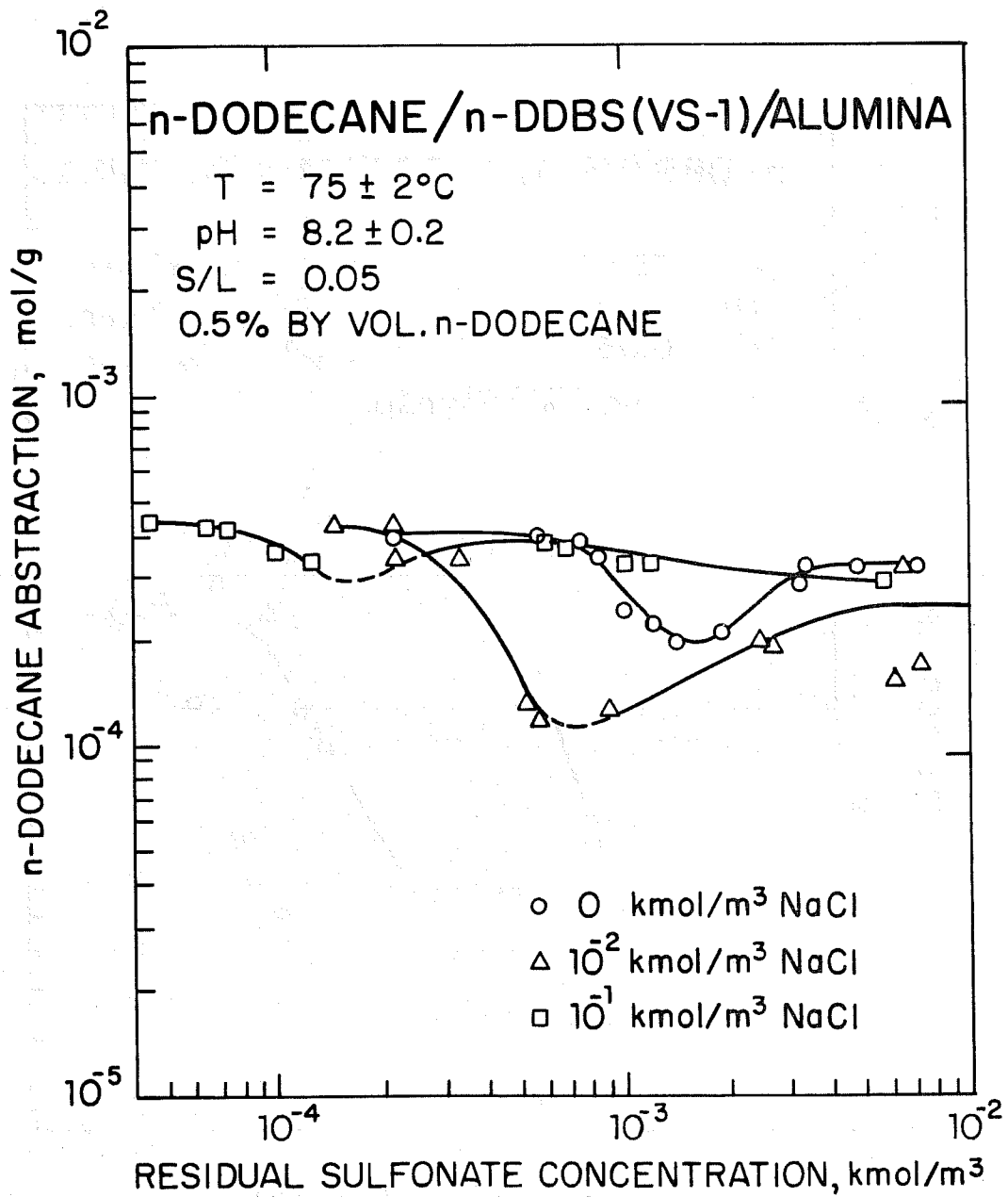


Figure II:19. Abstraction of n-dodecane by alumina in the presence of n-DDBS at 75°C.

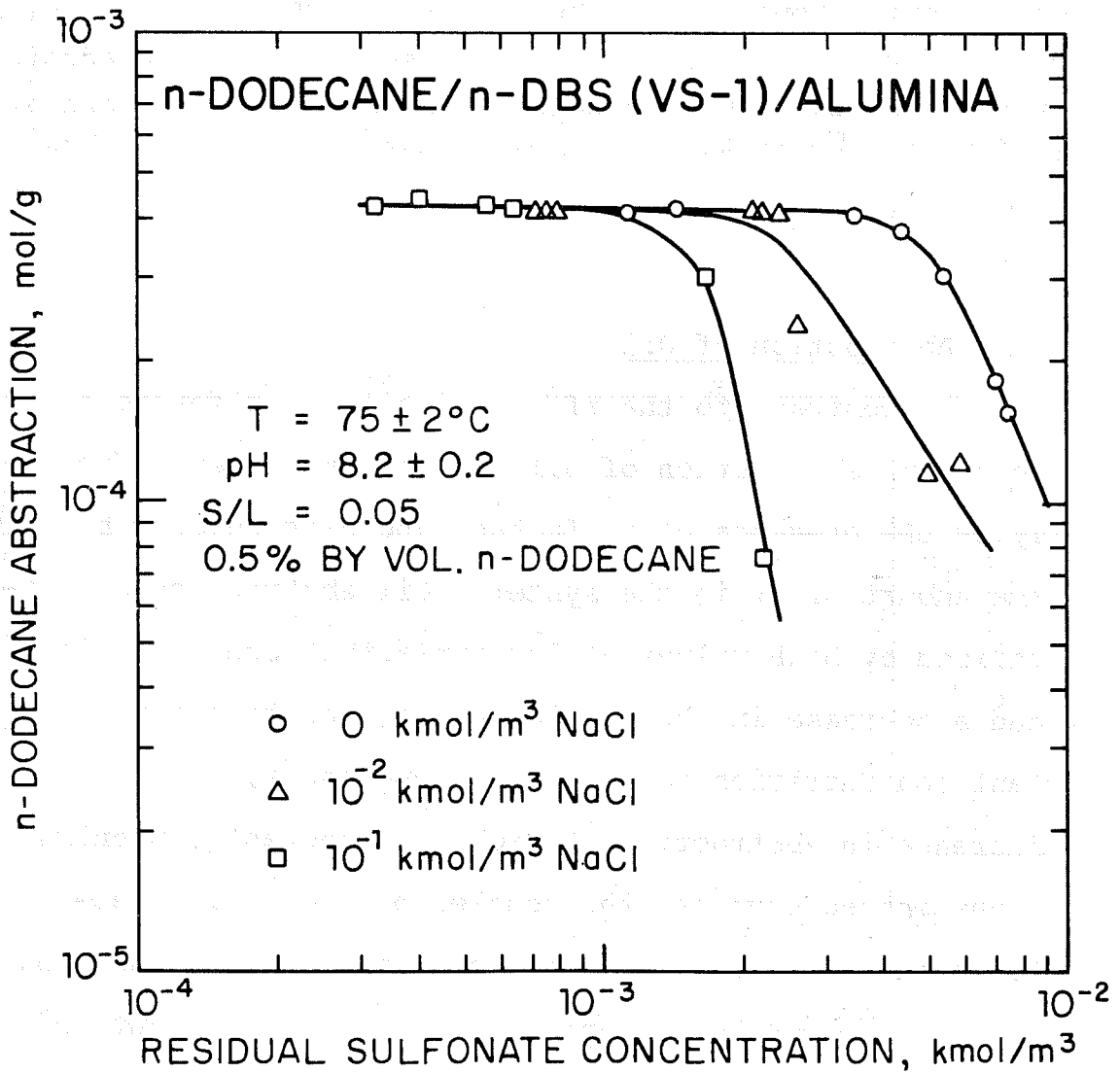


Figure II:20. Abstraction of n-dodecane from n-DBS solutions by alumina at three NaCl levels at 75°C.

C4a. Effect of Oil on Sulfonate Adsorption

The effect of n-dodecane on the plateau adsorption of n-NaDDBS and n-NaDBS on alumina is given in Table II:3a. It is clear from these figures that n-dodecane did not significantly affect the plateau adsorption behavior of n-DBS under the tested conditions. However, in the case of n-DDBS at 75°C presence of n-dodecane resulted in an increase in sulfonate adsorption at 10^{-2} and 10^{-1} kmol/m³ NaCl. Similarly, at 65°C and at 10^{-2} kmol/m³ NaCl n-dodecane enhanced the sulfonate adsorption in the plateau region.

C4b. Abstraction of Oil

In contrast to the effect of oil on sulfonate adsorption, abstraction of oil was influenced significantly by the presence of surfactant and particularly by the amount of it in the system. Oil abstraction characterized by high values at low surfactant concentrations and a decrease in abstraction above a certain surfactant concentration followed, in some cases, by an increase in abstraction at higher surfactant concentrations indeed suggests the complex nature of interactions in this system. Additional information regarding the state of emulsions, partitioning of surfactant and oil between the emulsion and aqueous phase, etc., is, however, required for a full analysis of the results of adsorption of sulfonates and uptake of oil in the presence of one another. Nevertheless, based upon the available results as well as the present knowledge of

the system, an attempt is made below to examine possible mechanisms of the observed effects.

Adsorption of n-dodecane (0.5% vol) at low surfactant concentrations is almost 100% (adsorption $\cong 4 \times 10^{-4}$ mol/g) and is independent of the chain length of the surfactant. This adsorption, assuming an area per molecule of 20 \AA^2 for the hydrocarbon oil (vertical orientation), would correspond to more than 3 monolayers. Such a multilayer adsorption of oil is possible on a solid surface which is made partially hydrophobic due to the surfactant adsorption.

Multilayer coating of the solid by n-dodecane is further supported by the data given in Figure II:21 which shows that the adsorption continues to increase with increase in the percentage of oil in the bulk. The adsorption was also found not to be influenced significantly by the salinity of the system.

Examination of the solids after adsorption tests clearly indicated that they aggregated to form larger spherical particles (see Figure II:22). The size of the aggregate was found to increase with increase in the oil concentration. This phenomenon is similar to the "spherical agglomeration" process which is known to be caused by the coating of oil on the particles. Preliminary experiments conducted with silica (Bio-Sil)

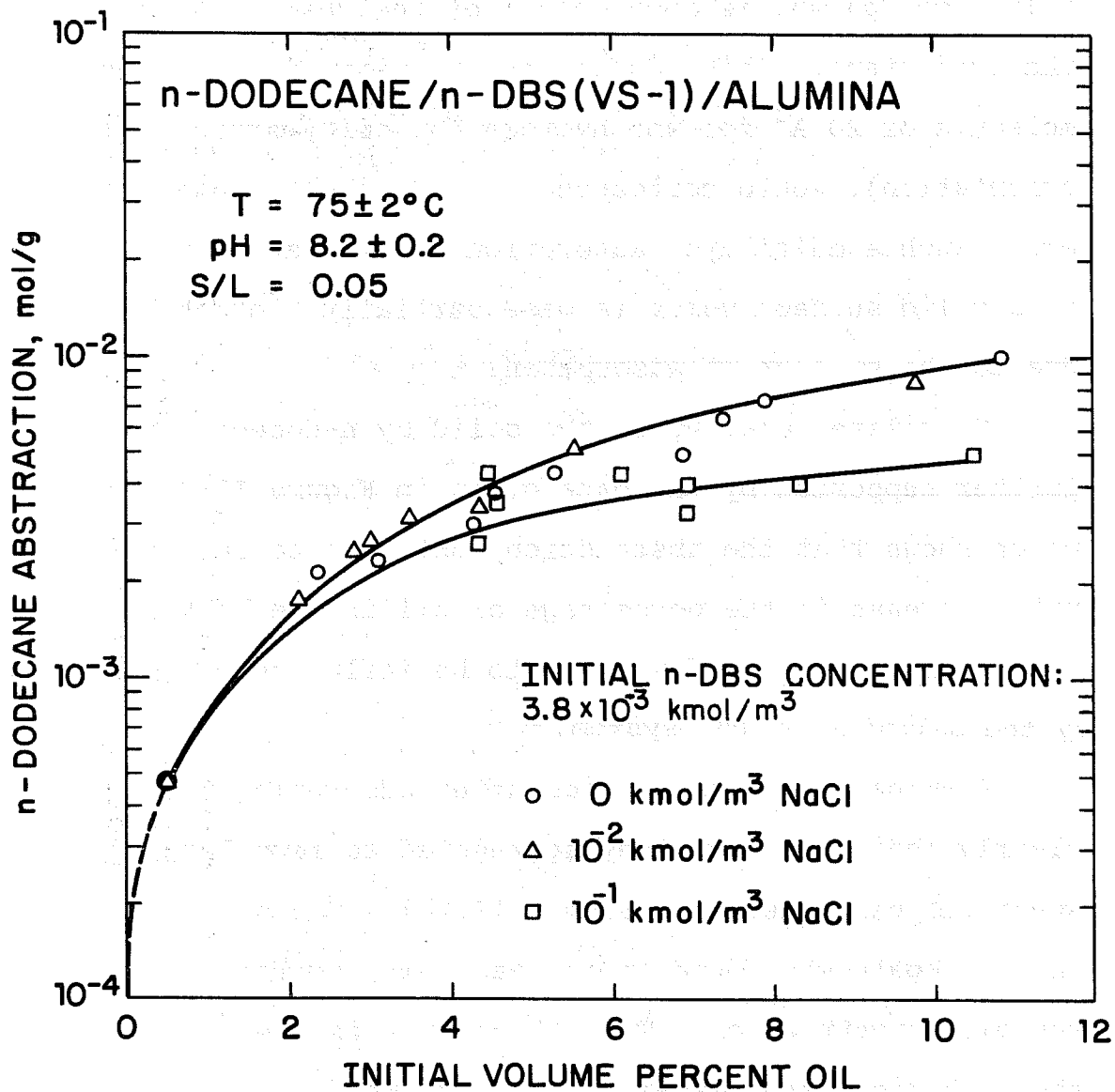


Figure II:21. Abstraction of n-dodecane by alumina in the presence of n-DBS at 75°C.

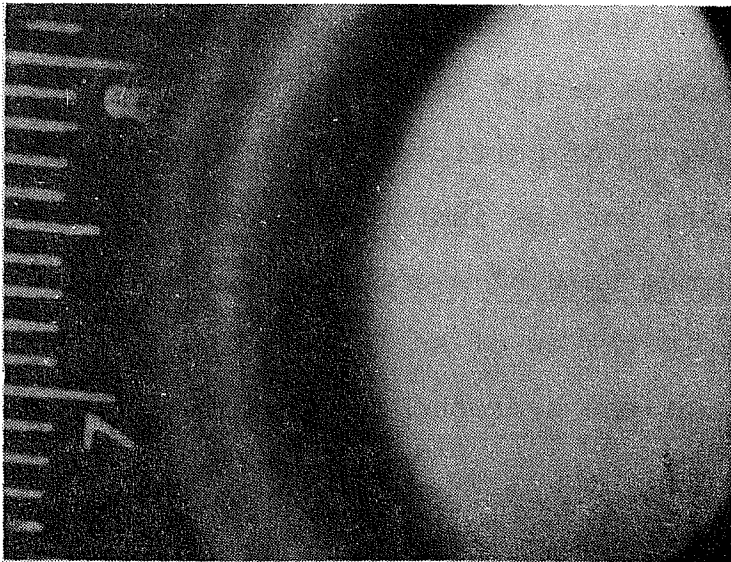
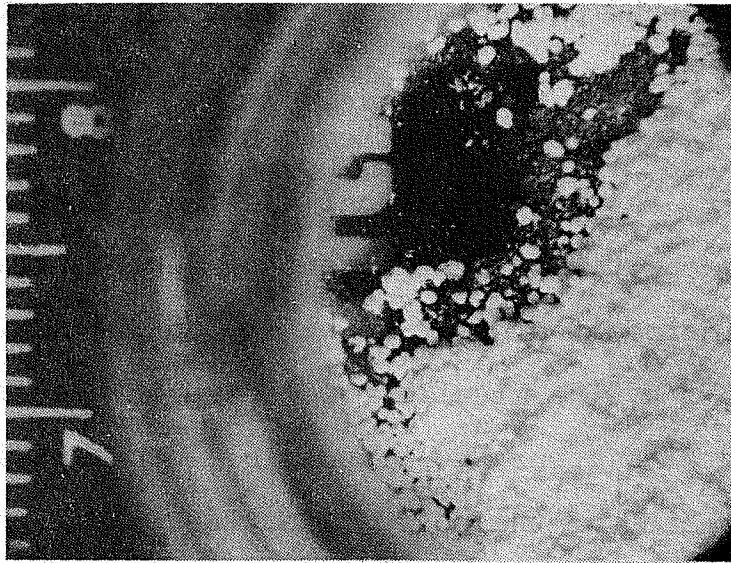
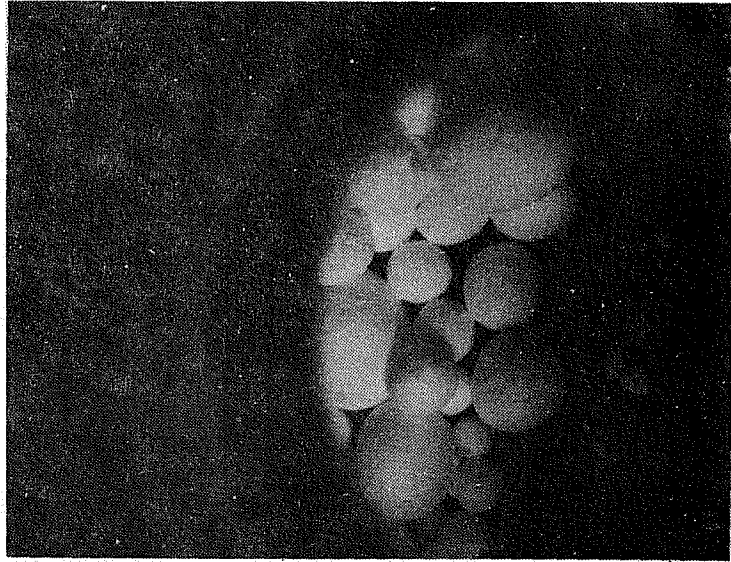


Figure II:22. Alumina particles showing spherical agglomeration with increase in oil abstraction. Initial oil concentrations (Vol. %): Left = 0.5, Center = 4.9, Right = 11.6.

(that does not adsorb sulfonate to any measurable extent), n-DDBS and n-dodecane did not result in spherical agglomeration of silica, indicating that adsorption of surfactant is a requirement for the coating of oil on such solids.

Aggregation of fine particles in the presence of surfactants and oil, may be deleterious for enhanced oil recovery process, if such aggregates can block the micropores and thus prevent the micellar fluid from entering such pores.

At intermediate surfactant concentrations, as mentioned earlier, abstraction of oil was found to decrease above a particular surfactant concentration. This is considered at present to be due to the solubilization of oil by the micelle. Decrease in oil abstraction can also occur due to possible decrease in the hydrophobicity of the solid under the conditions where sulfonate molecules can adsorb at the solid/liquid interface with a reverse orientation. This possibility can be easily tested by examining the aggregation tendency of particles under such conditions.

The reasons for the increase in oil abstraction above the minimum at 0.5% n-dodecane is not clear at present. Precipitation of sulfonates and the subsequent coating of the hydrophobic precipitate by oil or

the co-precipitation of oil with the surfactant are two of the possible reasons for such increase at high sulfonate concentrations. On similar grounds, the absence of minimum in oil uptake in DBS solutions can be attributed to the absence of sulfonate precipitation, owing to the higher solubility of n-DBS compared to n-DDBS.

According to the above reasoning, one should expect a minimum in oil uptake from 2.5% n-dodecane solutions also. This is, however, contrary to the experimental evidence given in Figure II:23. The only possible explanation in this case is that the abstracted amount of oil is relatively small compared to the amount in the aqueous phase, hence a reversal in the oil uptake is not observed.

Additional experiments as a function of key variables that might be helpful to elucidate the mechanisms of oil uptake in the presence of surfactants are in progress at present. The results for the effect of one such variable, namely solid to liquid ratio, on adsorption are given in Figure II:24. Adsorption of n-DDBS and abstraction of n-dodecane at fixed levels of residual sulfonate are plotted in this figure as a function of the solid to liquid ratio. The two levels of sulfonate were selected such that the lower one (2.4×10^{-4}

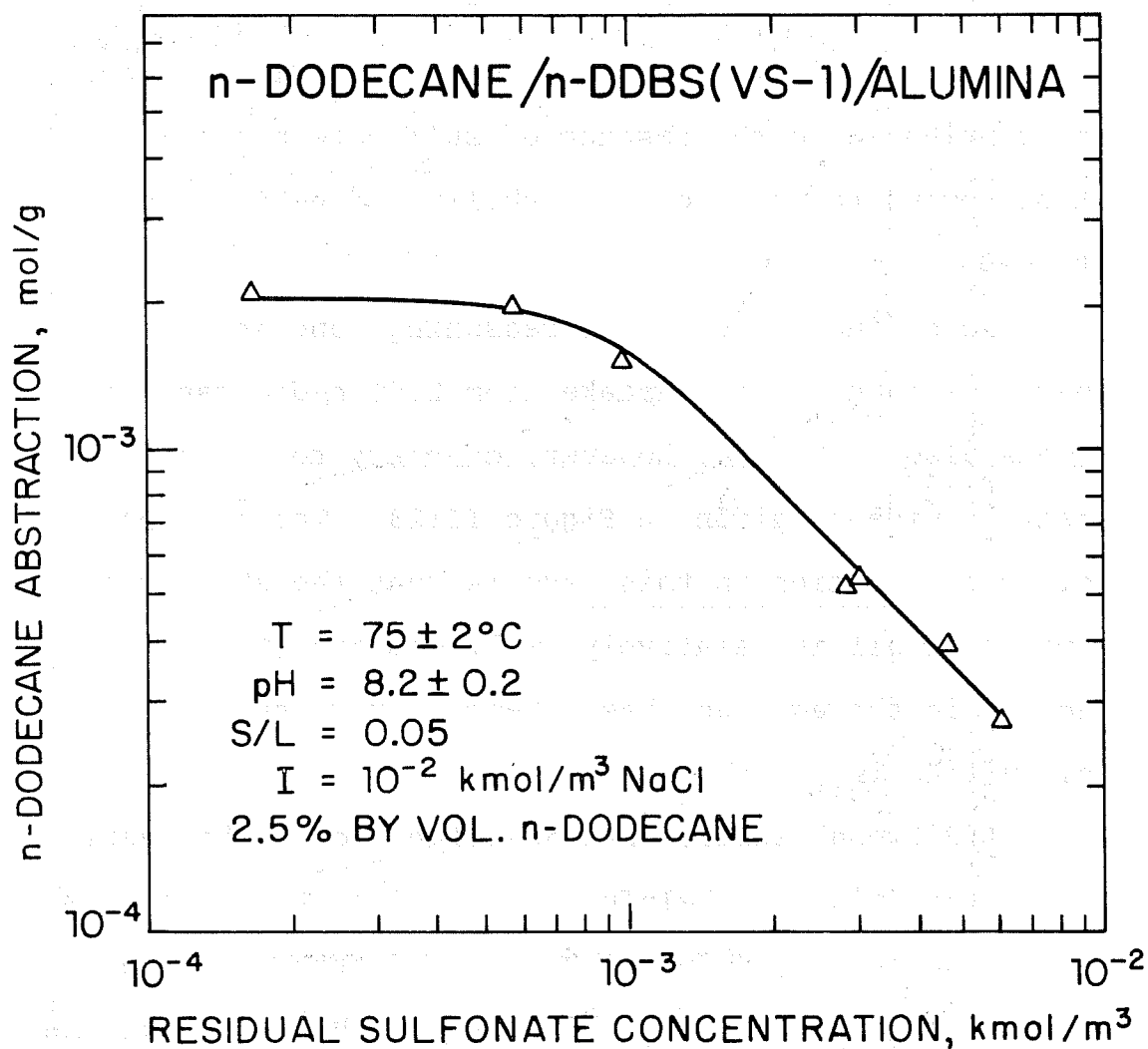


Figure II:23. Abstraction of n-dodecane by alumina in the presence of n-DDBS at 2.5% by volume of n-dodecane at 75°C.

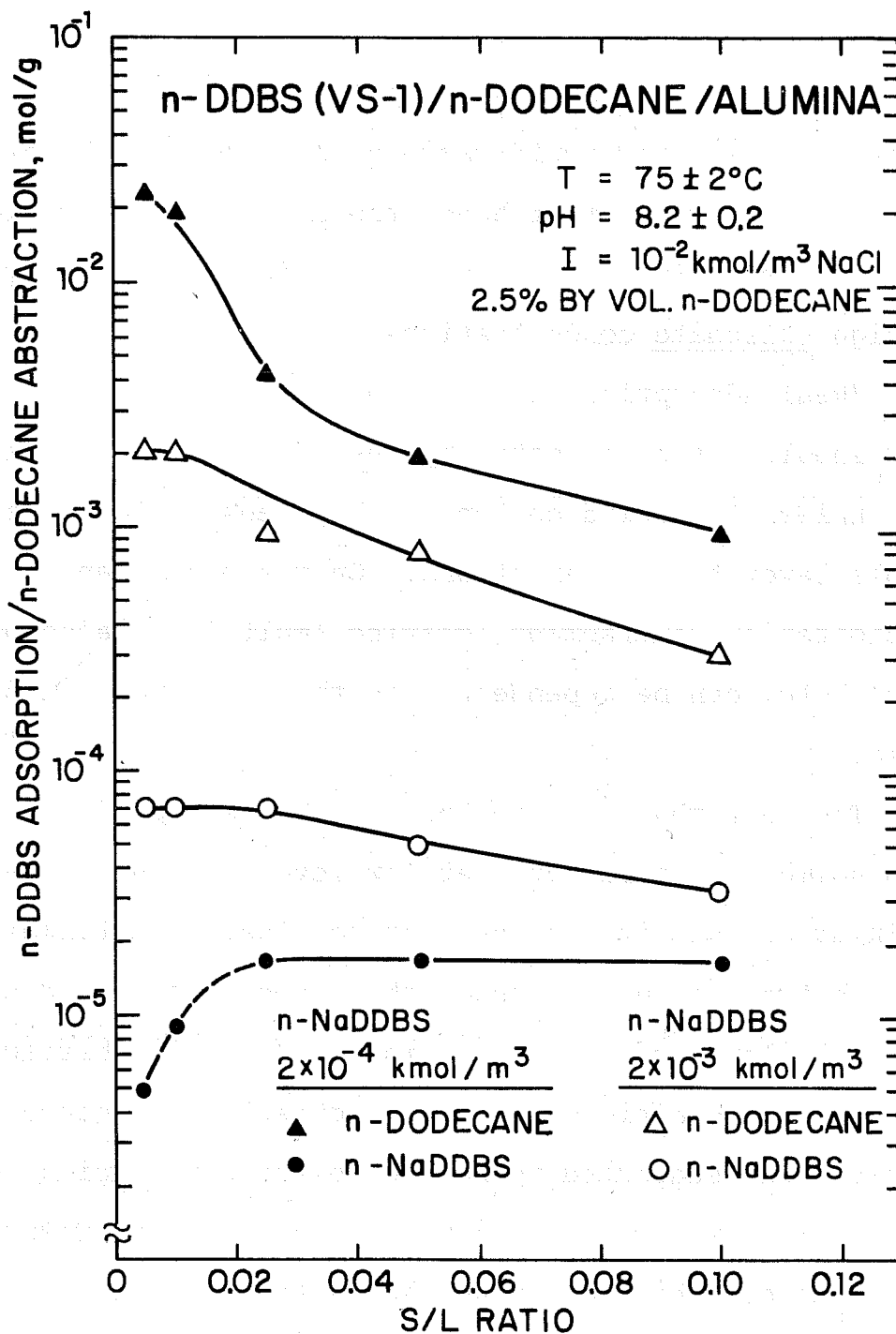


Figure II:24. The effect of solid to liquid ratio on the adsorption of n-DDBS and abstraction of n-dodecane on alumina at 75°C.

kmol/m³) corresponded to the plateau region in the oil abstraction and the upper (2.4×10^{-3} kmol/m³) to the plateau region on the sulfonate isotherm.

Abstraction of oil is found to decrease with increase in solid to liquid ratio at both the levels of sulfonate. On the other hand, the sulfonate adsorption decreased with increase in solid to liquid ratio only at high sulfonate concentrations.

"Real adsorption" from a thermodynamic point of view should not be affected by the solid to liquid ratio, unless the solid content is high enough to cause double layer type interactions. On the other hand, precipitation, entrapment, coating (multilayer adsorption), etc. can be dependent upon the solid to liquid ratio.

The fact that only the oil uptake is dependent upon solid to liquid ratio at low levels of sulfonate is in agreement with the earlier conclusion that the high abstraction of oil under these conditions is due to a multilayer coating. The increase in oil abstraction above the minimum (i.e. at high sulfonate concentration) was suggested to be due to the coprecipitation of oil along with the surfactant. The observed results that both oil abstraction and surfactant uptake under these conditions depend upon solid to liquid ratio support the above consideration.

C5. EFFECT OF TEMPERATURE

Temperature is one of the parameters that is known to affect the surfactant adsorption at interfaces. The effect of temperature on surfactant adsorption on reservoir rock minerals is important in micellar flooding mainly because of the reported variations in temperature among reservoir fields which may affect the performance of surfactants. Moreover, thermodynamic information such as the heat and entropy of adsorption which is necessary to elucidate adsorption mechanisms can be evaluated from the data on the dependence of adsorption on temperature.

Adsorption tests discussed in the previous sections were conducted at 75°C. The results for the adsorption of n-DDBS on alumina at 65°C, given in Figure II:25 show that the isotherm, like that at 75°C, consists of a rising part and a plateau region. Effect of NaCl, again similar to that at 75°C, was to increase the adsorption of sulfonate.

Comparison of figures II:14 and II:25 shows the adsorption to increase with decrease in temperature. This observation is in agreement with the reported dependence of dodecylsulfonate adsorption on alumina which was considered to be primarily electrostatic in nature (6). The temperature effect appears to be

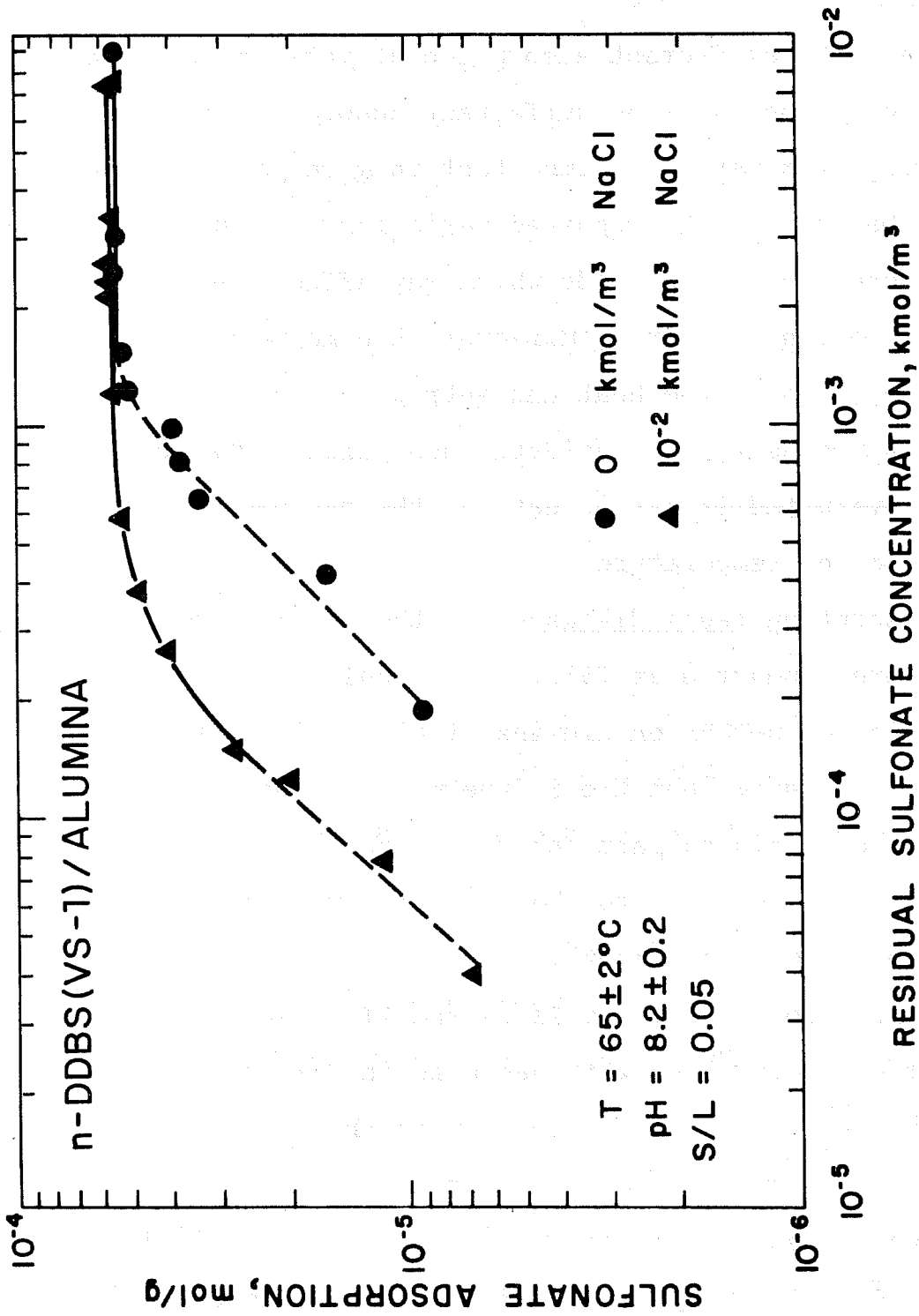


Figure II:25. Adsorption of n-DDBS on alumina at two levels of NaCl at 65°C.

pronounced in the rising part of the isotherm and marginal in the plateau region.

Adsorption of n-DDBS in the presence of n-dodecane and the uptake of the latter under the same conditions have been determined at 65°C also. Results given in Figures II:25,26 show that the adsorption of n-DDBS, at 10^{-2} kmol/m³ NaCl is enhanced by the presence of n-dodecane. Also, the uptake of n-dodecane (Figure II:27) exhibits a minimum as a function of sulfonate concentration. These observations are in agreement with those made at 75°C and possible reasons for such effects were discussed in section II:C4.

C6. EFFECT OF ALCOHOL

Alcohols are used as co-surfactants in micellar flooding. It is therefore important to determine the effect of alcohol on the adsorption and precipitation of surfactants under micellar flooding conditions. Preliminary results for the effect of n-propanol, a short chain alcohol, on the precipitation/redissolution behavior of recrystallized NaDDBS/CaCl₂ system are discussed in section IE1.

Results for the adsorption of n-NaDDBS on alumina in the presence of n-propanol at 75°C are given in Figure II:28. For the purpose of comparison n-DDBS adsorption in the absence of n-propanol is also included in this figure.

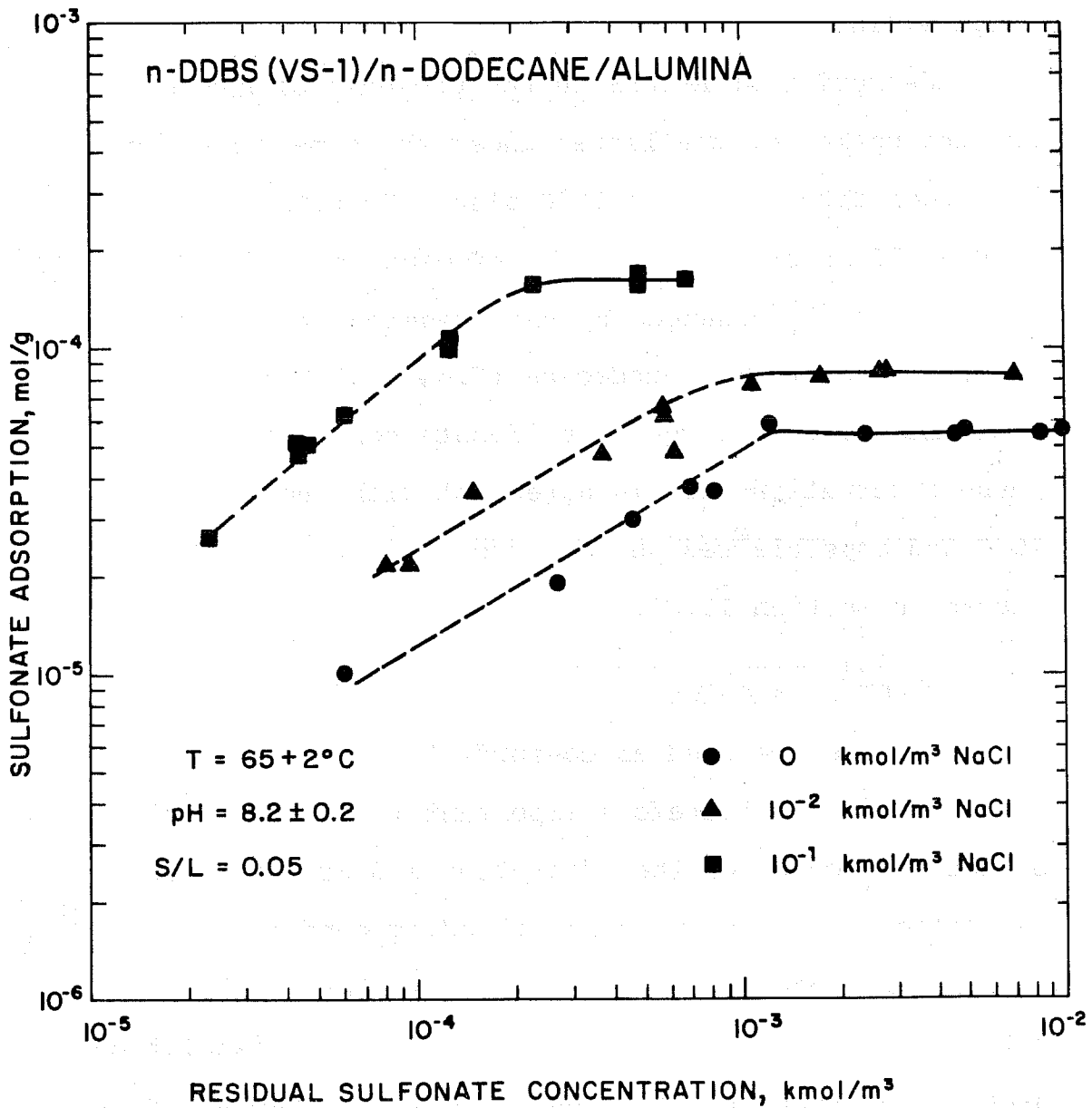


Figure II:26. Effect of oil, n-dodecane, on the adsorption of n-DDBS on alumina at 65°C.

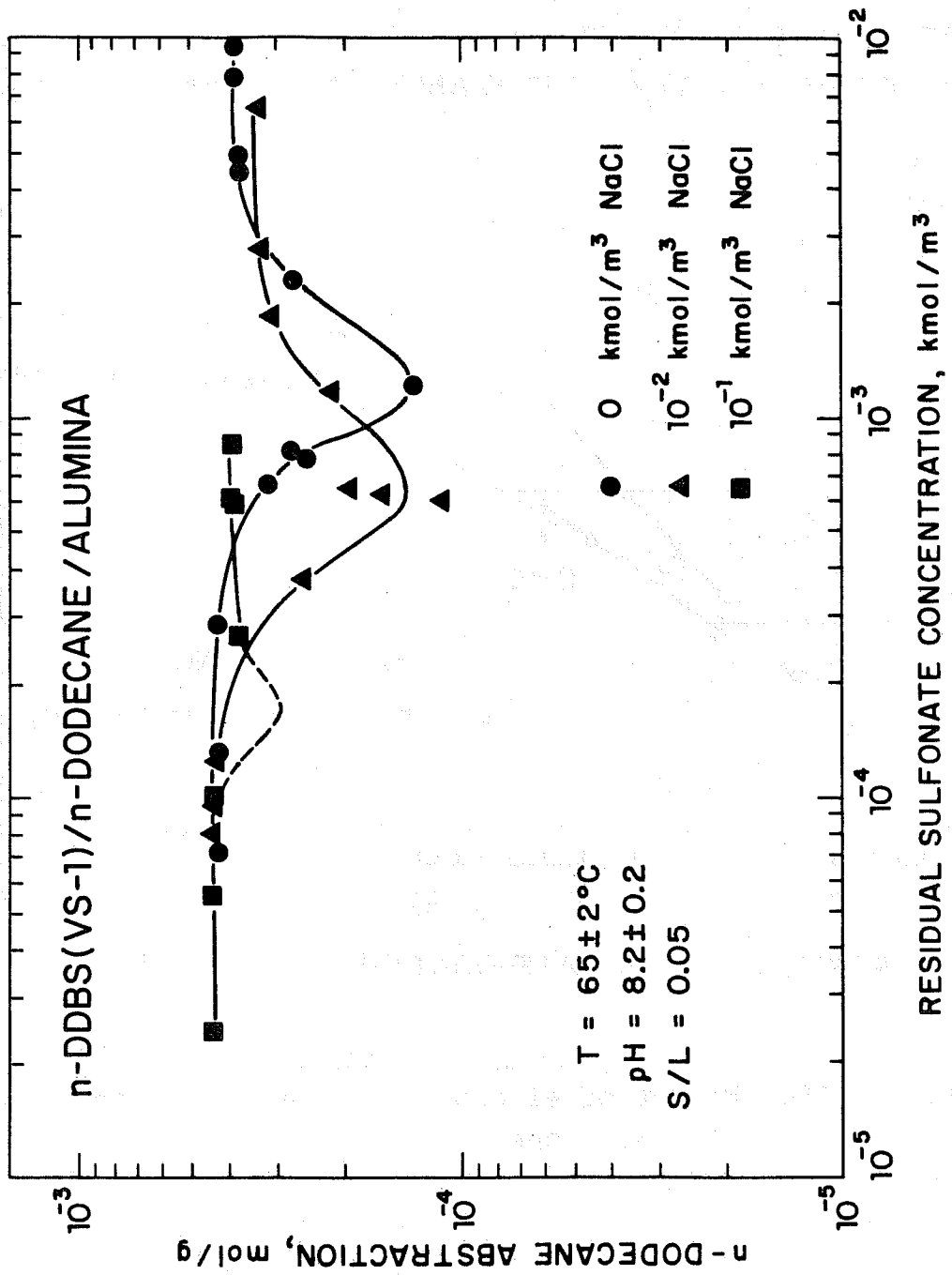


Figure II:27. Abstraction of n-dodecane by alumina at 65°C in the presence of n-DDBS.

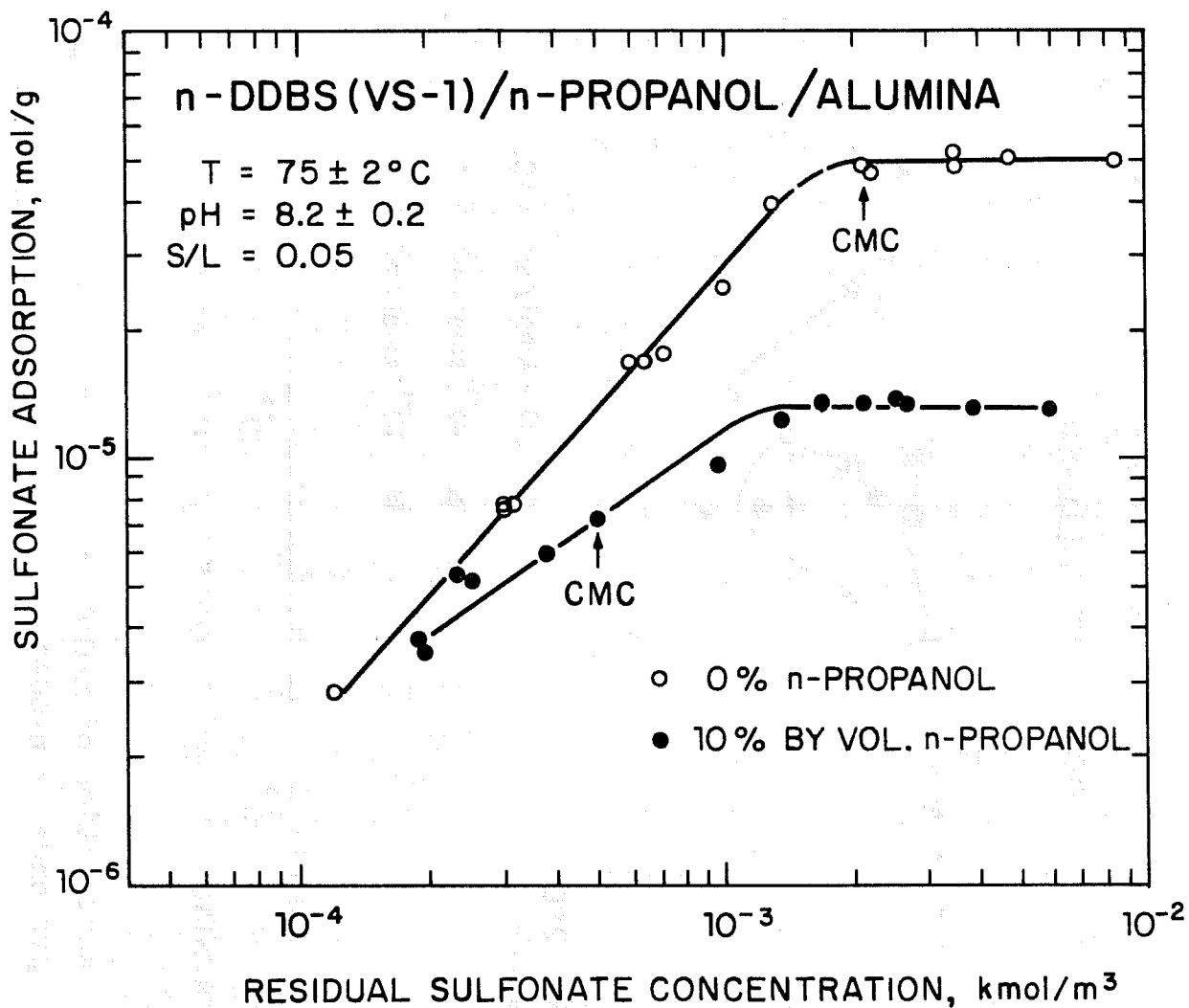


Figure II:28. Effect of alcohol, n-propanol, on the adsorption of n-DDBS on alumina at 75°C.

Adsorption is found to decrease significantly in the presence of n-propanol. Also, the slope of the rising part of the isotherm is reduced by n-propanol. CMC of n-DDBS was found to be reduced by propanol. Contrary to the earlier observation that the CMC coincided with the onset of the plateau region on the adsorption isotherms, in this case the CMC appears to be on the rising part of the isotherm. It is possible that the dye solubilization technique has its limitations in detecting the presence of micelles in n-propanol solutions. CMC of the surfactant in n-propanol solutions is therefore being determined at present using other techniques such as surface tension.

The reduction in surfactant adsorption caused by n-propanol is possible due to the increased solvent power of the water for amphipathic materials such as surfactants. Any such increase in solvent power of the medium can be expected to decrease the tendency of the surfactants to adsorb at interfaces. This would indeed be beneficial in reducing surfactant loss due to adsorption at the solid/liquid interface. On the other hand, presence of n-propanol can reduce the surfactant adsorption at the oil/water interface also, in which case the interfacial tension lowering, and hence the oil displacement efficiency, can be deleteriously affected.

Therefore, the determination of the optimum amount of alcohol which can reduce the surfactant loss without affecting the efficiency is important for micellar flooding.

A detailed investigation of the effect of alcohol as a function of its concentration and other relevant variables is planned for the coming year.

C7. ADSORPTION OF ALIPAL CO-436
ON ALUMINA AND Na-KAOLINITE

Surfactants which have a high salt tolerance and low adsorption capacity for solids are preferable for micellar flooding, provided they can also bring about the necessary oil/water interfacial tension lowering required for oil displacement. In this regard, potential use of ethoxylated surfactants which are reported to have a higher salt tolerance (10) compared to n-alkylbenzenesulfonates is being explored by industry at present. Adsorption properties of such ethoxylated surfactants have, however, remained unexplored, to our knowledge, so far. We have now initiated a study of the adsorption of ethoxylated surfactants on reservoir rock minerals. Preliminary results for the adsorption of Alipal Co-436, a sulfate ester of $(\text{alkyl})_9$ phenoxy poly (ethylene oxy)₃ ethanol, on alumina and Na-kaolinite are reported here.

It is evident from the kinetic data given in Figure II:29 for the adsorption Alipal Co-436 on Na kaolinite and alumina (at 25° and 75°C) that these systems attain equilibrium in about an hour. Since contact times used for n-alkylbenzenesulfonates on alumina and Na kaolinite were four and seventy-two hours respectively, similar time intervals were chosen for the study with Alipal also.

Results obtained for the adsorption of Alipal Co-436 on alumina and Na kaolinite are given in Figures II:30-31. These isotherms are similar to those presented earlier for n-alkylbenzenesulfonates and consist of a rising part and a plateau region. NaCl again, as in the case of alkylbenzenesulfonates, increase the surfactant adsorption. However, the plateau adsorption on alumina did not increase significantly above 10^{-2} kmol/m³ NaCl.

The effect of salinity on Alipal Co-436 adsorption at a fixed initial surfactant concentration can be seen from Figures II:32,33. Adsorption is found to increase with NaCl concentration. Surfactant precipitation was observed to occur at about 0.45 and 0.425 kmol/m³ NaCl at 75° and 25°C respectively. It is to be noted that DDBS (recrystallized) precipitates at about 0.5 kmol/m³ NaCl at 25°C indicating that the tolerance of DDBS and

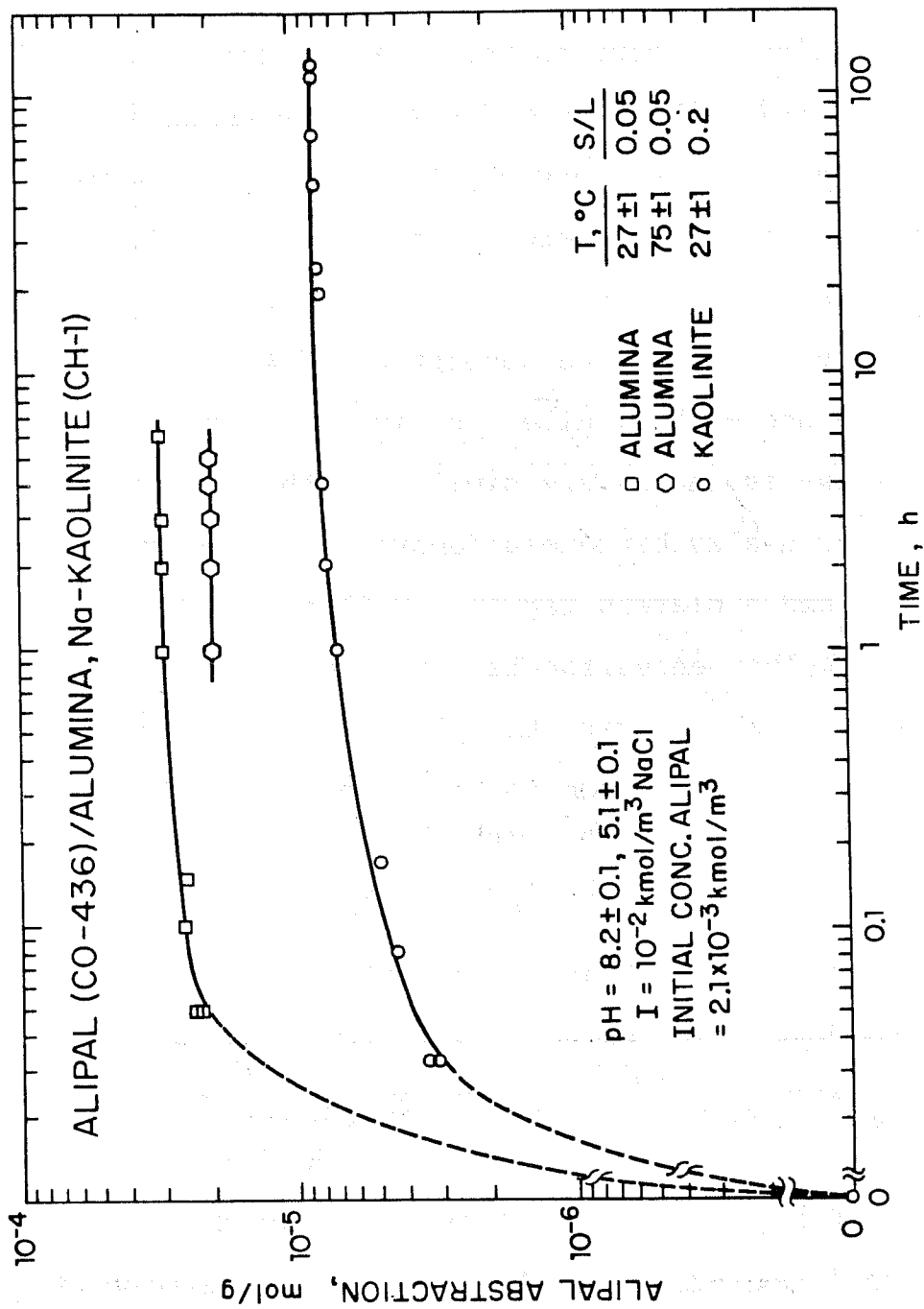


Figure II:29. Kinetics of abstraction of Alpal Co-436 on alumina at 75° and 27°C and on Na-kaolinite at 27°C.

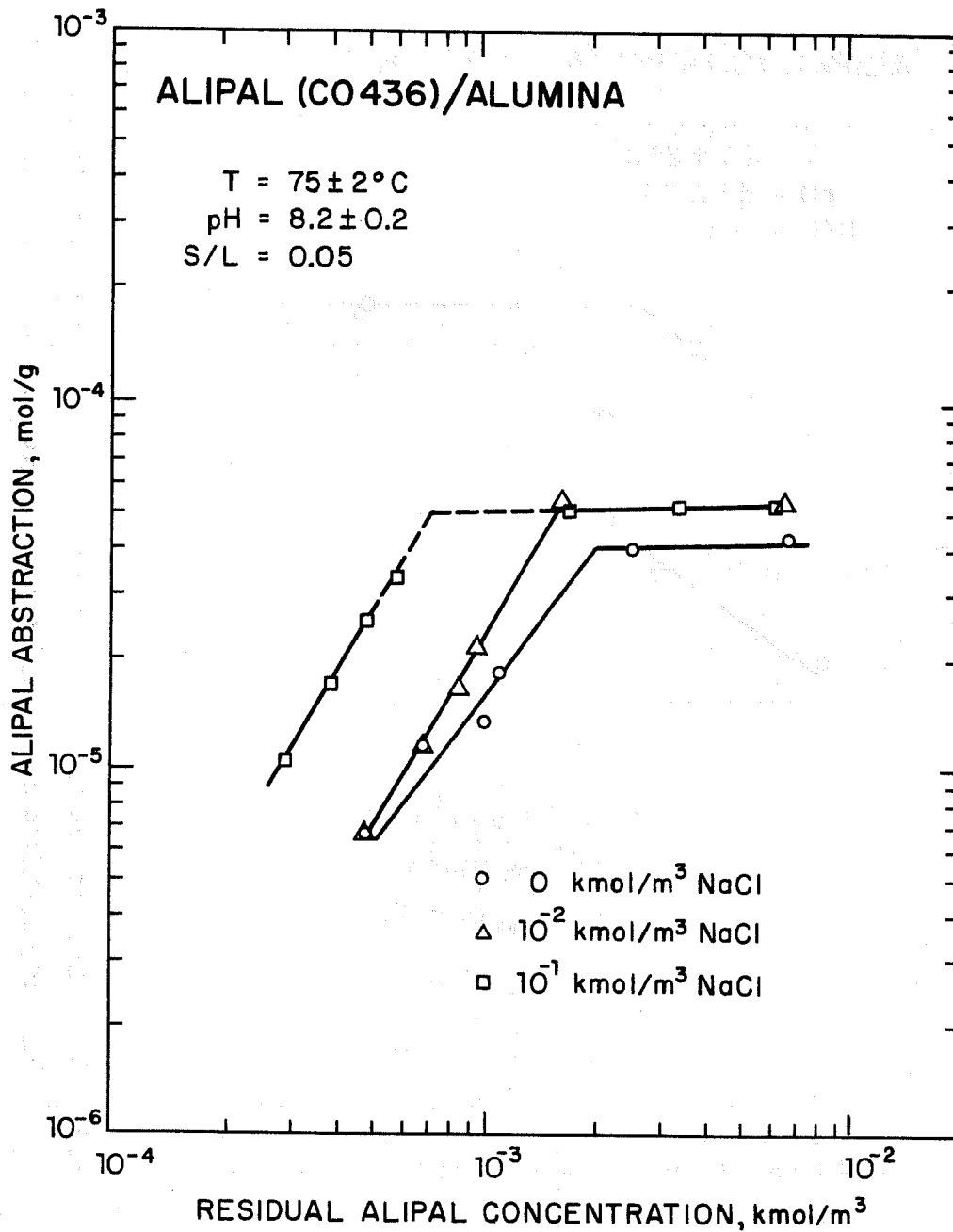


Figure II:30. Adsorption of Alipal Co-436 on alumina at three levels of NaCl at 75°C.

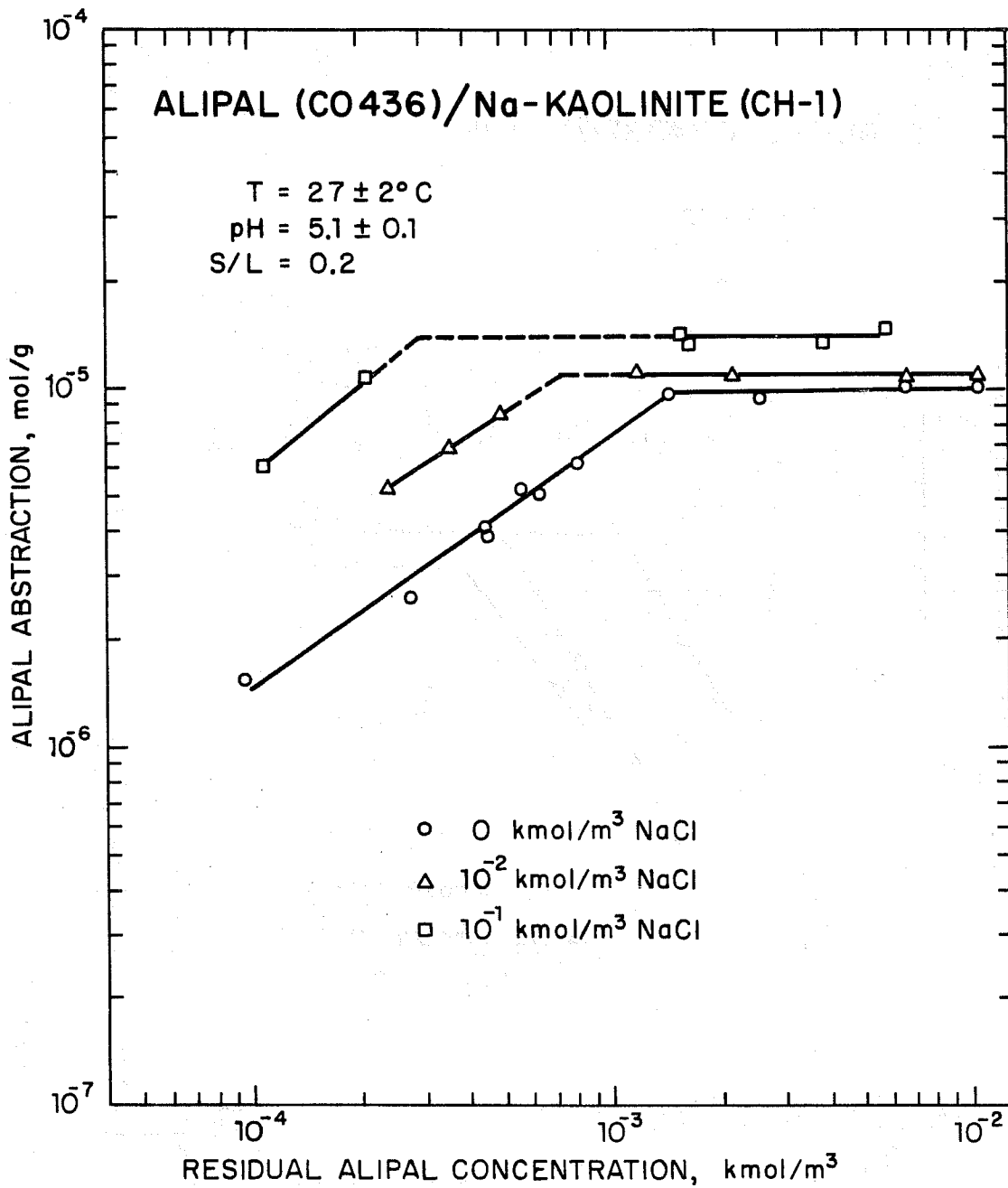


Figure II:31. Adsorption of Alipal Co-436 on Na-kaolinite at three levels of NaCl at 27°C.

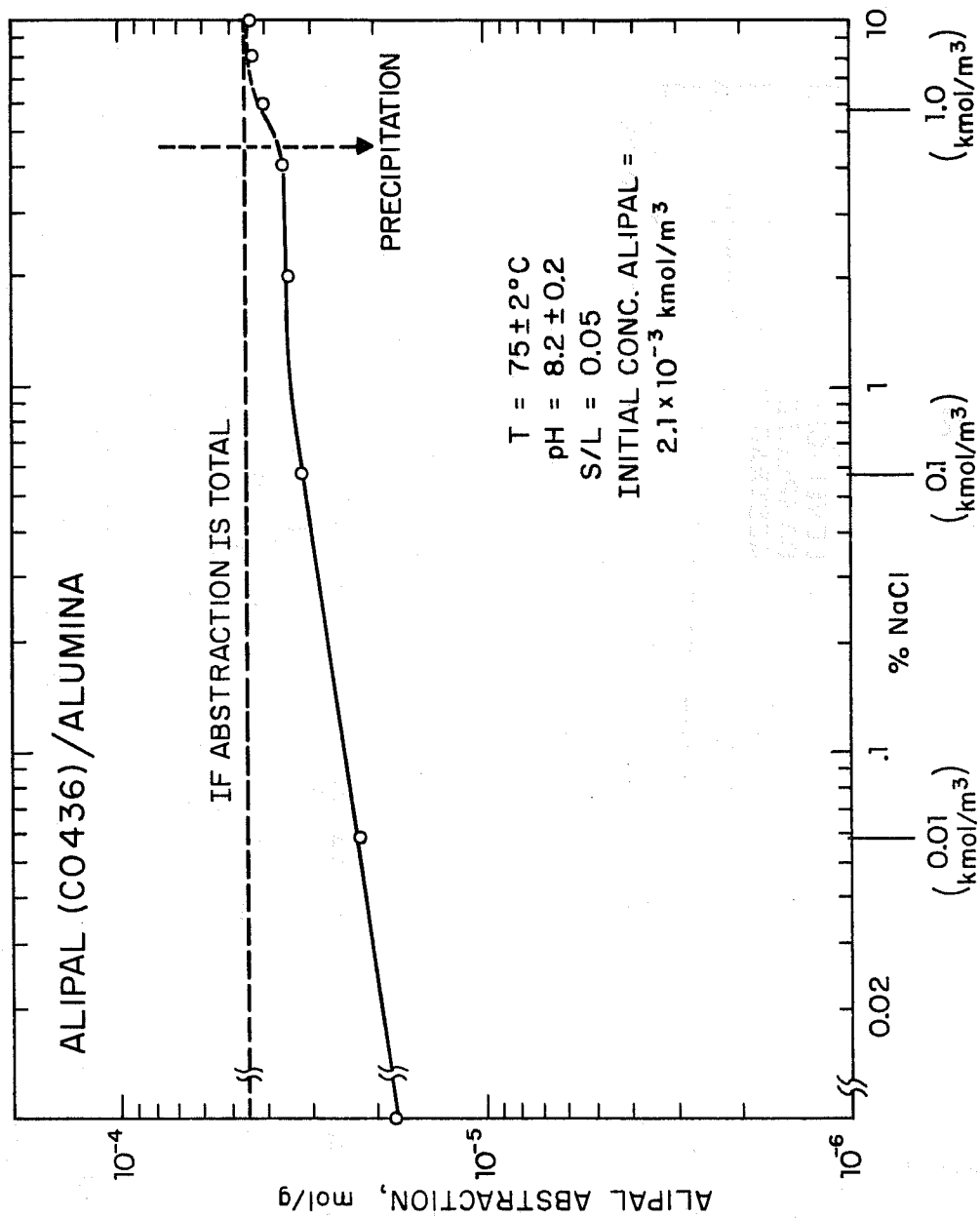


Figure II:32. Effect of salinity on the adsorption of Alipal Co-436 on alumina at 75°C.

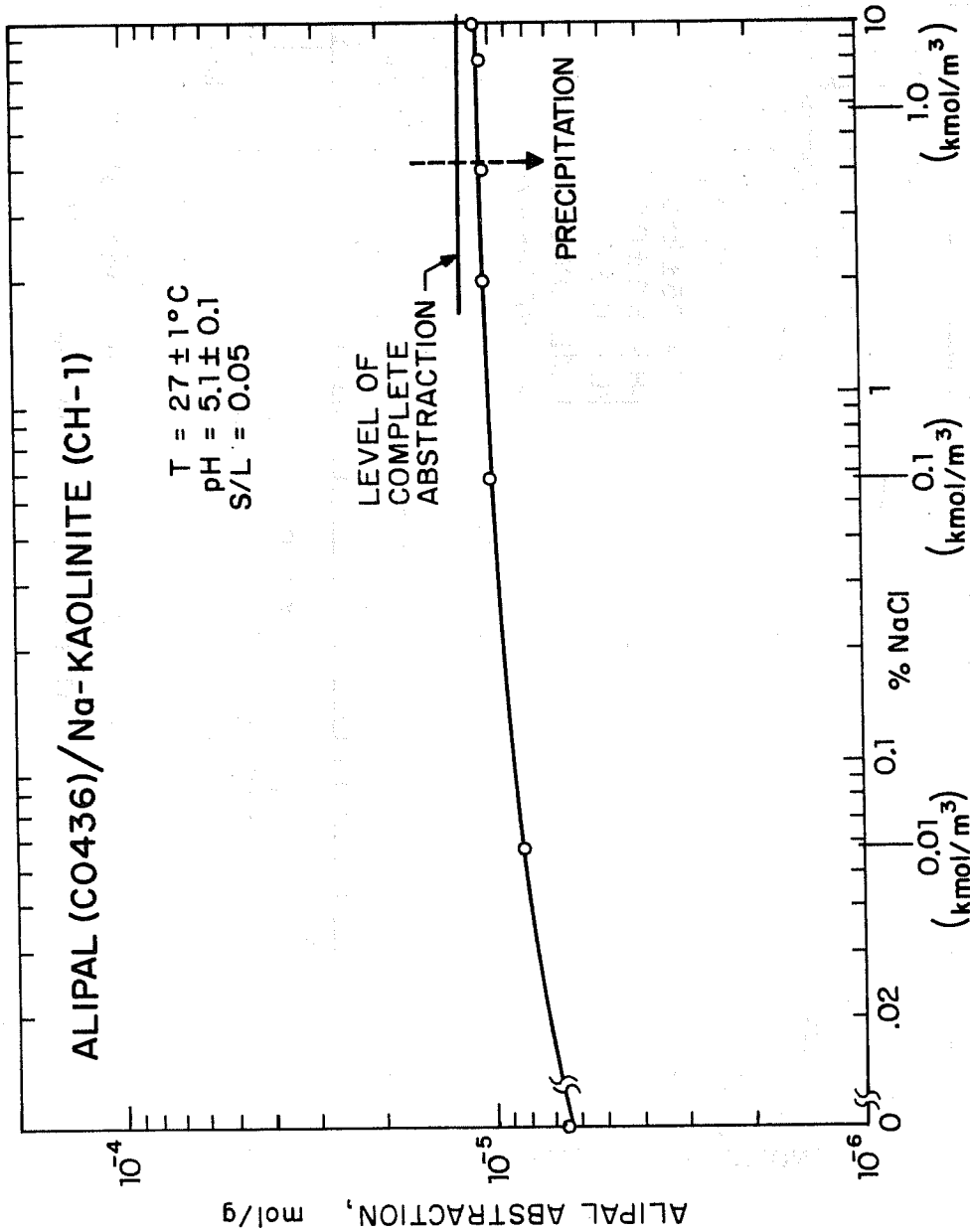


Figure II:33. Effect of salinity on the adsorption of Alipal Co-436 on Na-kaolinite at 27°C.

TABLE II: 4

Comparison of Plateau Adsorption on Alumina

NaCl conc. kmol/m ³	Plateau Adsorption		
	ALIPAL mol/g	n-DDBS mol/g	n-DBS mol/g
0	4×10^{-5}	5.0×10^{-5}	2×10^{-5}
10^{-2}	5×10^{-5}	6.0×10^{-5}	3.2×10^{-5}
10^{-1}	5×10^{-5}	5.6×10^{-5}	5.2×10^{-5}

Alipal Co-436 for NaCl are almost identical. This is contrary to the currently accepted belief that the ethoxylated surfactants have a higher salt tolerance compared to the alkyl sulfonates. Tolerance of these sulfates to multivalent ions will be tested in the future.

A comparison of the plateau adsorption of Alipal Co-436, n-DBS and n-DDBS on alumina, given in Table II:4, shows that the saturation adsorption of Alipal is about the same as those of the other two surfactants.

Detailed tests to determine the adsorption behavior of Alipal Co-436 and similar surfactants are in progress at present.

III. POLYMER-SURFACTANT INTERACTIONS

A. Introduction

Interactions of polymers and surfactants with one another are of major importance for a number of reasons in tertiary oil recovery by micellar flooding. For example, polymer/surfactant interactions can lead to precipitation of surfactant or polymer or even that of polymer-surfactant complexes. All such interactions will affect the concentrations of the surfactant and the polymer in the system and thus influence the interfacial tension lowering at the oil/water interface and the viscosity of the polymer slug (both from their expected values in the absence of any interaction). In addition to the above, polymer-surfactant interactions can modify their adsorption at the reservoir rock/liquid and the oil/aqueous phase interfaces. While the former can affect the wettability of reservoir rocks and the loss of surfactants and polymers due to adsorption, the latter can affect the oil/water interfacial tension reduction and hence the efficiency of the oil displacement process.

Our preliminary work (1) on the adsorption of polymer (polyacrylamide) and surfactant (sodium

dodecylbenzenesulfonate) on kaolinite has given indications for the presence of some interactions between these two reagents as adsorbates, but these tests also showed several precautions to be taken during such a study and could be considered only as exploratory in nature.

During the current year, a detailed investigation of the interactions of acrylamide based nonionic (polyacrylamide), anionic (sulfonated polyacrylamide) and cationic (aminated polyacrylamide) polymers with anionic (dodecylsulfonate) and cationic (dodecylamine-hydrochloride) surfactants has been initiated. Specifically, adsorption of surfactant and polymer at the solid/liquid interface, and the wettability of the solid subsequent to its contact with polymer-surfactant solutions were determined under selected conditions. In addition, surface tension, viscosity and precipitation behavior of certain combinations of surfactants and polymers mentioned above were also tested under specific conditions. The results of these investigations are discussed in the following sections.

B. Wettability of Reservoir Rock Minerals in Polymer-Surfactant Solutions

B1. INTRODUCTION

Since the wetting characteristics of reservoir rocks and alterations in them during micellar flooding can influence the displacement of oil from micropores, an understanding of such properties is important in enhanced oil recovery by micellar flooding. Our past work (1, 2) on water wettability and oil wettability of Berea sandstone, Agricultural limestone and Na-kaolinite upon contacting them with Mahogany sulfonate-AA and Na-dodecylbenzenesulfonate clearly showed that the wettability, in all these cases as a function of surfactant concentration, exhibited a maximum and was influenced significantly by the surfactant concentration.

Alterations in wettability brought about by the surfactant can be influenced by the presence of other components such as polymers. The changes in wettability in these cases can also depend upon the order in which the rocks are exposed to different chemical environments.

Apart from the practical implications of understanding the changes in wettability of reservoir rocks in the presence of chemicals, the wettability studies can also yield information on the orientation of surfactant

molecules at the solid/liquid interface. This information will be useful in revealing the nature of polymer/surfactant interactions that occur at the solid/liquid interface.

During the current year we have initiated a study to determine the wettability of reservoir rock minerals in the presence of polymers and surfactants. The results for the wettability of one of the reservoir rock mineral, quartz, in the presence of surfactants such as dodecylaminehydrochloride and dodecylsulfonate, and polymers such as polyacrylamide, sulfonated polyacrylamide and aminated polyacrylamide are included in the subsequent sections.

B2. METHODS AND MATERIALS

B2a. Materials

Quartz. Brazilian quartz purchased from Wards Natural Science Establishment was crushed using a roll crusher. The -28 +65 fraction was separated from the crushed product and was subjected to magnetic separation and dilute HNO_3 leaching. After leaching, the product was washed using triple distilled water until the material was free of acid and was finally stored under triple distilled water.

Polymers. Polyacrylamide (PAM), sulfonated polyacrylamide (PAMS), and aminated polyacrylamide (PAMD) were synthesized in our laboratory according to the

procedure discussed elsewhere (3). The molecular weight and charge density of these polymers are given in Table III:1.

Surfactants. Sodium dodecylsulfonate (NaDDS) (>99.9% purity) was purchased from Aldrich Chemical Co. Dodecylammonium hydrochloride (DDA.HCl) was purchased from Eastman Kodak Co. and was used without further purification.

B2b. Methods

Wettability. Wettability was determined by conducting flotation tests and the % floated was taken as an indicator for the degree of non-wettability by water (hydrophobicity). The reasons for using flotation as the hydrophobicity index as opposed to conventional parameters such as contact angle, have been discussed in our earlier Annual Reports (1, 2). Briefly, flotation tests permitted use of irregular particles whereas contact angle measurements required use of smooth polished surfaces that cannot be considered representative of the rock surface.

Flotation tests were conducted in a Hallimond tube using a procedure described elsewhere (1).

Approximately 1 g of the mineral was reagentized in a 100 cm³ volumetric flask for ten minutes. At the end of ten minutes the contents of the flask were

TABLE III:1

Properties of Polymers Used in the Present Investigation

Polymer	Molecular weight	Charge density (mol%)
PAM	2×10^6	-
PAMS	2×10^6	3%
PAMD	-	10%

transferred to the Hallimond tube and flotation was conducted. For tests with polymers and surfactants together, the solution was premixed (without the mineral) for two hours prior to its use for flotation.

B3. RESULTS AND DISCUSSION

B3a. Wettability of Quartz in Amine Solutions

Results obtained for the hydrophobicity of quartz as a function of DDA-HCl are given in Figure III:1. It is evident from this Figure that the flotation increases with increase in concentration up to a certain value and decreases above it. The surfactant concentration corresponding to the maximum flotation is $3.4-4.0 \times 10^{-4} \text{ kmol/m}^3$ DDA-HCl.

Since minerals such as quartz must be made hydrophobic for flotation to occur, the increase in flotation observed up to the maximum must be due to the increase in hydrophobicity of the surface resulting from surfactant adsorption. The sharp increase in flotation above a certain amine concentration has been attributed to the formation of two dimensional surfactant aggregates at the solid/liquid interface (4).

The decrease in flotation above the maximum with increase in amine concentration does not, however, imply that the adsorption density at the solid/liquid

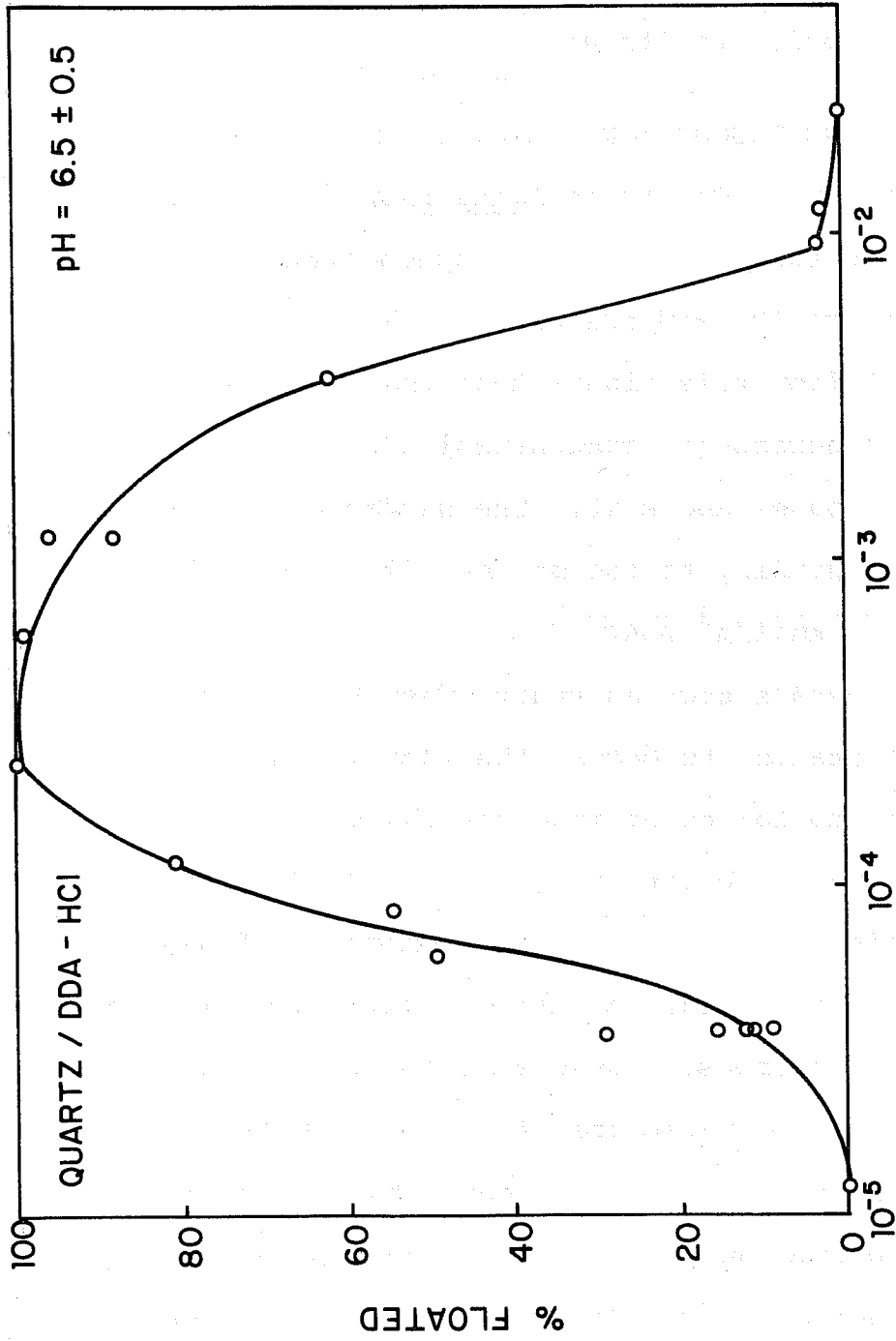


Figure III:1. Hydrophobicity of quartz, as measured by flotation, as a function of concentration of DDA-HCl.

interface is decreasing. This is because, in addition to adsorption density, the hydrophobicity imparted to the mineral depends also upon a number of other factors. For example, at high concentrations, surfactant can adsorb forming a bilayer, the second layer having its ionic heads oriented towards the solution. Similarly, adsorption of doubly charged dimers (5) with their ionic heads at the opposite ends can also have ionic heads exposed to solution. In both these cases, flotation can decrease with further increase in surfactant concentration. It is to be noted that the surfactant adsorbs at the liquid/air (bubble) interface during flotation with the ionic heads towards the solution. Therefore, under conditions of high adsorption density at both solid/liquid and liquid/air interfaces, there can be incompatibility between these two surfaces for attachment. Finally, at high surfactant concentration, the bubble size decreases and as a result the particle-bubble aggregate may not be able to levitate to the surface. Thus, the decrease in flotation at high surfactant levels can be due to any one or a combination of the above factors. It would be interesting to determine changes brought about by the polymer in the wettability of quartz in amine solutions, and particularly that above the flotation maximum.

B3b. Non-ionic Polymer

The effect of the non-ionic polymer, PAM, on the wettability of quartz at different levels of DDA-HCl is shown in Figure III:2. It is clear from the figure that PAM alone does not impart any hydrophobicity to quartz. Also, PAM (up to about 100 mg/kg at the tested levels of amine does not appear to influence the flotation significantly. At 1000 mg/kg of PAM and 3.6×10^{-5} kmol/m³ DDA-HCl, a marginal increase in flotation is observed.

PAM is a hydrophilic polymer and hence, even if it adsorbs on quartz, it cannot be expected to impart any hydrophobicity to the mineral. Moreover, based upon the results for the adsorption of PAM on quartz and silica (See Figure III:3 and Table III:2) significant adsorption of PAM cannot be expected. Therefore, the absence of any major effect of PAM on amine flotation of quartz can be due to its relatively low adsorption at the solid/liquid interface.

The observed small increase in flotation at 1000 mg/kg of PAM is possibly due to the increase in the effective concentration of surfactant resulting from the decrease in the solvent power of water under these conditions. The latter effect is caused by the hydration of polymer and the consequent decrease in the amount of "free water".

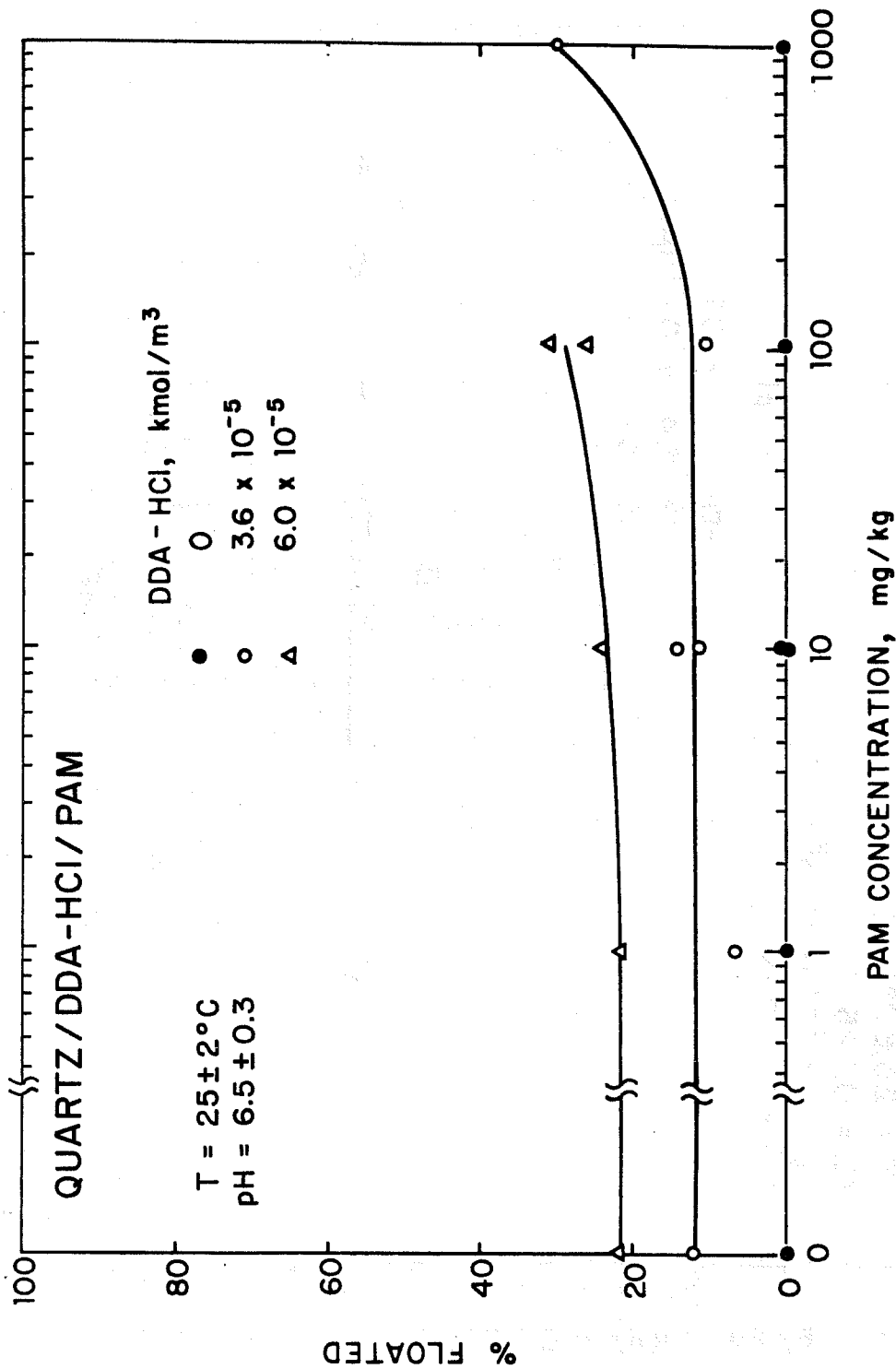


Figure III:2. Effect of the non-ionic polymer, PAM, on the wettability of quartz, as measured by its flotation in DDA-HCl solutions.

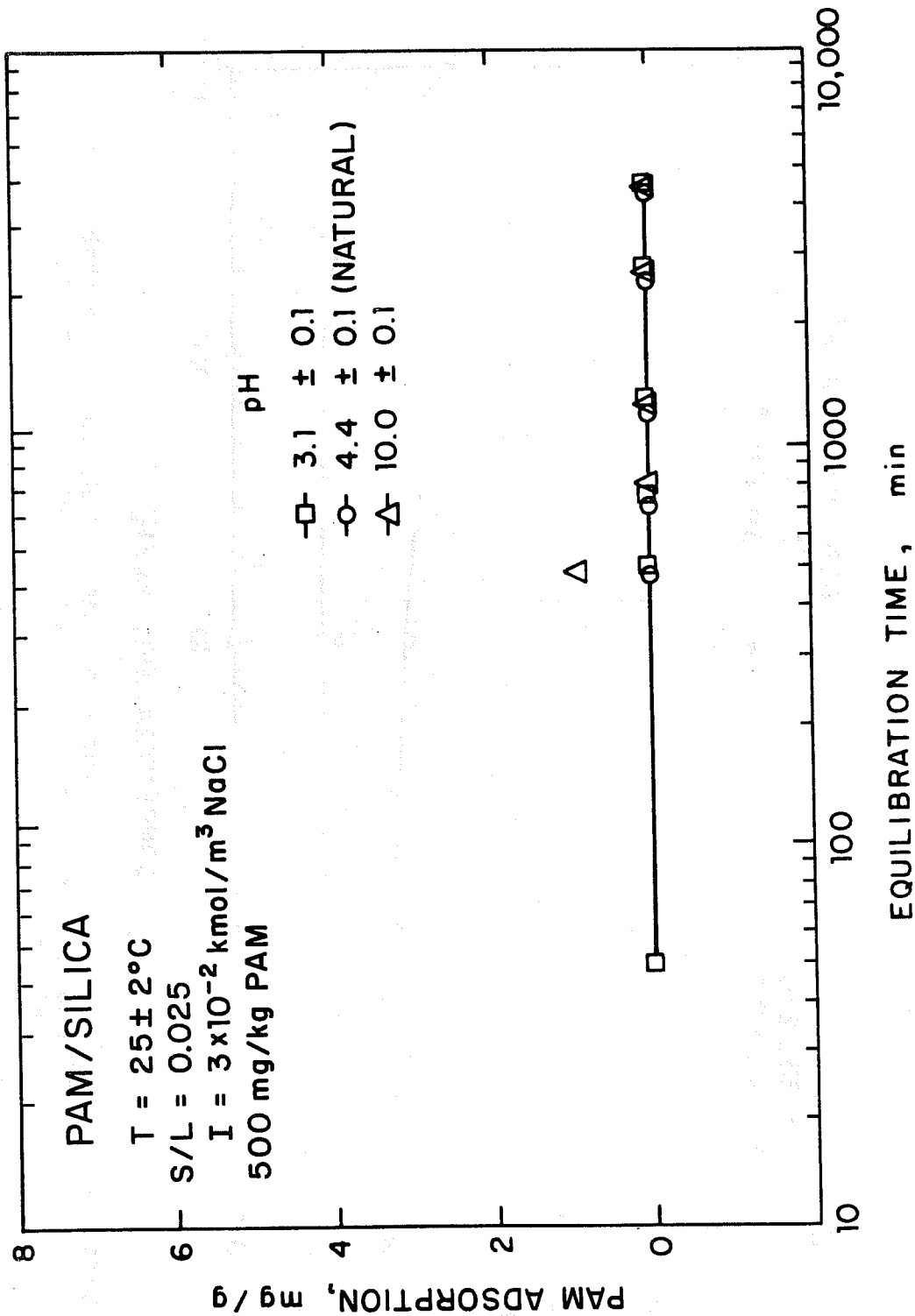


Figure III:3. Adsorption of PAM on silica as a function of time at three pH values.

TABLE III:2

Adsorption of PAM Under Natural pH Conditions

Initial PAM Concentration 533mg/kg

<u>Mineral</u>	<u>Adsorption Density</u> (mg/g)
Quartz	0.3
Biosil(Silica)	0
Hematite	9.2
Alumina	7.2

B3c. Cationic Polymer

Cationic PAMD, as shown in Figure III:4, is found to depress the amine flotation. Flotation is completely depressed at an addition of 10 mg/kg of PAMD.

PAMD, being cationic, can be expected to adsorb on quartz and in fact, the results of PAMD adsorption on silica (Figure III:5) show this to be the case. PAMD can compete with amine for adsorption sites on quartz even though studies on a similar surfactant/polymer system suggest the effect of competition on surfactant adsorption to be minimal (6). In addition to any possible competition with amines for the surface sites, polymer can also mask the effect of adsorbed surfactants as shown in Figure III:6.

It is interesting to note that, while competition effects can reduce the loss of surfactants at the expense of polymers, the effect due to masking results in loss of both surfactant and the polymer. Determination of the adsorption of both polymers and surfactants simultaneously can distinguish between the above two proposed mechanisms. Such tests are in progress at present.

B3d. Anionic Polymer

The effect of sulfonated PAM (PAMS) on the wettability of quartz is given in Figure II:7. PAMS at

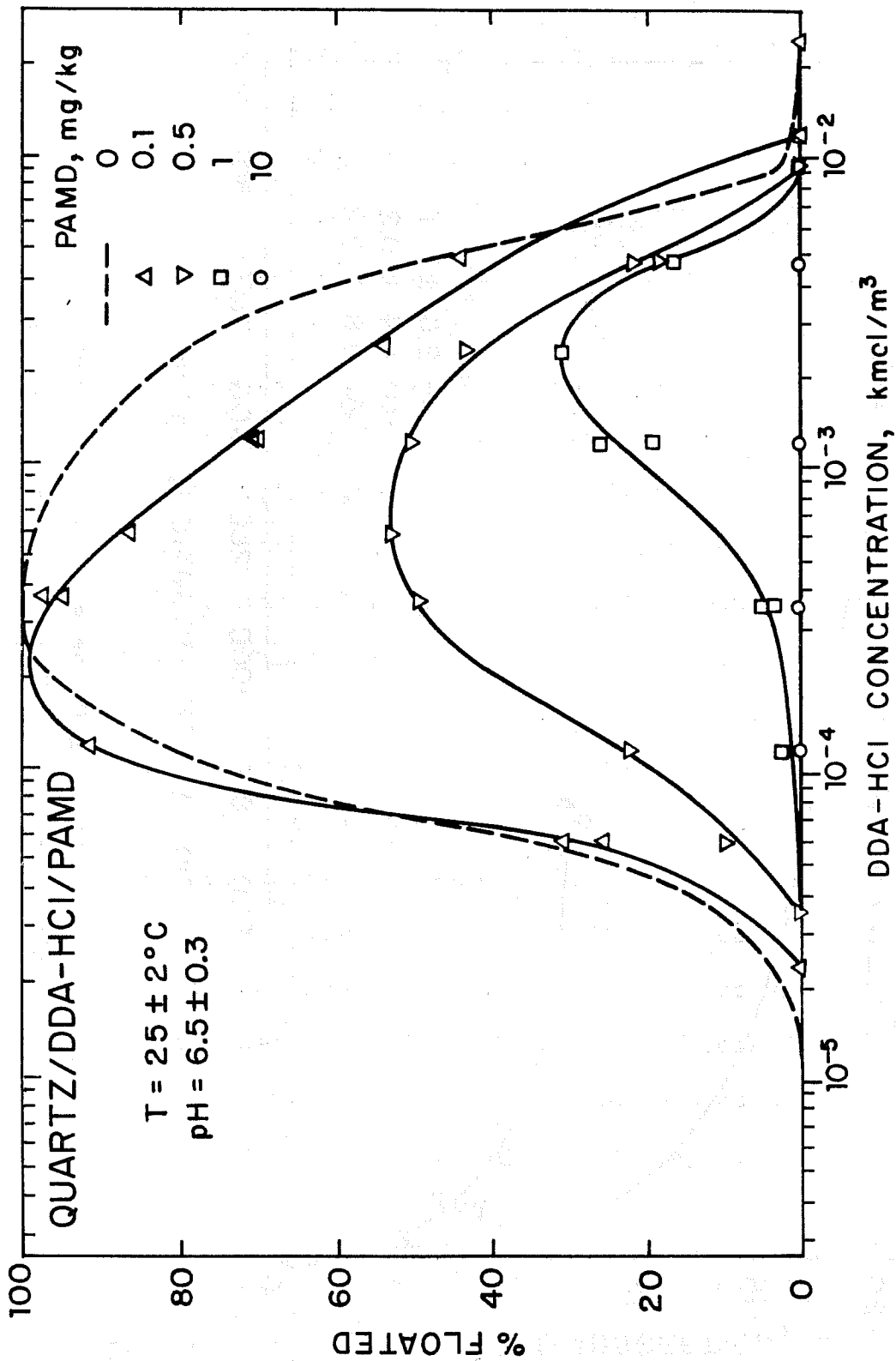


Figure III:4. Effect of the cationic polymer, PAMD, on the wettability of quartz, as measured by its flotation, in DDA-HCl solutions.

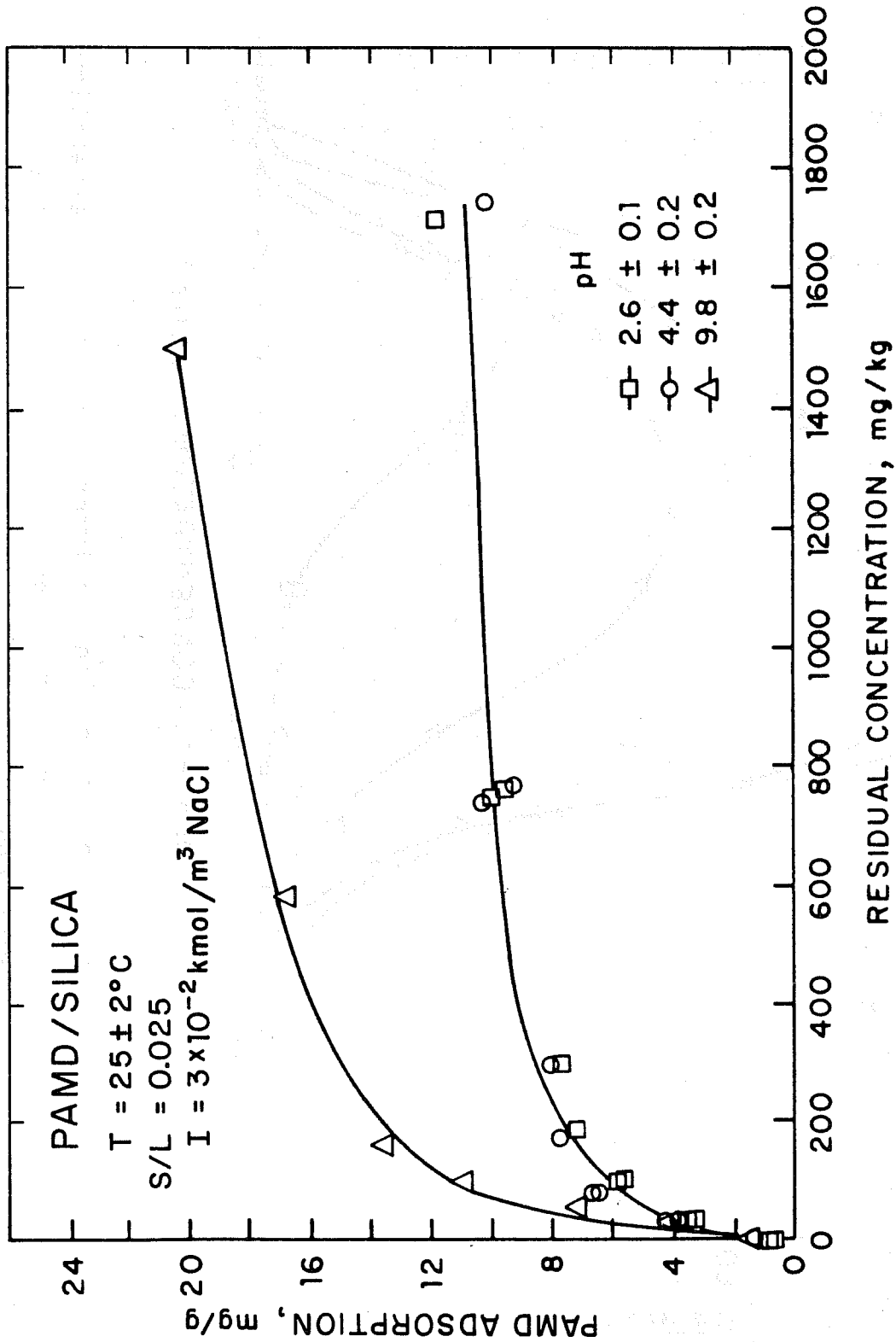


Figure III:5. Adsorption of PAMD on silica as a function of the residual concentration at three pH values.

DEPRESSION OF CATIONIC FLOTATION
OF QUARTZ BY PAMD

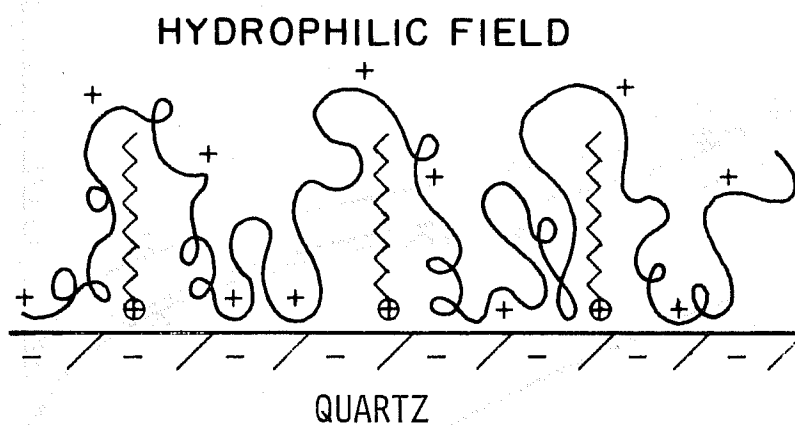


Figure III:6. A schematic diagram showing the polymer, PAMD, masking the effect of the adsorbed DDA^+ on quartz.

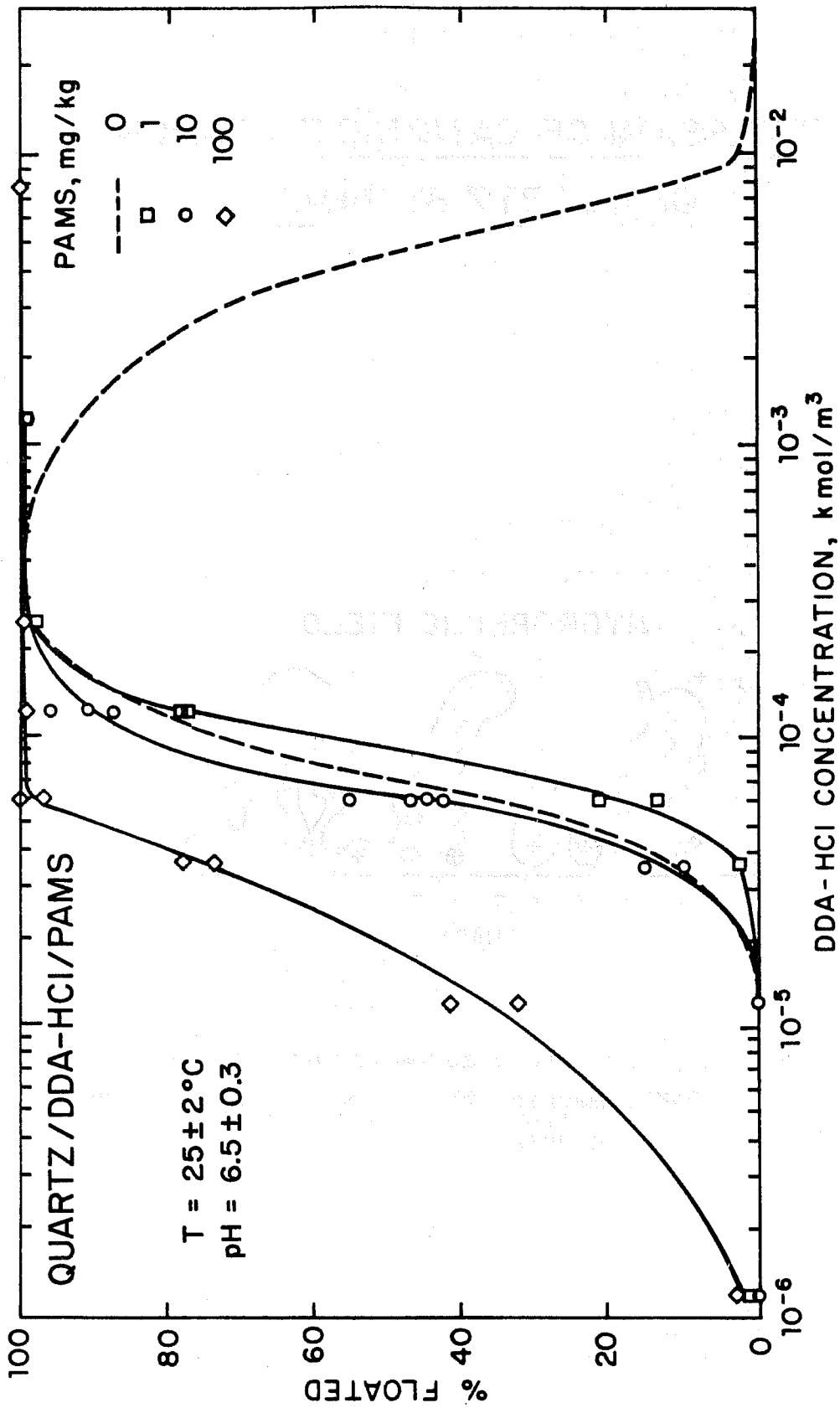


Figure III:7. Effect of the anionic polymer, PAMS, on the wettability of quartz, as measured by its flotation, in DDA-HCl solutions.

low concentrations (1 and 10 mg/kg) does not appear to have any significant effect on the amine flotation of quartz. However, at 100 mg/kg polymer, quartz flotation is enhanced at low surfactant concentrations and most interestingly, at high surfactant levels, the depression in flotation observed in the absence of the polymer is eliminated in the tested range. Thus, the anionic polymer appears to increase the range of amine concentration over which the system exhibits maximum non-wettability for water.

PAMS, which has both acrylamide as well as sulfonate functional groups may not adsorb in significant amounts on quartz, since both acrylamide (as evident from PAM adsorption on silica) and sulfonate (because of the negative charge) are not expected to cause significant adsorption. On the other hand, the opposite nature of charges on the polymer and surfactant can result in electrostatic interactions between them in the bulk. Such a surfactant/polymer complex formed can be surface active, and may also adsorb at interfaces. At the solid/liquid interface polymer can adsorb under conditions when surfactant is adsorbed with a reverse orientation. Apart from such electrostatic interactions in the bulk and at interfaces, presence of polymer can influence the system behavior also by

decreasing the solvent power of the medium. A decrease in the solvent power of the medium is equivalent to an apparent increase in the concentration of the surfactant in the system. Based upon the above considerations, the following mechanism is proposed for the observed effects in this system.

The enhancement of flotation at low surfactant concentration is attributed mainly to the increased adsorption of the surfactant at the solid/liquid interface, the increase being due to the decrease in the solvent power of the medium. The adsorption of polymer/surfactant complex itself is not considered under these low surfactant concentration conditions, since such adsorption requires surfactants either at the solid/liquid interface or on the sulfonate sites of the polymer with their polar heads oriented towards the solution. In either case, determination of the adsorption of polymer and surfactant in the presence of one another can distinguish between these two mechanisms.

As mentioned earlier, the decrease in flotation at high surfactant concentrations can be due to the formation of a bilayer at the solid/liquid interface and to the incompatibility of the bubble/particle for attachment. Presence of an oppositely charged polymer, in such a system can cause aggregation between the bubble and the particle (see Figure III:8). Such a

POSSIBLE PAMS-AMINE INTERACTIONS

1. "SANDWICHING EFFECT"

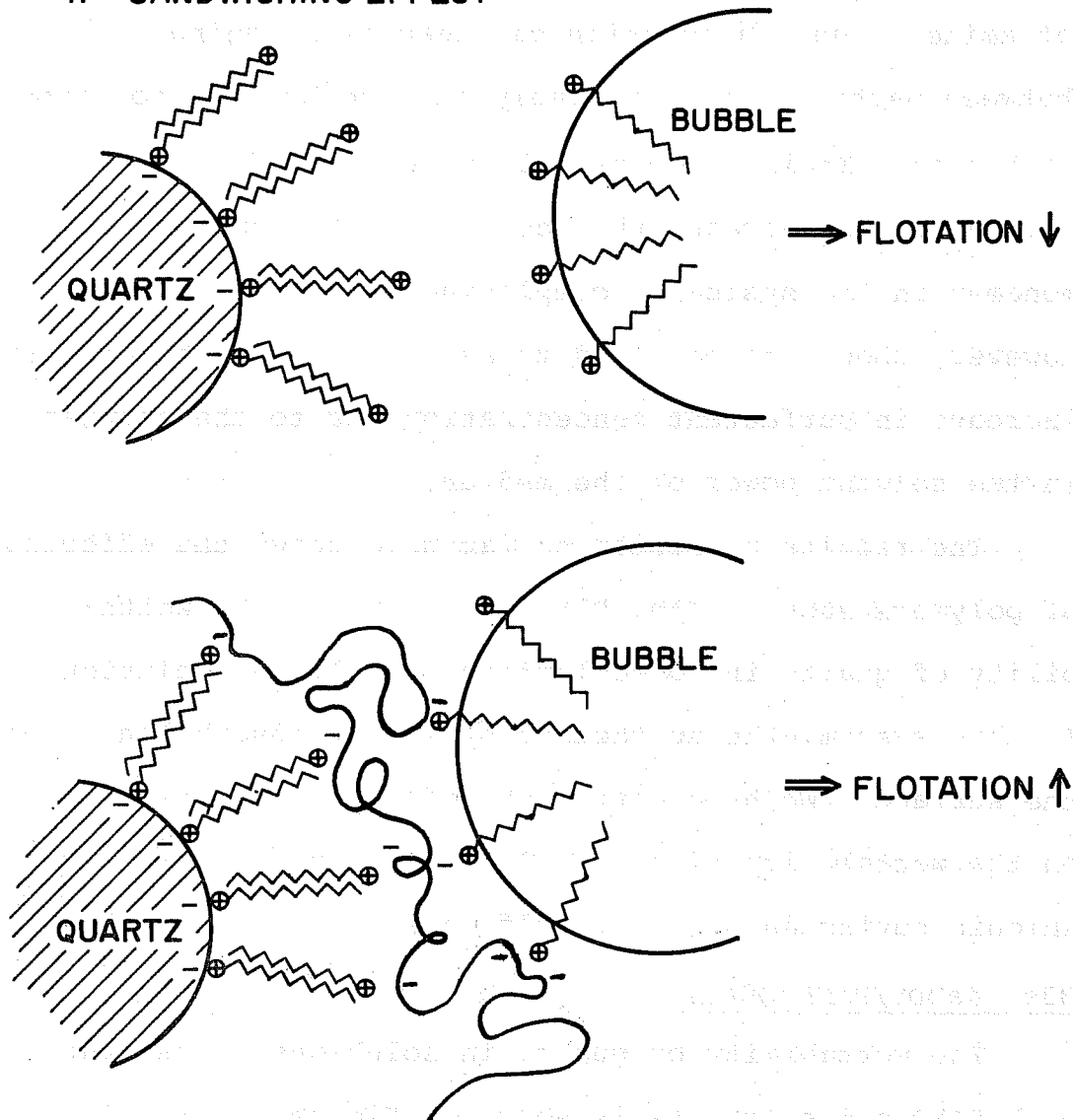


Figure III:8. A schematic diagram showing the aggregation between the surfactant coated bubble and quartz in the presence of a polymer charged oppositely to the surfactant--the aggregation process is referred to as "Sandwiching Effect."

bridging of the bubble and particle can prevent excessive depression in flotation. Preliminary results for the adsorption of PAMS on silica (6) clearly show that the polymer can adsorb on silica in the presence of amine. Such adsorption can lead to bridging between particles and similarly charged bubbles to cause flotation. It is also possible that the effect of polymer is to decrease the activity of the surfactant monomer in the system by complexing it. This effect, however, should be balanced to some extent by the effective increase in surfactant concentration due to the changes in the solvent power of the medium.

The results presented so far have shown the effects of polymers such as PAM, PAMS, and PAMD on the wettability of quartz in dodecylaminehydrochloride solutions. In this system, the surfactant by itself adsorbs on the surface. We have tested the effect of polymers on the wettability of quartz in the presence of an anionic surfactant, dodecylsulfonate.

B3e. NaDDS/PAMD/QUARTZ

The wettability of quartz in solutions containing both PAMD and sulfonate is shown in Figure III:9. Both PAMD and sulfonate independently do not impart any non-wettability to quartz. This is expected because, (a) the negatively charged NaDDS does not adsorb on

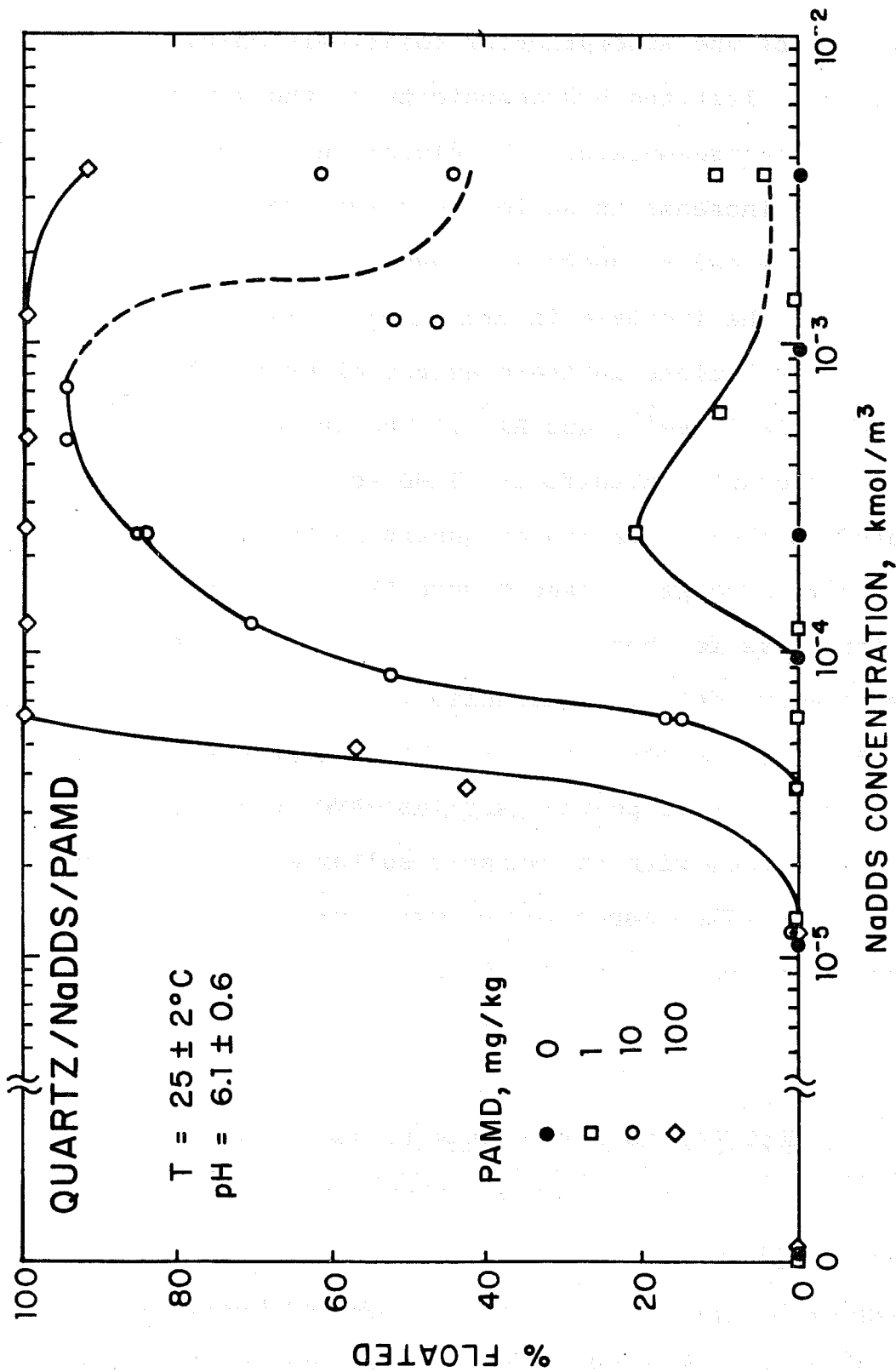


Figure III:9. Effect of the cationic polymer, PAMD, on the wettability of quartz, as measured by flotation, in NaDDS solutions.

quartz, and (b) the adsorption of positively charged PAMD will not alter the hydrophobicity of the surface. However, in the presence of PAMD, flotation is found to increase with increase in sulfonate concentration up to a certain value and to decrease above it. This behavior is similar to the increase in non-wettability of quartz in sulfonate solutions in the presence of multivalent ions such as Ca^{2+} , Fe^{2+} , and Al^{3+} . The increase in flotation of quartz in sulfonate/PAMD solutions is attributed to the activation of quartz surface by PAMD for sulfonate adsorption (see Figure III:10). Again, adsorption tests for both sulfonate and PAMD are in progress to elucidate the mechanisms.

In addition to activating the adsorption of NaDDS on quartz, a cationic polymer such as PAMD can be expected to interact with the anionic sulfonate also in the bulk solution. This aspect of polymer/surfactant interaction in the bulk is discussed in the next section.

C. PAMD/NaDDBS - Interactions in Bulk Solution: Precipitation/Redissolution Phenomenon

C1. INTRODUCTION

PAMD, being cationic, can be expected to interact electrostatically with the anionic sulfonate in the

ACTIVATION OF ANIONIC FLOTATION OF QUARTZ BY PAMD

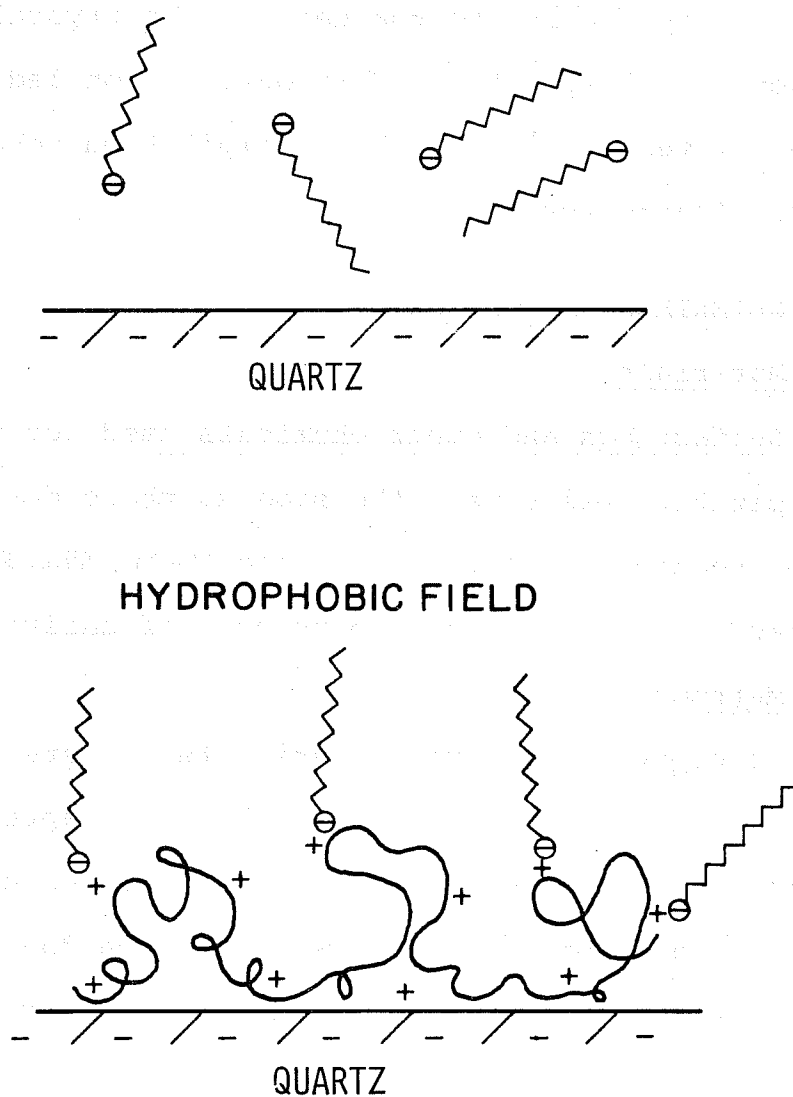


Figure III:10. A schematic diagram showing the activation of the adsorption of DDS^- on quartz in PAMD solutions.

bulk solution. In fact, during the preparation of solutions containing both PAMD and NaDDS for the wettability studies, precipitation was found to occur under certain conditions. Visual examination clearly indicated the fibrous, gel-like structure of the precipitate, as opposed to the needle-like crystalline surfactant precipitate. This observation led to a series of tests to study the precipitation behavior of the PAMD/sulfonate system.

C2. MATERIALS AND METHODS

C2a. Materials

Surfactants and other chemicals used for the precipitation tests were the same as those described in the section on wettability (page 149). The PAMD used was tagged with C-14 for the purpose of analysis.

C2b. Methods

Precipitation. Precipitation tests were conducted according to the procedure described in Chapter I. The polymers used for precipitation tests were tagged with C-14 and hence the analysis could be done easily using the liquid scintillation counter (Beckman LS 100C).

Surface Tension. Surface tension of polymer/surfactant solutions was measured using the Wilhelmy plate technique. (See Chapter I for details of the procedure).

Viscosity. Viscosity measurements were carried out using a suspended level Ubbelohde Capillary Viscometer.

C3. RESULTS AND DISCUSSION

C3a. NaDDBS/PAMD Precipitation Behavior

Results obtained for the precipitation behavior of PAMD upon increasing the NaDDBS concentration are given in Figure III:11. It is evident from this figure that precipitation of both the surfactant and polymer took place upon increasing the sulfonate and most interestingly, the precipitate redissolved above a certain surfactant concentration. This phenomenon of the redissolution of polymer/surfactant complex appears to be similar to the redissolution of multivalent ion/sulfonate precipitates discussed in Chapter I. Unlike the latter system, in this case the polymer precipitate did not undergo complete redissolution. About 20% of the polymer remained in the precipitated form even at high sulfonate concentrations in the tested range.

The results for the relative viscosity of PAMD/NaDDBS system showed a minimum with increase in sulfonate concentration and the position of the minimum corresponded to the point of maximum polymer precipitation (see Figure III:12). These observations are in agreement with the expected changes in the viscosity due

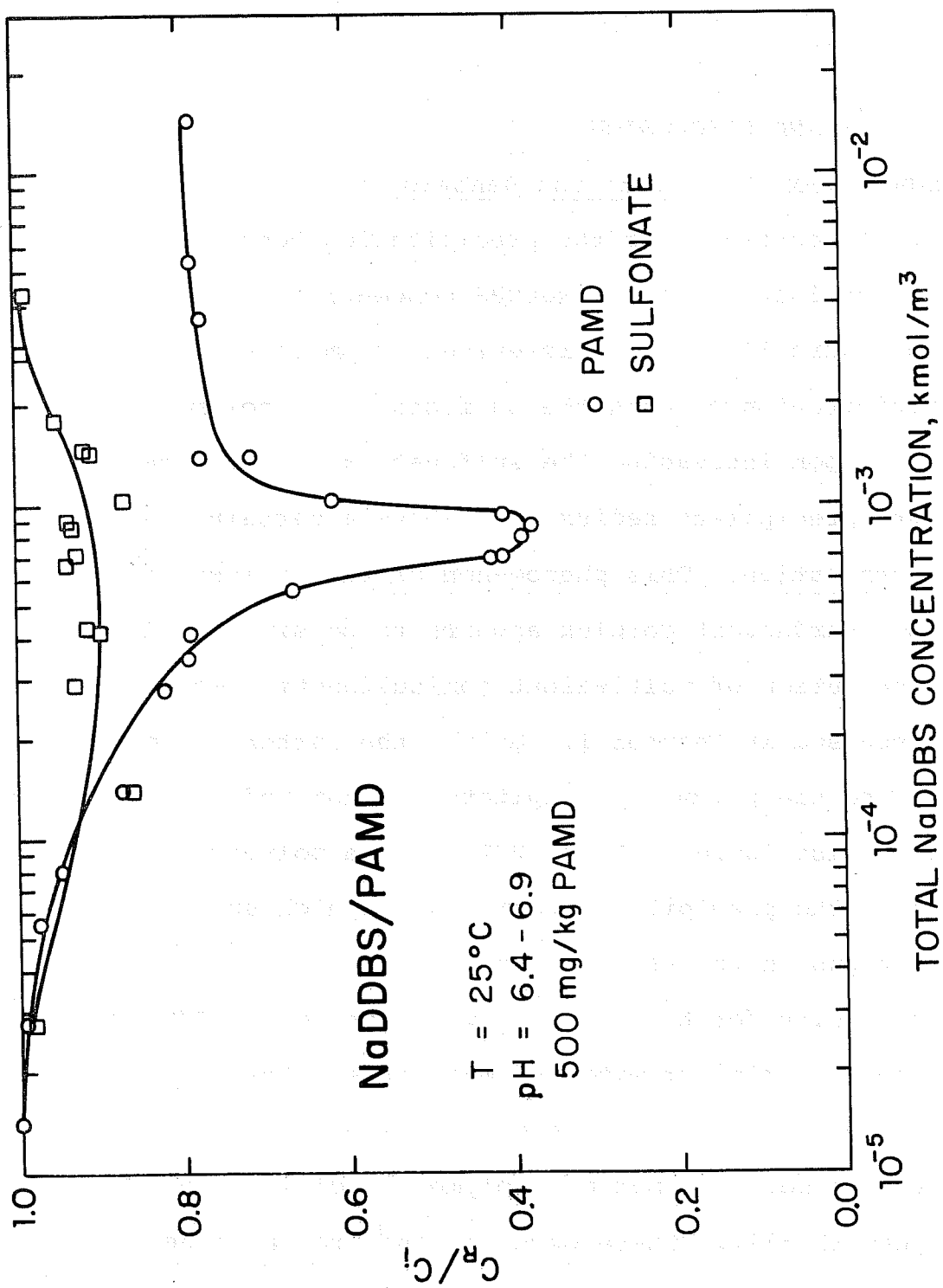


Figure III:11. Precipitation behavior of DDDBS and PAMD as a function of sulfonate concentration.

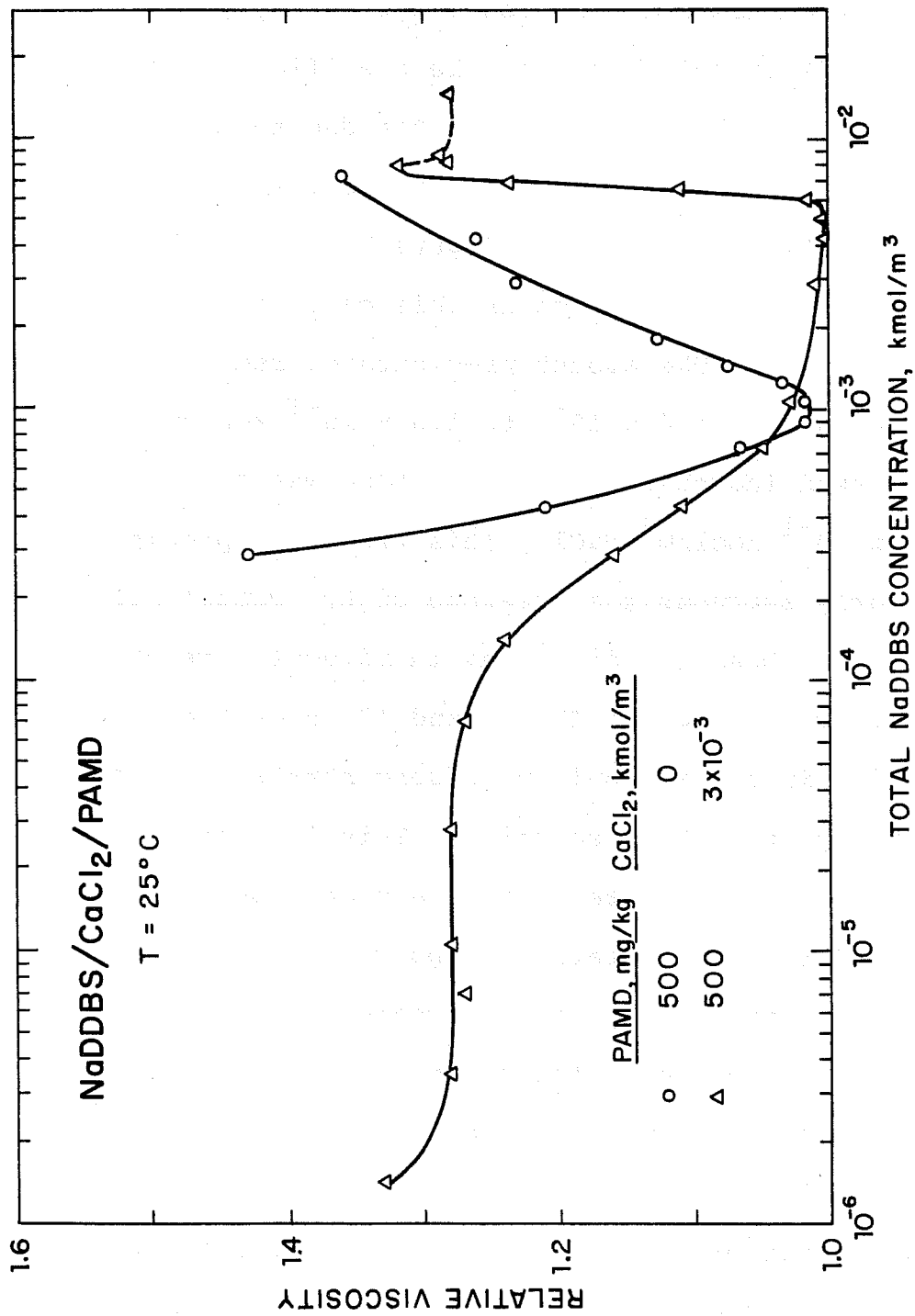


Figure III:12. Relative viscosity of PAMD/NaDDBS solutions as a function of sulfonate concentration.

to the precipitation and the redissolution of the polymer.

Since the above tests were conducted at 0 kmol/m^3 NaCl (without controlling the ionic strength), it is difficult to distinguish between the specific interactions of sulfonate with the polymer from that due to the changes in ionic strength. Therefore, similar data was generated as a function of NaCl (see Figure III:13). The onset of polymer precipitation in this case was around 10^{-3} kmol/m^3 NaCl. The amount precipitated remained constant ($\approx 20\%$) from 4×10^{-3} to $1.5 \times 10^{-1} \text{ kmol/m}^3$ NaCl. A marked increase in precipitation was observed above $1.5 \times 10^{-1} \text{ kmol/m}^3$ NaCl. This two stage precipitation clearly suggests the presence of two components in the polymer, possibly differing in molecular weight.

Comparison of Figures III:11 and 13 shows that the precipitation in certain sulfonate concentration regions is more than that in NaCl solution. This indicates the specific nature of interaction between PAMD and sulfonate and the precipitation of polymer/surfactant complex. Most importantly, in the redissolution region, the system could not cause the redissolution of about 20% of the precipitate which is the same amount that was found to precipitate in NaCl solutions. Thus, the precipitation of 20% fraction is attributed to the ionic strength effect.

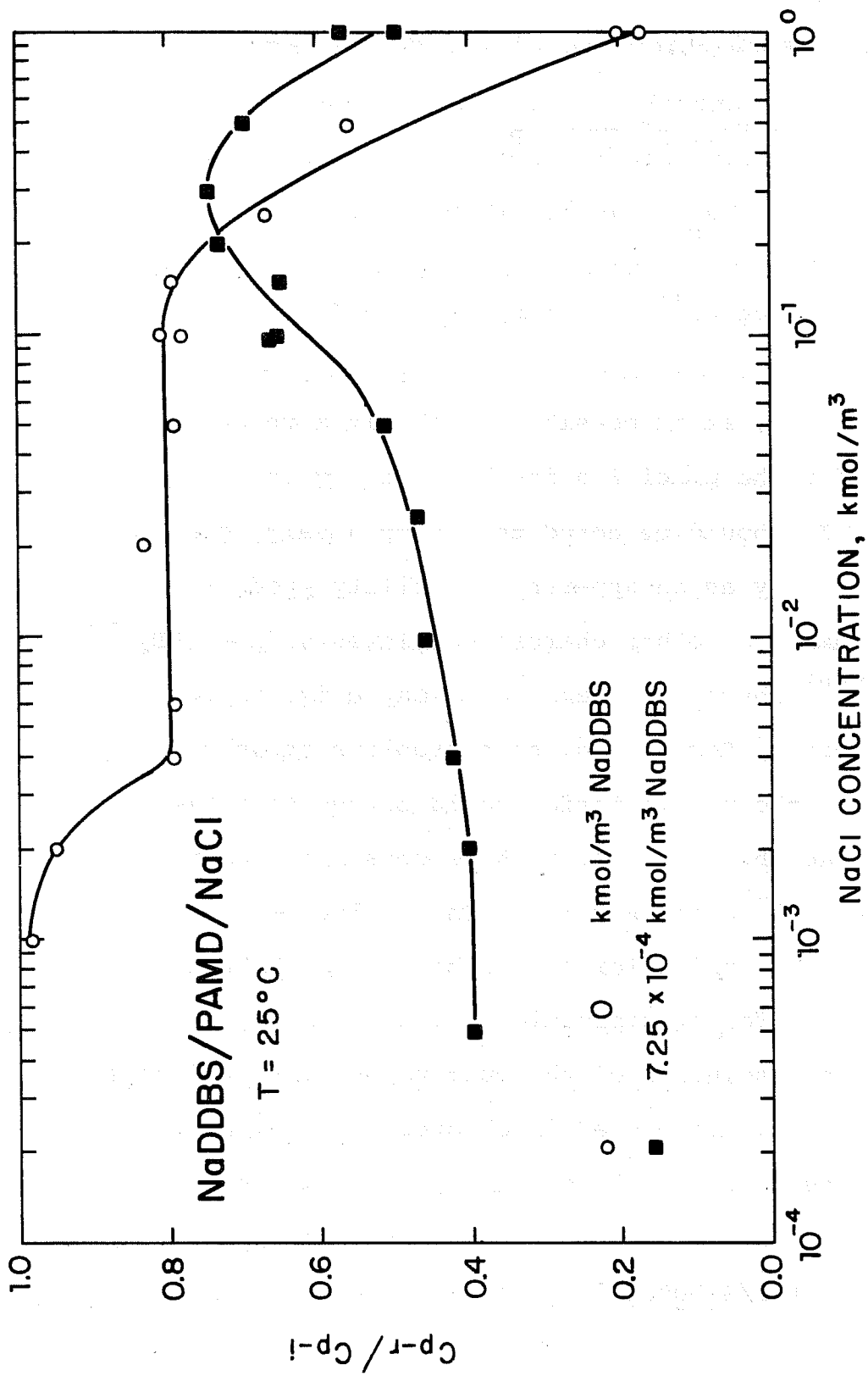


Figure III:13. The effect of NaCl on the precipitation behavior of PAMD, both in the presence and absence of NaDDBS.

The interaction of the polymer with the surfactant leading to precipitation can be represented as:



$$K_{sp} = [P^{+n}] [R^{-}]^n \quad (2)$$

$$\log [P^{+n}] = \log K_{sp} - n \log [R^{-}] \quad (3)$$

Therefore, it is possible to obtain a reaction constant for the precipitation by plotting $\log(R^{-})$ vs. $\log(P^{+n})$. It should be noted that such a value can be considered only as an apparent solubility product, since a number of other charged complexes such as $PR_x^{+(n-x)}$ and $PR_y^{-(y-n)}$ where $x < n$ and $y > n$ may exist in the aqueous phase. Recognizing such problems and noting that 20% of the precipitation could be due to a high molecular weight fraction, we have obtained a value of $K_{sp} = 1.4 \times 10^{-10}$ and $n = 1.2$. This value of n can be taken as an indication of 1:1 binding of PAMD and sulfonate for precipitation.

The redissolution of the multivalent ion/sulfonate precipitates, as discussed in Chapter I occurred only in the presence of micelles. In order to determine the onset of redissolution in the present case, surface tension of PAMD/NaDDBS solutions was measured (see

Figure III:14). The onset of precipitation and point of complete redissolution (for the 80% fraction) are indicated. In the presence of PAMD, the surface tension of NaDDBS is reduced significantly up to about 10^{-3} kmol/m³ NaDDBS. Also, the slope of the surface tension vs. log (concentration) curve is reduced in the presence of PAMD. Most importantly, the onset of redissolution is below the CMC of the surfactant. This behavior is different from that observed in multivalent ion/sulfonate systems where the redissolution was found to occur only in the presence of micelles.

The surface tension lowering of sulfonate solutions due to the addition of PAMD to the system is caused either by the "salting out" of the surfactant or by the adsorption polymer-surfactant complex at the interface. The decrease in $\partial\gamma/\partial\log c_T$, on the other hand, suggests that the monomer activity in the bulk is not increasing in the presence of PAMD in a manner similar to that in the absence of it. This is also conceivable since part of the added sulfonate is being used by the polymer to form the polymer/surfactant complex.

CMC of the PAMD/sulfonate system, as detected by the dye solubilization technique coincided with the onset of redissolution of the precipitate. Since it is known that the solubilization of dye can occur

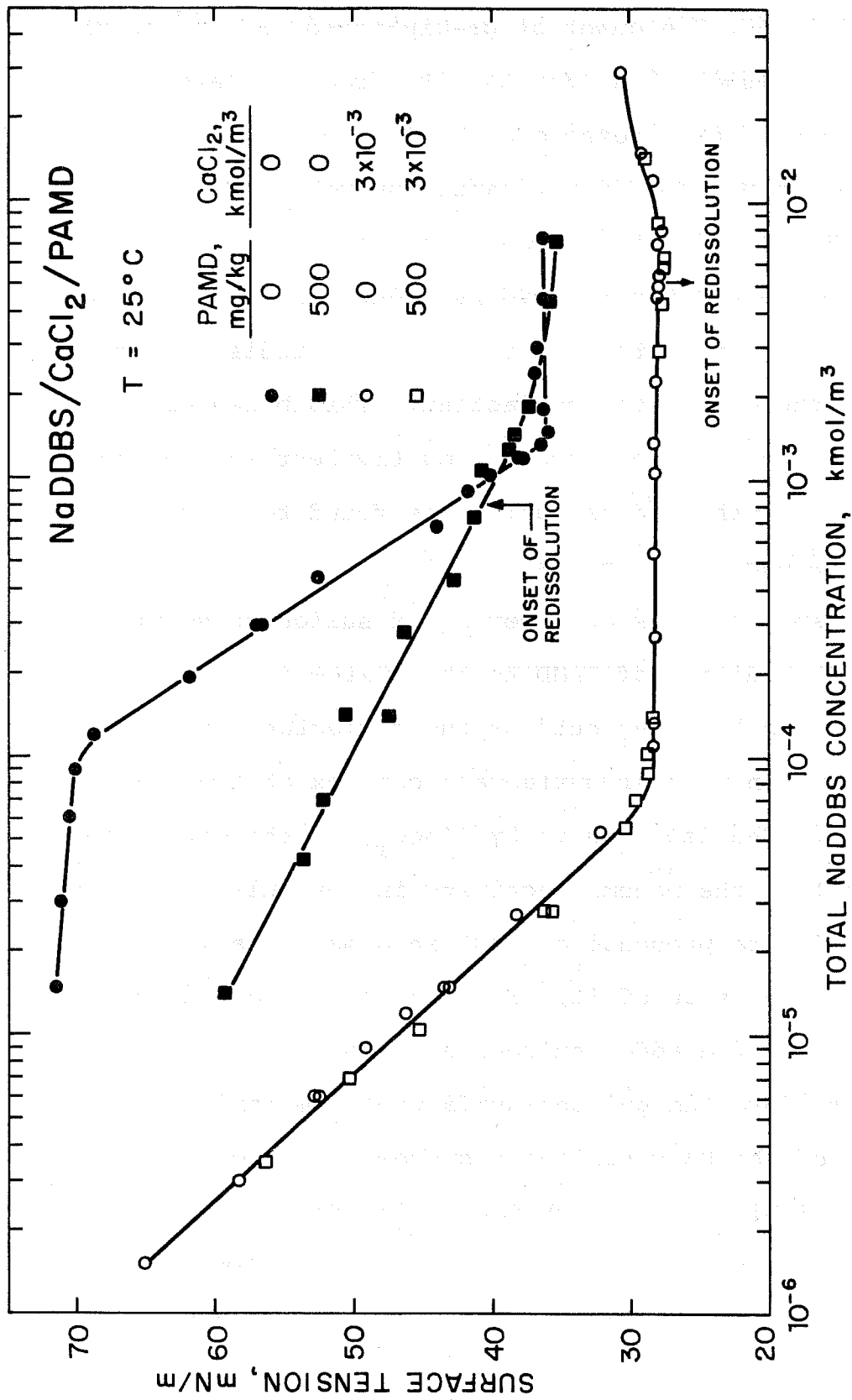
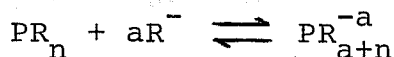


Figure III:14. Surface tension of NaDDBS/PAMD and NaDDBS/PAMD/CaCl₂ systems as a function of sulfonate concentration.

much before the conventional micelle formation (7), the dye solubilization observed at the onset of redissolution was not considered as indicative of micelle formation.

Since the redissolution of the polymer/surfactant complex takes place below the CMC, it must be due to a complexation process such as



Such a reaction can result from the chain-chain interaction of a surfactant molecule with another surfactant which is already electrostatically bound to the polymer. Interaction of doubly charged dimers, which are expected to form at high surfactant concentrations (5), with the polymer can also result in soluble complexes.

C3b. Effect of NaCl on PAMD/NaDDBS Precipitation

The effect of addition of NaCl to PAMD (500 mg/kg) and NaDDBS ($7.5 \times 10^{-4} \text{ kmol/m}^3$) is given in Figure III:13. Concentrations of PAMD and NaDDBS selected for these tests correspond to the maximum precipitation condition in Figure III:11. Increase in the NaCl concentration is found to cause a decrease in precipitation up to $3 \times 10^{-1} \text{ kmol/m}^3$ NaCl. Further increase in NaCl, however, resulted in increased precipitation. Similar effects of NaCl have been observed also for $\text{CaCl}_2/\text{NaDDBS}$ system (see Chapter I, also References 1-3).

The reasons for the observed effects of NaCl on the precipitation behavior of PAMD/NaDDBS system are not clear at present. "Salting-out" of the surfactant by NaCl can enhance also the precipitation and redissolution reactions given earlier (see Equations 1 & 2). Therefore, both precipitation and redissolution can occur in NaCl solutions at lower surfactant concentrations than in the absence of NaCl. According to this hypothesis, the redissolved species will have an excess negative charge (see Equation 2). On the other hand, the salting-out effect may simply result in lowering the monomer activity (also CMC) in which case, the reverse of reaction



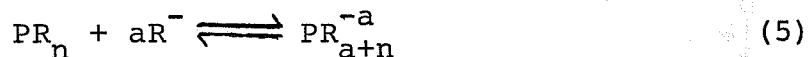
can take place. The charge on the precipitate under these conditions would be positive. The former hypothesis of enhanced complexation is equivalent to moving to the right of the curve in Figure III:11, and the latter, to the left. Measurement of charge on the precipitate upon adding NaCl can indicate the nature of interactions responsible for the redissolution of PAMD/DDBS complex.

C3c. Effect of CaCl₂ on PAMD/NaDDBS Precipitation

The precipitation/redissolution behavior of CaCl₂/NaDDBS system both in the presence and absence of

is given in Figures III:15 and 16. Comparison of these figures clearly shows that PAMD did not affect the precipitation/redissolution behavior of the calcium/sulfonate system. However, the presence of calcium increased the onset of precipitation as well as that of redissolution of the polymer to higher initial sulfonate concentrations. Also the range of sulfonate concentration over which the polymer complex was stable was increased significantly by the presence of calcium.

The need for higher initial sulfonate concentration for the precipitation of PAMD/sulfonate complex is expected since a significant amount of surfactant is used up by calcium to form the calcium sulfonate precipitate. With further increase in sulfonate concentration, the monomer activity increases significantly to cause reactions such as



leading to the redissolution of the polymer precipitates. The calcium sulfonate redissolution will occur once the monomer activity reaches the CMC.

It is not possible from the data given in Figure III:15 to distinguish between the onset of redissolution of the polymer precipitate and calcium sulfonate, particularly because of the low sulfonate requirement for the

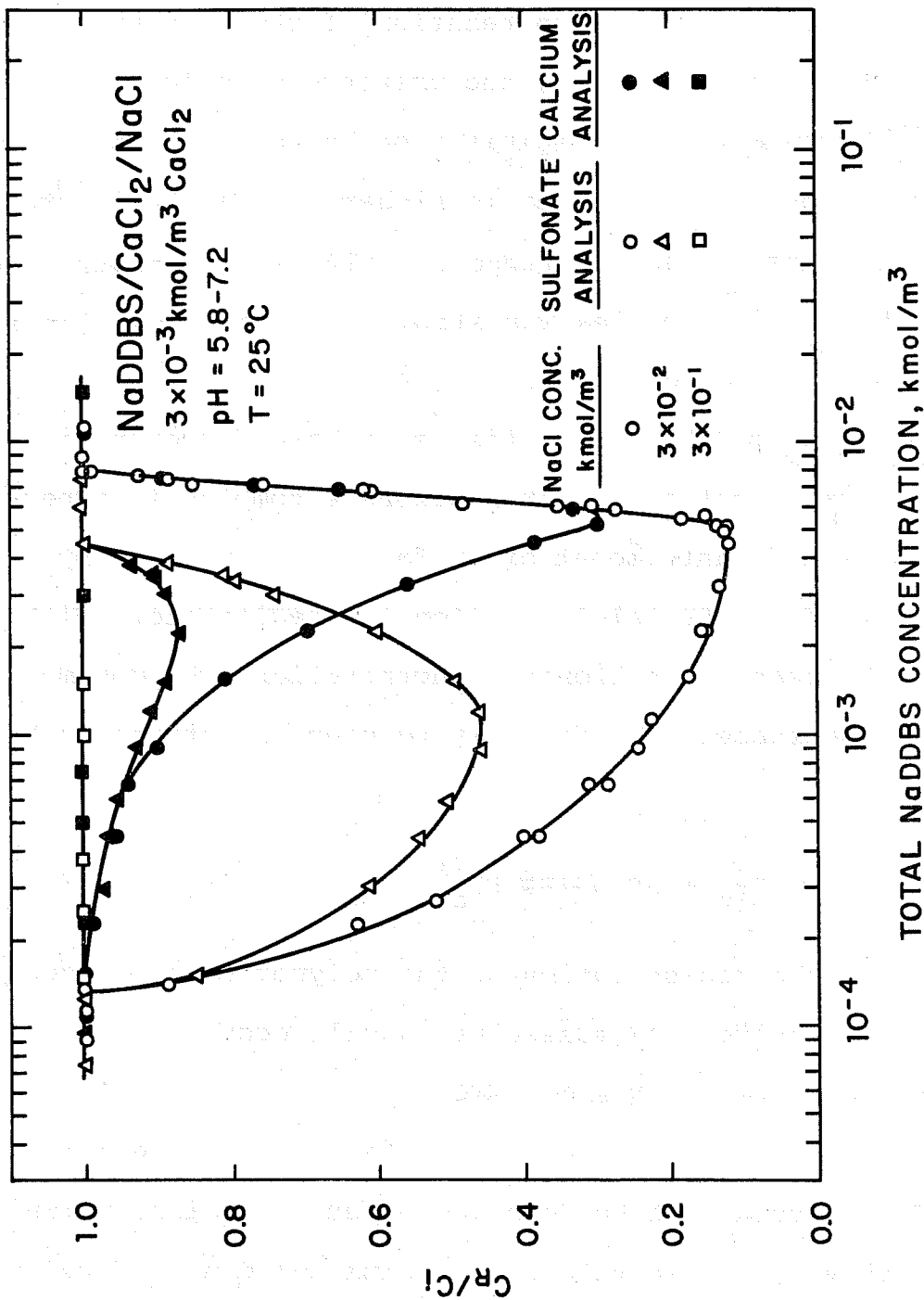


Figure III:15. Precipitation behavior of NaDDBS/CaCl₂ system as a function of sulfonate concentration.

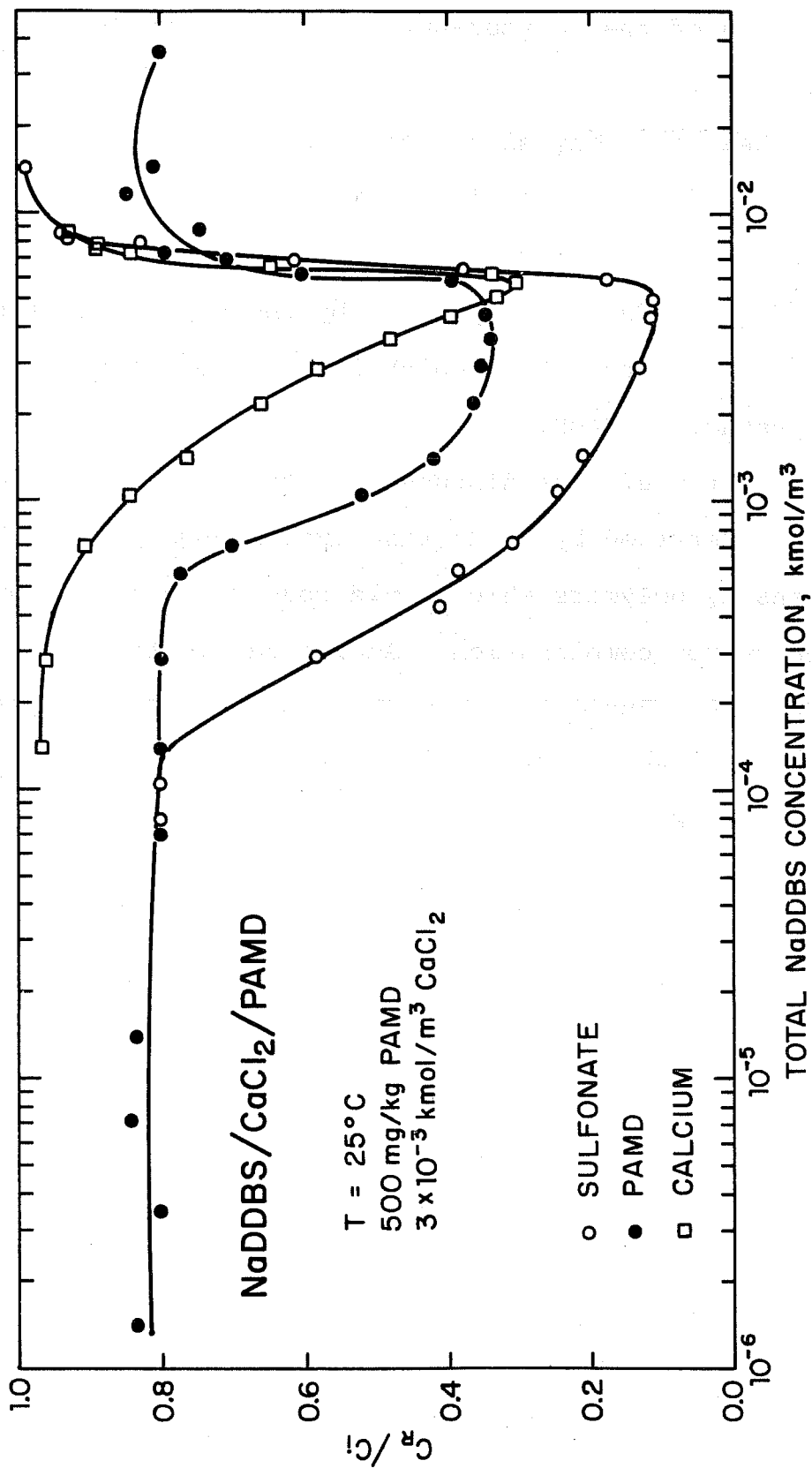


Figure III:16. Precipitation behavior of NaDDBS/CaCl₂/ PAMD system as a function of sulfonate concentration.

redissolution of the polymer-surfactant complex (see Figure III:11).

The absence of any significant influence of PAMD on calcium sulfonate precipitation/redissolution clearly indicates the dominant effect of calcium in the system. This is further supported by the surface tension data given in Figure III:14 which is also not affected by the presence of PAMD.

Some of the effects discussed in this section could be better understood by conducting experiments with higher charge density polymers which would require larger amounts of sulfonate for complexation. Additional tests are in progress to elucidate the mechanisms of polymer/surfactant interactions in this system as well as in other polymer/surfactant systems.

IV. FLOW DISTRIBUTIONS IN CONSOLIDATED SANDSTONE UTILIZING A TOMOGRAPHIC TECHNIQUE

A. Introduction

In the past fifteen months, my laboratory at Columbia University has been using CAT scanning to observe the possibilities for core research. We use the Delta 50 (Ohio Nuclear) CAT scanner on the campus, located at St. Luke's Medical Center. It scans a core with a collimated 120 Kev X-ray beam. We recover the binary data matrix on the scanner PDP-11 system on magnetic tape. Although experiments can interrupt the hospital machine at night, our needs for data analysis and reconstruction exceed its capacities. We are seeking capital funds to assist in our construction of an adequate facility.

B. Fluids that Can Be Observed in Berea Sandstone

We have demonstrated the quantitative nature of the CAT scan method for a number of different fluid combinations. In each experiment, displacing and displaced fluids are defined. Table 1 summarizes the fluid pairs having significant variations in X-ray attenuation. From these combinations, it is evident that the principal fluid and rock parameters can be independently controlled.

Table IV:1 Displacing Fluid/Displaced Fluid Combinations
that Can Be Observed in Berea Sandstone

Fluid One	Fluid Two
1. Aqueous 1 Molar KI	- Aqueous 1 M NaCl - Oil or other hydrocarbon
2. Aqueous 1 Molar KI with polymer such as poly(acryl- amide) or with sucrose	- Aqueous 1 M NaCl - Oil or other hydrocarbon
3. Exxon-1 Micellar Fluid in 1 M KI	- Oil or other hydrocarbon
4. Carbon tetrachloride	- Polystyrene in toluene - Toluene - Oil
5. Chlorinated polyisobutylene	- Polystyrene in toluene - Oil or other hydrocarbon

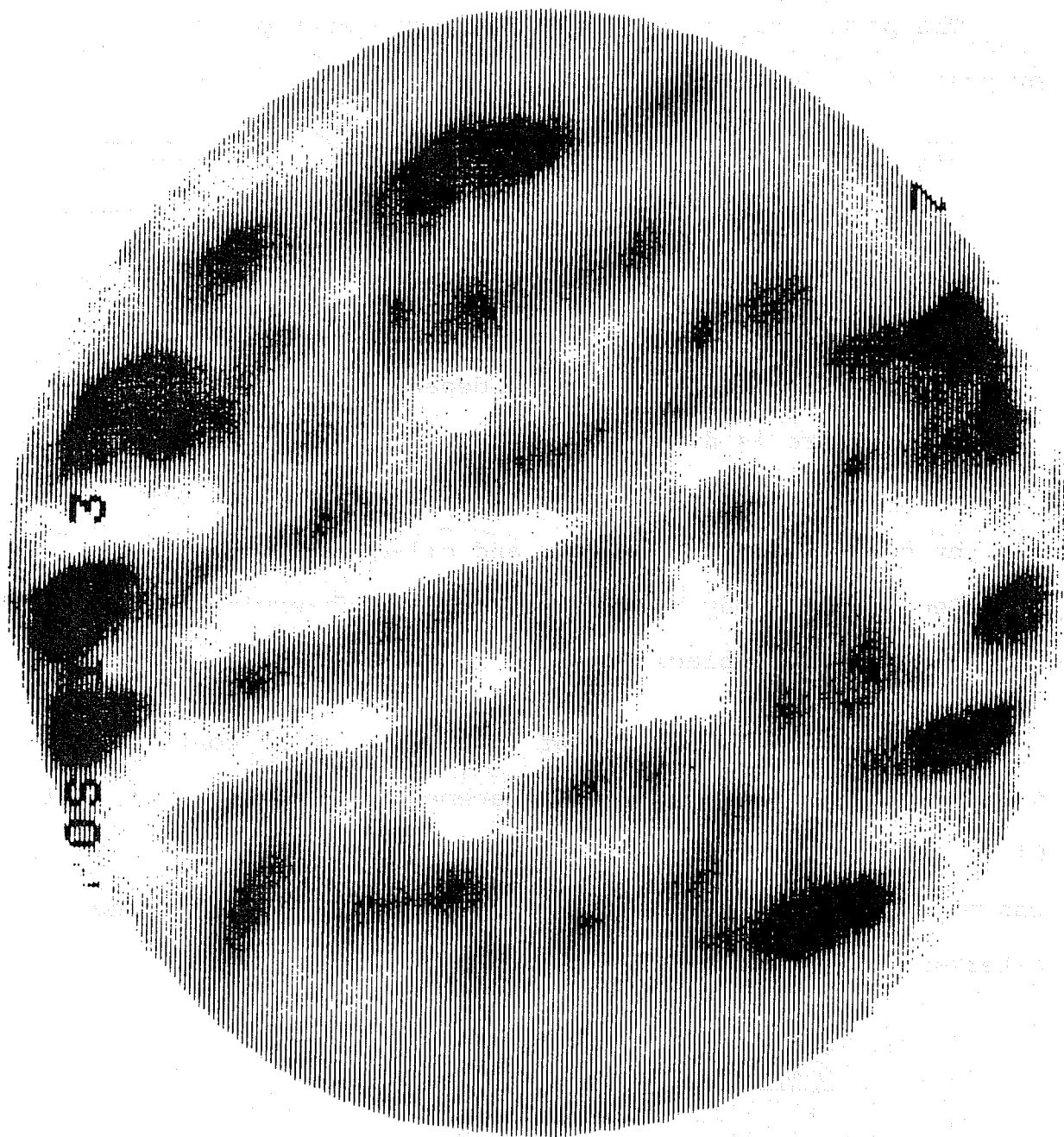


Figure IV:1. CAT scan image of oil-rich (white) and water-rich (black) regions in Berea core cross-section.

(1 molar KI displacing oil after 3 pore volumes of flow)

The parameters to be the primary subjects of this proposal include the following:

- 1) Viscosity may be identified either by polymeric or low molecular weight species.
- 2) The fluid character may be either water displacing oil, water displacing water, or oil displacing oil. Rock-fluid interactions will vary depending on the extent to which there is differential wetting.
- 3) The interfacial tension effect can be observed directly by comparing the oil-water and oil-oil combinations.
- 4) Bed porosity may be characterized by observing 1 M aqueous KI displace 1 M NaCl solution.

Tomographic observation of these cases will contribute to our understanding of oil displacement and mobility control. Given our ability to measure composition quantitatively, we can measure the local response of the pixel domains to the external flow parameters.

C. Initial Results for 1 M KI Displacing Oil from Berea Core

Initial experiments were performed with a Berea core (300 millidarcy, 6.3 cm diameter, 20 cm long, initially filled with 15 cp oil). This oil was displaced with a 1 M KI solution at a flow rate of 10 cc/hour (3 ft per day). Scans were taken as a function of position and time. Figure 1 shows a cross-section image of the core after 3 pore volumes

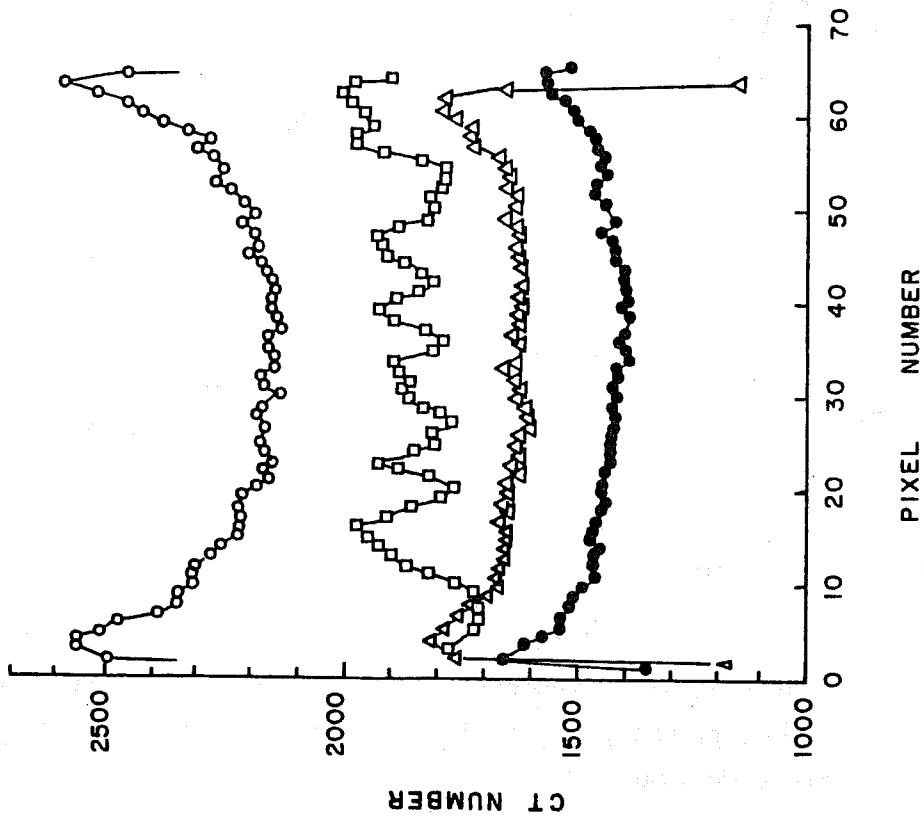
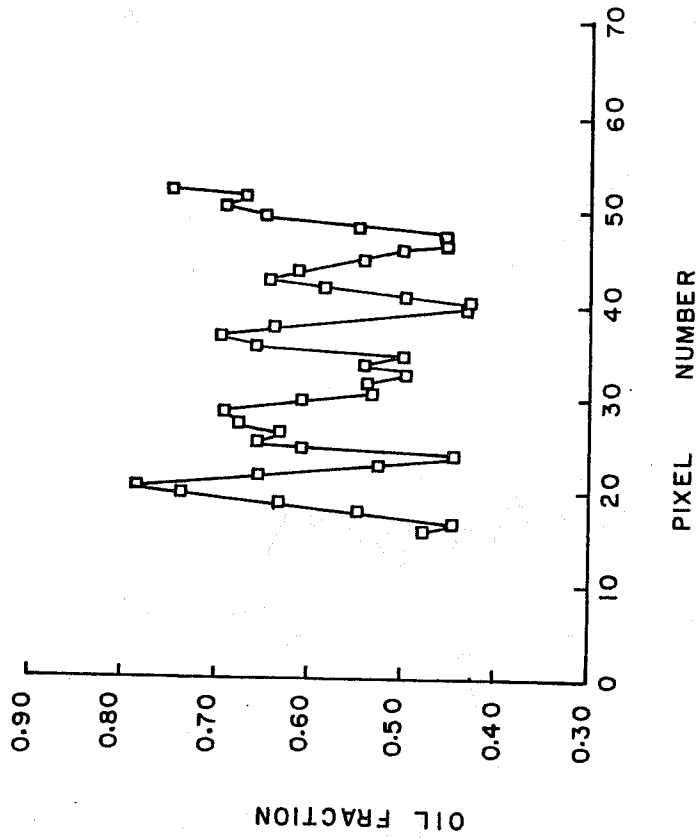


Figure IV:2. Traverse of Berea Sandstone core.

- 1 M KI filled core
- air filled core
- oil filled core
- core as in Figure 3

Figure IV:3. Local oil fraction for traverse of core shown in Figure 4.



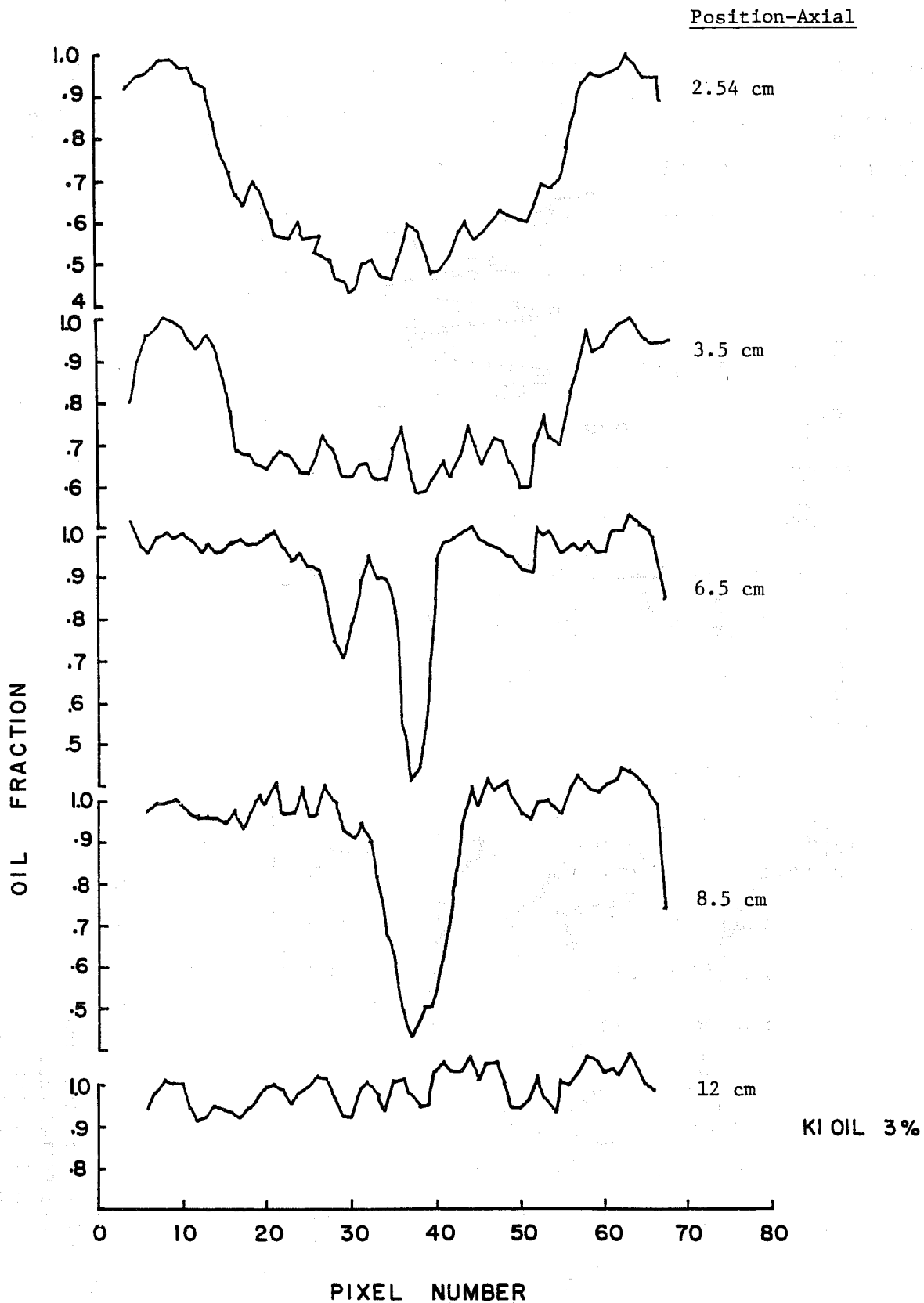


Figure IV:4. Profiles of traverse local oil fraction at different axial positions, 1M KI displacing oil, 3 percent of pore volumes injected.

of flow. Dark regions are KI rich, and lighter regions are oil-rich. In Fig. 2, a traverse (series of pixels along one diameter trace) through this cross-section is presented as a function of position. One observes that the local X-ray attenuation coefficient varies in a periodic manner across the core. In the same figure, traverses are given for similar core filled with only oil and only 1 M KI. By assuming a linear relationship with composition, these data may be used to compile the pixel average composition. The nonuniformity of the reference trace is the result of beam hardening due to the extent of X-ray absorption. In Fig. 3, the data for local oil fraction in this traverse are observed to vary across the cross-section of the core. These data show a periodicity that reflects the bedding planes in the initial Berea sandstone material. We have observed similar nonuniform distributions of flow in all of our experiments. We estimate that the uncertainty in our local composition is ± 5 percent. Some problems remain near the air/core interface due to the catastrophic change in the X-ray attenuation.

In Fig. 4, oil fraction traverse data are presented for the time at which any 3 percent of the core volume has been displaced. The KI was injected from a point source. One observes traces at planes 2.54 cm, 3.5 cm, 6.5 cm, 8.5 cm, and 12 cm from the injection point. One observes spreading of the KI about the injection point, the wide neck of the advancing water, and its development into narrow fingers as

it proceeds down the core. All of these data have been manually extracted from the 32,000 obtained for these tomographic traces. Automation of data manipulation is a key requirement if future studies are to take full advantage of these experimental data.

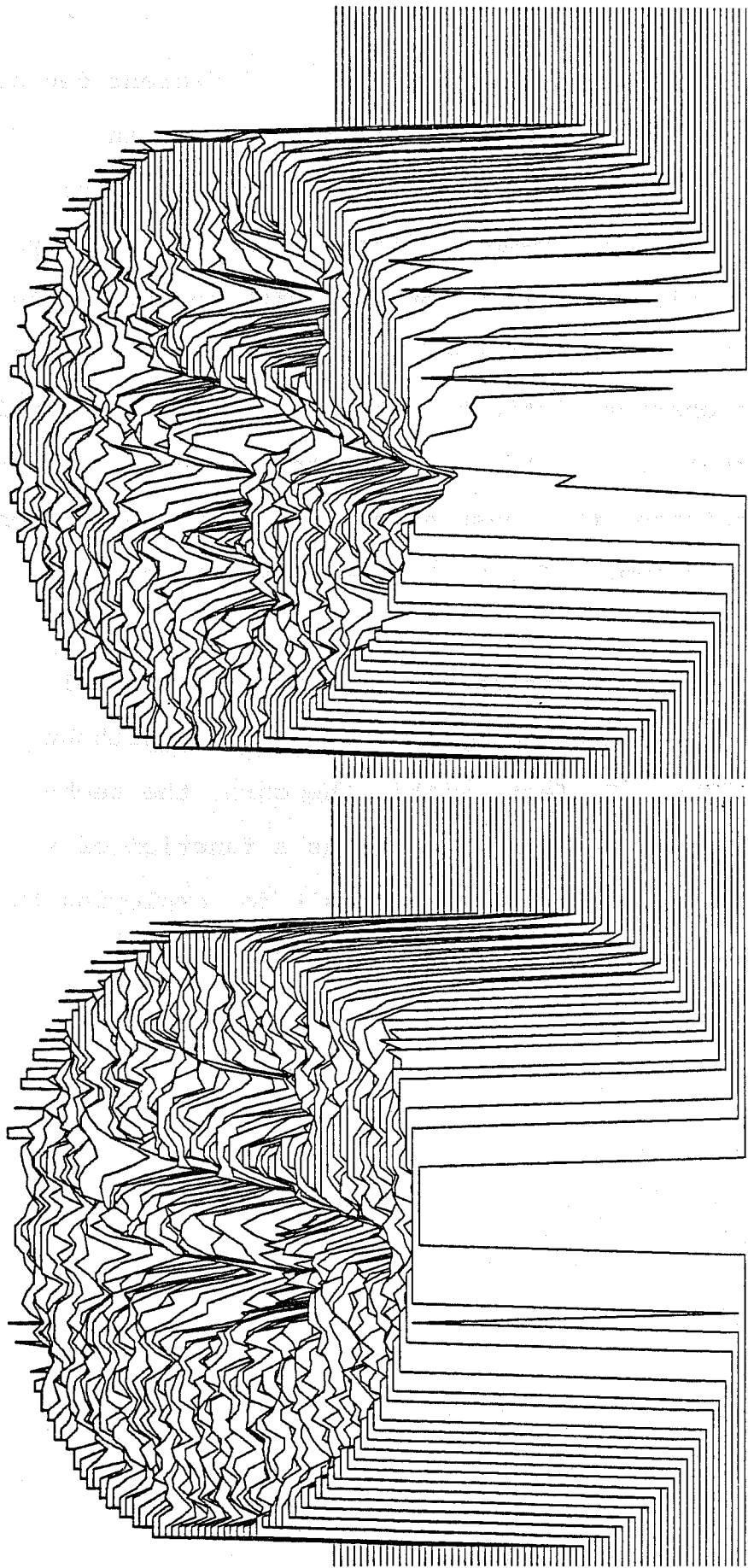
In Fig. 5, we have illustrated pixel composition data for a constant cross-section at three different times during KI injection. In order to visualize the effect most clearly, we have employed a "hidden lines removal subroutine" developed and written by the laboratory of Cyrus Levinthal. This software was originally intended for reconstruction of all shapes taken from electron micrographs of thin sections of biological material. We extend use and interact widely with this laboratory. In Fig. 5(a-c), the height of the cylindrical object is the local pixel oil fraction. The "canyons" that develop in the surface reflect the invasion of the aqueous KI solution into that region of the cross-section.

By looking at a specific pixel position as a function of time, we may measure its compositional change and determine the rate of change as a function of time from the slope. From Fig. 6, it is evident that pixel composition changes slowly as the displacement proceeds, depending on the region in which the pixel is located.

CAT scan results may be compared with other displacement experimental results. The added information from digital data is evident. In Fig. 7, the area average composition is

plotted as a function of axial position for different degrees of recovery. 1 M KI is displacing oil as it would in conventional brine flooding. One observes the startling result that, in this core sample, fingering is so extensive that core composition is almost constant with position. As time evolves, the geometry of the fingers widens. One does not observe the characteristic breakthrough profile observed in the measurement of output flows. In this figure, the bar on the right indicates the measured average core composition after three pore volumes of 1 M KI have passed through the core.

These data indicate the extent to which local pixel composition can be determined by CAT scan methods without disturbing the flow. In fact, within the core, the techniques yield core composition, C_{pixel} , as a function of x , y , z , and t . These results form the basis for employing the CAT scan method in our study of flow in porous media.



(a) **Figure IV:5. Initial attempt at graphic representation of cross-section and fraction matrix.**

Base plane represents x-y position in core cross-section. Height represents oil fraction; top is oil fraction 1.0. Conditions: 1 M KI displacing oil in Berea; position: 5 cm from injection (a) after 0.03 pore volumes; (b) after 0.45 pore volumes; (c) after 0.15 pore volumes injected.

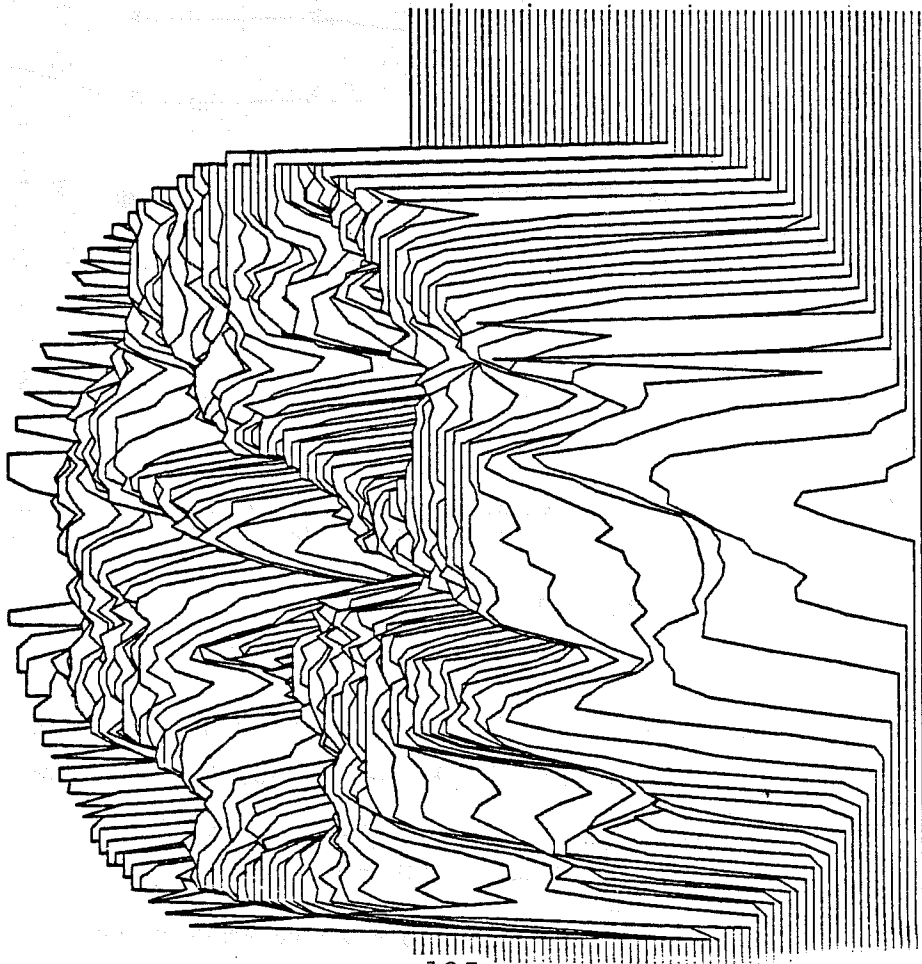


Figure IV:5

(cont 'd)

(c)

Pixel Oil Fraction

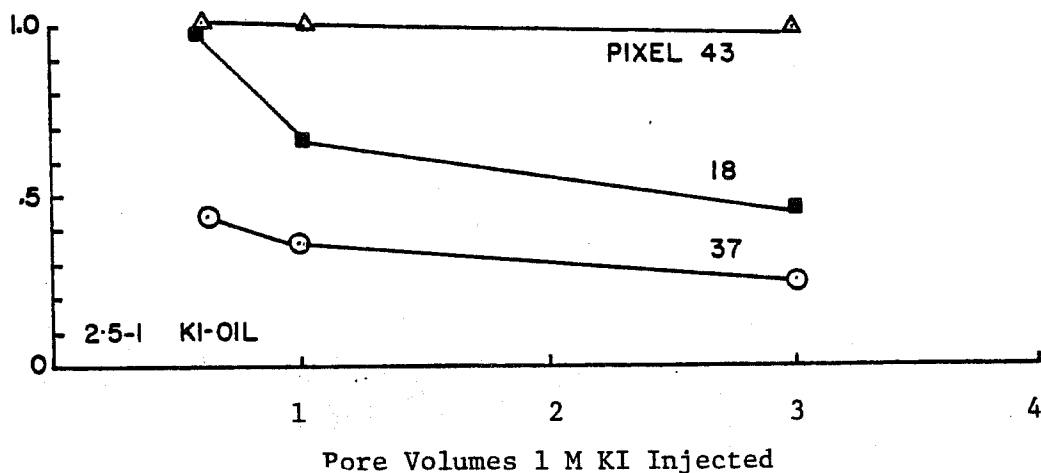


Figure IV:6. Pixel composition as a function of injected 1M KI volume (time); Position: 5 cm from injection point.

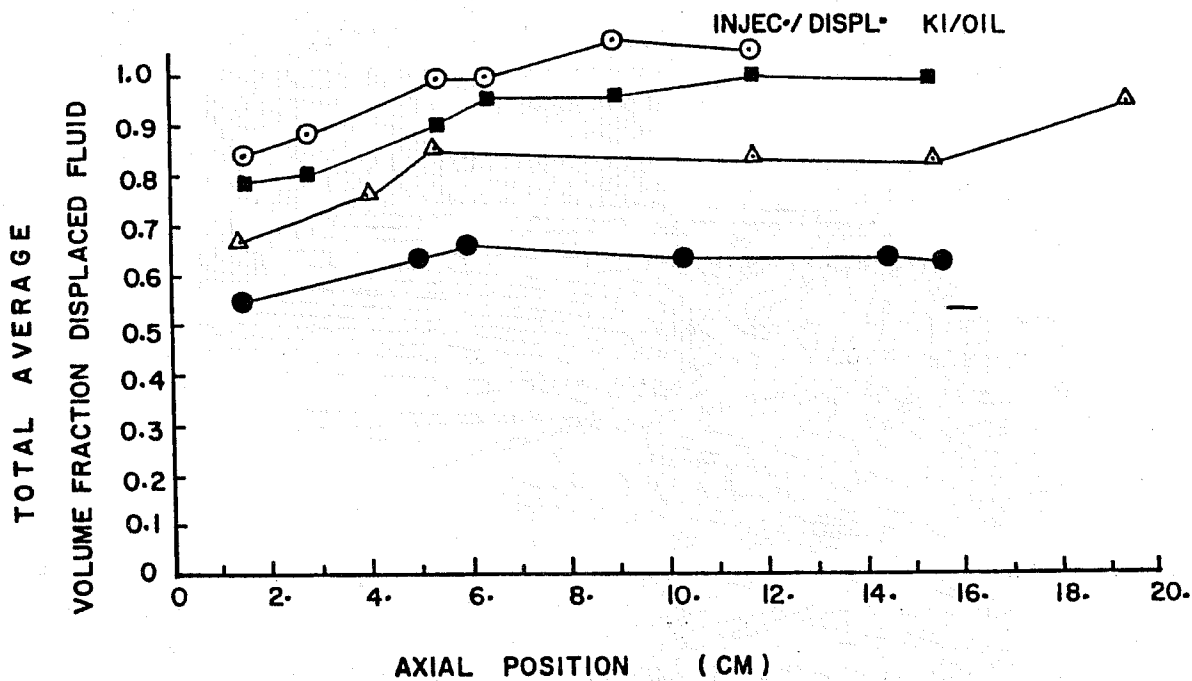


Figure IV:7. Area average oil fraction as a function of axial positions for 1M KI displacing oil from Berea core.

Conditions:
 ○ — 0.03 pore volumes
 ■ — 0.15 pore volumes
 ▲ — 0.45 pore volumes
 ● — 3.0 pore volumes injected

REFERENCES

Chapter I

1. Celik, M., Goyal, A., Manev, E., and Somasundaran, P., "The Role of Surfactant Precipitation and Redissolution in the Adsorption of Sulfonate on Minerals," SPE Paper 8263, presented at the 54th Annual SPE Meeting, Las Vegas, 1979.
2. Somasundaran, P., Celik, M., and Goyal, A., "Precipitation and Redissolution of Sulfonates and Their Role in Adsorption on Minerals," presented at the 3rd International Conference on Surface Active and Coll. Sci., August 1979, Stockholm.
3. Somasundaran, P., "Adsorption from Flooding Solutions in Porous Media," Annual Report submitted to DOE, NSF, and a Consortium of Supporting Industrial Organizations, Columbia University, New York, June 1980.
4. Celik, M., Manev, E., and Somasundaran, P., "Sulfonate Precipitation-Redissolution-Reprecipitation in Inorganic Electrolytes," presented at the 90th AIChE National Meeting, April 1981, Houston.
5. Mukerjee, P. and Mysels, K.J., "Critical Micelle Concentrations of Aqueous Surfactant Systems," NSRDS-NBS 36, U.S. Dept. of Commerce, Washington, D.C., 1971.
6. Mukerjee, P. and Mysels, K.J., "A Re-evaluation of the Spectral Change Method of Determining Critical Micelle Concentration," J. Am. Chem. Soc., 77, 2937 (1955).
7. Biswas, A.K. and Mukherji, B.K., "Studies on Micellar Growth in Surfactant Solutions With and Without Additives," J. Phys. Chem., 64, 1 (1960).
8. Corrin, M.L. and Harkins, W.D., "Determination of the Critical Concentration for Micelle Formation in Solution of Colloidal Electrolytes by the Spectral Change of a Dye," J. Am. Chem. Soc., 69, 683 (1947).

9. Orion Instruction Manual for Sodium Selective Electrodes, 1980.
10. Fuerstenau, M.C. and Miller, J.D., "The Role of the Hydrocarbon Chain in Anionic Flotation of Calcite," *Trans. AIME*, 238, 153 (1967).
11. Jung, R.F., "Oleic Acid Adsorption at the Goethite/Water Interface," M.S. Thesis, University of Melbourne, 1976.
12. Mukerjee, P., "Dimerization of Anions of Long-Chain Fatty Acids in Aqueous Solutions and the Hydrophobic Properties of the Acids," *J. Phys. Chem.*, 69, 2821 (1965).
13. Evans, D.R., Personal Communications, 1979.
14. Dick, S.G., Fuerstenau, D.W., and Healy, T.W., "Adsorption of Alkylbenzene Sulfonate Surfactants at the Alumina-Water Interface," *J. Coll. Int. Sci.*, 37, 595 (1971).
15. Evans, H.C., "Alkyl Sulfates. Part I: Critical Micelle Concentrations of the Sodium Salts," *J. Chem. Soc.*, 579 (1956).
16. Shinoda, K.J., in Colloidal Surfactants, Academic Press, New York, 1963.
17. Larsen, J.W. and Tepley, L.B., "Effect of Aqueous Alcoholic Solvents on Counterion Binding to CTAB Micelles," *J. Coll. Int. Sci.*, 49, 113 (1974).
18. Ananthapadmanabhan, K.P., "Associative Interactions in Surfactant Solutions and Their Role in Flotation," D.Eng.Sc. Thesis, Columbia University, New York, 1980.
19. Lange, H., "Kolloid-Z," 121, 66 (1951).
20. McBain, J.W. and Hutchinson, E., in Solubilization and Related Phenomena, Academic Press, New York, 1955.
21. Mukerjee, P., "Solubilization in Aqueous Micellar Systems," in Solution Chemistry of Surfactants, Vol. 1, ed. Mittal, K.L., Plenum Press, New York, 1979, p 86.

22. Nakagawa, T., "Solubilization" in Nonionic Surfactants, Vol. 1, Schick, M.J., ed., p. 558, Marcel Dekker, New York, 1967.
23. Elworthy, P.H., Florence, A.T., and Macfarlane, C.B., "Solubilization by Surface Active Agents," Chapman and Hall, London, 1968.
24. Klevens, H.B., "Effect of Electrolytes Upon the Solubilization of Hydrocarbons and Polar Compounds," J. Am. Chem. Soc. 72, 3780 (1950).
25. Richards, P.H., and McBain, J.W., "Effect of Salts on the Solubilization of Insoluble Organic Liquids by Cetylpyridinium Chloride," J. Am. Chem. Soc. 70, 1338 (1948).
26. Tartar, H.V. and Lelong, A.L.M., "Micellar Molecular Weights of Some Paraffin Chain Salts by Light Scattering," J. Phys. Chem., 59, 1185 (1956).
27. Celik, M.S., Ananthapadmanabhan, K.P., Somasundaran, P., and Manev, E.D., "Mechanism of Dissolution of Calcium Sulfonate Precipitates by Micelles--Role of Counterion Binding," presented at ACS 55th Colloid & Surface Science Symposium, June 1981, Cleveland.
28. Ludlum, D.B., "Micelle Formation in Solutions of Some Isomeric Detergents," J. Phys. Chem., 60, 1240 (1956).

Chapter II

1. Somasundaran, P., "Adsorption from Flooding Solutions in Porous Media," Annual Report submitted to NSF and a Consortium of Supporting Industrial Organizations, Columbia University, New York, July 1978.
2. Somasundaran, P., "Adsorption from Flooding Solutions in Porous Media," Annual Report submitted to DOE, NSF, and a Consortium of Supporting Industrial Organizations, Columbia University, New York, July 1979.

3. Somasundaran, P., "Adsorption from Flooding Solutions in Porous Media," Annual Report submitted to DOE, NSF, and a Consortium of Supporting Industrial Organizations, Columbia University, New York, June 1980.
4. Smolin, W., Private Communication, 1980.
5. Reid, V.W., Longman, G.F., and Heinerth, E., "Determination of Anionic-Active Detergents by Two-Phase Titration," *Tenside*, 5, (3-4), 90 (1968).
6. Somasundaran, P. and Fuerstenau, D.W., "Mechanisms of Alkyl Sulfonate Adsorption at the Alumina-Water Interface," *J. Phys. Chem.*, 70, 90 (1966).
7. Wakamatsu, T. and Fuerstenau, D.W., "The Effect of Hydrocarbon Chain Length on the Adsorption of Sulfonates at the Solid-Water Interface," *Advan. Chem. Ser.* 79, 161, 1968.
8. Somasundaran, P., Healy, T.W., and Fuerstenau, D.W., "Surfactant Adsorption at the Solid-Liquid Interface--Dependence of Mechanism on Chain Length," *J. Phys. Chem.*, 68, 3562 (1964).
9. Somasundaran, P. and Kulkarni, R.D., "Effect of Chain Length of Perfluoro Surfactants as Collectors," *Trans. Inst. Mining Met., Sect. C.*, 82, C-164 (1973).
10. Hato, M and Shinoda, K., "Kraft Points of Calcium and Sodium Dodecyl Poly(Oxyethylene) Sulfates and their Mixtures," *J. Phys. Chem.*, 77, 378 (1973).

Chapter III

1. Somasundaran, P., "Adsorption from Flooding Solutions in Porous Media," Annual Report submitted to NSF and a Consortium of Supporting Industrial Organizations, Columbia University, New York, 1978.
2. Somasundaran, P., "Adsorption from Flooding Solutions in Porous Media," Annual Report submitted to DOE, NSF, and a Consortium of Supporting Industrial Organizations, Columbia University, New York, 1980.

3. Somasundaran, P., "Adsorption from Flooding Solutions in Porous Media," Annual Report submitted to DOE, NSF, and a Consortium of Supporting Industrial Organizations, Columbia University, New York, 1979.
4. Fuerstenau, D.W., Healy, T.W., and Somasundaran, P., "The Role of the Hydrocarbon Chain of Alkyl Collectors in Flotation," *Trans. AIME*, 229, 321 (1964).
5. Ananthapadmanabhan, K.P., "Associative Interactions in Surfactant Solutions and their Role in Flotation," D.Eng.Sc. Thesis, Columbia University, New York, 1980.
6. Moudgil, B.M. and Somasundaran, P., Unpublished Results, 1980.
7. Goddard, E.D. and Hannan, R.B. in Micellization, Solubilization and Microemulsions, ed., Mittal, K.L., Plenum Press, New York, 1977.

